Ovules, megagametophytes and embryos
Ultrastructural studies after cryofixation

Marja H. Thijssen

Promotor: Prof.dr. J.L. Van Went
Hoogleraar in de Experimentele plantenmorfologie en celbiologie

Co-promotor: Prof.dr. A.M.C. Emons
Hoogleraar in de Plantencelbiologie

Samenstelling promotiecommissie:
Prof.dr. R.J. Bino, Wageningen Universiteit
Prof.dr. M. Cresti, Universita di Siena, Italie
Prof.dr. C. Mariani, Universiteit Nijmegen
Dr. W.H. Müller, Universiteit Utrecht

Ovules, megagametophytes and embryos
Ultrastructural studies after cryofixation

Marja H. Thijssen

Proefschrift

ter verkrijging van de graad van doctor
op gezag van de rector magnificus
van Wageningen Universiteit,
prof.dr.ir. L. Speelman,
in het openbaar te verdedigen
op maandag 15 september 2003
des namiddags te 13.30 uur in de Aula

Thijssen, Marja H.

Ovules, megagametophytes and embryos - Ultrastructural studies after cryofixation
Thijssen, Marja H.
Thesis Wageningen University, the Netherlands
With references – with summary in Dutch

ISBN 90-5808-882-0

Ovules, megagametophytes and embryos
Ultrastructural studies after cryofixation

Marja H. Thijssen

Proefschrift

ter verkrijging van de graad van doctor
op gezag van de rector magnificus
van Wageningen Universiteit,
prof.dr.ir. L. Speelman,
in het openbaar te verdedigen
op maandag 15 september 2003
des namiddags te 13.30 uur in de Aula

Thijssen, Marja H.

Ovules, megagametophytes and embryos - Ultrastructural studies after cryofixation
Thijssen, Marja H.
Thesis Wageningen University, the Netherlands
With references – with summary in Dutch

ISBN 90-5808-882-0

Stellingen

1. De isolatie van vrouwelijke gametofyten uit zaadbeginsels haalt deze juist uit hun geïsoleerde positie. (hoofdstuk 4 en 5 van dit proefschrift)

2. De belangrijkste vraag in de ontwikkelingsbiologie is: "Hoe doen ze dat?" Ultrastructurele analyses met behulp van cryofixatie kunnen het "dat" goed definiëren, maar extrapolaties naar het "hoe" mogen niet zondermeer gemaakt worden. (hoofdstuk 4 en 5 van dit proefschrift)

3. Het zoeken naar alternatieven voor potgrond-substraat en het gebruik hiervan in de tuinbouw draagt meer bij aan de bescherming van de Korhoen dan de daarop gerichte natuurbeschermingsmaatregelen op de Sallandse Heuvelrug.

4. Duurzame landbouw is gebaat bij de toepassing van gentechnologie.

5. Ontwikkelingslanden moeten capaciteit opbouwen op het gebied van gentechnologie om een gewogen oordeel te kunnen vellen over de voordelen en de risico's van de toepassing in eigen land.

6. Wageningen Universiteit dreigt het vermogen te verliezen om studenten uit ontwikkelingslanden een opleiding te bieden waarin technologie in een ontwikkelingsgericht kader geplaatst wordt.

7. Meer vrouwen aan de top heeft geen meerwaarde voor de vrouwenemancipatie indien deze vrouwen zich als mannen gaan gedragen.

Stellingen behorend bij het proefschrift 'Ovules, megagametophytes and embryos – Ultrastructural studies after cryofixation'.

Marja H. Thijssen
Wageningen, 15 september 2003

Contents

Chapter 1

General introduction

Plant life cycle

The life cycle of a flowering plant is marked by an alternation between the diploid generation, the sporophyte, and the haploid generation, the gametophyte. Meiotic divisions in the sporophyte result in the formation of microspores in the anther and megaspores in the ovules of the pistil.

Microspores develop into male gametophytes, i.e. microgametophytes or pollen grains. Pollen grains consist of a vegetative cell and a generative cell. Mitotic division of the generative cell, either within the pollen grain, or after germination within the pollen tube, results in the formation of the two male gametes, the sperm cells.

Generally, in each ovule one megaspore develops into the female gametophyte, i.e. the megagametophyte or embryo sac. The embryo sac contains the two female gametes, the egg cell and the central cell.

A pistil is composed of an ovary, a style, and a stigma. Generally, the stigma is positioned at the apex of an elongated style and promotes the adherence and germination of pollen grains. Pollen tubes are guided through the style and grow towards the ovules (reviewed by Wilhelmi & Preuss, 1997). The pollen tube finally enters the embryo sac and the two sperm cells are delivered into the embryo sac to effect double fertilization, a process typically occurring in angiosperms (reviewed by Russell, 1992). During the double fertilization process one sperm cell fuses with the egg cell, resulting in the formation of the diploid zygote, which subsequently develops into a new diploid sporophyte, the embryo. The second sperm cell fuses with the central cell, resulting in the formation of the endosperm, a tissue with a nutritive function for the developing embryo (Friedman, 1998).

Patterns of female gametophyte development

The formation of the megaspore and female gametophyte in angiosperms occurs according to various patterns, which differ between species (Willemse & Van Went, 1984; Haig, 1990). Usually within a species one distinct pattern is followed, which leads to a specific type of embryo sac, though, sometimes more than one embryo sac type can be recognized within a species (Haig, 1990).

Generally, during megasporogenesis, meiotic division of the megaspore mother cell within the nucellar tissue results in the formation of four haploid nuclei. Depending on the occurrence of cytokinesis after each meiotic division, the megaspore nuclei are situated within four individual cells each containing one nucleus, within two cells each containing two nuclei, or all four within the same cell. Depending on the number of

megaspore nuclei present in the initial cell from which the embryo sac is formed, megasporogenesis is designated as monosporic (one nucleus), bisporic (two nuclei), or tetrasporic (four nuclei) (Haig, 1990).

During megagametogenesis, which is development of the functional megaspore into the mature megagametophyte, variations between species occur in the number of nuclear divisions, nuclear migration and positioning, nuclear fusion, nuclear degeneration, cellularization pattern, and organization of the mature embryo sac (Haig, 1990). As a result an embryo sac can be composed of different cell numbers, with cells containing various numbers of nuclei and with nuclei varying in ploidy level. But, although the developmental patterns of megasporogenesis and megagametogenesis differ among species, the functional organization of the cells at the micropylar pole of the mature embryo sac, i.e. the cells that participate in the fertilization process, is remarkably similar (Russell, 1993).

The most common type of megagametophyte development found in flowering plants is the *Polygonum* type. After megasporogenesis, the three megaspores located at the micropylar pole degenerate and the one-nucleate megaspore at the chalazal pole undergoes megagametogenesis. This functional megaspore undergoes three rounds of mitotic nuclear divisions which results in a coenocytic, eight-nucleate cell. Subsequently, nuclear migration and cellularization result in the formation of an embryo sac consisting of seven cells that after differentiation fall into four distinct cell types, i.e. the egg cell, two synergid cells, one central cell and three antipodal cells.

Structural studies on female gametophyte development

During the last decades structural studies have greatly extended our knowledge on the angiosperm female gametophyte (reviewed by Kapil & Bhatnagar, 1981; Willemse & Van Went, 1984; Huang & Russell, 1992). However, compared to other cell types within flowering plants, there are only a few rapidly developing cells involved in megagametogenesis. Generally, female gametophyte development and differentiation take place deeply embedded in the sporophytic tissues of the ovule, which hampers the accessibility of the female gametophyte for cytological, biochemical and molecular characterization. Ultrastructural studies are mainly restricted to the stage of the mature embryo sac, focusing on the characteristics of the synergid cells, egg cell and central cell. A number of developmental aspects of megagametogenesis are still poorly understood, like the regulation and establishment of megagametophyte polarity, nuclear division, nuclear migration and nuclear positioning, cell plate formation in the eight-

nucleate megagametophyte, and the initiation and control of cell specification.

Most structural studies on megagametogenesis are based on chemically fixed ovules and embryo sacs (reviewed by Kapil & Bhatnagar, 1981; Willemse & Van Went, 1984). Due to the nature and duration of a chemical fixation process, a variety of structural artifacts can be induced (Mersey & McCully, 1978; Hayat, 1986). Because female gametophytes are highly vacuolated and surrounded by rigid embryo sac walls and several layers of ovular tissues, they are supposed to be particularly sensitive to chemical fixation.

Cryofixation physically arrests cell structure and cellular processes within milliseconds and is supposed to lead to a preservation of the cellular ultrastructure that more closely resembles the native state (reviewed by Menco, 1986; Galway *et al.*, 1995). With high pressure freezing, samples are frozen under a pressure of 2100 bar (Müller & Moor, 1984; Moor, 1987), which in theory, increases the vitrification depth compared to ultra-rapid freeze-fixation from 20 to 200 μm (Sartori *et al.*, 1993). Applying this technique for ultrastructural studies on ovules could reveal new details on megagametophyte development.

Isolation of female gametophytes and *in vitro* systems

Since the mid 1980s, the availability of methods to isolate fixed as well as living embryo sacs and their component cells from the surrounding sporophytic tissues has facilitated the characterization of the female gametophyte (reviewed by Theunis *et al.*, 1991; Huang & Russell, 1992; Dumas & Mogensen, 1993). Megagametophytes are integral parts of the ovules and can only be released with the help of enzymatic digestion of the ovules, squashing, micro-dissection, or a combination of these techniques.

The isolation techniques for female gametophytes enabled cytological studies on megasporogenesis and megagametogenesis (Yang & Zhou, 1984), fertilization (Zhou, 1987; Huang *et al.*, 1990), and early embryogenesis (Zhou & Yang, 1984, 1985; Huang *et al.*, 1990). The application of fluorescent probes to isolated megaspores and megagametophytes made it possible to study the distribution of nuclear and organellar DNA (Huang *et al.*, 1990; Huang & Russell, 1993; Huang & Sheridan, 1994), and the microtubular and actin cytoskeleton (Bednara *et al.*, 1990; Huang *et al.*, 1990, 1993; Webb & Gunning, 1990, 1994; Murgia *et al.*, 1993; Huang & Russell, 1994; Huang & Sheridan, 1994, 1996). In this way the isolation technique offers an alternative for sectioning, and enables easier integration of structural information and three-dimensional observations.

Most studies reporting on the isolation of viable female gametophyte cells, concern mature embryo sacs or their component cells. In some species the isolation of living megasporocytes, megaspores, and immature megagametophytes was reported (Wagner *et al.*, 1989; Wu *et al.*, 1993; Mouritzen & Holm, 1995; Kristóf & Imre, 1996; Imre & Kristóf, 1999). The access to isolated viable megasporocytes, megaspores, and immature megagametophytes enables experimental studies of megasporogenesis and female gametophyte differentiation at the single cell level and creates possibilities for *in vitro* manipulation of female gametophyte development. This may contribute to a better understanding of the process of megagametophyte differentiation and function.

Access to viable isolated embryo sac cells and sperm cells, has in the case of maize enabled experimental studies of gametes, fertilization and embryogenesis (reviewed by Dumas & Mogensen,1993; Faure *et al.*, 1994, Kranz & Dresselhaus, 1996). Kranz *et al.* (1991a, 1991b) established an *in vitro* fertilization system, based on electrofusion of maize gametes. Many steps of early zygote and endosperm development *in vitro*, highly resembled zygote and endosperm development *in planta*, making this system a useful model for studies on embryogenesis and endosperm development (Kranz *et al.*, 1995, 1998). Fertile maize plants could be regenerated (Kranz & Lörz, 1993). Also *in vitro* fertilized wheat egg cells divided in culture, though the multicellular structures that developed from the zygotes did not regenerate into plants (Kovács *et al.*, 1995).

In our laboratory the maize somatic embryogenesis system has been extensively explored (Fransz & Schel, 1987, 1991; Emons *et al.*, 1993b). The development of maize somatic embryos originating from exogenic meristems on embryogenic callus (Emons *et al.*, 1993b) shows many similarities with zygotic embryo development, including morphogenesis (Emons & De Does, 1993), histodifferentiation (Emons & Kieft, 1991), starch accumulation (Emons *et al.*, 1993a) and the suppression of lignin formation (Mulder & Emons, 1993). Under appropriate conditions plant regeneration is possible (for reviews, see Emons, 1994; Emons & Kieft, 1995).

Scope of the thesis

The aim of the thesis work was to obtain further insight in the process of female gametophyte differentiation and function. Insight in this process may contribute to the application of plant breeding techniques like the production of haploid plants by gynogenesis, and *in vitro* fertilization in higher plants. In our studies we mainly used *Petunia* x *hybrida* with its *Polygonum* type of embryo sac development as a

representative angiosperm.

The work was particularly focused on two aspects: (1) the analysis of the cytological and ultrastructural changes during megagametophyte development *in planta*, with the aim to identify and characterize factors and mechanisms playing a role in this process. We explored and developed the high pressure freezing technique to obtain detailed ultrastructural information on the cytoplasmic organization of *P.* x *hybrida* female gametophyte cells, information that may be destroyed by conventional chemical fixation. Information can be compared with the information already available from observations on chemically fixed mature embryo sacs (Van Went, 1970a, 1970b), and will be especially valuable now mutants become available (reviewed by Drews & Yadegari, 2002).

(2) The characterization of isolated viable female gametophyte cells, as they can be directly observed and are uninfluenced by the sporophytic cells that surround them *in planta*. Successful female gametophyte cell culture will create possibilities for *in vitro* manipulation of megagametophyte development. We could use the enzymatic maceration technique developed at our laboratory for the isolation of living mature *P.* x *hybrida* embryo sacs (Van Went & Kwee, 1990) as a starting point for further characterization of *P.* x *hybrida* embryo sacs, the isolation of megaspores and immature megagametophytes, and *in vitro* culture experiments.

Outline of the thesis

In chapter 2 the results of ultrastructural preservation of *P.* x *hybrida* as well as *Brassica napus* ovules obtained by cryofixation methods, propane plunge freezing and high pressure freezing, were compared with the results obtained by conventional chemical fixation methods.

Though leading to improved ultrastructural preservation, the application of high pressure freezing and freeze substitution yielded only a low percentage of adequately preserved ovules. We presumed this was due to the embedding fluid used in this cryofixation procedure. Chapter 3 describes the tests and comparisons of different compounds for the suitability as embedding fluids in the high pressure freezing/ freeze substitution procedure, with the aim to increase the percentage of well preserved ovules.

With this for *P.* x *hybrida* ovules optimized cryofixation procedure, the ultrastructural aspects of female gametophyte development as well as the ultrastructural organization of the mature embryo sac were studied. The results of these studies are

described in chapter 4 and chapter 5, respectively.

Chapter 6 describes the use of the enzymatic maceration technique to isolate different developmental stages of *P.* x *hybrida* megagametophytes and the characterization of the female gametophyte cells. Attempts of megagametophyte *in vitro* culture and the effects of culture on the structure and organization of the female gametophytes are described.

Chapter 7 presents a study in which maize *in planta* and *in vitro* embryo development are compared at the structural level, with special focus on globulin storage proteins.

References

Bednara, J., Willemse, M.T.M. & Van Lammeren, A.A.M. (1990). Organization of the actin cytoskeleton during megasporogenesis in *Gasteria verrucosa* visualized with fluorescent-labelled phalloidin. Acta Bot. Neerl. 39, 43-48.

Drews, G.N. & Yadegari, R. (2002). Development and function of the angiosperm female gametophyte. Annu. Rev. Genet. 36, 99-124.

Dumas, C. & Mogensen, H.L. (1993). Gametes and fertilization: Maize as a model system for experimental embryogenesis in flowering plants. Plant Cell 5, 1337-1348.

Emons, A.M.C. (1994). Somatic embryogenesis: Cell biological aspects. Acta Bot. Neerl. 43, 1-14.

Emons, A.M.C. & De Does, H. (1993). Origin and development of embryo and bud primordia during maturation of embryogenic calli of *Zea mays*. Can. J. Bot. 71, 1349-1356.

Emons, A.M.C. & Kieft, H. (1991). Histological comparison of single somatic embryos of maize from suspension culture with somatic embryos attached to callus cells. Plant Cell Rep. 10, 485-488.

Emons, A.M.C. & Kieft H. (1995). Somatic embryogenesis in maize (*Zea mays* L.). Biotechnology in agriculture and forestry, Vol. 31, Somatic embryogenesis and synthetic seed II (ed. by Y.P.S. Bajaj), pp. 24-39. Springer-Verlag, Berlin.

Emons, A.M.C., Mulder, M.M. & Kieft, H. (1993a). Pyrolysis mass spectrometry of developmental stages of maize somatic embryos. Acta Bot. Neerl. 42, 319-339.

Emons, A.M.C., Samallo-Droppers, A. & Van der Toorn, C. (1993b). The influence of sucrose, mannitol, L-proline, abscisic acid and gibberellic acid on the maturation of somatic embryos of *Zea mays* L. from suspension cultures. J. Plant Physiol. 142, 597-604.

Faure, J.-E., Digonnet, C., Mòl, R., Matthys-Rochon, E. & Dumas, C. (1994). *In vitro* pollination and fertilisation in maize (*Zea mays* L.): Technical procedures and prospects for the dissection of the double fertilisation process. Plant Sci. 104, 1-10.

Fransz, P.F. & Schel, J.H.N. (1987). An ultrastructural study on the early callus development from immature embryos of the maize strains A188 and A632. Acta Bot. Neerl. 36, 247-260.

Fransz, P.F. & Schel, J.H.N. (1991). Cytodifferentiation during the development of friable embryogenic callus of maize (*Zea mays*). Can. J. Bot. 69, 26-33.

Friedman, W.E. (1998). The evolution of double fertilization and endosperm: An "historical" perspective. Sex. Plant Reprod. 11, 6-16.

Galway, M.E., Heckman, J.W. Jr, Hyde, G.J. & Fowke, L.C. (1995). Advances in high-pressure and plunge-freeze fixation. Methods in cell biology, Vol. 49 (ed. by D.W. Galbraith, H.J. Bohnert and D.P. Bourque), pp. 3-19. Academic Press, Inc., San Diego, CA.

Haig, D. (1990). New perspectives on the angiosperm female gametophyte. Bot. Rev. 56, 236-274.

Hayat, M.A. (1986). Glutaraldehyde: Role in electron microscopy. Micron Microsc. Acta 17, 115-135.

Huang, B.-Q., Pierson, E.S., Russell, S.D., Tiezzi, A. & Cresti, M. (1993). Cytoskeletal organisation and modification during pollen tube arrival, gamete delivery and fertilisation in *Plumbago zeylanica*. Zygote 1, 143-154.

Huang, B.-Q. & Russell, S.D. (1992). Female germ unit: Organization, isolation, and function. Int. Rev. Cytol. 140, 233-293.

Huang, B.-Q. & Russell, S.D. (1993). Polarity of nuclear and organellar DNA during megasporogenesis and megagametogenesis in *Plumbago zeylanica*. Sex. Plant Reprod. 6, 205-211.

Huang, B.-Q. & Russell, S.D. (1994). Fertilization in *Nicotiana tabacum*: Cytoskeletal modifications in the embryo sac during synergid degeneration. A hypothesis for short-distance transport of sperm cells prior to gamete fusion. Planta 194, 200-214.

Huang, B.-Q., Russell, S.D., Strout, G.W. & Mao, L.-J. (1990). Organization of isolated embryo sacs and eggs of *Plumbago zeylanica* (Plumbaginaceae) before and after fertilization. Am. J. Bot. 77, 1401-1410.

Huang, B.-Q. & Sheridan, W.F. (1994). Female gametophyte development in maize: Microtubular organization and embryo sac polarity. Plant Cell 6, 845-861.

Huang, B.-Q. & Sheridan, W.F. (1996). Embryo sac development in the maize *indeterminate gametophyte1* mutant: Abnormal nuclear behavior and defective microtubule organization. Plant Cell 8, 1391-1407.

Imre, K. & Kristóf, Z. (1999). Isolation and osmotic relations of developing megagametophytes of *Torenia fournieri*. Sex. Plant Reprod. 12, 152-157.

Kapil, R.N. & Bhatnagar, A.K. (1981). Ultrastructure and biology of female gametophyte in flowering plants. Int. Rev. Cytol. 70, 291-341.

Kovács, M., Barnabás, B. & Kranz, E. (1995). Electro-fused isolated wheat (*Triticum aestivum* L.) gametes develop into multicellular structures. Plant Cell Rep. 15, 178-180.

Kranz, E., Bautor, J. & Lörz, H. (1991a). *In vitro* fertilization of single, isolated gametes of maize mediated by electrofusion. Sex. Plant Reprod. 4, 12-16.

Kranz, E., Bautor, J. & Lörz, H. (1991b). Electrofusion-mediated transmission of cytoplasmic organelles through the *in vitro* fertilization process, fusion of sperm cells with synergids and central cells, and cell reconstitution in maize. Sex. Plant Reprod. 4, 17-21.

Kranz, E. & Dresselhaus, T. (1996). *In vitro* fertilization with isolated higher plant gametes. Trends Plant Sci. 1, 82-89.

Kranz, E. & Lörz, H. (1993). *In vitro* fertilization with isolated, single gametes results in zygotic embryogenesis and fertile maize plants. Plant Cell 5, 739-746.

Kranz, E., Von Wiegen, P. & Lörz, H. (1995). Early cytological events after induction of cell division in egg cells and zygote development following *in vitro* fertilization with angiosperm gametes. Plant J. 8, 9-23.

Kranz, E., Von Wiegen, P., Quader, H. & Lörz, H. (1998). Endosperm development after fusion of isolated, single maize sperm and central cells *in vitro*. Plant Cell 10, 511-524.

Kristóf, Z. & Imre, K. (1996). Isolation of living megaspores of *Torenia fournieri.* Protoplasma 192, 245-248.

Menco, B.P.M. (1986). A survey of ultra-rapid cryofixation methods with particular emphasis on applications to freeze-fracturing, freeze-etching, and freeze-substitution. J. Electron Microsc. Tech. 4, 177-240.

Mersey, B. & McCully, M.E. (1978). Monitoring the course of fixation in plant cells. J. Microsc. 114, 49-76.

Mouritzen, P. & Holm, P.B. (1995). Isolation and culture of barley megasporocyte protoplasts. Sex. Plant Reprod. 8, 321-325.

Mulder, M.M. & Emons, A.M.C. (1993). Cell wall development in maize somatic embryos studied by pyrolysis mass spectrometry. J. Anal. Appl. Pyrolysis 25, 255-264.

Murgia, M., Huang, B.-Q., Tucker, S.C. & Musgrave, M.E. (1993). Embryo sac lacking antipodal cells in *Arabidopsis thaliana* (Brassicaceae). Am. J. Bot. 80, 824-838.

Russell, S.D. (1992). Double fertilization. Int. Rev. Cytol. 140, 357-388.

Russell, S.D. (1993). The egg cell: Development and role in fertilization and early embryogenesis. Plant Cell 5, 1349-1359.

Sartori, N., Richter, K. & Dubochet, J. (1993). Vitrification depth can be increased more than 10-fold by high-pressure freezing. J. Microsc. 172, 55-61.

Theunis, C.H., Pierson, E.S. & Cresti, M. (1991). Isolation of male and female gametes in higher plants. Sex. Plant Reprod. 4, 145-154.

Van Went, J.L. (1970a). The ultrastructure of the synergids of *Petunia*. Acta Bot. Neerl. 19, 121-132.

Van Went, J.L. (1970b). The ultrastructure of the egg and the central cell of *Petunia*. Acta Bot. Neerl. 19, 313-322.

Van Went, J.L. & Kwee, H.-S. (1990). Enzymatic isolation of living embryo sacs of *Petunia*. Sex. Plant Reprod. 3, 257-262.

Wagner, V.T., Kardolus, J.P. & Van Went, J.L. (1989). Isolation of the lily embryo sac. Sex. Plant Reprod. 2, 219-224.

Webb, M.C. & Gunning, B.E.S. (1990). Embryo sac development in *Arabidopsis thaliana*. I. Megasporogenesis, including the microtubular cytoskeleton. Sex. Plant Reprod. 3, 244-256.

Webb, M.C. & Gunning, B.E.S. (1994). Embryo sac development in *Arabidopsis thaliana*. II. The cytoskeleton during megagametogenesis. Sex. Plant Reprod. 7, 153-163.

Wilhelmi, L.K. & Preuss, D. (1997). Blazing new trails. Pollen tube guidance in flowering plants. Plant Physiol. 113, 307-312.

Willemse, M.T.M. & Van Went, J.L. (1984). The female gametophyte. Embryology of angiosperms (ed. by B.M. Johri), pp. 159-196. Springer-Verlag, Berlin.

Wu, Y., Zhou, C. & Koop, H.-U. (1993). Enzymatic isolation of viable nucelli at the megaspore mother cell stage and in developing embryo sacs in *Nicotiana tabacum*. Sex. Plant Reprod. 6, 171-175.

Yang, H.-Y. & Zhou, C. (1984). Observations on megasporogenesis and megagametophyte development in *Paulownia* sp. and *Sesamum indicum* by enzymatic maceration technique. Acta Bot. Sin. 26, 342-346.

Zhou, C. (1987). A study of fertilization events in living embryo sacs isolated from sunflower ovules. Plant Sci. 52, 147-151.

Zhou, C. & Yang, H.-Y. (1984). The enzymatic isolation of embryo sacs from fixed and fresh ovules of *Antirrhinum majus* L. Acta Biol. Exp. Sin. 17, 141-147.

Zhou, C. & Yang, H.-Y. (1985). Observations on enzymatically isolated, living and fixed embryo sacs in several angiosperm species. Planta 165, 225-231.

Chapter 2

Improved ultrastructural preservation of *Petunia* and *Brassica* ovules and embryo sacs by high pressure freezing and freeze substitution

M.H. THIJSSEN, F. MITTEMPERGHER, A.C. VAN AELST & J.L. VAN WENT

(1997) Protoplasma 197, 199-209

Summary

In order to improve the ultrastructural preservation of the female gametophyte of *Petunia* x *hybrida* and *Brassica napus* we tested several cryofixation techniques and compared the results with those of conventional chemical fixation methods. Ovules fixed with glutaraldehyde and osmium tetroxide in the presence or absence of potassium ferrocyanide showed poor cell morphological and ultrastructural preservation. In ovules cryo-fixed by plunging into liquid propane, the cell morphology was well preserved. However, at the ultrastructural level structure-distorting ice crystals were detected in all tissues. Due to the large size of the ovules, cryofixation by plunging in liquid propane is not adequate for ultrastructural studies. In contrast, *P.* x *hybrida* and *B. napus* ovules cryo-fixed by high pressure freezing showed improved cell morphological as well as ultrastructural preservation of the embryo sac and the surrounding integumentary tissues. The contrast of the cellular membranes after freeze substitution with 2% osmium tetroxide and 0.1% uranyl acetate in dry acetone was high. At the ultrastructural level, the most prominent improvements were: straight plasma membranes which were appressed to the cell walls; turgid appearing organelles with smooth surface contours; minimal extraction of cytoplasmic and extracellular substances. In contrast to the chemically fixed ovules, in high pressure frozen ovules numerous microtubules and multivesicular bodies could be distinguished.

Key words: *Brassica napus*, embryo sac, freeze substitution, high pressure freezing, ovule, *Petunia* x *hybrida*.

Introduction

For many years, the development of the female gametophyte has been a topic of interest, as is reflected in the large amount of literature concerning embryo sac cytology and ultrastructure (for reviews, see Kapil & Bhatnagar, 1981; Willemse & Van Went, 1984; Haig, 1990; Reiser & Fischer, 1993). One reason for that interest is the high specialization of the embryo sac cells, of which each has a unique ultrastructural configuration related to its specific role during the fertilization process. However, most knowledge on embryo sac development to this day is based on light and electron microscopical studies of chemically fixed material. Embryo sacs are composed of large, highly vacuolate cells, which are deeply embedded in the ovular tissues, thus, making them very difficult cells to fix particularly for ultrastructural observations.

Fixation with aldehydes may require several seconds up to minutes to arrest biological processes (Mersey & McCully, 1978); the slow penetration rate of these fixatives through the sample may not be rapid enough to trap fast occurring processes, such as fertilization. Chemical fixatives generally cause swelling or shrinkage artifacts of tissues, cells, and organelles, thereby inducing a variety of structural and elemental changes (Hayat, 1986).

An alternative to chemical fixation is cryofixation, ideally resulting in an instant stabilisation of the native state of dynamic structures with the ultrastructural images obtained being more realistic. Many advances have been achieved in ultra-rapid freeze-fixation (Severs *et al.*, 1995), which have extended our knowledge of cellular organization. However, because the cooling rate of an ultra-rapid freezing system should be higher than 10^4 °C/s, the size of specimens that can be frozen without the formation of structure-distorting ice crystals is limited to 10 to 20 μm (Severs *et al.*, 1995).

High pressure freezing can reduce this limitation. The sample is exposed to a pressure of 2100 bar just before freezing, resulting in a lowered freezing point, a decreased formation of ice nucleation sites and a reduced rate of ice crystal growth. In this way the depth of good freezing is increased, even though a relatively slow cooling rate is employed. This technique allows good freezing of larger samples, such as compact tissues without the use of cryoprotectants (Müller & Moor, 1984; Moor, 1987). High pressure freezing, followed by freeze substitution or freeze-fracturing has been successfully applied to stabilize a variety of unfixed plant tissues, without the use of cryoprotectants, like root tips (Craig & Staehelin, 1988; Kaeser *et al.*, 1989; Kiss *et al.*, 1990), root nodules (Studer *et al.*, 1992; Berg, 1994), and anthers (Hesse & Hess,

1993; Hess & Hesse, 1994).

The present study contains a description of the use of cryo-techniques versus chemical fixation procedures on the ultrastructure of *Petunia* x *hybrida* (Hook.) Vilm. and *Brassica napus* L. ovules and embryo sacs. The results achieved with high pressure frozen ovules are discussed and compared with those obtained by plunge freezing in liquid propane and chemical fixation techniques.

Materials and methods

Plant material

Plants of *Brassica napus* L. var. *oleifera* Del., cv. Drakkar, and cv. Tanto were grown in the greenhouse at an average temperature of 20 °C. With tweezers, the ovules (450 μm in diameter) were removed one by one from the placenta of flowers in anthesis. Plants of *Petunia* x *hybrida* (Hook.) Vilm. cv. Bluebedder were grown under growth chamber conditions with a daylength of 16 h and a temperature of 20 °C. From flowers in anthesis the petals and sepals were removed by hand, while the carpels were carefully removed with a tweezer. Using a dissecting microscope the ovules (200 μm in diameter) could be easily detached from the placenta with a needle.

Chemical fixation

Ovules were fixed for 4 h with 3% glutaraldehyde in 0.1 M phosphate buffer (pH 7.2), containing 0.01% Triton X-100. After rinsing in phosphate buffer, the samples were post-fixed for 6 h with 1% OsO_4 in the same buffer. To enhance the contrast of the cellular membranes, in some cases, 1.5% $K_4Fe(CN)_6 \cdot 3H_2O$ was added to the post-fixative (Janson *et al.*, 1994). A number of *B. napus* ovules were fixed for 2 h with 2% glutaraldehyde and 4% paraformaldehyde in 0.05 M phosphate buffer and post-fixed for 2 h with 1% OsO_4 in the same buffer. All samples were dehydrated in a graded ethanol series and stained en bloc with 1% uranyl acetate in 70% ethanol for 1 h, and finally embedded in Spurr's low viscosity resin (Spurr, 1969).

Cryofixation by plunge freezing in liquid propane

Ovules of *B. napus* were mounted on the flat surface of a rivet, with a 10% sucrose solution in phosphate buffer or a thin layer of Tissue-Tek glue (Miles Inc., Elkhart, IN, U.S.A.). *Petunia* x *hybrida* ovules were attached to nickel grids with a 10% sucrose

solution in phosphate buffer. The samples were plunged into liquid propane that was pre-cooled by liquid nitrogen.

Cryofixation by high pressure freezing

Either seven to eight *B. napus* ovules or up to 30 *P.* x *hybrida* ovules were placed in gold specimen holders, previously filled with 1-hexadecene to remove the air. Pairs of holders were clamped together and frozen in a Balzers HPM 010 high pressure freezing machine. To facilitate the separation of the pair of holders, one of them was coated with 3% lecithin in chloroform prior to freezing.

Freeze substitution

Frozen samples were kept under liquid nitrogen and transferred to cryo-vials onto the surface of the frozen substitution fluid and placed in a Reichert-Jung freeze substitution apparatus (CS Auto). Ovules were freeze substituted with 1% or 4% OsO_4, or 2% OsO_4 with 0.1% uranyl acetate in anhydrous acetone. Freeze substitution was performed for 48 h at -80 °C and for 8 h at -40 °C to permit the OsO_4 to react with the cellular components. Afterwards the samples were slowly brought back to room temperature. After washing in acetone, the samples were stained en bloc with 1% uranyl acetate in methanol for 1 h, then brought back to acetone, and finally embedded in Spurr's low viscosity resin (Spurr, 1969).

Electron microscopy

Ultrathin sections were cut with a diamond knife on an LKB ultramicrotome and collected on formvar coated 100 mesh copper grids. The sections were counterstained with uranyl acetate and lead citrate, and examined with a JEOL 1200 EXII electron microscope at 80 kV.

Results

Chemical fixation

Chemically fixed *P.* x *hybrida* and *B. napus* ovules had deformed integumentary tissues as well as considerably deformed embryo sacs (Figs. 1a and 3a). The cells were not turgescent, which was especially apparent in the highly vacuolate embryo sac cells in which the undulate cell membranes were no longer appressed to the cell

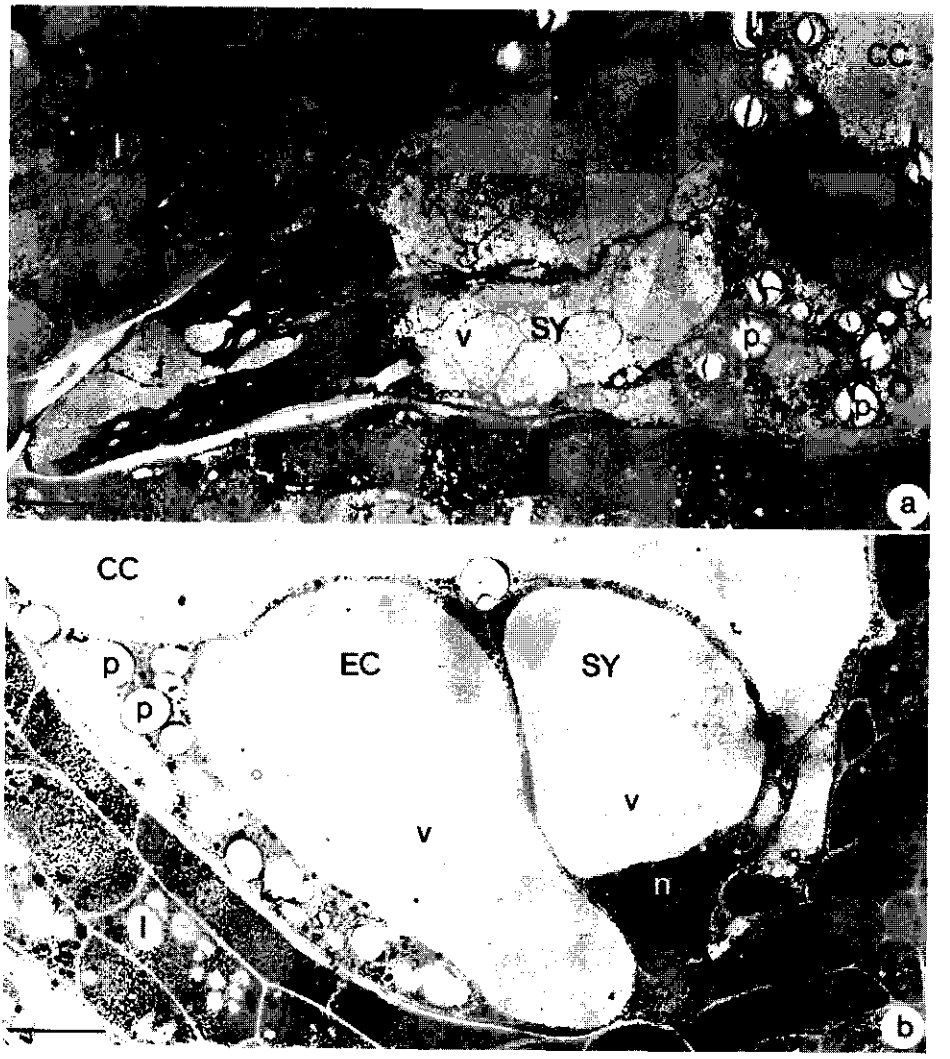

Fig. 1 a, b. Overviews of the egg apparatus of *P.* x *hybrida*. **a** Chemically fixed ovule (glutaraldehyde, OsO_4, and $K_4Fe(CN)_6$). The synergids show deformation in cell shape; cellular membranes are undulating or even absent. **b** Propane plunged frozen and freeze substituted ovule (1% OsO_4). The cell morphology of the egg apparatus cells is well preserved. However, ice crystal damage is visible in all ovular cells. *CC* Central cell; *EC* egg cell; *f* filiform apparatus; *I* integumentary tissues; *n* nucleus; *p* plastid; *SY* synergid; *v* vacuole. Bars: 5 µm.

walls (Fig. 1a). The vacuoles had lost their round shape and they often appeared translucent (Fig. 3a). Sometimes vacuolar membranes were not visible at all, whereas inside the vacuoles different membranous structures were present (Fig. 1a). Inside the irregularly shaped nuclei membranous structures could sometimes be found as well (Fig. 1a). A large number of membranes was often situated at the periphery of the integumentary cells (Fig. 3a).

Chemical fixation seemed to rearrange the normal distribution of organelles within the cells. The nuclear envelope showed invaginations where plastids were located (Fig. 3a). Organelles were irregularly shaped and seemed to be shrunken and extracted (Fig. 3a). This shrinkage was especially visible in the area of the plastids surrounding the starch (Fig. 3a). Some mitochondria had an electron translucent area in the centre of the interior structure while the matrix had low contrast (Fig. 3a). Microtubules were never observed.

The cellular membranes of sections of *P.* x *hybrida* and *B. napus* ovules, post-fixed with osmium tetroxide only, showed poor contrast (results not shown). The addition of ferrocyanide to the post-fixative greatly enhanced the contrast of most of the cellular membranes.

Cryofixation by plunge freezing in liquid propane

After plunge freezing and freeze substitution of *P.* x *hybrida* and *B. napus* ovules the cell morphology of the integumentary cells as well as the embryo sacs was well preserved. The cells appeared turgescent with straight plasma membranes, which were tightly appressed to the cell walls. Thin layers of cytoplasm were present along the plasma membranes at the chalazal side of the highly vacuolate egg apparatus cells of *P.* x *hybrida* embryo sacs (Fig. 1b).

However, at the ultrastructural level ice crystal damage was observed in all ovular tissues, including the embryo sac. This damage was visible as electron translucent spaces, the former location of the ice crystals, surrounded by a network of electron dense material. This segregation pattern was not only detectable throughout the groundplasm but also inside the nuclei (Fig. 1b). Growing ice crystals in the groundplasm had also caused deformation in the shape of the organelles. The severity of ice crystal damage varied between neighbouring cells.

In *P.* x *hybrida* embryo sacs most of the organelles showed an altered structure, but could still be recognized. The ultrastructure of plunged frozen *B. napus* ovules was totally destroyed due to ice crystal damage (results not shown).

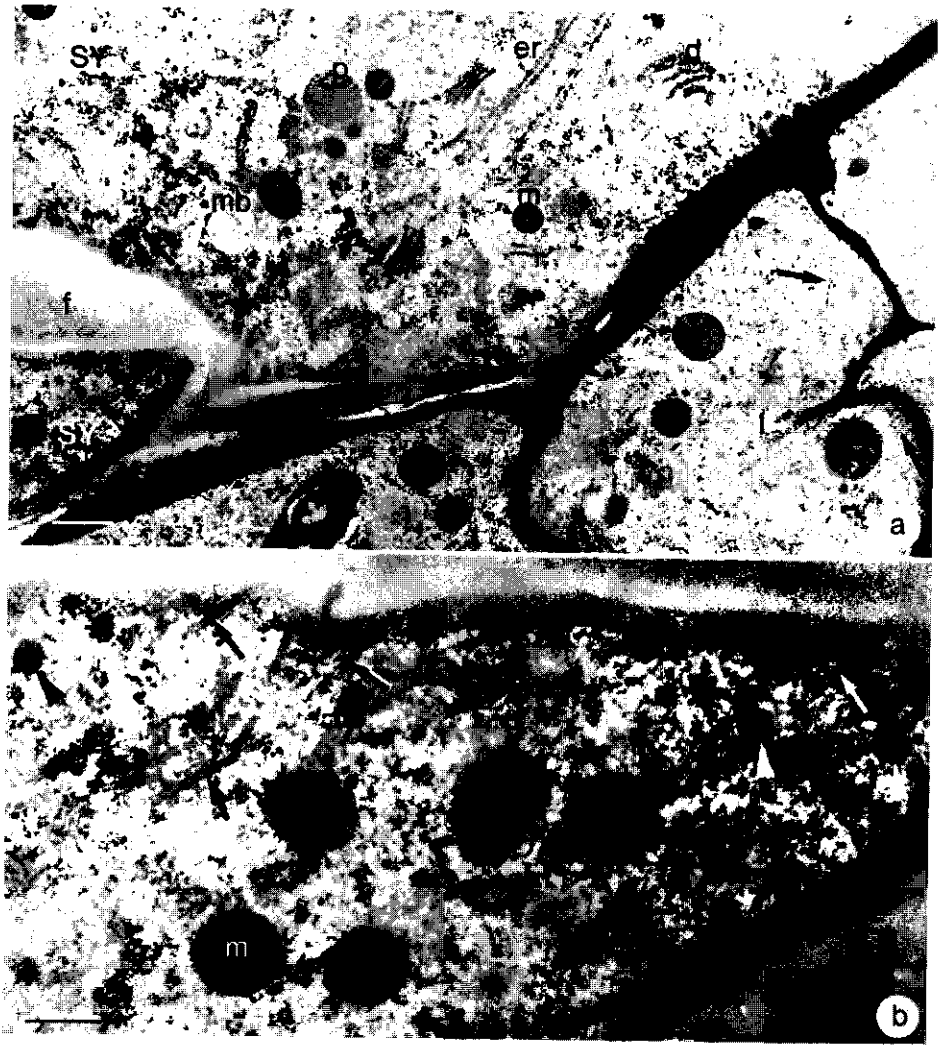

Fig. 2 a, b. High pressure frozen and freeze substituted *P.* x *hybrida* ovule (2% OsO_4 and 0.1% uranyl acetate). **a** Micrograph showing the well preserved ultrastructure of the synergids as well as the surrounding integumentary tissues. Bar: 500 nm. **b** Higher magnification showing many coated vesicles (arrowheads) close to the filiform apparatus and the well preserved microtubules. Bar: 200 nm. *d* Dictyosome; *er* endoplasmic reticulum; *f* filiform apparatus; *l* integumentary tissues; *m* mitochondrion; *mb* multivesicular body; *p* plastid; *SY* synergid; arrow, microtubule.

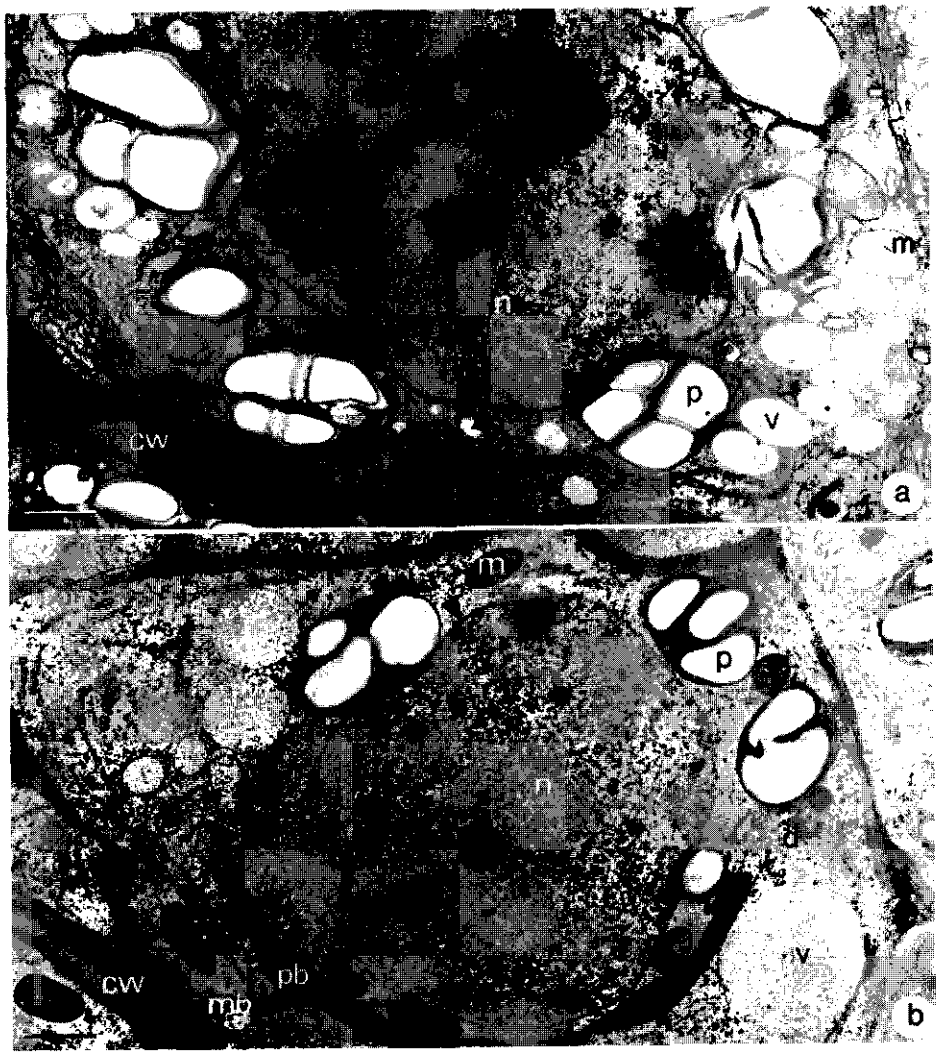

Fig. 3 a, b. Integumentary cells of *B. napus* ovules. **a** Cell from a chemically fixed ovule (glutaraldehyde, OsO_4, and $K_4Fe(CN)_6$), showing a deformed nucleus and plastids, extracted mitochondria and wavy endoplasmic reticulum at the periphery of the cell. **b** Cell from a high pressure frozen, freeze substituted ovule (2% OsO_4 and 0.1% uranyl acetate), showing several ultrastructural details recognisable throughout the cytoplasm. Organelles have a turgid appearance and are much less extracted than with a chemical fixation. *cw* Cell wall; *d* dictyosome; *er* endoplasmic reticulum; *m* mitochondrion; *mb* multivesicular body; *n* nucleus; *p* plastid; *pb* protein body; *v* vacuole; arrowhead, nuclear envelope. Bars: 1 μm.

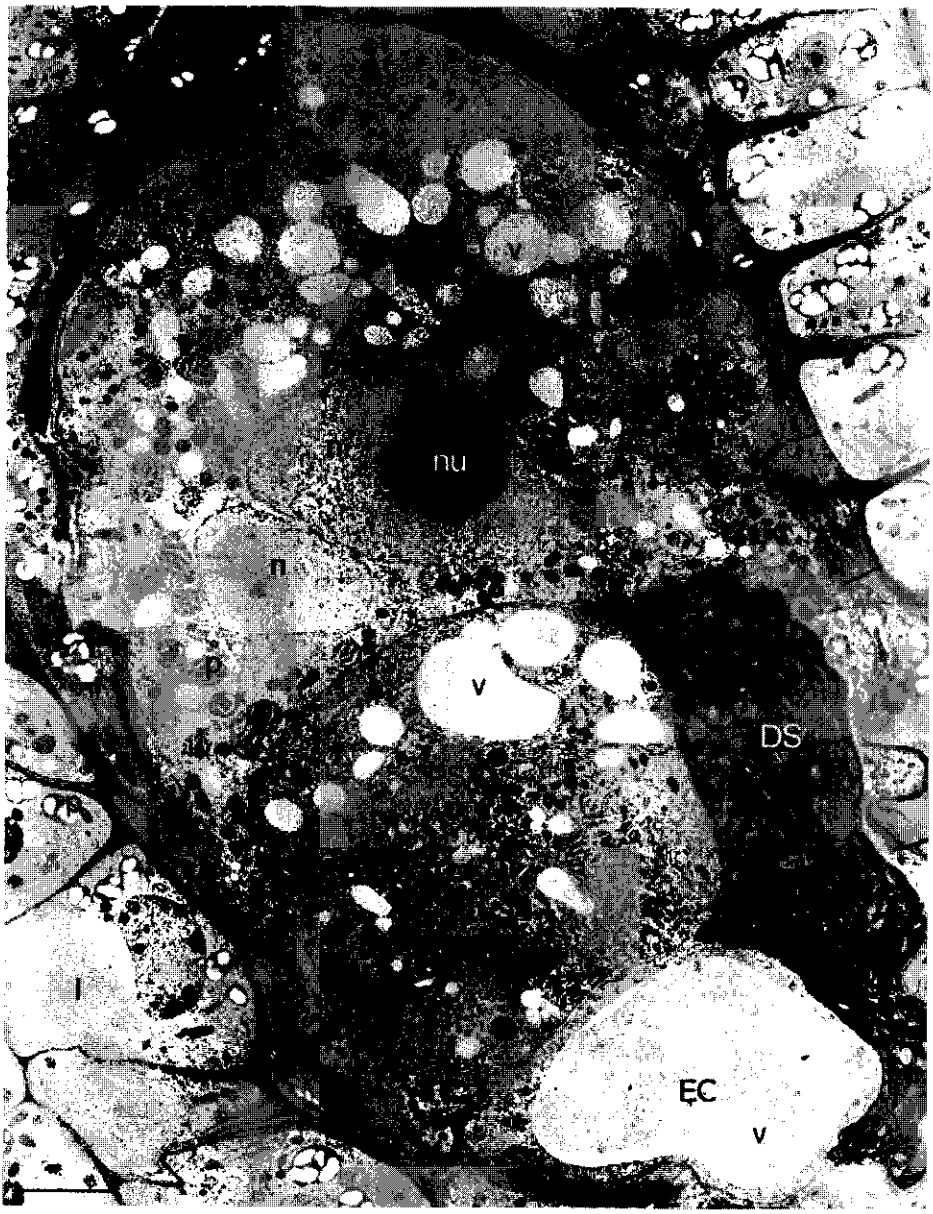
nu
n
v
DS
EC
v

Cryofixation by high pressure freezing

With the high pressure freezing and freeze substitution methods used, visible ice crystal damage could not be detected in 5 to 10% of *P.* x *hybrida* ovules and up to 50% of *B. napus* ovules. In ovules in which distortion of the cytoplasm by ice crystals had occurred, the damage varied between cells and between different cellular components. In general the morphology of the ovular cells was well preserved, showing turgescent integumentary and embryo sac cells. However, breakage of the cell walls and cytoplasmic strands, especially at the chalazal side of the highly vacuolate cells of the egg apparatus, was regularly observed (results not shown). This artifact did not disturb the ultrastructure of the surrounding area. The cell walls, including the thin walls of the synergids and egg cell of the embryo sacs, were regular in appearance with straight plasma membranes tightly appressed against them (Figs. 2a and 4). Also, the abundantly developed system of wall ingrowths in the central cell of *B. napus* was continuously associated with an appressed plasma membrane (Fig. 5a, b). Many cortical microtubules could be detected in the integumentary cells, and in the *P.* x *hybrida* synergids microtubules parallel to the long axis of these cells were visible (Fig. 2a, b). Microfilaments were never observed.

In contrast to the organelles of chemically fixed ovules, nuclei, plastids, and mitochondria of high pressure frozen and freeze substituted ovules had a turgid appearance with smooth surface contours (compare Fig. 3a to b). The two membranes of the nuclear envelope were evenly spaced with ribosomes detectable on the cytoplasmic surface of the outer membrane (Fig. 3b). Mitochondria had an electron dense matrix and even at low magnification the cristae could be discerned (Fig. 3b). In the highly active synergids, numerous dictyosomes associated with vesicles with a content could be distinguished (Figs. 2a and 5a, c). Dictyosomes often showed an evident cis-trans polarity (Fig. 5c). Close to the filiform apparatus of *P.* x *hybrida* many coated vesicles could be discerned (Fig. 2b).

Fig. 4. Overview of a *B. Napus* embryo sac of a high pressure frozen and freeze substituted ovule (2% OsO_4 and 0.1% uranyl acetate), showing the well preserved cell morphology of the egg cell (*EC*), the persistent synergid (*PS*), the degenerating synergid (*DS*), and the central cell (*CC*) with the two polar nuclei (*n*). *I* Integumentary tissues; *m* mitochondrion; *nu* nucleolus; *p* plastid; *v* vacuole. Bar: 5 μm.

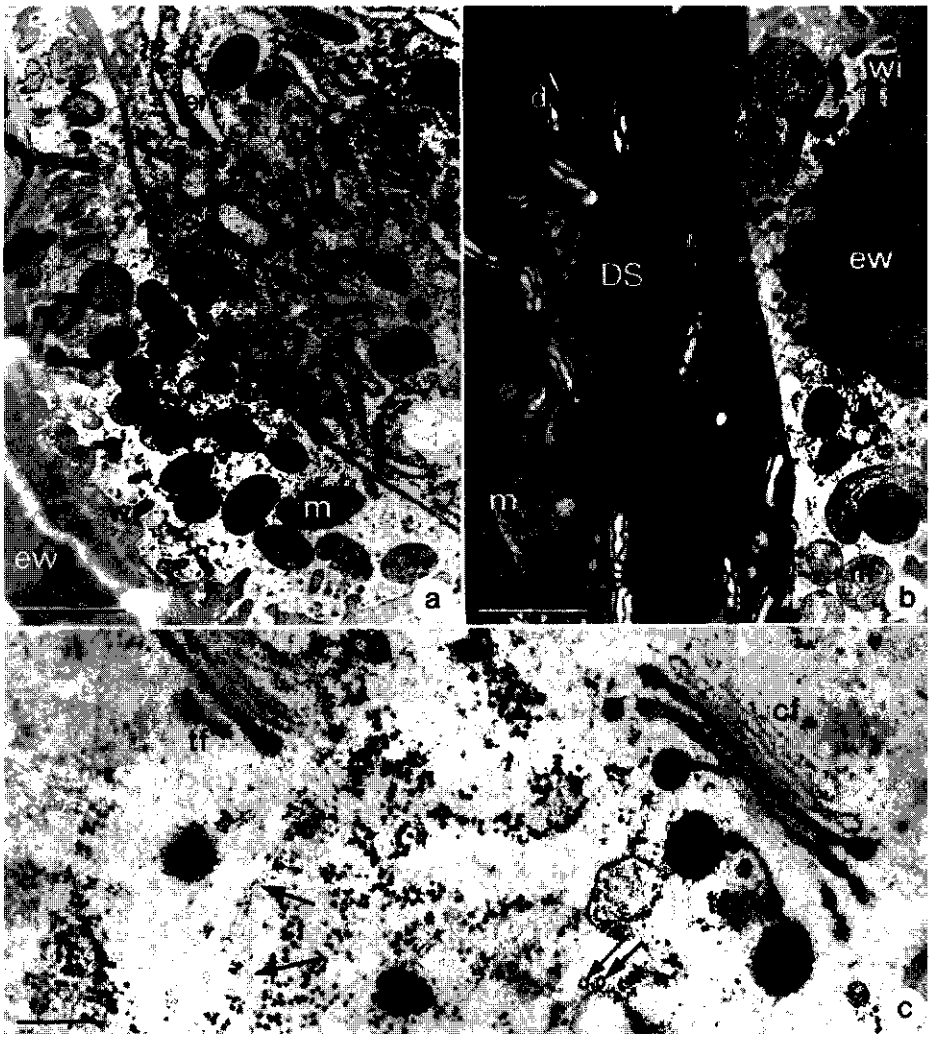

Fig. 5 a-c. Details from embryo sacs of *B. Napus* of high pressure frozen and freeze substituted ovules. **a** Detail from Fig. 4 of the persistent synergid (*PS*) and the adjacent micropylar portion of the central cell, showing typical cell wall ingrowths. Bar: 1 μm. **b** Equivalent part on the other side of the embryo sac of Fig. 4 showing the ultrastructure of the degenerating synergid (*DS*), and the adjacent central cell. Bar: 1 μm. **c** Micrograph from the cytoplasm of a synergid (freeze substituted with 4% OsO_4) showing dictyosomes with an evident cis-trans polarity. Bar: 200 nm. *CC* Central cell; *cf* cis face of dictyosome; *d* dictyosome; *er* endoplasmic reticulum; *ew* embryo sac wall; *m* mitochondrion; *tf* trans face of dictyosome; *wi* cell wall ingrowth; arrow, microtubule; arrowhead, polysome.

Vacuoles were visible throughout the cytoplasm, displaying continuous and regular tonoplasts. The presence of material in the vacuoles was clear, in contrast to the electron translucent appearance of the vacuoles in the chemically fixed ovules (compare Fig. 3a to b). Multivesicular bodies could often be observed (Figs. 2a and 3b). In the integumentary cells of the *B. napus* ovules protein bodies were distinct, displaying a regular inner structure and ribosomes aligned on the outer surface of the surrounding membrane (Fig. 3b).

One of the *B. napus* synergids showed some shrinkage, which reflects its degenerating state (Fig. 4). In the electron dense cytoplasm many ultrastructural details could still be observed (Fig. 5b).

Freeze substitution

The freeze substitution medium consisting of acetone with 2% of osmium tetroxide and 0.1% of uranyl acetate yielded the best results with *B. napus* as well as *P.* x *hybrida* ovules, as seen by high contrast and low extraction (Figs. 2a, b and 3b-5b). Ovules freeze substituted with a medium containing 1% of osmium tetroxide generally had lower contrast, whereas ovules freeze substituted with 4% of osmium tetroxide showed a higher extraction of cytoplasmic components (Fig. 5c).

Discussion

Most previous ultrastructural studies on embryo sac development are based on chemically fixed ovules. These studies have lead to an extensive knowledge on embryo sac development and important insights into the relationship between structure and function of the embryo sac cells (reviewed by Kapil & Bhatnagar, 1981; Willemse & Van Went, 1984; Haig, 1990; Reiser & Fischer, 1993). However, chemical fixation by aldehydes is known to induce a variety of structural artifacts (Mersey & McCully, 1978; Hayat, 1986). In our studies on *P.* x *hybrida* and *B. napus* embryo sac development we found that the highly vacuolate cells of the mature embryo sacs reacted very sensitively to aldehyde fixation, resulting in a severely altered morphology. At the ultrastructural level, organelles often appeared to be deformed and extracted, and membranes were undulating, redistributed, or even absent (Figs. 1a and 3a). The combination of the faster penetrating paraformaldehyde with glutaraldehyde slightly improved the ultrastructural preservation of *B. napus* ovules (results not shown). Compared to post-fixation with osmium tetroxide only, the addition of potassium ferrocyanide to the post-fixative (Janson *et al.*, 1994) greatly enhanced

the contrast of the cellular membranes.

Cryofixation is now generally recognized to result in superior ultrastructural preservation compared to conventional chemical fixation (Severs *et al.*, 1995). Recently, ultrastructural studies based on ultra-rapid freeze-fixation of unicellular or relatively small multicellular specimens revealed previously unreported details of cellular and cytoskeletal organization (Cresti *et al.*, 1987, 1990; Fitzgerald & Knox, 1995; Lancelle *et al.*, 1986, 1987; Lancelle & Hepler, 1992; McCauley & Hepler, 1992; Tiwari & Polito, 1988). The size of the samples which can be ultra-rapidly frozen without the occurrence of ultrastructure-distorting ice crystals is limited. However, Huang and coworkers (1993) reported in an ultrastructural study on fertilization in *Nicotiana tabacum* an acceptable freezing quality in 10% of propane-jet frozen, partly dissected ovules. Due to the considerable size of *P.* x *hybrida* and *B. napus* ovules at anthesis (approximately 200 and 450 μm in diameter, respectively) plunge freezing in liquid propane followed by freeze substitution resulted in the formation of ultrastructure-distorting ice crystals (Fig. 1b). Without the application of cryoprotectants plunge freezing in liquid propane is not a suitable method for ultrastructural studies on *B. napus* and *P.* x *hybrida* embryo sac development. However, this type of cryofixation caused less alterations in cell organization and morphology of the ovules than chemical fixation (compare Fig. 1a to b), and therefore would be very appropriate for structural studies at the light microscopical level. Several authors (Fisher & Jensen, 1969; Cass & Jensen, 1970; Russell, 1982; Russell & Cass, 1988) have earlier reported on the use of cryofixation techniques in their studies on female gametophytes and fertilization in light microscopical studies.

To our knowledge this is the first ultrastructural study on high pressure freezing and freeze substitution of ovules. Generally, high pressure freezing and freeze substitution of ovules of both *P.* x *hybrida* and *B. napus* lead to major improvements in the ultrastructural preservation of the ovular tissues, including the embryo sacs when compared to chemical fixation. Freeze substitution with acetone containing 2% osmium tetroxide and 0.1% uranyl acetate yielded the best preservation in terms of high contrast combined with low extraction of the cytoplasm. By comparing Fig. 3a to b, it is evident that the distribution of organelles is more ordered in the high pressure frozen cells than in the chemically fixed samples allowing easier identification of the different cellular structures. General ultrastructural improvements also reported by other authors (Craig & Staehelin, 1988; Hesse & Hess, 1993; Kiss *et al.*, 1990) include the appearance of straight plasma membranes, which were closely appressed to the

cell walls. The organelles had smooth surface contours and a turgid appearance. Plastids and mitochondria were less extracted and showed clear internal structures. The well preserved dictyosomes had regularly stacked cisternae which clearly differed in content, and secretory vesicles could be observed on the trans face. Close to the plasma membranes, coated vesicles could be identified. Multivesicular bodies, which could not be recognized after a chemical fixation, were easily detectable in the high pressure frozen cells. The microtubular cytoskeleton was also well preserved. In this study microfilaments were never detected, which was also reported by Kiss and coworkers (1990) for high pressure frozen root tips of *Nicotiana* and *Arabidopsis*. However, Ding and coworkers (1992) found good preservation of single microfilaments and microtubule-associated microfilaments in high pressure frozen leaves of *Nicotiana*.

5 to 10% of *P.* x *hybrida* ovules and up to 50% of *B. napus* ovules could be adequately cryo-fixed and freeze substituted without ultrastructure-perturbing ice crystal damage. In those cases where ice crystal damage occurred, a big difference between cells and also between cellular compartments was sometimes visible. Moor (1987) points out that this heterogeneous crystallinity is caused by a difference in the critical cooling rate, which depends on the actual water content of cells and cellular compartments, and a difference in the supercoolability, which depends on the presence and activity of heterogeneous crystallization nuclei.

Even optimally frozen specimens may undergo recrystallization during the freeze substitution step. The desired amorphous or micro-crystalline state can be easily lost by conversion to larger crystals, which are in fact thermodynamically more stable (Steinbrecht, 1985). Hohenberg and coworkers (1994) reported that 1-hexadecene, used to fill the residual space between the ovules in the specimen holders, is not readily soluble in acetone at -80 °C, possibly being a barrier for freeze substitution. After opening of the specimen holders, most of the large *B. napus* ovules (450 μm in diameter) will have a part directly exposed to the freeze substitution medium, whereas most of the small *P.* x *hybrida* ovules (200 μm in diameter) will be completely covered by 1-hexadecene. This could possibly explain the higher percentage of *B. napus* ovules preserved without ice crystal damage. To overcome this problem we are presently testing the usefulness of other substances as embedding media.

An artifact observed in high pressure frozen ovules was the presence of local fractures in cell walls and cytoplasmic strands, in integumentary tissues as well as in

the cells of the embryo sac. Highly vacuolate cells seemed to be more sensitive to this fracturing than cells richer in cytoplasm. Fortunately, this artifact, also observed in other tissues by other authors (Kiss *et al.*, 1990), is easily recognized and is not affecting the preservation of the neighbouring cells and bordering cytoplasm. Craig and coworkers (1987) blame the cracking of frozen specimens on the vibration of the specimen cups, which after a certain number of freezing shots do not fit exactly in the slightly deformed specimen holder. Tears and folds in the plasma membrane could also be due to the collapse of air spaces during the pressurization before freezing (Craig & Staehelin, 1988). Moor (1987) emphasizes that to prevent the distortion of the specimen exposed to a pressure of 2100 bar, freezing has to follow pressurization instantaneously, which means within 0.1 s. An artifact we sometimes observed, like the presence of gaps in the nuclear envelope could be a result of exposure to high pressure (Kiss & Staehelin, 1995).

In conclusion, the present study has demonstrated the usefulness of high pressure freezing and freeze substitution in improving the ultrastructural preservation of *P.* x *hybrida* and *B. napus* ovules. In our future research these techniques are used to study a number of aspects on gametophyte differentiation and fertilization.

Acknowledgements

We thank S. Massalt for photography and Dr. D. Miller for text editing.

References

Berg, R.H. (1994). Symbiotic vesicle ultrastructure in high pressure-frozen, freeze-substituted actinorhizae. Protoplasma 183, 37-48.

Cass, D.D. & Jensen, W.A. (1970). Fertilization in barley. Am. J. Bot. 57, 62-70.

Craig, S., Gilkey, J.C. & Staehelin, L.A. (1987). Improved specimen support cups and auxiliary devices for the Balzer's high pressure freezing apparatus. J. Microsc. 148, 103-106.

Craig, S. & Staehelin, L.A. (1988). High pressure freezing of intact plant tissues. Evaluation and characterization of novel features of the endoplasmic reticulum and associated membrane systems. Eur. J. Cell Biol. 46, 80-93.

Cresti, M., Lancelle, S.A. & Hepler, P.K. (1987). Structure of the generative cell wall complex after freeze substitution in pollen tubes of *Nicotiana* and *Impatiens*. J. Cell Sci. 88, 373-378.

Cresti, M., Milanesi, C., Salvatici, P. & Van Aelst, A.C. (1990). Ultrastructural observations of *Papaver rhoeas* mature pollen grains. Bot. Acta 103, 349-354.

Ding, B., Turgeon, R. & Parthasarathy, M.V. (1992). Effect of high-pressure freezing on plant microfilament bundles. J. Microsc. 165, 367-376.

Fisher, D.B. & Jensen, W.A. (1969). Cotton embryogenesis: The identification, as nuclei, of the X-bodies in the degenerated synergid. Planta 84, 122-133.

Fitzgerald, M.A. & Knox, B. (1995). Initiation of primexine in freeze-substituted microspores of *Brassica campestris*. Sex. Plant Reprod. 8, 99-104.

Haig, D. (1990). New perspectives on the angiosperm female gametophyte. Bot. Rev. 56, 236-274.

Hayat, M.A. (1986). Glutaraldehyde: Role in electron microscopy. Micron Microsc. Acta 17, 115-135.

Hess, M.W. & Hesse, M. (1994). Ultrastructural observations on anther tapetum development of freeze-fixed *Ledebouria socialis* Roth (Hyacinthaceae). Planta 192, 421-430.

Hesse, M. & Hess, M.W. (1993). Recent trends in tapetum research. A cytological and methodological review. Plant Syst. Evol. Suppl. 7, 127-145.

Hohenberg, H., Mannweiler, K. & Müller, M. (1994). High-pressure freezing of cell suspensions in cellulose capillary tubes. J. Microsc. 175, 34-43.

Huang, B.-Q., Strout, G.W. & Russel, S.D. (1993). Fertilization in *Nicotiana tabacum*: Ultrastructural organization of propane-jet-frozen embryo sacs *in vivo*. Planta 191, 256-264.

Janson, J., Reinders, M.C., Valkering, A.G.M., Van Tuyl, G.M. & Keijzer, C.J. (1994). Pistil exudate production and pollen tube growth in *Lilium longiflorum* Thu. Ann. Bot. 73, 437-446.

Kaeser, W., Koyro, H.W. & Moor, H. (1989). Cryofixation of plant tissues without pretreatment. J. Microsc. 154, 279-288.

Kapil, R.N. & Bhatnagar, A.K. (1981). Ultrastructure and biology of female gametophyte in flowering plants. Int. Rev. Cytol. 70, 291-341.

Kiss, J.Z., Giddings, T.H. Jr, Staehelin, L.A. & Sack, F.D. (1990). Comparison of the ultrastructure of conventionally fixed and high pressure frozen/ freeze substituted root tips of *Nicotiana* and *Arabidopsis*. Protoplasma 157, 64-74.

Kiss, J.Z. & Staehelin, L.A. (1995). High pressure freezing. Rapid freezing, freeze fracture and deep etching (ed. by N.J. Severs and D.M. Shotton), pp. 89-104. Wiley-Liss, New York.

Lancelle, S.A., Callaham, D.A. & Hepler, P.K. (1986). A method for rapid freeze fixation of plant cells. Protoplasma 131, 153-165.

Lancelle, S.A., Cresti, M. & Hepler, P.K. (1987). Ultrastructure of the cytoskeleton in freeze-substituted pollen tubes of *Nicotiana alata*. Protoplasma 140, 141-150.

Lancelle, S.A. & Hepler, P.K. (1992). Ultrastructure of freeze-substituted pollen tubes of *Lilium longiflorum*. Protoplasma 167, 215-230.

McCauley, M.M. & Hepler, P.K. (1992). Cortical ultrastructure of freeze-substituted protonemata of the moss *Funaria hygrometrica*. Protoplasma 169, 168-178.

Mersey, B. & McCully, M.E. (1978). Monitoring the course of fixation in plant cells. J. Microsc. 114, 49-76.

Moor, H. (1987). Theory and practice of high pressure freezing. Cryotechniques in biological electron microscopy (ed. by R.A. Steinbrecht and K. Zierold), pp. 175-191. Springer-Verlag, Berlin.

Müller, M. & Moor, H. (1984). Cryofixation of thick specimens by high pressure freezing. Science of biological specimen preparation (ed. by J.P. Revel, T. Barnard and G.H. Haggins), pp. 131-138. SEM, AMF O'Hare, Chicago.

Reiser, L. & Fischer, R.L. (1993). The ovule and the embryo sac. Plant Cell 5, 1291-1301.

Russell, S.D. (1982). Fertilization in *Plumbago zeylanica*: Entry and discharge of the pollen tube in the embryo sac. Can. J. Bot. 60, 2219-2230.

Russell, S.D. & Cass, D.D. (1988). Fertilization in *Plumbagella micrantha*. Am. J. Bot. 75, 778-781.

Severs, N.J., Newman, T.M. & Shotton, D.M. (1995). A practical introduction to rapid freezing techniques. Rapid freezing, freeze fracture and deep etching (ed. by N.J. Severs and D.M. Shotton), pp. 31-49. Wiley-Liss, New York.

Spurr, A.R. (1969). A low-viscosity epoxy resin embedding medium for electron microscopy. J. Ultrastruct. Res. 26, 31-43.

Steinbrecht, R.A. (1985). Recrystallization and ice-crystal growth in a biological specimen, as shown by a simple freeze substitution method. J. Microsc. 140, 41-46.

Studer, D., Hennecke, H. & Müller, M. (1992). High-pressure freezing of soybean nodules leads to an improved preservation of ultrastructure. Planta 188, 155-163.

Tiwari, S.C. & Polito, V.S. (1988). Organization of the cytoskeleton in pollen tubes of *Pyrus communis*: A study employing conventional and freeze-substitution electron microscopy, immunofluorescence, and rhodamine-phalloidin. Protoplasma 147, 100-112.

Willemse, M.T.M. & Van Went, J.L. (1984). The female gametophyte. Embryology of angiosperms (ed. by B.M. Johri), pp. 159-196. Springer-Verlag, Berlin.

Chapter 3

Heptane and isooctane as embedding fluids for high-pressure freezing of *Petunia* ovules followed by freeze-substitution

M.H. THIJSSEN, J.L. VAN WENT & A.C. VAN AELST

(1998) J. Microsc. 192, 228-235

Summary

In comparison with other fixation methods, high-pressure freezing and freeze-substitution of *Petunia* ovules lead to improved ultrastructural preservation of all tissues. Crucial for adequate high-pressure freezing is the absence of air in the specimen sandwich; air has to be replaced by an embedding fluid. Frequently, 1-hexadecene is used for this purpose. Using 1-hexadecene as an embedding fluid resulted in only 5-10% of *Petunia* ovules being preserved without disturbance of the ultrastructure due to ice-crystal damage. Since 1-hexadecene is not soluble in acetone at -90 °C, freeze-substitution is hindered when ovules remained completely surrounded by it; this results in recrystallization when the temperature is raised. We tested and compared the suitability of heptane and isooctane as embedding fluids for high-pressure freezing and freeze-substitution, reasoning that because of their low melting points and low relative densities, phase separation during freeze-substitution would result in complete exposure of the ovules to the substitution medium, leading to adequate freeze-substitution. Using either heptane or isooctane as an embedding fluid yielded up to 90% ice-crystal-free ovules. Both compounds, however, have some damaging effects on the outer one or two cell layers of the ovule, but not on the inner tissues.

Key words: Cryofixation, freeze-substitution, heptane, 1-hexadecene, high-pressure freezing, isooctane, ovule, *Petunia* x *hybrida*.

Introduction

During the past few decades many advances have been made in cryofixation techniques for the preservation of cellular ultrastructure, and the advantages of cryofixation over conventional chemical fixation has become obvious (Menco, 1986; Galway *et al.*, 1995). Although techniques based on ultrarapid freeze-fixation have been employed successfully for ultrastructural studies of a variety of primarily unicellular organisms and relatively small plant tissues, good ultrastructural preservation is generally limited to a shell of 8-20 μm from the specimen surface (Sitte *et al.*, 1987).

With the technique of high-pressure freezing a sample is exposed to a pressure of 2100 bar, which lowers the freezing point and reduces the rate of ice nucleation and ice-crystal growth (Müller & Moor, 1984; Moor, 1987). The resulting reduced critical cooling rate allows adequate freezing of relatively large specimens such as compact tissues without the application of cryoprotectants (Müller & Moor, 1984; Moor, 1987). Satori *et al.* (1993) reported a more than 10-fold increase in vitrification depth by high-pressure freezing compared with rapid freezing at ambient pressure by plunge-freezing in liquid ethane.

The female gametophyte of *Petunia* x *hybrida* (Hook.) Vilm. develops deep inside the sporophytic tissues of the ovule. The mature embryo sac consists of seven cells, of which the three egg apparatus cells and the central cell are large and highly vacuolate. The embryo sac is surrounded by a layer of remnants of squeezed nucellar cells, forming a barrier for chemical fixatives. High-pressure freezing followed by freeze-substitution of *P.* x *hybrida* ovules resulted in an improved ultrastructural preservation compared with chemical fixation and propane plunge-freeze-fixation (Thijssen *et al.*, 1997). However, the percentage of ovules eventually appearing without ice-crystal-induced segregation patterns was low. We presumed that ice-crystal damage was not the result of inadequate cryofixation, but the result of inadequate freeze-substitution, owing to the use of 1-hexadecene as an embedding fluid.

Prior to high-pressure freezing the sample has to be sandwiched between a pair of metal specimen holders. To optimize pressure transfer and heat conductivity, the free space inside the specimen holders has to be filled completely with a liquid. Even intercellular gases have to be replaced by a liquid to prevent distortion of the cell structure by compression of these gases under high pressure (Welter *et al.*, 1988; Studer *et al.*, 1989). Different media have been applied for these purposes.

1-hexadecene is the most commonly used embedding fluid, having the advantages of being chemically inert, hydrophobic, and of low viscosity and surface tension (Studer *et al.*, 1989). 1-hexadecene is successfully used as an embedding fluid for high-pressure freezing of a variety of plant tissues such as root nodules (Studer *et al.*, 1992), root tips (Ding *et al.*, 1991), anthers (Hess, 1993; Hesse & Hess, 1993) and leaves (Studer *et al.*, 1989; Michel *et al.*, 1991; Kaneko & Walther, 1995). 1-hexadecene has the disadvantage that it does not dissolve in acetone, methanol or ethanol at freeze-substitution temperatures. As a consequence, if samples are completely surrounded by this compound, freeze-substitution is severely hindered and inadequate, resulting in the formation of secondary ice crystals during specimen rewarming (Hohenberg *et al.*, 1994).

Other embedding fluids described in the literature for high-pressure freezing of botanical tissues and cells include water (Craig & Staehelin, 1988) and mineral salt solutions (Meindl *et al.*, 1992). When water, buffer solutions or culture media are used as an embedding fluid, they are often supplemented with cryoprotectants such as methanol (Welter *et al.*, 1988; Pain *et al.*, 1994; Rodríguez-Gálvez & Mendgen, 1995), sucrose (Kandasamy *et al.*, 1991; Ding *et al.*, 1992; Zhang & Staehelin, 1992), or dextran (Kiss *et al.*, 1990; Staehelin *et al.*, 1990). Sometimes a small percentage of agarose is added to the medium to protect cells from physical damage during handling and to keep them together during subsequent processing (Lichtscheidl *et al.*, 1990; Galway *et al.*, 1993).

To improve the yield of adequately high-pressure frozen and freeze-substituted *P.* x *hybrida* ovules for our ultrastructural studies on female gametophyte differentiation and fertilization, we tested and compared different embedding fluids. The results of preliminary experiments using buffer solutions and solutions of high-molecular-weight dextran as embedding fluids were unsatisfactory. Using heptane or isooctane as embedding fluids for high-pressure freezing and freeze-substitution increased dramatically the percentage of ice-crystal-free ovules.

Materials and methods

Plant material

Plants of *Petunia* x *hybrida* (Hook.) Vilm. cv. Bluebedder were grown in a growth chamber with a day length of 16 h and a temperature of 20 °C. Using a dissecting microscope the ovules can be removed easily from the placenta using a needle. The

time between dissection of the ovules from the placental tissues of the ovary and cryofixation was approximately 30 s. For cryofixation, ovules at different developmental stages were used; the ovule diameters ranged from 100 to 230 μm.

Cryofixation by high-pressure freezing

P. x *hybrida* ovules were frozen in a sandwich of aluminium specimen holders. Specimen holders of different sizes were used (Heinz Waldner, Ottenhoterstr. 101, 8738 Uetliburg, Switzerland, and Leica, Germany), the cavity diameter was 1 or 2 mm and the cavity depth was between 100 and 300 μm. Just before the ovules were dissected from the placenta, one of the specimen holders was positioned in the sample holder of the high-pressure freezing apparatus and filled with a droplet of embedding fluid. Between 10 and 25 ovules were put in the medium and covered with the flat side of another specimen holder. The sample holder was closed and the sandwich of specimen holders was frozen in a Balzers HPM 010 (Moor, 1987) or Leica EM HPF (Studer *et al.*, 1995) high-pressure freezing device. The two holders of the specimen sandwich have to fit onto each other well to prevent the embedding fluid from being blown out of the sandwich during pressurization. To sandwich the specimen holders as tightly as possible a TEM grid was placed in the high-pressure freezing sample holder if necessary. After freezing the sandwich was split and the specimen holders were stored in liquid nitrogen.

Embedding fluids

The embedding fluids employed to encapsulate the ovules and fill the entire space between the specimen holders were 1-hexadecene (melting point, 4 °C), heptane (m.p. -90.6 °C), or isooctane (2,2,4-trimethylpentane; m.p. -107.4 °C).

Freeze-substitution

For freeze-substitution anhydrous acetone with 2% OsO_4 and 0.1% uranyl acetate was used (Steinbrecht & Müller, 1987). Freeze-substitution was performed in a recently developed device (A. Van Aelst, WAU, Wageningen). Samples were freeze-substituted for 8 h at -90 °C, 8 h at -60 °C and 8 h at -30 °C, and subsequently brought to room temperature. After washing in pure anhydrous acetone the samples were embedded in Spurr's low-viscosity resin (Serva, Germany) (Spurr, 1969).

Transmission electron microscopy

Ultrathin sections were cut on a Reichert Jung Ultracut S microtome equipped with a diamond knife, and collected on formvar-coated 100-mesh copper grids. After counterstaining with uranyl acetate and lead citrate the sections were examined with a JEOL 1200 EXII transmission electron microscope at 80 kV.

Cryo-scanning electron microscopy

Ovaries were dissected from the flowers, mounted on a specimen holder using conductive carbon cement (Leit C, Neubauer, Germany) and immediately frozen in liquid nitrogen. The holder was transferred under vacuum at near liquid nitrogen temperature to the cold stage of a CT 1500-HF cryo-preparation chamber (Cryotrans System, Oxford Instruments, U.K.). The specimens were fractured with a cold scalpel knife, partly freeze-dried at -90 °C at 10^{-6} Torr for 2 min, and sputter-coated with 3 nm platinum. The samples were subsequently transferred to the cryostage of a field emission scanning electron microscope (JEOL 6300F) and observed at 5 kV.

Results

Each *P.* x *hybrida* flower contains an ovary with 300-400 ovules. Figure 1 shows a SEM image of an ovary; the carpels have been partly removed to show the position of the ovules at the placenta. At anthesis a *P.* x *hybrida* ovule measures 150 and 200 μm in diameter and contains a mature embryo sac. The embryo sac is positioned in the centre of the ovule and, at maturity, consists of three small antipodal cells, three large, highly vacuolate cells forming the egg apparatus, and one extensively vacuolate central cell, which occupies the main volume of the embryo sac (Fig. 2).

With the use of 1-hexadecene in the high-pressure freezing/ freeze-substitution procedure, 5-10% of the *P.* x *hybrida* ovules were preserved adequately, without structural disturbance from ice crystals (Thijssen *et al.*, 1997). Cells of adequately cryofixed and freeze-substituted ovules show low extraction of the cytoplasm, organelles with a turgid appearance and smooth surface contours, and plasma membranes which are tightly pressed against the cell walls (Figs. 3 and 4). At higher magnifications the double lipid layer of the plasma membrane is clearly visible and many cortical microtubules can be observed (Fig. 4). Sometimes in cells of adequately preserved ovules an ice-crystal-induced segregation pattern could be observed inside the nuclei (Fig. 4). Using 1-hexadecene as an embedding fluid did not damage the

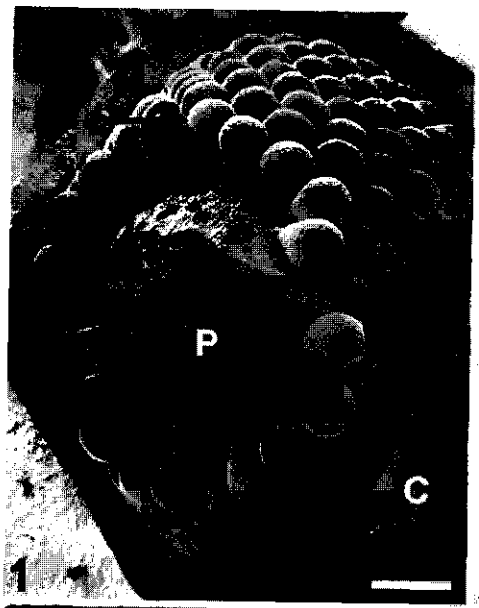
P
C
1

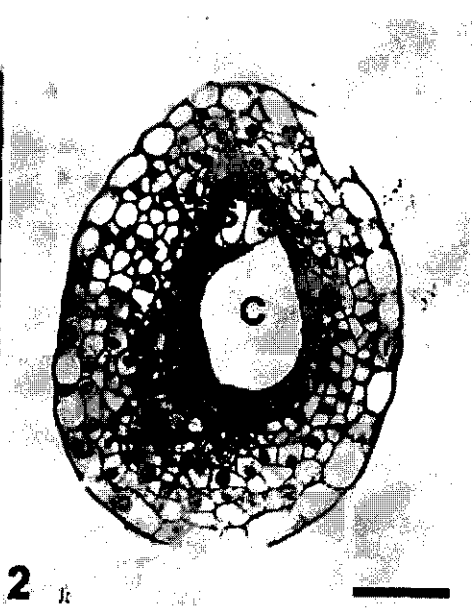
C
2

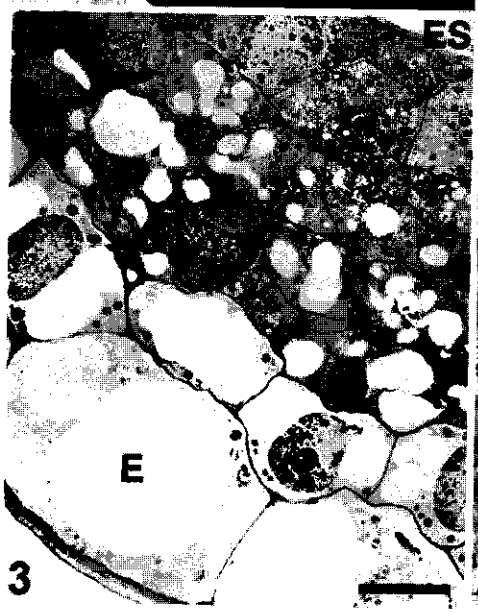
ES
E
3

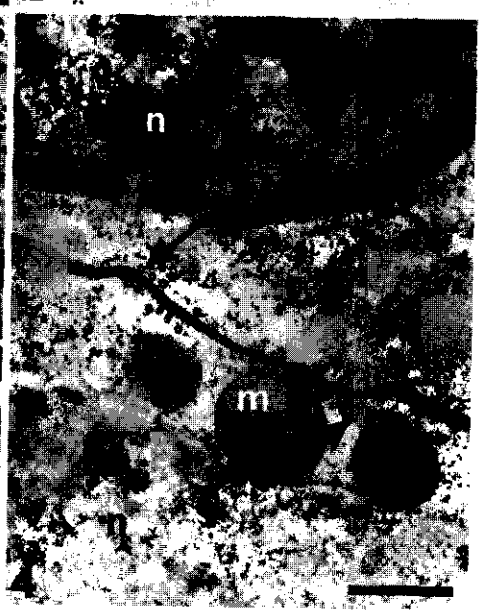
n
m

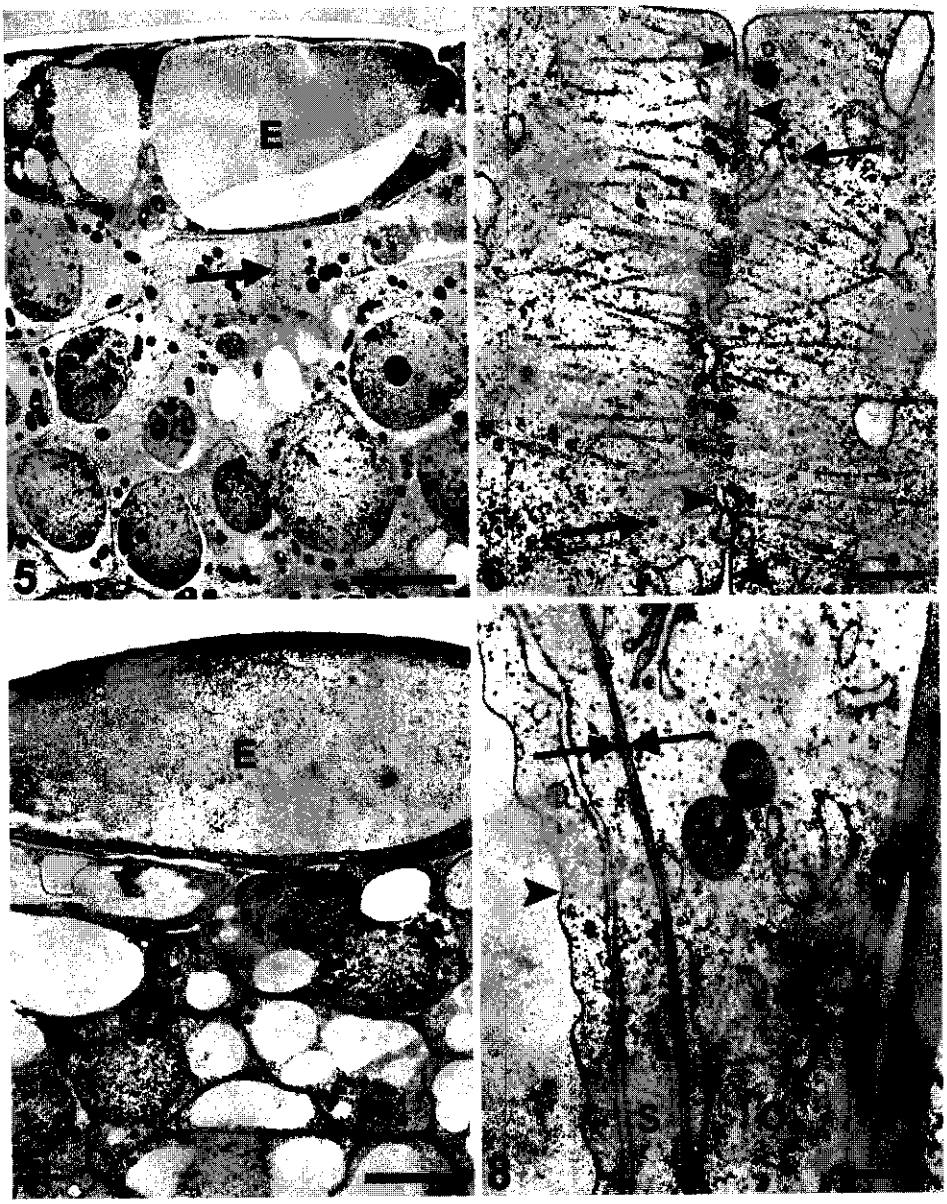
E
5
E
S
6

ovular tissues, including the epidermal cell layer (Fig. 3).

Ovules frozen in heptane show some structural damage in the outer one or two cell layers of the ovule (Fig. 5). Figure 6 shows a nicely preserved phragmoplast; at the site of the cell plate many microtubules and polysaccharide-containing vesicles are visible. The position of this cell, just underneath the epidermal cell layer (see Fig. 5), demonstrates that the damaging effect of the heptane did not extend far into the ovular tissue.

Fig. 1. Cryo-SEM image of a *P.* x *hybrida* ovary; the carpels (C) have been partly removed to show the position of the ovules (arrows) on the placenta (P). Bar: 200 μm.

Fig. 2. Light microscopic image of a transverse section through a high-pressure frozen and freeze-substituted ovule, stained with toluidine blue, showing the cell layers of the integument (I) and the centrally located mature embryo sac with the central cell (C) and the two synergids (S). Bar: 40 μm.

Fig. 3. Transmission electron micrograph of an ovule high-pressure frozen in 1-hexadecene. Different cell layers of the integumentary tissues; the epidermal cell layer (E) is hardly affected by the 1-hexadecene. ES, Embryo sac. Bar: 5 μm.

Fig. 4. Transmission electron micrograph of an ovule high-pressure frozen in 1-hexadecene. Detail of the cytoplasm of an integumentary cell showing the double lipid layer of the cell membranes, cortical microtubules (arrows), and two nuclei (n) one of which shows a crystal-induced segregation pattern. m, Mitochondrion. Bar: 400 nm.

Fig. 5. Transmission electron micrograph of an ovule high-pressure frozen in heptane. The damaging effect of the heptane on the epidermis (E) is visible; the next cell layers are not affected. Bar: 4 μm.

Fig. 6. Transmission electron micrograph of an ovule high-pressure frozen in heptane. Phragmoplast in the integumentary cell located next to an epidermal cell (see Fig. 5, arrow), showing many microtubules along which vesicles (arrows) are transported to the newly synthesized cell wall (arrowheads). Bar: 500 nm.

Fig. 7. Transmission electron micrograph of an ovule high-pressure frozen in isooctane. The damaging effect of the isooctane on the outer layer of the ovule (E) is visible. Bar: 4 μm.

Fig. 8. Transmission electron micrograph of an ovule high-pressure frozen in isooctane. Detail of the cytoplasm of a synergid (S) and the central cell (C) of the embryo sac, showing the excellently preserved plasma membranes (arrows), the tonoplast of the synergid (arrowhead), and plasma membrane aligning ER (er) covered with ribosomes on the cytoplasmic side only. I, Integumentary cell. Bar: 400 nm.

Figure 7 shows the integumentary tissues of an ovule frozen in isooctane. The effect of isooctane on the outer cell layers is comparable with the effect of heptane. At higher magnifications of the embryo sac cells, the excellently preserved cellular membranes are visible (Fig. 8). No differences in ultrastructural preservation were observed between ovules frozen in heptane or isooctane. Between 80 and 90% of the ovules, using either heptane or isooctane as an embedding fluid, appeared without ice-crystal damage after freeze-substitution.

For high-pressure freezing, specimen holders with different cavity depths and diameters were used. We did not observe an effect of the different inner sizes of the specimen holders used on the freezing quality of the ovules.

Discussion

In comparison with other fixation methods, high-pressure freezing and freeze-substitution of *P.* x *hybrida* ovules lead to improved ultrastructural preservation of all tissues, including the embryo sac (Thijssen *et al.*, 1997). However, when ovules were frozen in 1-hexadecene, the percentage of adequately cryofixed and freeze-substituted ovules appeared to be relatively low (5-10%). We assumed that recrystallization resulting from incomplete freeze-substitution was the problem.

Because of its insolubility in acetone at -90 °C, the 1-hexadecene has to be removed from the sample surface before freeze-substitution, in order to have sufficient exchange between ice and the substitution medium (Hohenberg *et al.*, 1994). When 10-25 *P.* x *hybrida* ovules are placed in one specimen holder, most of the ovules will remain completely surrounded by 1-hexadecene after opening the sandwich of holders, and freeze-substitution of these ovules will be severely hindered. Attempts to remove the 1-hexadecene from the ovules by scratching the surface with a needle resulted in a lot of tissue damage and loss of samples.

Using specimen holders with a cavity depth close to the ovule diameter, the ovules are forced into a monolayer. In this situation a lower percentage of the ovules will be completely surrounded by 1-hexadecene after opening the specimen sandwich, and thereby a higher percentage of the ovules will be in part directly exposed to the freeze-substitution medium. However, in practice this method resulted in only a slight increase in the percentage of adequately preserved ovules.

To overcome the problem of inadequate freeze-substitution caused by 1-hexadecene, we examined and compared the suitability of various other substances as embedding fluids for high-pressure freezing and freeze-substitution of *P.* x *hybrida*

ovules, i.e. water-based embedding fluids and organic embedding fluids.

Water-based embedding fluids

Despite the cryoprotective effects of the high pressure during freezing, specimens frozen in water or dilute solutions often show severe ice-crystal damage (Welter *et al.*, 1988; Kiss *et al.*, 1990; Meindl *et al.*, 1992). To suppress the formation of extracellular ice crystals and thereby increase the rate of specimen cooling, cryoprotectants should be added to watery embedding fluids.

The cryoprotectant methanol has been added to water to improve the yield of well-frozen leaf and root tissues (Welter *et al.*, 1988; Xu & Mendgen, 1994; Rodríguez-Gálvez & Mendgen, 1995). Welter *et al.* (1988) reported that the addition of 8% methanol to water increased the yield of well-frozen fungus-infected bean leaves from approximately 10% to 80%. Although methanol can easily enter and thereby harm the cells, these authors observed no structural alterations as compared with preparations frozen in pure water.

Despite the potential osmotic effects, sugar solutions are often used as cryoprotectants (Kandasamy *et al.*, 1991; Ding *et al.*, 1992; Zhang & Staehelin, 1992). Ding *et al.* (1992) reported that incubation and freezing in a 0.2 M sucrose-containing buffer solution increased the depth of good freezing but did not induce plasmolysis or cause other structural artifacts for high-pressure frozen and freeze-substituted tobacco leaves. *P.* x *hybrida* ovules high-pressure frozen in buffer solutions containing different percentages of mannitol suffered either from plasmolysis or showed ice-crystal damage in all ovular tissues.

Several authors have reported good results using aqueous solutions of dextran as embedding fluids for high-pressure freezing (Kiss *et al.*, 1990; Staehelin *et al.*, 1990; Czymmek & Klomparens, 1992), dextran being mentioned as an osmotically inactive and effective cryoprotectant. Kiss *et al.* (1990) reported less high-pressure-induced shearing with freezing in 15% aqueous dextran solutions than with freezing in 1-hexadecene. They assumed that this result was due to the higher viscosity of the dextran solution. In our experiments the use of a 40 000 MW dextran solution as an embedding fluid resulted in very brittle specimens after freeze-substitution.

Organic embedding fluids

An advantage of applying organic fluids as embedding media for high-pressure freezing is that they have a lower heat capacity than water. The two alkanes tested,

heptane and isooctane, are of low relative density, low viscosity, and low surface tension, and therefore, like 1-hexadecene, are easy to work with. Because heptane and isooctane are more volatile than 1-hexadecene, the specimen holder containing the ovules was 'overfilled' with embedding fluid just before the sample sandwich was closed.

The melting points of 1-hexadecene (4 °C) and heptane/ isooctane (-90.6 °C/ -107.4 °C) imply a difference in freezing temperature of the embedding fluids and the tissues. Although a pressure of 2100 bar will lower the freezing point of water to -20 °C, it will raise the freezing points of the organic embedding fluids. This means that when tissues are frozen in 1-hexadecene, the embedding fluid will solidify before the tissues, even above 4 °C under high pressure. The early freezing of 1-hexadecene can have a negative effect on the cooling rate of the embedded tissue because of its crystallization heat, shrinkage during phase change and drop of thermal conductivity in the solid state. The advantage of freezing tissues in heptane and isooctane is that these embedding fluids maintain the liquid state during the most critical period of tissue freezing.

The low melting points of heptane and isooctane, -90.6 °C and -107.4 °C, respectively, provide the advantage that these compounds are liquid at freeze-substitution temperatures. Heptane and isooctane do not dissolve in acetone at -90 °C but become phase separated at the surface of the freeze-substitution medium, leading to complete exposure of the ovules to the substitution medium, and thereby resulting in ideal freeze-substitution conditions. Using heptane or isooctane as an embedding fluid for high-pressure freezing and freeze-substitution yielded 90% well-frozen and well freeze-substituted ovules.

Studer *et al.* (1995) mentioned that the size limit for vitrification by high-pressure freezing of most biological samples will probably not exceed 200 μm. We did not find a relation between the fixation quality of ovules frozen in heptane or isooctane and the dimensions of the inner space of the specimen holders (100-300 μm). Adequate cryofixation for ultrastructural studies does not necessarily mean complete vitrification. In the samples there might be a gradient from water frozen in the amorphous state to microcrystalline ice. Sometimes, in cells which we considered adequately cryofixed, we observed a well-preserved cytoplasm, combined with microcrystal-induced segregation patterns within the nucleus. Such cells could be found in all positions within the ovule, indicating that there is not a clear segregation gradient from the outside to the inside of the ovule.

We did not find qualitative differences in ultrastructural preservation between ovules frozen in heptane or isooctane. After the analysis of many preparations we have the impression that the structural preservation of the inner tissues of ovules frozen in heptane or isooctane was slightly better than the structural preservation of the best preparations frozen in 1-hexadecene. Freezing ovules in heptane and isooctane resulted in somewhat better preservation of the thin cytoplasmic strands traversing the large vacuoles of some cells, as well as the unit membrane structure of the tonoplasts.

Since heptane and isooctane are apolar solvents, they can interact physically with hydrophobic cellular components such as the cuticle covering the epidermal cell layer of the ovules. Even though we observed some damaging effects on the outer layer of the ovules, heptane and isooctane did not affect the ultrastructural preservation of the inner tissues, including the embryo sac. Up to now we have only used heptane and isooctane to high-pressure freeze ovules. We consider these embedding fluids to be suitable for other tissues, although some damage to the outer cells could occur. Therefore, these embedding fluids are not recommended for studying single cells or epidermal cell layers. To minimize the damaging effects of the embedding fluid in general, as well as self-deterioration of the tissues, the time between dissection of the tissues and cryofixation must be kept to a minimum.

Compared with the use of 1-hexadecene as an embedding fluid for the high-pressure freezing/ freeze-substitution procedure, the use of heptane and isooctane increased the percentage of ovules without structure-disturbing ice-crystal formation, from 5 to 90%. This striking increase in yield of well-preserved specimens leads to a tremendous improvement in preparation efficiency in our ultrastructural studies on female gametophyte development.

Acknowledgements

We thank Felix Thiel, Johan Hazekamp, Bruno Humbel, Paul Walther and Eyal Shimoni for assistance with the high-pressure freezing and useful discussion, Martin Müller for the opportunity to work at the Laboratory for Electron Microscopy I, ETH Zürich, Adri Minnaard and Ton Marcelis for valuable advice on the use of organic chemicals, Sijbout Massalt for printing the micrographs, Mark Alberda and Jan van Kreel for the design and manufacture of the freeze-substitution apparatus, and Daphne Foreman for text editing.

References

Craig, S. & Staehelin, L.A. (1988). High pressure freezing of intact plant tissues. Evaluation and characterization of novel features of the endoplasmic reticulum and associated membrane systems. Eur. J. Cell Biol. 46, 80-93.

Czymmek, K.J. & Klomparens, K.L. (1992). The ultrastructure of ascosporogenesis in freeze-substituted *Thelebolus crustaceus*: Enveloping membrane system and ascospore initial development. Can. J. Bot. 70, 1669-1683.

Ding, B., Turgeon, R. & Parthasarathy, M.V. (1991). Microfilaments in the preprophase band of freeze-substituted tobacco root cells. Protoplasma 165, 209-211.

Ding, B., Turgeon, R. & Parthasarathy, M.V. (1992). Substructure of freeze-substituted plasmodesmata. Protoplasma 169, 28-41.

Galway, M.E., Heckman, J.W. Jr, Hyde, G.J & Fowke, L.C. (1995). Advances in high-pressure and plunge-freeze fixation. Methods in cell biology, Vol. 49 (ed. by D.W. Galbraith, H.J. Bohnert and D.P. Bourque), pp. 3-19. Academic Press, Inc., San Diego, CA.

Galway, M.E., Rennie, P.J. & Fowke, L.C. (1993). Ultrastructure of the endocytotic pathway in glutaraldehyde-fixed and high-pressure frozen/ freeze-substituted protoplasts of white spruce (*Picea glauca*). J. Cell Sci. 106, 847-858.

Hess, M.W. (1993). Cell-wall development in freeze-fixed pollen: Intine formation of Ledebouria socialis (*Hyacinthaceae*). Planta 189, 139-149.

Hesse, M. & Hess, M.W. (1993). Recent trends in tapetum research. A cytological and methodological review. Plant Syst. Evol. Suppl. 7, 127-145.

Hohenberg, H., Mannweiler, K. & Müller, M. (1994). High-pressure freezing of cell suspensions in cellulose capillary tubes. J. Microsc. 175, 34-43.

Kandasamy, M.K., Parthasarathy, M.V. & Nasrallah, M.E. (1991). High pressure freezing and freeze-substitution improve immunolabeling of S-locus specific glycoproteins in the stigma papillae of *Brassica*. Protoplasma 162, 187-191.

Kaneko, Y. & Walther, P. (1995). Comparison of ultrastructure of germinating pea leaves prepared by high-pressure freezing - freeze substitution and conventional chemical fixation. J. Electron Microsc. 44, 104-109.

Kiss, J.Z., Giddings, T.H. Jr, Staehelin, L.A. & Sack, F.D. (1990). Comparison of the ultrastructure of conventionally fixed and high pressure frozen/ freeze substituted root tips of *Nicotiana* and *Arabidopsis*. Protoplasma 157, 64-74.

Lichtscheidl, I.K., Lancelle, S.A. & Hepler, P.K. (1990). Actin-endoplasmic reticulum complexes in *Drosera*. Their structural relationship with the plasmalemma, nucleus, and organelles in cells prepared by high pressure freezing. Protoplasma 155, 116-126.

Meindl, U., Lancelle, S. & Hepler, P.K. (1992). Vesicle production and fusion during lobe formation in *Micrasterias* visualized by high-pressure freeze-fixation. Protoplasma 170, 104-114.

Menco, B.P.M. (1986). A survey of ultra-rapid cryofixation methods with particular emphasis on applications to freeze-fracturing, freeze-etching, and freeze-substitution. J. Electron Microsc. Tech. 4, 177-240.

Michel, M., Hillmann, T. & Müller, M. (1991). Cryosectioning of plant material frozen at high pressure. J. Microsc. 163, 3-18.

Moor, H. (1987). Theory and practice of high pressure freezing. Cryotechniques in biological electron microscopy (ed. by R.A. Steinbrecht and K. Zierold), pp. 175-191. Springer-Verlag, Berlin.

Müller, M. & Moor, H. (1984). Cryofixation of thick specimens by high pressure freezing. Science of biological specimen preparation (ed. by J.P. Revel, T. Barnard and G.H. Haggins), pp. 131-138. SEM, AMF O'Hare, Chicago.

Pain, N.A., O'Connell, R.J., Mendgen, K. & Green, J.R. (1994). Identification of glycoproteins specific to biotrophic intracellular hyphae formed in the *Colletotrichum lindemuthianum*-bean interaction. New Phytol. 127, 233-242.

Rodríguez-Gálvez, E. & Mendgen, K. (1995). The infection process of *Fusarium oxysporum* in cotton root tips. Protoplasma 189, 61-72.

Sartori, N., Richter, K. & Dubochet, J. (1993). Vitrification depth can be increased more than 10-fold by high-pressure freezing. J. Microsc. 172, 55-61.

Sitte, H., Edelmann, L. & Neumann, K. (1987). Cryofixation without pretreatment at ambient pressure. Cryotechniques in biological electron microscopy (ed. by R.A. Steinbrecht and K. Zierold), pp. 87-113. Springer-Verlag, Berlin.

Spurr, A.R. (1969). A low-viscosity epoxy resin embedding medium for electron microscopy. J. Ultrastruct. Res. 26, 31-43.

Staehelin, L.A., Giddings, T.H. Jr, Kiss, J.Z. & Sack, F.D. (1990). Macromolecular differentiation of Golgi stacks in root tips of *Arabidopsis* and *Nicotiana* seedlings as visualized in high pressure frozen and freeze-substituted samples. Protoplasma 157, 75-91.

Steinbrecht, R.A. & Müller, M. (1987). Freeze-substitution and freeze-drying. Cryotechniques in biological electron microscopy (ed. by R.A. Steinbrecht and K. Zierold), pp. 149-172. Springer-Verlag, Berlin.

Studer, D., Hennecke, H. & Müller, M. (1992). High-pressure freezing of soybean nodules leads to an improved preservation of ultrastructure. Planta 188, 155-163.

Studer, D., Michel, M. & Müller, M. (1989). High pressure freezing comes of age. Scanning Microsc. Suppl. 3, 253-269.

Studer, D., Michel, M., Wohlwend, M., Hunziker, E.B. & Buschmann, M.D. (1995). Vitrification of articular cartilage by high-pressure freezing. J. Microsc. 179, 321-332.

Thijssen, M.H., Mittempergher, F., Van Aelst, A.C. & Van Went, J.L. (1997). Improved ultrastructural preservation of *Petunia* and *Brassica* ovules and embryo sacs by high pressure freezing and freeze substitution. Protoplasma 197, 199-209.

Welter, K., Müller, M. & Mendgen, K. (1988). The hyphae of *Uromyces appendiculatus* within the leaf tissue after high pressure freezing and freeze-substitution. Protoplasma 147, 91-99.

Xu, H. & Mendgen, K. (1994). Endocytosis of 1,3-ß-glucans by broad bean cells at the penetration site of the cowpea rust fungus (haploid stage). Planta 195, 282-290.

Zhang, G.F. & Staehelin, L.A. (1992). Functional compartmentation of the Golgi apparatus of plant cells. Immunocytochemical analysis of high-pressure frozen- and freeze-substituted sycamore maple suspension culture cells. Plant Physiol. 99, 1070-1083.

Chapter 4

Female gametophyte development in wild type *Petunia* x *hybrida* studied by high pressure freezing and freeze substitution

M.H. THIJSSEN, A.C. VAN AELST, A.M.C. EMONS & J.L. VAN WENT

Submitted for publication

Summary

In this study female gametophyte development in the species *Petunia* x *hybrida* was investigated, with emphasis on the ultrastructural organization from the one-nucleate up to the four-nucleate stage. Simultaneously we monitored the developments in the tissues that surround the female gametophyte. To preserve cytoarchitecture in the best possible way, we cryofixed the ovules by high pressure freezing followed by freeze substitution.

In *P.* x *hybrida* the female gametophyte is monosporic and develops according to the *Polygonum* type. In the functional megaspore a vacuole forms at the micropylar pole. During vacuole formation, the chalazally located nucleus moves to an adaxial position compared to the funiculus, in the middle of the micropylar-chalazal megagametophyte axis. The cytoplasm surrounding the nucleus is packed with rough endoplasmic reticulum, polysomes, mitochondria, Golgi bodies with associated vesicles and starch containing plastids. Nucellus breakdown is already almost completed before the first mitotic division. After the first mitotic division, the two nuclei move to opposite poles of the megagametophyte. After simultaneous nuclear division the four-nucleate megagametophyte is established. Cytoplasmic constitution at the two poles is similar and comparable to the vacuolated one-nucleate megagametophyte. Microtubules can be observed throughout the cytoplasm and at the two- and four-nucleate gametophyte stage in addition in close association with the nuclear envelope. Plasmodesmata are only present in the most chalazal cell wall of the gametophyte and seem to be occluded.

With high pressure freezing and freeze substitution we were able to show details of cellular organization of the female gametophyte and the surrounding tissues that are often destroyed with chemical fixation. These include well preserved plasma membranes and vacuolar membranes; vesicles, including ring-like vesicles, along with and attached to the plasma membranes; the microtubule cytoskeleton; and details of cell degeneration.

Key words: Cryofixation, female gametophyte, freeze substitution, high pressure freezing, ovule, *Petunia* x *hybrida*.

Introduction

The mature female gametophyte (megagametophyte or embryo sac) is an essential group of cells in sexual reproduction of angiosperms. After the double fertilization process, the egg cell gives rise to the embryo and the central cell gives rise to the endosperm, a tissue with a nutritive function for the developing embryo. This paper reports on female gametophyte development in wild type *Petunia* x *hybrida* (Hook.) Vilm., from the one-nucleate stage up to the eight-nucleate stage. Special attention is given to the ultrastructural organization of the one-nucleate, two-nucleate and four-nucleate megagametophyte. Chapter 5 of this thesis deals with the organization of the mature embryo sac.

The type of female gametophyte development varies between species and the organization of the mature embryo sac is the result of the number of nuclear divisions occurring during its development, the nuclear migration pattern, the occurrence of nuclear fusion and nuclear degeneration, the pattern of cell plate formation, and the differentiation of the embryo sac cells after separate cells have been formed (Haig, 1990). In *P.* x *hybrida*, female gametophyte development is according to the *Polygonum* type, which is the most common type in angiosperms (Willemse & Van Went, 1984). In this type of development the one-nucleate megagametophyte undergoes three subsequent mitotic divisions without cytokinesis, resulting in an eight-nucleate coenocyte. Immediately after the third nuclear division cell plate formation results in an embryo sac consisting of one egg cell, two synergid cells, one central cell and three antipodal cells.

Information on female gametophyte differentiation and fertilization has mostly been based on microscopic studies of chemically fixed ovaries and ovules (reviewed by Kapil & Bhatnagar, 1981; Willemse & Van Went, 1984), and the studies are mainly restricted to the mature embryo sac stage. Chemical fixatives are known to induce morphological and ultrastructural artifacts, due to their slow penetration rate, their selectivity for certain cellular components, as well as due to osmolarity differences between different cell types and cellular compartments (reviewed by Mersey & McCully, 1978; Hayat, 1986). With cryofixation techniques, tissues and cells are physically arrested within milliseconds; the application of freeze fixation methods is supposed to lead to a more life-like preservation of cellular ultrastructure (reviewed by Menco, 1986; Severs *et al.*, 1995). With ultra-rapid freeze fixation good ultrastructural preservation is generally limited to the outer 8-20 µm of the specimen (Sitte *et al.*, 1987). With high pressure freezing, i.e. freezing a specimen under a pressure of 2100 bar, in theory, up

to 600 µm thick specimens can be preserved without the formation of detectable ice crystals (Müller & Moor, 1984; Moor, 1987). Compared to plunge freezing in liquid propane and compared to chemical fixation, high pressure freezing of *P.* x *hybrida* ovules resulted in a considerably improved ultrastructural preservation of the integument as well as the female gametophyte cells (Thijssen *et al.*, 1997). To obtain further insight in the process of female gametophyte development in *P. x hybrida* we analyzed the fine structural details of cellular organization at the different gametophyte stages with high pressure freezing followed by freeze substitution.

Materials and methods

Plant material

Plants of *Petunia* x *hybrida* (Hook.) Vilm. cv. Bluebedder were grown in a growth chamber at a temperature of 20 °C, and a relative humidity of 70%. In each photoperiod, plants were given 16 hours of illumination.

Light microscopy

Light microscopy of chemically fixed, resin embedded, and serially sectioned ovaries, allows a rapid screening of many ovules and enhances the possibility of capturing rapidly occurring events like the gametophyte mitotic divisions. Preparation of ovaries for light microscopy was as follows: The carpels of excised ovaries were removed and ovaries were fixed for 3 hours at room temperature with 3% glutaraldehyde in 0.1 M phosphate buffer at pH 7.2, for the first 30 minutes under vacuum. After rinsing in phosphate buffer, the ovaries were dehydrated through a graded ethanol series, and infiltrated with and embedded in the hydroxy-ethyl methacrylate Technovit 7100, according to the manufacturer's specifications (Kulzer Histo-Tec, Germany). 2 µm thick sections were cut with a rotary microtome HM 340 (Microm Laborgeräte GmbH, Heidelberg), and sections were attached serially onto microscope slides. Sections were stained with 0.1% toluidine blue O in water as a general cytological stain, or with periodic acid-Schiff (PAS) for non-water-soluble polysaccharides and 1% amido black 10B in 7% acetic acid for proteins (Fischer, 1968).

High pressure freezing and freeze substitution

High pressure freezing and freeze substitution were performed as previously reported

(Thijssen *et al.*, 1998). Briefly, in one shot 10 to 25 ovules were high pressure frozen in a sandwich of aluminum specimen cups, using heptane, isooctane, or 1-hexadecene as an embedding fluid. For freezing, the Balzers HPM 010 (Moor, 1987) or Leica EM HPF (Studer *et al.*, 1995) high pressure freezing device was used. The substitution procedure was performed with a FreasySub freeze substitution unit (Cryotech Benelux, Schagen-NL). Samples were freeze substituted in acetone with 2% OsO_4 and 0.1% uranylacetate for 8 hours at -90 °C, 8 hours at -60 °C, 8 hours at -30 °C, and warmed up to room temperature. After several rinses in acetone, samples were infiltrated with and embedded in Spurr's low viscosity resin (Spurr, 1969).

Transmission electron microscopy

Ultrathin sections were cut on a Reichert Jung Ultracut S microtome equipped with a diamond knife, and collected on 100 mesh copper grids coated with formvar. Sections were stained with uranyl acetate and lead citrate, and examined with a JEOL 1200 EXII transmission electron microscope at 80 kV.

Results

The description of the ultrastructure of the gametophytes is derived from 17 sectioned megagametophytes. Figures are micrographs of representative sections.

One-nucleate female gametophyte stage

After the megaspore mother cell has undergone meiosis, which results in the formation of four haploid megaspores, the three micropylar megaspores degenerate. The megaspore located at the chalazal side, called the functional megaspore, expands and gives rise to the embryo sac. From the onset of degeneration of the three micropylar megaspores we call the functional megaspore the one-nucleate gametophyte. Figure 1a shows a light microscopic image of a one-nucleate female gametophyte. The breakdown of the nucellus is almost complete, and only some remnants of crushed nucellus cells can be observed surrounding the one-nucleate megagametophyte. Generally, the nucleus is located adaxially, which means at the side of the funiculus, the tissue that connects the chalazal part of the ovule with the placenta. The vacuole of the one-nucleate gametophyte stains PAS-positive. The single integument consists of five to six cell layers, and has already completely enclosed the gametophyte at the one-nucleate stage. The integument consists of various cell types. In the cells of the micropylar region, in the cells of the inner epidermis, called the integument tapetum,

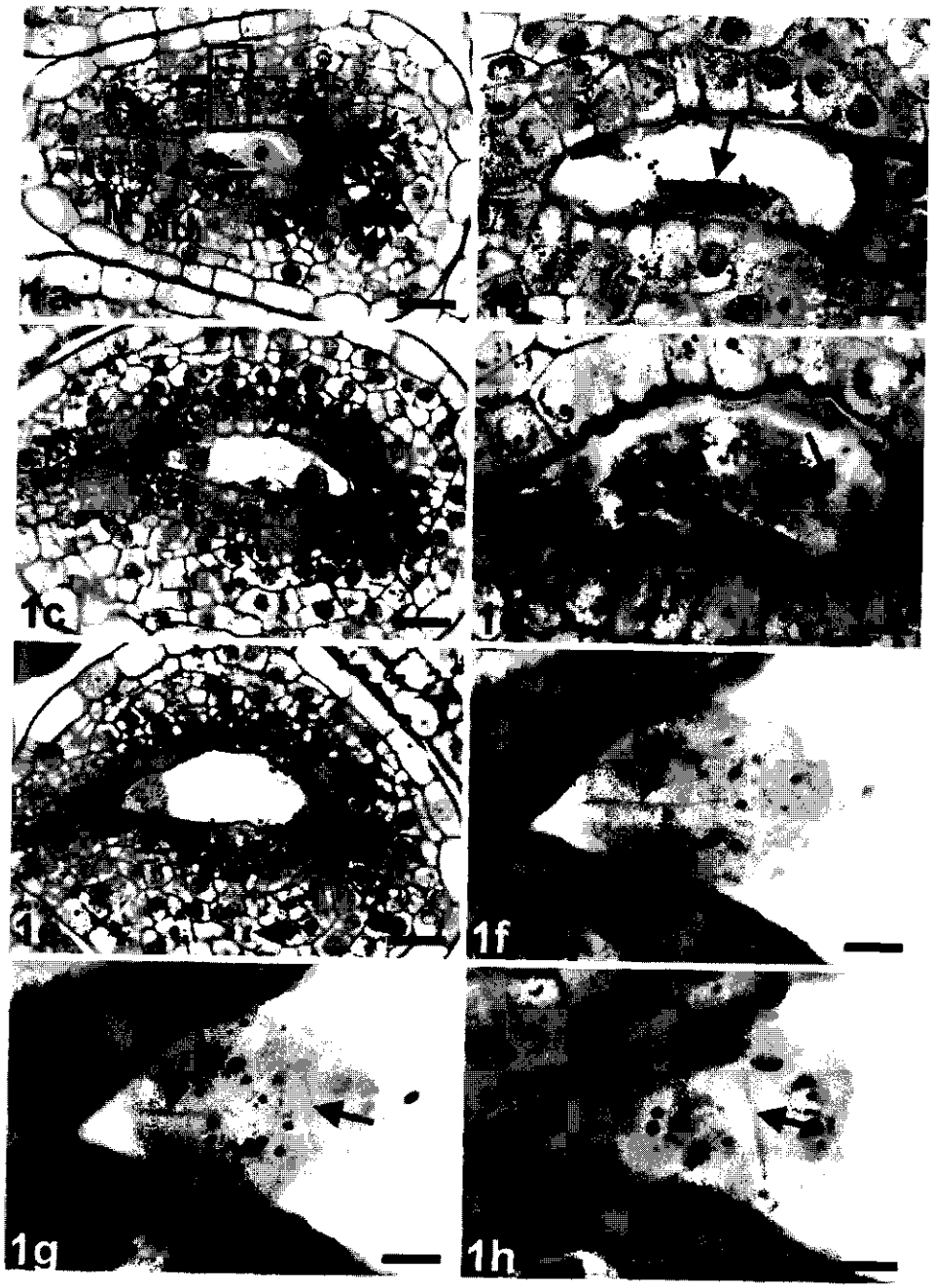
1c
1f
1g
1h

and in the cells of the hypostase, the tissue with cells with thickened cell walls, located at the chalazal side of the ovule, PAS-positive deposits are present. These are visible as darkly staining spherical structures (small arrows in Fig. 1a).

Figure 2a shows an electron micrograph of a one-nucleate megagametophyte. The large nucleus, with little heterochromatin and a large nucleolus, is still situated at the chalazal pole of the cell. The vacuole is located at the micropylar part and during development the vacuole will further expand, finally occupying the largest part of the one-nucleate gametophyte. Figure 2b and 2c show part of the cytoplasm and an adaxially located nucleus. The nuclear envelope is regular in outline and many nuclear pores can be observed (arrowheads in Fig. 2b). The cytoplasm is packed with RER strands, polysomes, mitochondria, Golgi bodies with associated vesicles and starch containing plastids. Cytoskeletal structures can be observed in the cortex, as well as throughout the cytoplasm (arrows in Fig. 2b,c). In the abaxial region and at both poles of the megagametophyte only a very thin layer of cytoplasm is present along the plasma membrane (Fig. 3a). In this layer strands of RER, Golgi bodies with associated vesicles, and mitochondria are present. Whereas mitochondria in the integument cells have a darkly staining matrix, most mitochondria in the one-nucleate gametophyte have a lightly staining matrix, and inter-membrane spaces are visible (compare Figs. 2c and 4b). In the megagametophyte cytoplasm, ring-like, membrane-bound structures, sometimes attached to the plasma membrane are present (arrows in Fig. 3a). Moreover, plasma membrane invaginations are observed (arrows in Fig. 3b). Also in the integument tapetum these type of structures are located (arrowhead in Fig. 4b).

Fig. 1 a-h. Light microscopy images of *P.* x *hybrida* megagametophytes at different developmental stages. Section (d) is stained with toluidine blue; the other sections are stained with PAS and amido black. (a) One-nucleate megagametophyte with almost completely degenerated nucellus. Square indicates area comparable to area of electron micrograph 4a. Small arrows indicate PAS-positive deposits. (b) First mitotic division; metaphase microtubules are visible (*large arrow*). (c) Two-nucleate megagametophyte with one nucleus at the micropylar and one at the chalazal pole, and a large central vacuole. (d) Second mitotic division; two spindles with microtubules in anaphase are visible (*arrows*). (e) Four-nucleate megagametophyte showing the two nuclei at the micropylar pole. (f-h) Serial sections through a gametophyte after the third mitotic division, showing the cell plates between sister nuclei at the micropylar pole (*arrows*). *H*, hypostase cells; *IT*, integument tapetum; *M*, micropyle; *NU*, degenerating nucellus cells; *arrowhead*, dividing cell in integument; *small arrows*, PAS positive deposits. Bars are (a,c,e) 20 μm, (b,d) 10 μm and (f-h) 5 μm.

Degenerating nucellus cells surround the one-nucleate gametophyte (Figs. 2 and 3a-c). In figure 3c a part of a nucellus cell adjacent to the chalazal side of the gametophyte can be seen. Most striking are the darkly staining vacuoles and the high ribosome density. Even in almost completely degenerated cells, the plasma membranes can still be distinguished (white arrowheads in Fig. 3a). The cell wall surrounding the megagametophyte shows a very typical ultrastructure, consisting of a translucent and an electron-dense, fibrous part (Figs. 2b, 3a). The nucellus is separated from the integument tapetum by a cuticle-like structure (black arrowhead in Fig. 3a). Adjacent to the nucellus cells, at the chalazal side of the one-nucleate gametophyte the hypostase is located. Figure 3d shows a hypostase cell with many mitochondria, Golgi bodies and deposit containing vacuoles. Cell walls are thickened and have ingrowths.

Figure 4a shows a section of the different integument cell layers (area indicated in Fig. 1a). The radially stretched cells of the integument tapetum, which surround the one-nucleate megagametophyte from the micropylar part up to the chalazal tissues, possess darkly staining vacuoles, which phenomenon is different from the vacuoles of the other cell types (Fig. 4a,b). Many plasmodesmata transfer the thin radial cell walls in between the integument tapetum cells (arrows in Fig. 4b). Besides the typical vacuoles, these cells possess numerous starch containing plastids, mitochondria, RER strands mainly along the cell walls, and Golgi bodies surrounded by vesicles. Many vesicles, mainly non-coated ones, are present along the cell walls, and are sometimes connected to the plasma membranes (white arrowheads in Fig. 2b,c).

Before undergoing division, the one-nucleate megagametophyte is approximately 54 μm long and 19 μm wide (Five megagametophytes from light microscopy preparations were measured).

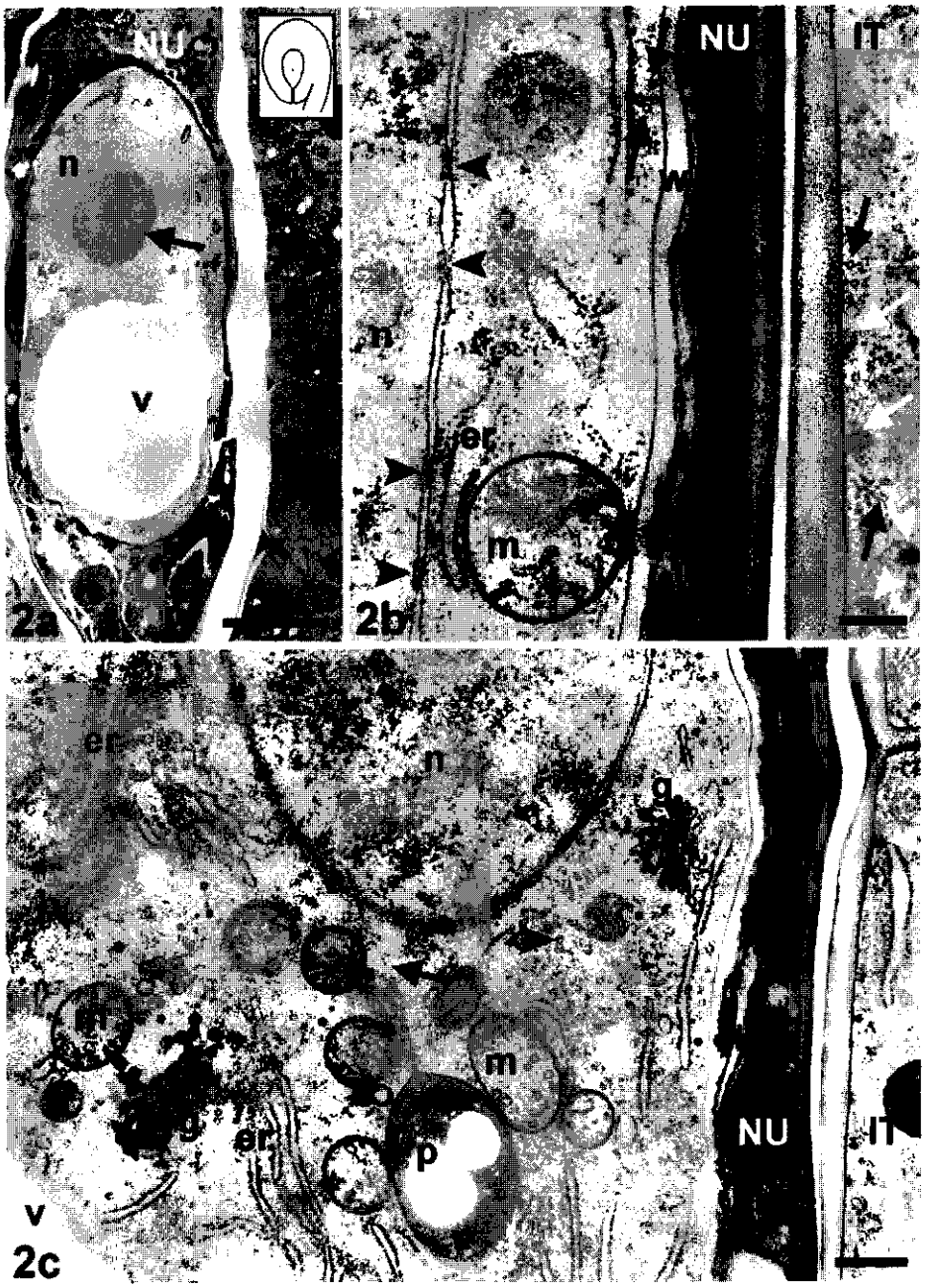
NU
n
v
2a
NU
IT
n
er
m
2b
er
n
g
m
p
er
v
NU
IT
2c

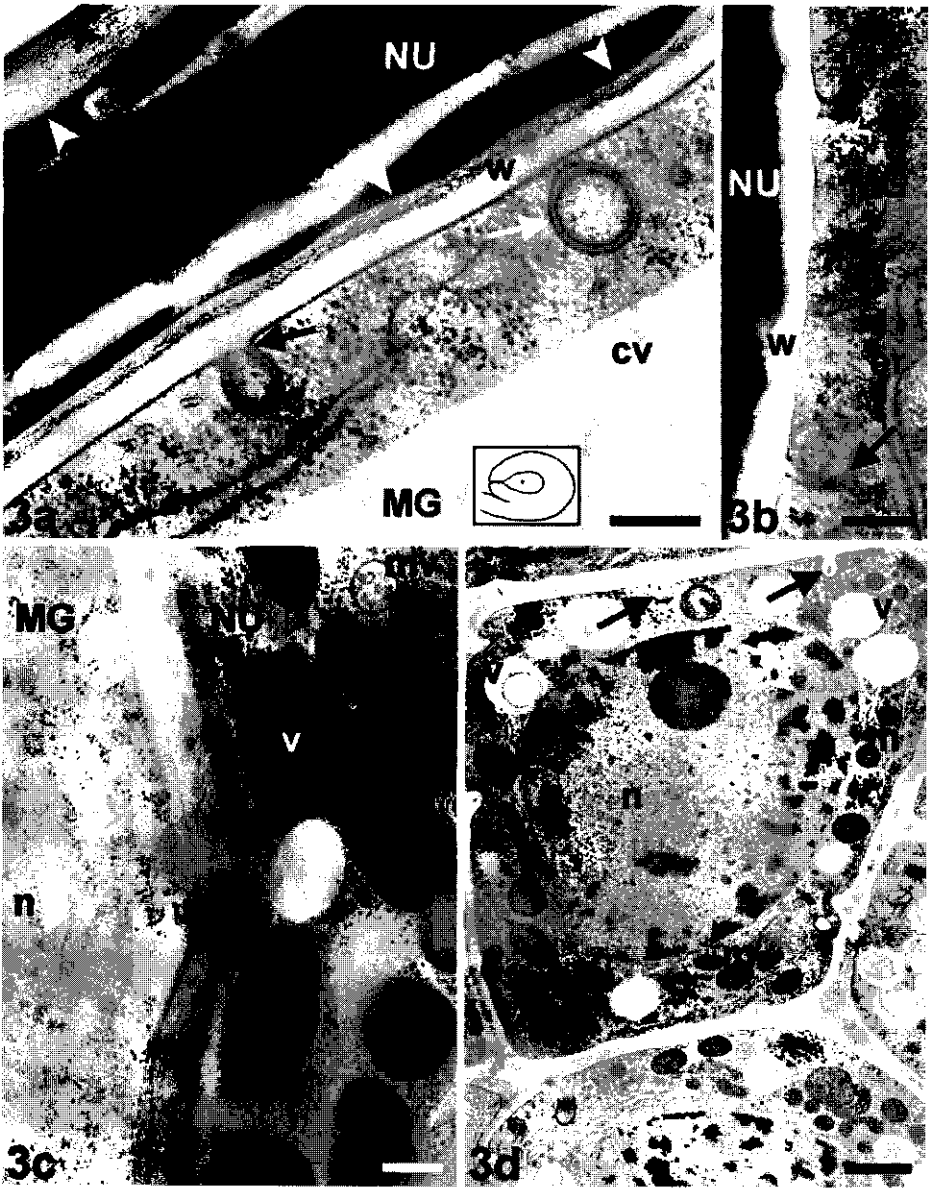
NU
w
cv
MG
3a
NU
w
3b
MG
NU
v
n
3c
v
n
3d

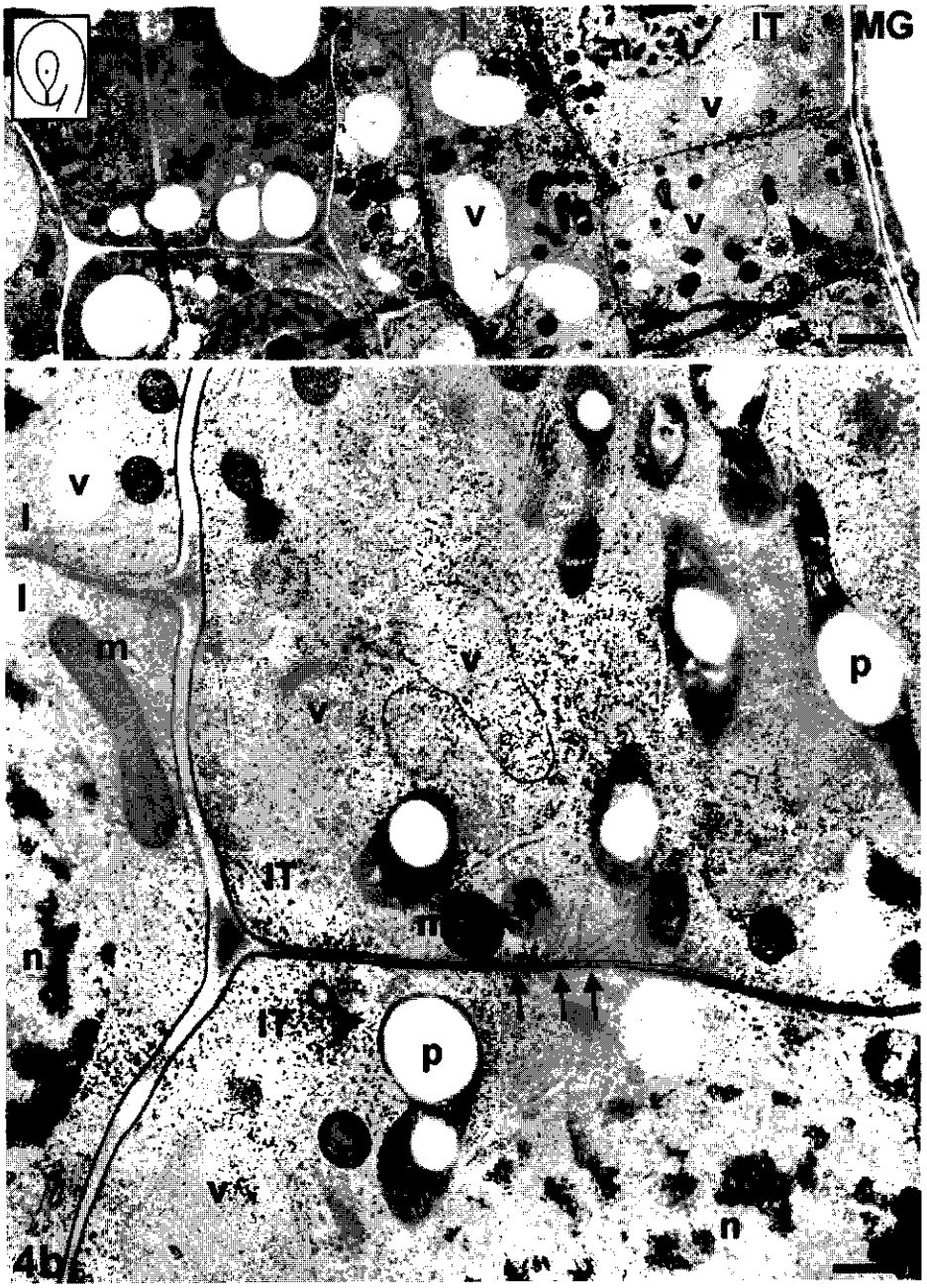
IT
MG
v
v
v
v
l
l
m
v
v
p
IT
n
n
IT
p
v
n
4b

Fig. 2 a-c. Electron micrographs of *P.* x *hybrida* ovules with one-nucleate megagametophytes. See inset for ovule orientation. (a) Longitudinal section through the one-nucleate megagametophyte. Most cytoplasm, including the relatively large nucleus (*n*), with a large nucleolus (*arrow*), is located at its chalazal side. Degenerating nucellus cells (*NU*) are surrounding the megagametophyte. (b) Detail of a longitudinal section through a megagametophyte with a nucleus positioned adaxially, in between the micropylar and chalazal pole. Remnants of degenerating nucellar cells (*NU*) are located in between the gametophyte and the integument tapetum (*IT*). Note the nuclear pores of the gametophyte nucleus (*black arrow heads*), the close relation between an ER strand (*er*) and a mitochondrion (*m*), the typical structure of the megagametophyte cell wall (*w*), cortical microtubules (*black arrows*), the plasma membrane invaginations of a cell of the integument tapetum (*white arrows*), and the vesicles along the integument tapetum cell walls (*white arrowheads*). (c) Cytoplasm of the same megagametophyte as in (b). Note the abundance of RER (*er*), polysomes (*arrowheads*), and mitochondria (*m*), the microtubule in the cytoplasm (*arrow*), and the vesicles along the integument tapetum cell walls (*white arrowheads*). *g*, Golgi bodies; *IT*, integument tapetum; *NU*, degenerating nucellus cells; *n*, nucleus; *p*, plastid; *v*, vacuole. Bars are (a) 5 μm, (b) 200 nm and (c) 500 nm.

Fig. 3 a-d. Electron micrographs of *P.* x *hybrida* ovules with one-nucleate megagametophytes. See inset for ovule orientation. (a) Note a ring-like membrane-bound structure attached to the plasma membrane of the megagametophyte (*black arrow*) and another ring within the cytoplasm (white arrow). Note the typical structure of the cell wall of the megagametophyte (*w*) and the cuticle-like structure (*black arrowhead*) separating the nucellus from the integument tapetum. Plasma membranes of the adjacent degenerating nucellus cell still seem intact (*white arrow heads*). (b) Plasma membrane invaginations at the megagametophyte cell wall (*arrows*). (c) Chalazal side of the megagametophyte and a degenerating nucellus cell. Note the high ribosome density and the darkly staining vacuoles of the nucellus cell (*v*). (d) Chalazal cell with cell wall ingrowths (*arrows*) and cytoplasm with vacuoles containing deposits (*v*), many mitochondria (*m*) and Golgi bodies with associated vesicles (*g*). *cv*, central vacuole; *er*, endoplasmic reticulum; *m*, mitochondrion; *MG*, megagametophyte; *mv*, multivesicular body; *n*, nucleus; *NU*, degenerating nucellar cells; *w*, megagametophyte cell wall. Bars are (a-c) 200 nm and (d) 1 μm.

Fig. 4 a,b. Electron micrographs of *P.* x *hybrida* ovules with one-nucleate megagametophytes. See inset for ovule orientation; integument tissues at the abaxial side of the ovule (megagametophyte at the right). (a) Different cell types of the integument. (b) Detail of two cells of the integument tapetum (*IT*) and bordering integument cells (*I*), showing many darkly stained vacuoles (*v*) and starch containing plastids (*p*) within the integument tapetum. Note the ring-like membrane-bound structure within the cytoplasm (*arrowhead*). *I*, integument cell; *IT*, integument tapetum; *m*, mitochondrion; *MG*, megagametophyte; *n*, nucleus; *v*, vacuoles; *arrows*, plasmodesmata. Bars are (a) 2 μm and (b) 500 nm.

Two-nucleate female gametophyte stage

The one-nucleate megagametophyte undergoes a nuclear division (Fig. 1b), giving rise to the two-nucleate female gametophyte. One of the nuclei migrates towards the micropylar pole, whereas the other nucleus migrates towards the chalazal pole, leaving a prominent central vacuole in between (Fig. 1c). The two nuclei are much smaller than the nucleus of the one-nucleate megagametophyte (Fig. 1a,c). The megagametophyte itself is enlarging. The morphological organization of the integument tissues of the two-nucleate gametophyte is similar to that of the vacuolated one-nucleate megagametophyte (Fig. 1a,c).

Figure 5a shows an electron micrograph overview of a two-nucleate megametophyte in which the micropylar nucleus is visible. Figure 5b shows the chalazal pole cytoplasm of a different gametophyte, with the nucleus, large starch containing plastids, many polysomes, strands of RER, numerous small vacuoles and microtubules throughout the cytoplasm. The microtubule density is especially high around the nucleus (arrows in Fig. 5b), with microtubules that seem to radiate from the nuclear envelope. In the nuclear envelope many pores can be seen (arrowheads in Fig. 5b). No differences in cytoplasmic organization between the micropylar and the chalazal side of the megagametophyte could be observed. At the lateral side of the gametophyte only a very thin cytoplasmic layer is present between the wall and the central vacuole (Fig. 5a). Only little remnants from nucellus cells are visible around the megagametophyte and the gametophyte is now directly bordered by the integument tapetum (Figs. 1c, 5a).

Before undergoing division the two-nucleate megagametophyte is around 68 μm long and 22 μm wide (as measured from five megagametophytes prepared for light microscopy).

Fig. 5 a,b. Electron micrographs of *P.* x *hybrida* ovules with megagametophytes at the two-nucleate stage. See inset for ovule orientation. (a) Longitudinal section through a megagametophyte showing the micropylar nucleus (*n*). (b) Chalazal cytoplasm of a megagametophyte with nucleus. *cv*, central vacuole; *er*, rough endoplasmic reticulum; *g*, Golgi bodies; *MG*, megagametophyte; *m*, mitochondrion; *n*, nucleus; *p*, plastid; *v*, vacuole; *arrow*, microtubule; *arrowhead*, nuclear pore. Bars are (a) 5 μm and (b) 500 nm.

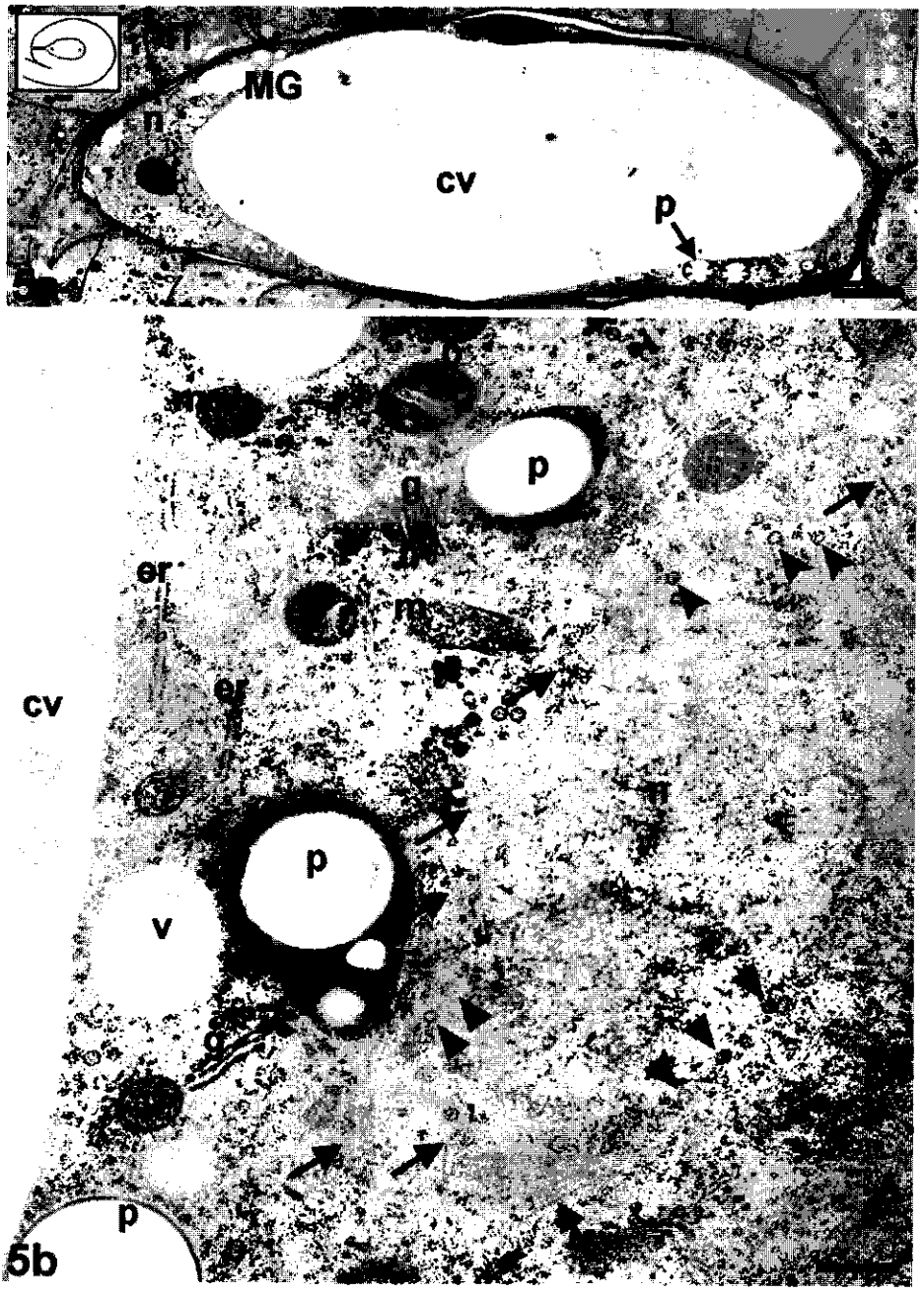
MG
n
cv
p
er
m
v
5b

Four-nucleate female gametophyte stage

The simultaneous division of both nuclei of the two-nucleate gametophyte (Fig. 1d) results in a megagametophyte with two nuclei at the micropylar pole and two nuclei at the chalazal pole. Figure 1e shows the two nuclei at the micropylar pole of a four-nucleate megagametophyte. The micropylar spindle is always found in a transverse orientation in relation to the micropylar-chalazal axis (left arrow in Fig. 1c); during development the axis between the two nuclei changes position from perpendicular to the micropylar-chalazal axis to parallel to the micropylar-chalazal axis. The chalazal spindle was found in various directions, from transverse to oblique to the micropylar-chalazal axis (right arrow in Fig. 1c).

In figure 6a one of the micropylar nuclei of a four-nucleate megagametophyte is visible. The nucleus is regular in outline and shows little evenly dispersed heterochromatin. In the cytoplasm mitochondria, Golgi bodies, starch containing plastids, and a network of RER are visible. At higher magnification many Golgi vesicles and many microtubules (arrows) in longitudinal as well as in cross section can be discerned (Fig. 6b). The organization of the cytoplasm at the chalazal pole of the megagametophyte is shown in figure 7 and is comparable to the cytoplasmic organization at the micropylar pole (compare Figs. 6b and 7c). Figure 7c shows a high magnification of the chalazal cytoplasm; an ER network is visible, as well as many microtubules (arrows). In figure 7a the two chalazal nuclei are visible; in one of them the nucleolus can be seen. In this gametophyte quite a large chalazal vacuole is visible. Around the nuclei a network of ER is present (Fig. 7b). In the nuclear envelope many nuclear pores are visible (arrowheads in Fig. 7b) and microtubules are closely associated with the nuclear envelope (arrows in Fig. 7b).

Plasmodesmata are present in the chalazal cell wall of the megagametophyte (Fig. 8a). They have a special feature on the aperture towards the cytoplasm of the megagametophyte; an electron dense disk suggests occlusion of the plasmodesmata (Fig. 8b). Towards the cytoplasm of the chalazal cells ER is attached to the plasmodesmata (not shown). In the megagametophytes micropylar (Fig. 8c) and lateral cell walls we never observed plasmodesmata.

In the different cell layers of the integument, dividing cells can be seen (Figs. 1e, 8d). Most cells of the integument tapetum are still radially stretched. The dark inclusions in the vacuoles, that are present in the integument tapetum cells of ovules with one-nucleate megagametophytes, have disappeared at this stage (compare Figs. 4a and 8d).

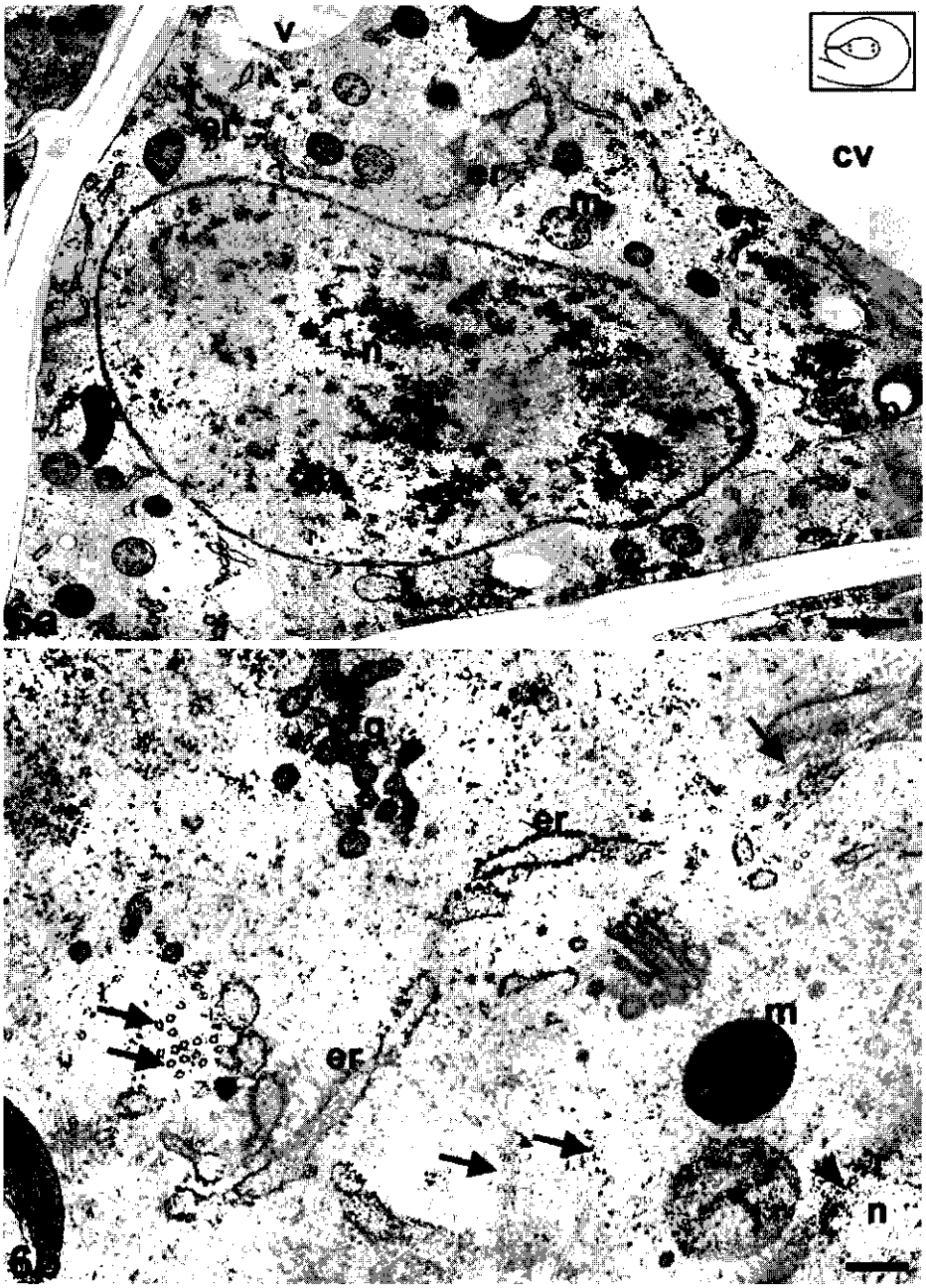
v
cv
er
m
n
ba
g
er
er
m
n

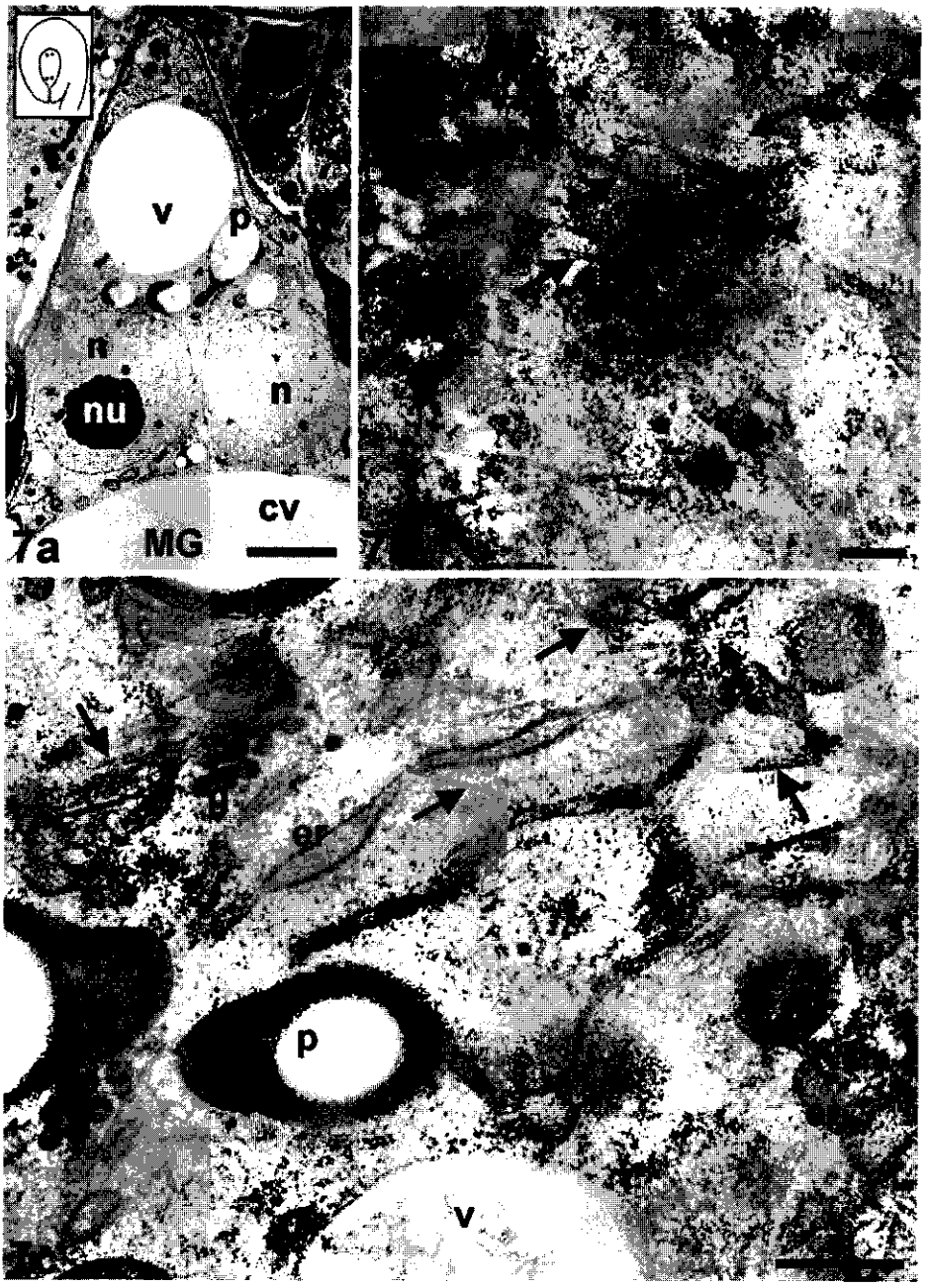
v
p
n
nu
n
cv
7a
MG
op
p
v

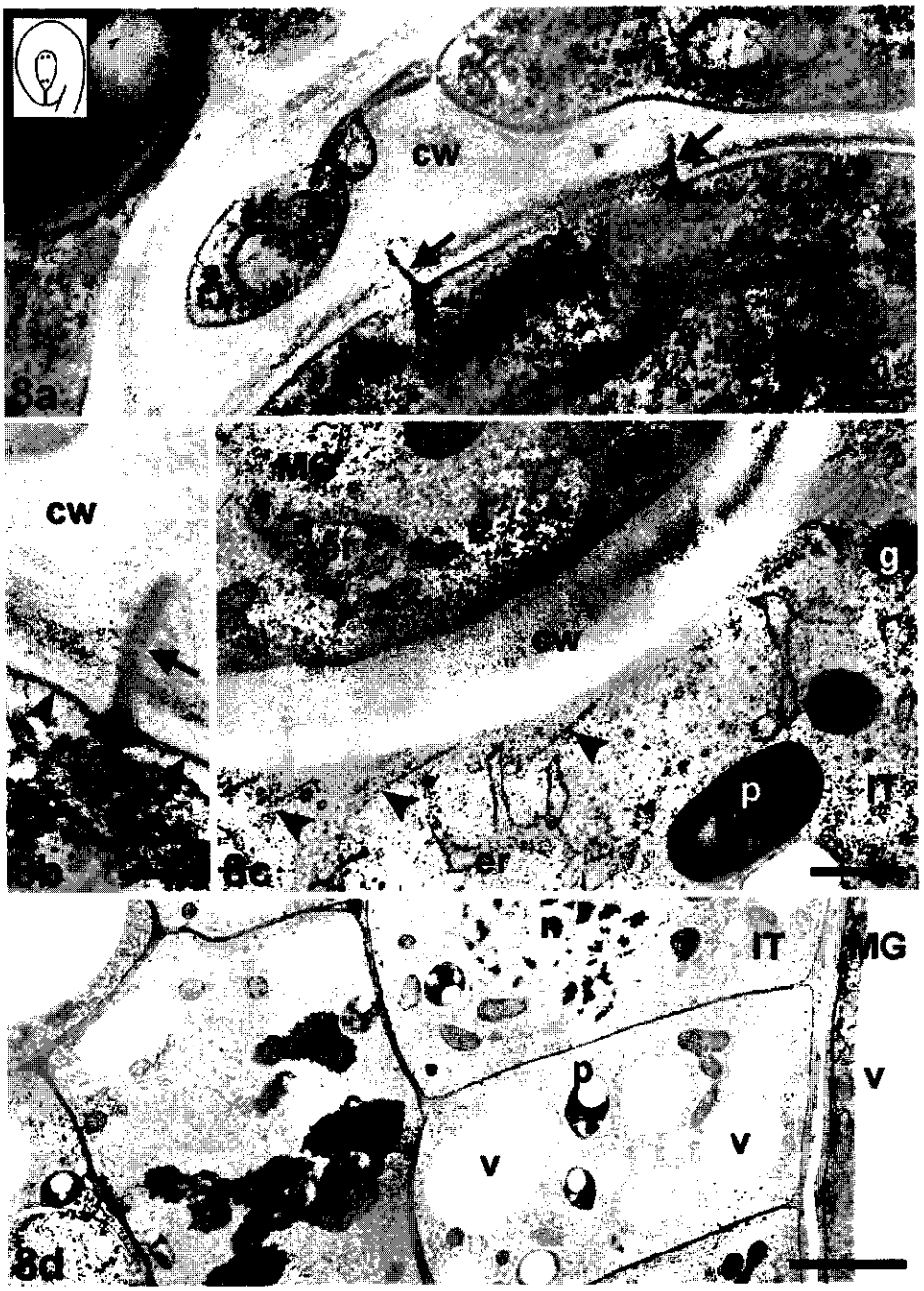
cw
8a
cw
MG
g
cw
p
IT
8b
8c
er
n
IT
MG
p
v
v
v
8d

The four-nucleate megagametophyte measures approximately 80 μm in length and 36 μm in width before the third mitosis (five light microscopy preparations were measured).

Fig. 6 a,b. Electron micrographs of the micropylar side of a *P.* x *hybrida* megagametophyte at the four-nucleate stage. See inset for ovule orientation. (a) Part of the cytoplasm with a cross section through one of the nuclei (*n*). Note the network of endoplasmic reticulum throughout the cytoplasm (*er*). (b) Detail of the cytoplasm showing rough endoplasmic reticulum (*er*), Golgi associated vesicles (g), and many microtubules throughout the cytoplasm (*arrows*). *cv*, central vacuole; *g*, Golgi bodies; *m*, mitochondrion; *n*, nucleus; *v*, vacuole; *arowhead*, nuclear envelope. Bars are (a) 1 μm and (b) 200 nm.

Fig. 7 a-c. Electron micrographs of the chalazal side of *P.* x *hybrida* megagametophytes at the four-nucleate stage. See inset for ovule orientation. (a) Part of the cytoplasm with both nuclei (*n*), one of them with a nucleolus (*nu*). (b) Detail of the cytoplasm showing the surface of one of the nuclei (n), with nuclear pores (*arrowheads*) and microtubules associated with the nuclear surface (*arrows*). (c) ER network within the cytoplasm and microtubules traversing the cytoplasm in all directions. *cv*, central vacuole; *er*, endoplasmic reticulum; *g*, Golgi bodies; *p*, plastid; *v*, vacuole; *arrow*, microtubule. Bars are (a) 2 μm, (b) 200 nm and (c) 500 nm.

Fig. 8 a-d. Electron micrographs of *P.* x *hybrida* ovules with megagametophytes at the four-nucleate stage. See inset for ovule orientation. (a) Chalazal cell wall of a megagametophyte showing plasmodesmata that seem occluded (*arrows*). (b) High magnification of a plasmodesma (*arrow*) with an electron-dense disk on the aperture towards the gametophyte cytoplasm. Arrowheads point to the plasma membrane. (c) Cell wall at the micropylar side of the gametophyte. Note the cortical microtubules (*arrowheads*). Plasmodesmata are absent. (d) Integument tapetum and adjacent dividing integument cell. *c*, chromosome; *cw*, cell wall; *er*, endoplasmic reticulum; *g*, Golgi bodies; *IT*, integument tapetum; *m*, mitochondrion; *MG*, megagametophyte; *n*, nucleus; *p*, plastid; *v*, vacuole. Bars are (a) 200 nm, (b) 100 nm, (c) 500 nm and (d) 2 μm.

Eight-nucleate female gametophyte stage

All four nuclei divide simultaneously (not shown). The spindle closest to the micropyle is oriented transversely to the micropylar-chalazal axis and gives rise to the two synergid nuclei, whereas the second micropylar spindle is oriented longitudinally to obliquely to the micropylar-chalazal axis and gives rise to the egg cell nucleus and the central cell nucleus. At the chalazal side of the embryo sac a transversely oriented and a longitudinally oriented spindle give rise to the three antipodal nuclei and the second polar nucleus of the central cell. The third nuclear division is followed by cell plate formation, resulting in a seven-celled embryo sac when cell walls are complete. Figure 1f-h shows the cell plates that are formed between the sister nuclei at the micropylar side of the megagametophyte. This stage was never detected in ovules prepared for electron microscopy. Chapter 5 of this thesis deals with the ultrastructural organization of mature *P.* x *hybrida* ovules and embryo sacs.

Discussion

There are not many publications available dealing with the ultrastructural analysis of female gametophyte development from the one-nucleate stage up to cell plate formation after the third mitotic division, and in all these studies chemical fixation methods were employed (reviewed by Kapil & Bhatnagar, 1981; Willemse & Van Went, 1984). Because chemical fixation is known to induce a variety of ultrastructural artifacts, we employed cryofixation by high pressure freezing in our studies on *P.* x *hybrida* female gametophyte development (Thijssen *et al.*, 1997). With high pressure freezing (freezing a specimen under a pressure of 2100 bar [Müller & Moor, 1984; Moor, 1987]) multicellular specimens can be fixed without structure disturbing ice crystal formation. At this moment it is considered the best state-of-the-art method for arresting multicellular tissues close to their *in vivo* state.

High pressure freezing and freeze substitution greatly enhanced ultrastructural preservation of *P.* x *hybrida* ovules compared to chemical fixation (Thijssen *et al.*, 1997). Cells appear turgescent, and generally plasma membranes are very well preserved, even those of degenerating cells. Vacuoles are straight in outline, nuclei and organelles are regular in profile, and the microtubular cytoskeleton is visible. However, also in ovules fixed with high pressure freezing and freeze substitution sometimes a number of artifacts could be observed. Disrupted nuclei, wavy cell walls and plasma membranes, and disrupted vacuolar membranes are thought to result from exposure to high pressure (Craig & Staehelin, 1988). Breaks in cell walls and cracks in the

cytoplasm are ascribed to either the vibration of specimen cups during freezing (Craig *et al.*, 1987) or the conversion of high density ice as formed during freezing, to low density ice as formed during re-warming of the specimen to freeze substitution temperatures (Studer *et al.*, 1989). These artifacts were more severe in the relatively large and highly vacuolated female gametophytes compared to the integument tissues.

Degenerating megaspores and nucellus cells surround the *P.* x *hybrida* megagametophyte at the one-nucleate gametophyte stage, but have almost completely disappeared at the two-nucleate stage; it is supposed that their degraded products are reabsorbed by the developing megagametophyte (reviewed by Willemse & Van Went, 1984). Whereas in *Capsella* small projections of the plasma membrane are supposed to facilitate the absorption of material from abortive megaspores (Schulz & Jensen, 1986), in cryofixed *P.* x *hybrida* megagametophytes these structures are not present, and plasma membranes are regular in outline. We did find these structures in chemically fixed *P.* x *hybrida* megagametophytes (not shown); we suppose these are fixation artifacts.

In the nucellus tissues various stages of degradation can be recognized with different organelles and plasma membranes still recognizable at late stages, showing that high pressure freeze fixation/ freeze substitution is a good tool to study the ultrastructural details of cell death. In line with this, Huang *et al.* (1993) concluded from observations of rapidly frozen and freeze substituted embryo sacs of *Nicotiana tabacum* that the breakdown of plasma membrane, organelles and vacuoles of degenerating synergid cells appeared to be later than concluded from chemically fixed ovules.

From the megaspore stage to the stage of the seven-celled embryo sac, the *P.* x *hybrida* megagametophyte is enlarging greatly, which is mainly attributed to the formation of a large central vacuole. In *P.* x *hybrida* formation of the central vacuole starts already in the one-nucleate gametophyte. In most other plants with *Polygonum* type of embryo sacs, including *Arabidopsis* (Christensen *et al.*, 1997), the megagametophyte only starts to vacuolize after the first mitotic nuclear division, when nuclei have been positioned at opposite poles (Maheshwari, 1950).

Plasmodesmata are only present in the chalazal cell wall of the *P.* x *hybrida* megagametophyte, which has been reported before for other species (reviewed by Willemse & Van Went, 1984). The plasmodesmata are covered with a small electron-dense disk in *P.* x *hybrida*, which suggests that the megagametophyte is symplastically isolated from the surrounding integument tissues. Symplastic isolation is believed to be required in specific cells and tissues to perform distinct functions and for morphogenesis (reviewed by Heinlein, 2002). In *Arabidopsis* it has been shown that

commitment to flowering involves a period of plasmodesmata closure and reduced intercellular communication (Gisel *et al.*, 2001).

During megagametophyte cell expansion a solute influx from the apoplast to the symplast is expected. The integument tapetum is proposed to have a role in providing nutrients to the developing megagametophyte (reviewed by Kapil & Tiwari, 1978). In *P.* x *hybrida* the cells of the integument tapetum seem highly metabolically active, but transfer walls as observed in *Vicia* and *Lathyrus* (Johansson & Walles, 1993) are not present and appear to be species related. In the expanding megagametophyte we found ring-like membrane-bound structures, free in the cytoplasm as well as associated with the plasma membrane (Fig. 3a). These structures were also observed in the integument tapetum cells. The function of these structures is not clear. They might be part of the endocytotic pathway; endocytosis is still the least characterized process in plant vesicular transport (reviewed by Ueda & Nakano, 2002).

The separation of cytoplasm and nuclei at the micropylar and chalazal pole by the formation of a central vacuole is thought to have an important role in establishing cell polarity and in subsequent development (Folsom & Cass, 1989; Huang & Sheridan, 1994). But, whereas during the vacuolization process of the two-nucleate megagametophyte in *Zea mays* the cytoplasm is unequally divided (Huang & Sheridan, 1994), in *P.* x *hybrida* the cytoplasm is equally distributed at both poles. The cytoplasm of the vacuolated one-nucleate megagametophyte and the two- and four-nucleate gametophyte appeared quite similar. This has also been reported for the vacuolated two- and four-nucleate megagametophyte stages of *Helianthus annuus* (Newcomb, 1973). In *Zea mays* an increased structural complexity, with well developed organelles, up to the two-nucleate stage, is followed by a simplification in the four-nucleate stage, where organelle degradation related to the expansion of the central vacuole occurs (Russell, 1979). In *P.* x *hybrida* the cytoplasm of the vacuolated one-nucleate gametophyte up to the four-nucleate gametophyte is packed with polysomes, rough endoplasmic reticulum, mitochondria, Golgi bodies with associated vesicles and plastids that contain starch.

Besides the central vacuole, several small vacuoles are present in the cytoplasm; it is not clear if these are connected. Remnants of membranes or other cytoplasmic components within the vacuoles, like described for the lytic complex in *Zea mays* (Russell, 1979), were not observed in high pressure frozen and freeze substituted *P.* x *hybrida* gametophytes. However, in cells of chemically fixed *P.* x *hybrida* megagametophytes these were present (not shown). Chemical fixatives are known to induce break down of complex membrane structures (Mersey & McCully, 1978; Hayat,

1986).

Mitochondria in the *P.* x *hybrida* integument tissues stain very darkly, and show closely associated cristae. Most mitochondria in the megagametophyte show a lightly staining matrix, as well as dilated internal membranes. Inter-membrane spaces in mitochondria of cryofixed tissues are supposed to be related to the physiological state of the organelles (Knoll *et al.*, 1987).

In high pressure frozen and freeze substituted *P.* x h*ybrida* ovules the microtubular cytoskeleton is well preserved; this is generally the case when cryofixation techniques are applied (reviewed by Ketelaar & Emons, 2001). In *P.* x *hybrida* integument cells the microtubules are mainly restricted to the cell cortex. In the megagametophytes, microtubules are internal rather than cortical and they can be found in random orientation throughout the cytoplasm. Especially in the perinuclear region of the two-nucleate and four-nucleate gametophytes a high density of microtubules could be observed, with microtubules that sometimes seemed to radiate from the nuclear envelope into the adjacent cytoplasm. This is normally only the case in the preprophase of plant cells. A similar microtubular organization was found with immunofluorescence studies in megagametophytes of *Arabidopsis* (Webb & Gunning, 1994) and *Zea mays* (Huang & Sheridan, 1994). From these studies it was concluded that the microtubular cytoskeleton has a role in maintaining cytoplasmic integrity and positioning of the nuclei and organelles. Especially in the free-nucleate stages, the microtubular organization could prevent random movement of nuclei within the developing megagametophyte, comparable to their supposed function within the free-nuclear endosperm (Van Lammeren, 1988). In the maize *ig1* gametophyte mutant disturbed in nuclear division and nuclear positioning, also the microtubular organization appeared aberrant (Huang & Sheridan, 1996).

Sections of *P.* x *hybrida* ovaries prepared for light microscopy showed that cell plate formation after the third mitotic division occurred simultaneously at the micropylar and the chalazal megagametophyte poles. Like described for *Zea mays* (Huang & Sheridan, 1994) the orientation of the two mitotic spindles at each pole, perpendicular to each other, with an orientation transverse to the micropylar-chalazal axis closest to the poles and an orientation longitudinal to the micropylar-chalazal axis more to the centre, seems to determine the fate of the eight nuclei that are formed. At the micropylar side, the two most micropylar nuclei become the synergid nuclei, and the most chalazal nucleus will become part of the central cell. At the chalazal side, the three most chalazal nuclei will become the antipodal nuclei and the most micropylar one will become the second polar nucleus of the central cell.

From our light microscopic studies it was not possible to deduce how cell walls between non-sister nuclei, like the egg cell and the synergid cells, are formed. Unfortunately, we were not able to catch this event in *P.* x *hybrida* megagametophytes prepared for electron microscopy. Besides the extreme rapidity of megagametophyte cell plate formation in flowering plants (Russell, 1993), this was further hampered by the fact that a precise developmental staging of ovules appeared to be impossible in *P.* x *hybrida*, due to asynchronous megagametophyte development within ovules (chapter 6 of this thesis). Different models of gametophyte cell plate formation are proposed in literature, involving two phragmoplasts (Cass *et al.*, 1985, 1986), three phragmoplasts (Bhandari & Chitralekha, 1989; Huang & Sheridan, 1994) or four phragmoplasts at one megagametophyte pole (Battaglia, 1991). In megagametophytes preprophase bands are absent (Russell, 1993). Russell (1993) proposed that sites of cell plate formation might be determined by cytoplasmic domains, with the domains established by microtubules radiating from individual nuclei. This has also been described for cell plate formation in syncytial endosperm cells (Van Lammeren, 1988; Otegui & Staehelin, 2000).

Over the past few years many female gametophyte mutants have been identified (reviewed by Drews & Yadegari, 2002). These include mutants that are arrested in the one-nucleate stage, are affected in nuclear number and positions, and are affected in cell plate formation and subsequent differentiation of the individual embryo sac cells. For most mutants the details of gametophyte cellular organization are not known yet, and the affected genes still have to be discovered. Studies addressing wild type gametophyte development have to provide essential reference data to locate and recognize developmental disturbances in these mutants. Ultrastructural studies employing high pressure freezing and freeze substitution that reveal high resolution cellular detail with temporal and spatial integrity may be an important tool to integrate information at the molecular level with the level of cellular organization, and enhance our insight in female gametophyte development.

Acknowledgements

We thank Martin Müller for giving Marja Thijssen the opportunity to visit the Laboratory for Electron Microscopy I, ETH Zurich; Felix Thiel, Johan Hazekamp, Bruno Humbel, Paul Walther and Eyal Shimoni for assistance with the high pressure freezing and useful discussion; and André van Lammeren for critical reading of the manuscript.

References

Battaglia, E. (1991). Embryological questions. 16. Unreduced embryo sac and related problems in angiosperms. Atti Della Societá Toscana di Scienze Naturali Memorie, Ser. B. 98, 1-134.

Bhandari, N.N. & Chitralekha, P. (1989). Cellularization of the female gametophyte in *Ranunculus sceleratus*. Can. J. Bot. 67, 1325-1330.

Cass, D.D., Peteya, D.J. & Robertson, B.L. (1985). Megagametophyte development in *Hordeum vulgare*. 1. Early megagametogenesis and the nature of cell wall formation. Can. J. Bot. 63, 2164-2171.

Cass, D.D., Peteya, D.J. & Robertson, B.L. (1986). Megagametophyte development in *Hordeum vulgare*. 2. Later stages of wall development and morphological aspects of megagametophyte cell differentiation. Can. J. Bot. 64, 2327-2336.

Christensen, C.A., King, E.J., Jordan, J.R. & Drews, G.N. (1997). Megagametogenesis in *Arabidopsis* wild type and the *Gf* mutant. Sex. Plant Reprod. 10, 49-64.

Craig, S., Gilkey, J.C. & Staehelin, L.A. (1987). Improved specimen support cups and auxiliary devices for the Balzer's high pressure freezing apparatus. J. Microsc. 148, 103-106.

Craig, S. & Staehelin, L.A. (1988). High pressure freezing of intact plant tissues. Evaluation and characterization of novel features of the endoplasmic reticulum and associated membrane systems. Eur. J. Cell Biol. 46, 80-93.

Drews, G.N. & Yadegari, R. (2002). Development and function of the angiosperm female gametophyte. Annu. Rev. Genet. 36, 99-124.

Fischer, D.B. (1968). Protein staining of ribboned epon sections for light microscopy. Histochemie 16, 92-96.

Folsom, M.W. & Cass, D.D. (1989). Embryo sac development in soybean: Ultrastructure of megasporogenesis and early megagametogenesis. Can. J. Bot. 67, 2841-2849.

Gisel A., Hempel, F.D., Barella, S., Zambryski, P. (2001). Leaf-to-shoot apex movement of symplastic tracer is restricted coincident with flowering in *Arabidopsis*. Proc. Natl. Acad. Sci. USA 99, 1713-1717.

Haig, D. (1990). New perspectives on the angiosperm female gametophyte. Bot. Rev. 56, 236-274.

Hayat, M.A. (1986). Glutaraldehyde: Role in electron microscopy. Micron Microsc. Acta 17, 115-135.

Heinlein, M. (2002). Plasmodesmata: Dynamic regulation and role in macromolecular cell-to-cell signaling. Curr. Opin. Plant Biol. 5, 543-552.

Huang, B.-Q. & Sheridan, W.F. (1994). Female gametophyte development in maize: Microtubular organization and embryo sac polarity. Plant Cell 6, 845-861.

Huang, B.-Q. & Sheridan, W.F. (1996). Embryo sac development in the maize *indeterminate gametophyte1* mutant: Abnormal nuclear behavior and defective microtubule organization. Plant Cell 8, 1391-1407.

Huang, B.-Q., Strout, G.W. & Russell, S.D. (1993). Fertilization in *Nicotiana tabacum*: Ultrastructural organization of propane jet-frozen embryo sacs *in vivo*. Planta 191, 256-264.

Johansson, M. & Walles, B. (1993). Functional anatomy of the ovule in broad bean (*Vicia faba* L.) I. Histogenesis prior to and after pollination. Int. J. Plant Sci. 154, 80-89.

Kapil, R.N. & Bhatnagar, A.K. (1981). Ultrastructure and biology of female gametophyte in flowering plants. Int. Rev. Cytol. 70, 291-341.

Kapil, R.N. & Tiwari, S.C. (1978). The integument tapetum. Bot. Rev. 44, 457-490.

Ketelaar, T. & Emons, A.M.C. (2001). The cytoskeleton in plant cell growth: Lessons from root hairs. New Phytol. 152, 409-418.

Knoll, G., Verkleij, A.J. & Plattner, H. (1987). Cryofixation of dynamic processes in cells and organelles. Cryotechniques in biological electron microscopy (ed. by R.A. Steinbrecht and K. Zierold), pp. 258-271. Springer-Verlag, Berlin.

Maheshwari, P. (1950). An introduction to the embryology of angiosperms. McGraw-Hill Book Co., New York.

Menco, B.P.M. (1986). A survey of ultra-rapid cryofixation methods with particular emphasis on applications to freeze-fracturing, freeze-etching and freeze-substitution. J. Electron Microsc. Tech. 4, 177-240.

Mersey, B. & McCully, M.E. (1978). Monitoring the course of fixation in plant cells. J. Microsc. 114, 49-76.

Moor, H. (1987). Theory and practice of high pressure freezing. Cryotechniques in biological electron microscopy (ed. by R.A. Steinbrecht and K. Zierold), pp. 175-191. Springer-Verlag, Berlin.

Müller, M. & Moor, H. (1984). Cryofixation of thick specimens by high pressure freezing. Science of biological specimen preparation (ed. by J.P. Revel, T. Barnard and G.H. Haggins), pp. 131-138. SEM, AMF O'Hare, Chicago.

Newcomb, W. (1973). The development of the embryo sac of sunflower *Helianthus annuus* before fertilization. Can. J. Bot. 51, 863-878.

Otegui, M. & Staehelin, L.A. (2000). Syncytial-type cell plates: A novel kind of cell plate involved in endosperm cellularization of *Arabidopsis*. Plant Cell 12, 933-947.

Russell, S.D. (1979). Fine structure of megagametophyte development in *Zea mays*. Can. J. Bot. 57, 1093-1110.

Russell, S.D. (1993). The egg cell: Development and role in fertilization and early embryogenesis. Plant Cell 5, 1349-1359.

Schulz, R. & Jensen, W.A. (1986). Prefertilization ovule development in *Capsella*: the dyad, tetrad, developing megaspore, and two-nucleate gametophyte. Can. J. Bot. 64, 875-884.

Severs, N.J., Newman, T.M. & Shotton, D.M. (1995). A practical introduction to rapid freezing techniques. Rapid freezing, freeze fracture and deep etching (ed. by N.J. Severs and D.M. Shotton), pp. 31-49. Wiley-Liss, New York.

Sitte, H., Edelmann, L. & Neumann, K. (1987). Cryofixation without pretreatment at ambient pressure. Cryotechniques in biological electron microscopy (ed. by R.A. Steinbrecht and K. Zierold), pp. 87-113. Springer-Verlag, Berlin.

Spurr, A.R. (1969). A low-viscosity epoxy resin embedding medium for electron microscopy. J. Ultrastruct. Res. 26, 31-43.

Studer, D., Michel, M. & Müller, M. (1989). High pressure freezing comes of age. Scanning Microsc. Suppl. 3, 253-269.

Studer, D., Michel, M., Wohlwend, M., Hunziker, E.B. & Buschmann, M.D. (1995). Vitrification of articular cartilage by high-pressure freezing. J. Microsc. 179, 321-332.

Thijssen, M.H., Mittempergher, F., Van Aelst, A.C. & Van Went, J.L. (1997). Improved ultrastructural preservation of *Petunia* and *Brassica* ovules and embryo sacs by high pressure freezing and freeze substitution. Protoplasma 197, 199-209.

Thijssen, M.H., Van Went, J.L. & Van Aelst, A.C. (1998). Heptane and isooctane as embedding fluids for high-pressure freezing of *Petunia* ovules followed by freeze-substitution. J. Microsc. 192, 228-235.

Ueda, T. & Nakano, A. (2002). Vesicular traffic: An integral part of plant life. Curr. Opin. Plant Biol. 5, 513-517.

Van Lammeren, A.M.M. (1988). Structure and function of the microtubular cytoskeleton during endosperm development in wheat: An immunofluorescence study. Protoplasma 146, 18-27.

Webb, M.C. & Gunning, B.E.S. (1994). Embryo sac development in *Arabidopsis thaliana*. II. The cytoskeleton during megagametogenesis. Sex. Plant Reprod. 7, 153-163.

Willemse, M.T.M. & Van Went, J.L. (1984). The female gametophyte. Embryology of angiosperms (ed. by B.M. Johri), pp. 159-196. Springer-Verlag, Berlin.

Chapter 5

The mature embryo sac of wild type *Petunia* x *hybrida* studied by high pressure freezing and freeze substitution

M.H. THIJSSEN, A.C. VAN AELST, A.M.C. EMONS & J.L. VAN WENT

Submitted for publication

Summary

In this study we analyzed the ultrastructural organization of the mature embryo sac of *Petunia* x *hybrida* and the tissues surrounding it. To preserve cytoarchitecture in the best possible way, we cryofixed ovules with high pressure freezing followed by freeze substitution. The *P.* x *hybrida* embryo sac develops according to the *Polygonum* type and the mature embryo sac consists of an egg cell, two synergid cells, a central cell and three antipodal cells. The synergid cells are highly polarized with in the micropylar cytoplasm high numbers of mitochondria, Golgi bodies with associated vesicles, and extensive rough endoplasmic reticulum. The filiform apparatus is regular in appearance. Microtubules protrude from the filiform apparatus into the synergid cell cytoplasm, and along the plasma membrane that aligns the filiform apparatus, many vesicles are located. Cellular organization of both synergid cells is similar and degeneration before pollen tube penetration does not occur. The *P.* x *hybrida* egg cell is extremely vacuolated with only a thin layer of cytoplasm, containing few organelles along the plasma membrane and around the chalazally located nucleus. The central cell is characterized by the accumulation of high amounts of starch at maturity. At the most chalazal side of the synergid cells and the egg cell, and the most micropylar side of the central cell, plasma membranes lay very closely together and cell walls in this area seem absent. The antipodal cells initially have the appearance of highly metabolically active cells, with Golgi bodies with associated vesicles, rough endoplasmic reticulum, polysomes, and starch containing plastids, but degeneration starts upon embryo sac maturity. Cell wall ingrowths are not present in the embryo sac cells. Plasmodesmata are present between all embryo sac cells, but in the embryo sac surrounding cell wall, only at the most chalazal side. Differences in cytoarchitecture obtained after chemical fixation and after high pressure freezing are discussed.

Key words: Cryofixation, embryo sac, female gametophyte, freeze substitution, high pressure freezing, ovule, *Petunia* x *hybrida*.

Introduction

The aim of ultrastructural studies is to correlate information on cell structure and organization with functioning of cells and cellular components. This is only possible if biological specimens are preserved in a way resembling the living state, with temporal and spatial integrity. Dynamic organelles like the endoplasmic reticulum (reviewed by Staehelin, 1997), the Golgi apparatus (reviewed by Nebenführ & Staehelin, 2001), plant cell vacuoles (reviewed by Bethke & Jones, 2000) and the cytoskeleton (reviewed by Ketelaar & Emons, 2001) are difficult to preserve with relatively slow chemical fixation methods, and changes in cytoarchitecture will occur.

With cryofixation methods all cell components are simultaneously stabilized, at a much faster rate than with chemical fixation, resulting in a preserved ultrastructure more closely reflecting the living state. Ultra-rapid freezing techniques can only adequately preserve the ultrastructure of the outer 10-20 µm of a specimen (Severs *et al.*, 1995). With the technique of high pressure freezing (freezing a specimen under a pressure of 2100 bar (Müller & Moor, 1984; Moor, 1987)) multicellular specimens of up to 600 µm can be fixed without structure disturbing ice crystal formation. Fixation by high pressure freezing and freeze substitution considerably improved the ultrastructural preservation of *P.* x *hybrida* ovules and female gametophytes as compared to chemical fixation techniques (Thijssen *et al.*, 1997).

The *P.* x *hybrida* embryo sac is monosporic and develops according to the *Polygonum* type (Willemse & Van Went, 1984). The nucleus of the functional megaspore divides three times and only after the third mitotic division cell plates are formed. The resulting embryo sac consists of an egg cell, a central cell with two polar nuclei, two synergid cells and three antipodal cells. These four cell types each have their own identity, displayed by their location in the embryo sac, a specific function in the reproductive processes and their own morphology, cytoarchitecture and ultrastructure.

This paper reports on the ultrastructural organization of the mature embryo sac of *P.* x *hybrida*. Another manuscript in this thesis deals with the organization of the megagametophyte from the one-nucleate up to the eight-nucleate stage. Most structural studies on the organization of the mature embryo sac used chemical fixation techniques (reviewed by Kapil & Bhatnagar, 1981; Willemse & Van Went, 1984), including studies on the ultrastructure of the synergid cells, egg cell and central cell of *P.* x *hybrida* (Van Went, 1970a, 1970b). To obtain further insight in the organization of the *P.* x *hybrida* female gametophyte we analyzed the fine structural details of cellular organization with high pressure freezing and freeze substitution, the most appropriate state-of-the-art

cryofixation method for this purpose.

Materials and methods

Plant material

Petunia x *hybrida* (Hook.) Vilm. cv. Bluebedder plants were grown in a growth chamber at 20 °C, 70% relative humidity, and 16 hours light per day.

High pressure freezing and freeze substitution

High pressure freezing and freeze substitution were as described by Thijssen *et al.* (1998). Ovules were cryofixed with the high pressure freezing device of Balzers HPM 010 (Moor, 1987) or Leica EM HPF (Studer *et al.*, 1995). Heptane, isooctane, or 1-hexadecene was used to replace the air in the specimen sandwich. Freeze substitution was performed with a FreasySub freeze substitution unit (Cryotech Benelux, Schagen-NL), for 8 hours at -90 °C, 8 hours at -60 °C and 8 hours at -30 °C. The substitution medium consisted of 2% OsO_4 and 0.1% uranylacetate in acetone. Samples were embedded in Spurr's low viscosity resin (Spurr, 1969).

Microscopy

Sections were cut on a Reichert Jung Ultracut S microtome. 1 μm sections were adhered to glass slides and stained with toluidine blue. Ultrathin sections were collected on 100 mesh copper grids coated with formvar and stained with uranyl acetate and lead citrate. Ultrathin sections were examined with a JEOL 1200 EXII transmission electron microscope at 80 kV.

Results

The description of the ultrastructure of the embryo sac cells is derived from ten sectioned embryo sacs. Figures are micrographs of representative sections.

Synergid cells

At anthesis the *P.* x *hybrida* synergid cells are pear-shaped, polarized cells, with their cytoplasm located at the micropylar side of the embryo sac, and a large vacuole, surrounded by a thin layer of cytoplasm at the chalazal side of the embryo sac. Figure 1 shows light microscopy overviews of longitudinal sections through synergid cells, an

egg cell and a central cell; figure 2a shows an electron micrograph of a synergid cell, the adjacent egg cell and part of a central cell of a mature gametophyte.

At the micropylar side a thick cell wall, called the filiform apparatus, is situated between the two synergid cells (Figs. 2a, 3c-f). The filiform apparatus is quite regular in outline (Fig. 3c-e). Some parts of the filiform apparatus are very granular in appearance (Fig. 3c,f). The presence of exudates is visible within the micropyle (arrow in Fig. 3f). In the vicinity of the synergid plasma membranes that border the filiform apparatus, many coated as well as non-coated vesicles are present (arrowheads in Figs. 3c,d). Many microtubules, oriented longitudinally compared to the micropylar-chalazal embryo sac axis, are closely associated with the filiform apparatus (arrows in Fig. 3d).

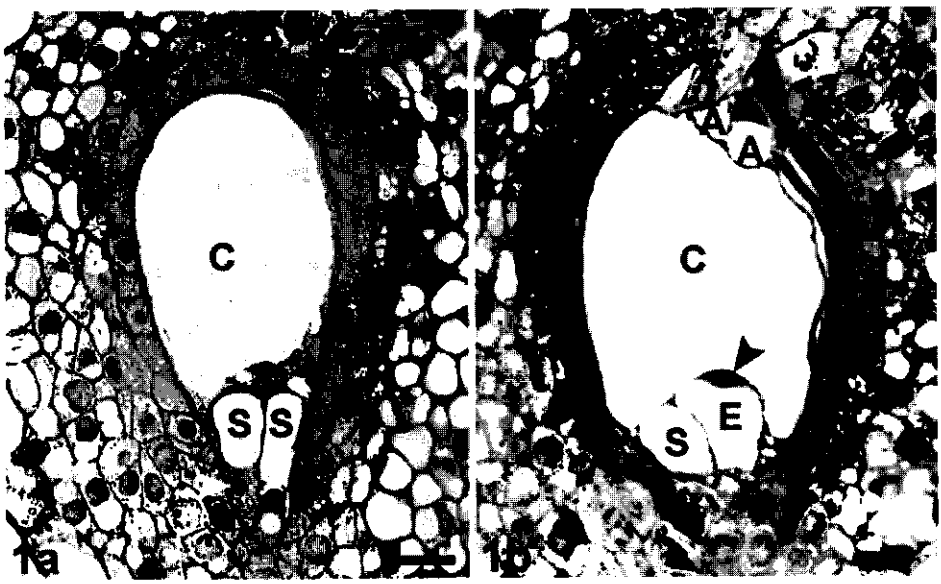

Fig. 1 a-b. Light microscopic images of *P.* x *hybrida* ovules with mature embryo sacs. Sections are stained with toluidine blue. (a) Section through the two synergid cells (*S*) and the central cell (*C*). (b) Section through the egg cell (*E*), one of the synergid cells (*S*), two of the antipodal cells (*A*), and the central cell (*C*). Arrowhead points to the egg cell nucleus. Bar is 10 μm; magnification of (a) and (b) are the same.

From the filiform apparatus onwards to the chalazal side of the cells, the cell wall between the two synergid cells is diminishing in thickness. At the most chalazal side of the synergid cells and the egg cell, and the most micropylar side of the central cell, plasma membranes lay very closely together and cell walls in this area seem absent (Fig. 5a,b). In the cell wall between the two synergid cells, as shown in figure 2b, plasmodesmata can be observed (arrowheads). Many microtubules that are closely associated with the plasma membranes of the synergid cells are visible (arrows in Fig. 2b).

Within their micropylar cytoplasm, the synergid cells have a large spherical nucleus (Fig. 2a,c). No lobes or invaginations are present and many nuclear pores can be observed in the nuclear envelope (arrowheads in Fig. 3a). Ribosomes are attached to the outer nuclear membrane and at some places the RER is attached to the nuclear envelope (not shown).

The cytoplasm shows abundant RER, high concentration of polysomes, numerous mitochondria, and Golgi bodies with many vesicles (Figs. 2c, 3a). The RER can sometimes be observed as long strands that are dilated at some places (Fig. 2c). Polysomes are observed free in the cytoplasm as well as attached to ER strands (small arrows in Fig. 3b). Mitochondria are evenly distributed throughout the cytoplasm (Figs. 2c, 3a). In the synergid cells two different types of plastids can be observed; darkly staining plastids with mainly short dilated thylakoid membranes and lighter staining ones with only very few thylakoid membranes tightly pressed together (Fig. 3a). Sometimes plastids have a small starch grain (arrow in Fig. 2b). The cytoplasm contains a high number of Golgi bodies with many associated vesicles. The Golgi bodies consist of three to six cisternae, and the contents of the cisternae differ in staining (Fig. 3b). Besides the large chalazal vacuole, some small vacuoles can be discerned inside the cytoplasm (Fig. 2c); it is not clear whether these are connected with each other or not. Also multi-vesicular bodies are present (Fig. 3b). Figure 3b shows such a multi-vesicular body with some vesicles around it and one vesicle being incorporated (see arrow).

At anthesis no difference between the two synergid cells can be discerned; the cells do not degenerate prior to fertilization.

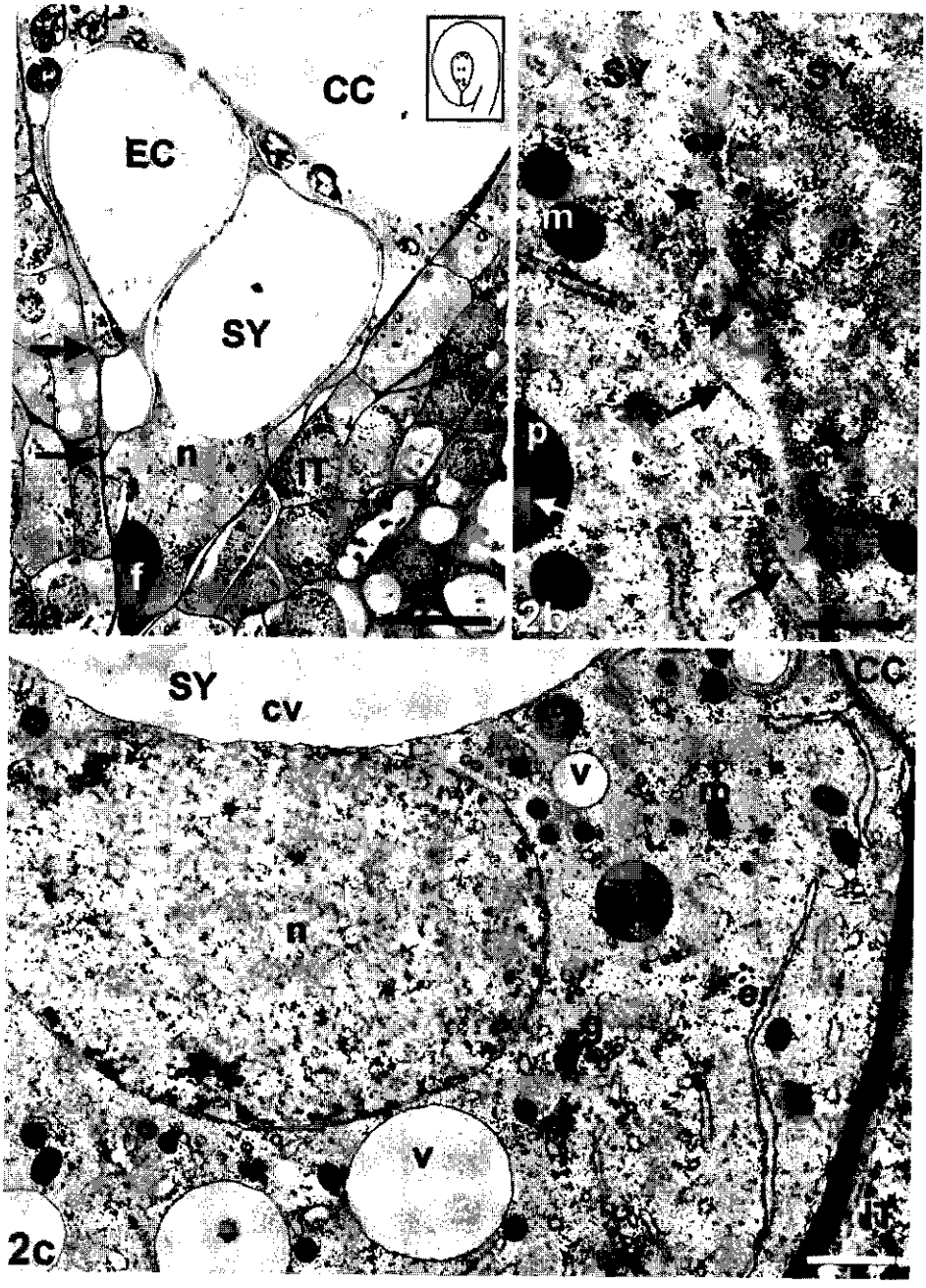
CC
EC
SY
n
m
f
2a
2b
SY
cv
CC
v
n
n
v
2c

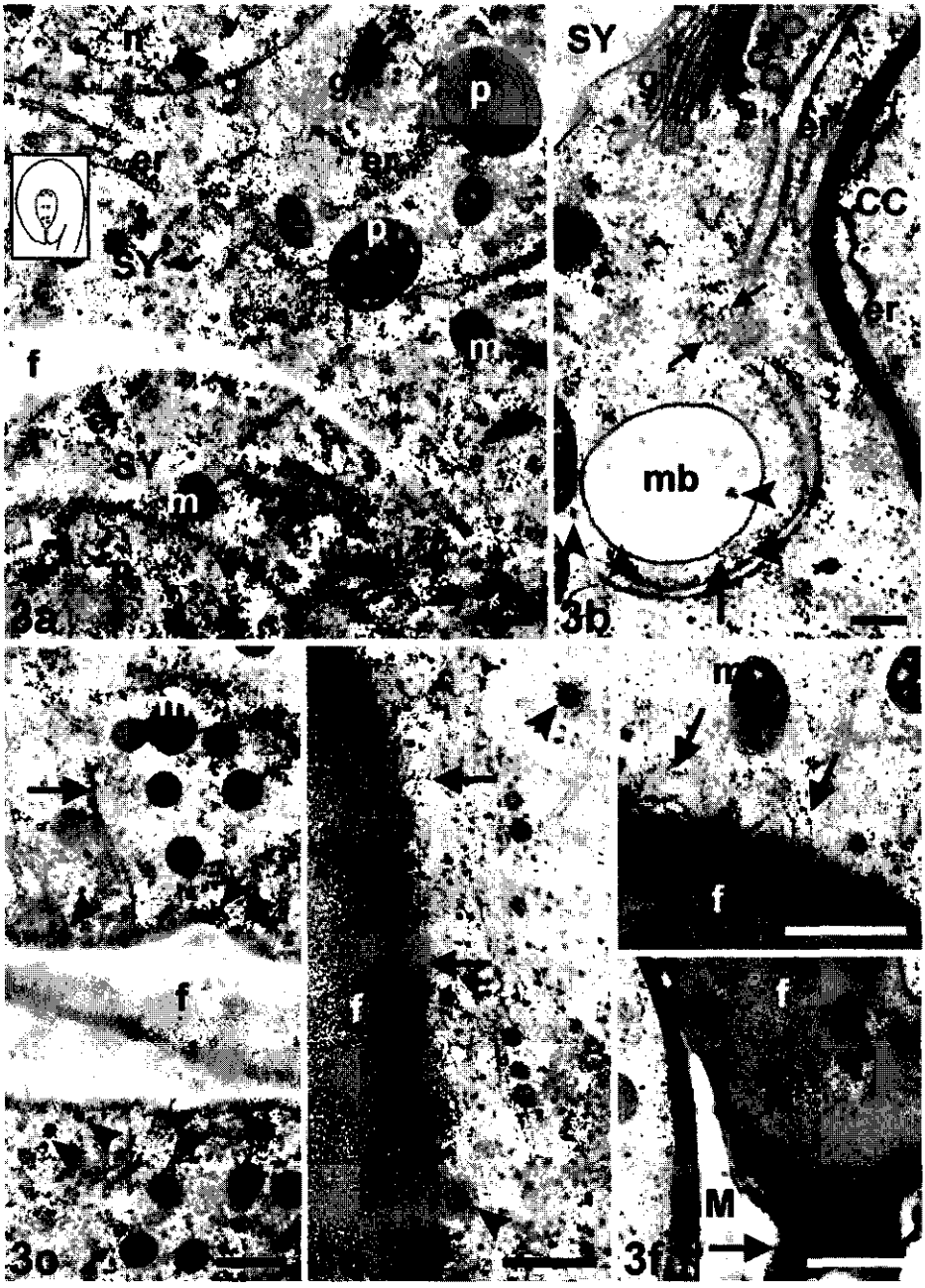
n
g
p
er
SY
m
f
mb
CC
M
3a
3b
3c
3f

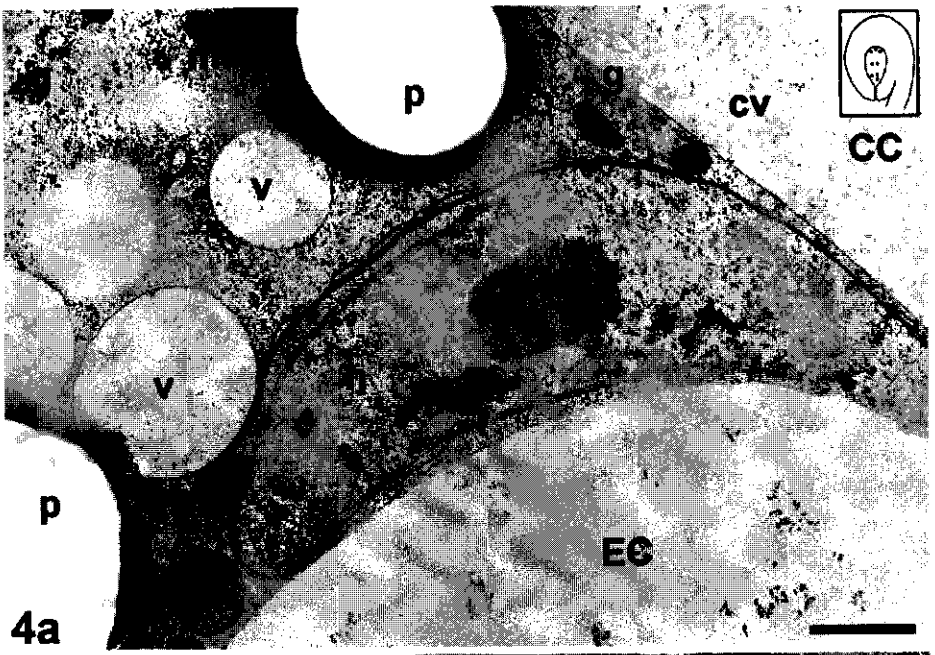

4a

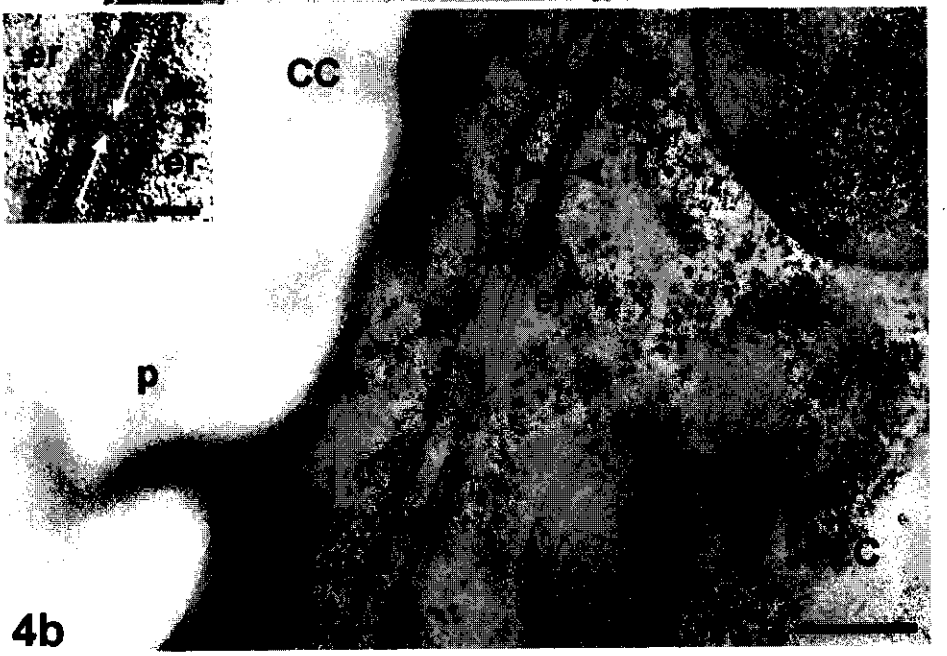

4b

Fig. 2 a-c. Electron micrographs of the egg apparatus of mature *P.* x *hybrida* embryo sacs. See inset for ovule orientation. (a) Overview of the egg apparatus showing the egg cell, one of the synergid cells and part of the central cell. Note the lateral attachment of the egg cell to the embryo sac wall (*arrows*). (b) Cell wall between the two synergid cells. Note plasmodesmata (*arrowheads*) and microtubules associated with the cell wall (*black arrows*). Note the small starch grain (*white arrow*) in the plastid. (c) Synergid cell cytoplasm, rich in RER (*er*), Golgi bodies (*g*), mitochondria (*m*), and with several small vacuoles (*v*). *CC*, central cell; *cv*, central vacuole; *EC*, egg cell; *er*, endoplasmic reticulum; *f*, filiform apparatus; *IT*, integument; *m*, mitochondrion; *n*, nucleus; *p*, plastid; *SY*, synergid cell; *v*, vacuole. Bars are (a) 10 μm, (b) 500 nm and (c) 1 μm.

Fig. 3 a-f. Electron micrographs of the *P.* x *hybrida* synergid cells. See inset for ovule orientation. (a) Cytoplasm of the two synergid cells; no difference in organization between the two cells can be observed. Note the nuclear pores in the nuclear envelope (*white arrowheads*). (b) Detail of synergid cell cytoplasm and the cell wall between a synergid and central cell, which is aligned with endoplasmic reticulum (*er*). Note the multi-vesicular body (*mb*) in the synergid cell, with vesicles inside and around (*arrowheads*), and one vesicle attached (*large arrow*). Note the polysomes attached to the endoplasmic reticulum (*small arrows*). (c) Filiform apparatus between the two synergid cells with many vesicles close to the plasma membranes (*arrowheads*). Arrow points at microtubule. (d) Detail of the filiform apparatus showing microtubules associated with the plasma membrane (*arrows*) and coated vesicles (*black arrowheads*) as well as non-coated vesicles (*white arrowheads*) in this area. (e) Endoplasmic reticulum associated with the filiform apparatus (*arrows*). (f) Granular appearance of the lowest part of the filiform apparatus and excreted products within the micropyle (*arrow*). *CC*, central cell; *er*, endoplasmic reticulum; *f*, filiform apparatus; (*g*) Golgi bodies; *m*, mitochondrion; *M*, micropyle; *n*, nucleus; *p*, plastid; Bars are (a,c,e) 500 nm, (b,d) 200 nm and (f) 1 μm.

Fig. 4 a,b. Electron micrographs of the *P.* x *hybrida* egg cell. See inset for ovule orientation. (a) Chalazal part of the egg cell and adjacent central cell cytoplasm. (b) Detail of the cell wall between the egg cell and the central cell. Note the ER along the central cell plasma membrane with ribosomes attached to one side only (*er*) and the plasmodesma (*black arrow*). Inset shows a higher magnification of this plasmodesma (*white arrows*). *CC*, central cell; *cv*, central vacuole; *EC*, egg cell; *er*, endoplasmic reticulum; *m*, mitochondrion; *n*, nucleus; *nu*, nucleolus; *p*, plastid; *v*, vacuole; *arrowhead*, plasma membrane. Bars are (a) 1 μm, (b) 200 nm, and inset (b) 25 nm.

Egg cell

Whereas the synergid cells are located at the most micropylar end of the embryo sac, the egg cell is placed more chalazally, attached laterally to the embryo sac wall (arrows in Fig. 2a). At anthesis the cell is pear-shaped and highly vacuolated (Figs. 1b, 2a). Only a very thin layer of cytoplasm aligns the plasma membrane, with the nucleus situated at the chalazal side of the cell (Figs. 1b, 4a). The nucleus lays between the large vacuole and de egg cell wall. In figure 4a the nucleolus is visible. The nucleus has only little heterochromatin.

The egg cell wall diminishes in thickness from the micropylar side towards the chalazal side of the cell. Figure 5b shows a high magnification of the borders at the chalazal side of the egg apparatus between the egg cell, one of the synergid cells and the central cell. Membranes appear almost to be attached to each other and cell walls seem absent. Some cortical microtubules can be observed close to the plasma membranes (Fig. 5b). Few plasmodesmata are present between the egg cell and other embryo sac cells (see inset in Fig. 4b).

The egg cell contains only little cytoplasm with few mitochondria, undifferentiated plastids, mostly without starch, some Golgi bodies and few ER strands. The density of non-membrane bound ribosomes is low.

Central cell

The central cell is the largest cell of the embryo sac, with its main volume occupied by a large vacuole (Fig. 1a,b). A thin layer of cytoplasm is located along its lateral and chalazal wall and at anthesis the major portion of the cytoplasm, including the two polar nuclei, is situated at the micropylar side (Figs. 1a, 5a). Besides the central vacuole the cell possesses several small vacuoles (Fig. 4a). Fusion of the two polar nuclei does mostly not occur before anthesis. Figure 5c shows a micrograph of two polar nuclei that lay very close to each other, and may already have fused in an area out of the section. The polar nuclei are regular in profile and possess a large round nucleolus (not shown) and little heterochromatin (Fig. 5a). Many large starch containing plastids surround the polar nuclei. Also mitochondria, ER strands and Golgi bodies can be observed (Figs. 4a, 5a). Strands of ER are aligning the plasma membranes of the central cell and the egg apparatus cells; in some areas the alignment is very closely and ribosomes are adhered to one side of the ER only (Fig. 4b). At some places plasmodesmatal contact between the central cell and the egg apparatus cells exists (see inset in Fig. 4b).

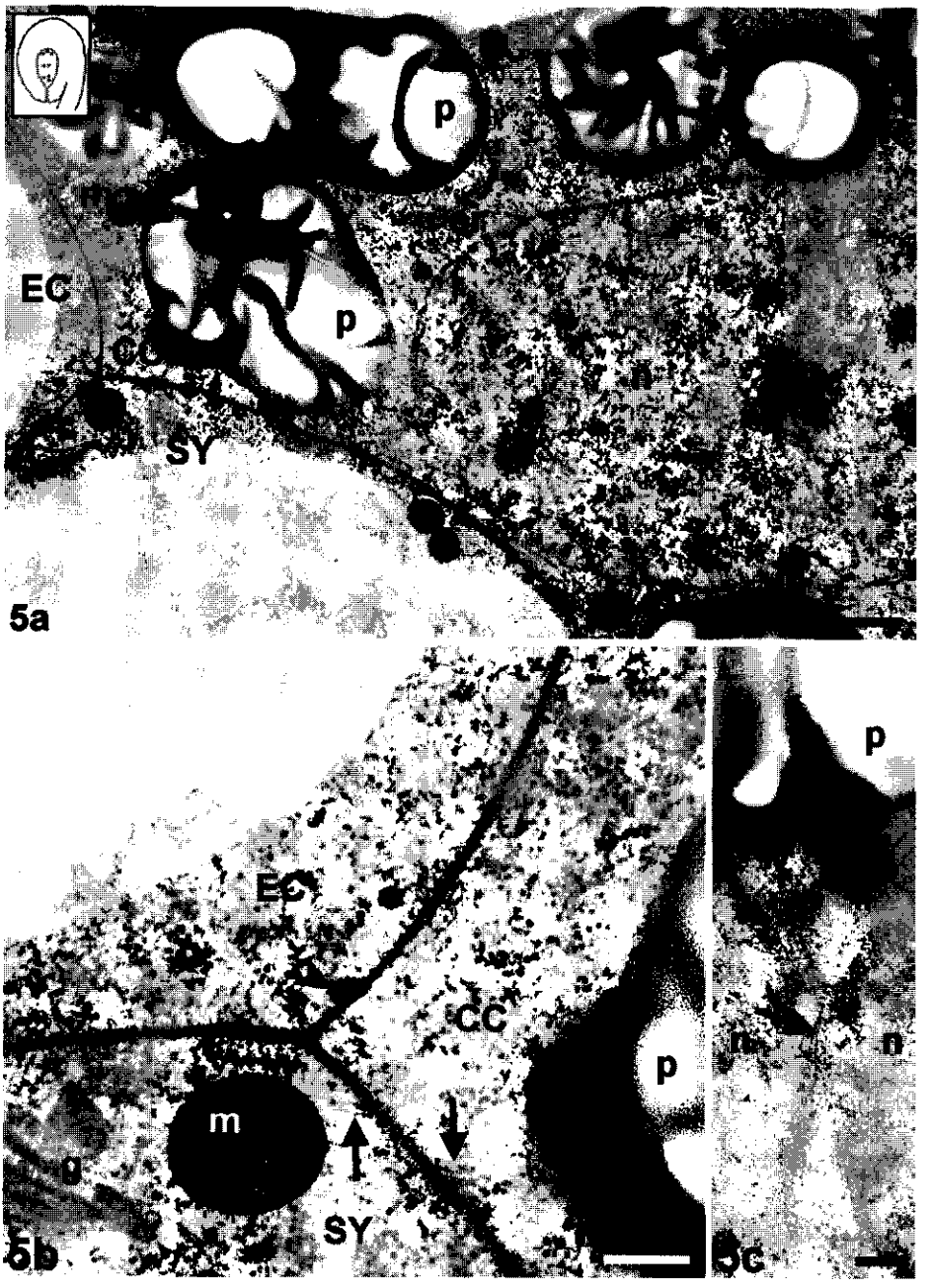
p
EC
p
CC
n
SY
5a
EC
CC
p
m
SY
5b
p
n
5c

Antipodal cells

The three smallest embryo sac cells, the antipodal cells, are situated at the chalazal end of the embryo sac. Figure 1b shows a light microscopic image of an embryo sac in which two of the antipodal cells are visible. The antipodal cells are arranged in a triangular way similar to the cells of the egg apparatus. In *P.* x *hybrida* these cells are like the other embryo sac cells highly vacuolated. Generally, we observed that two of the antipodal cells posses a large vacuole at the micropylar side (Fig. 1b), whereas the third has its large vacuole located at the chalazal side.

The developmental stage of the antipodal cells at anthesis varied between embryo sacs (compare Fig. 6a, 6b and 6c). Whereas the antipodal cells shown in figure 6a only have started to vacuolize, the highly vacuolated antipodal cells of figure 6c are already degenerating, as can be observed from the thin layers of very dense cytoplasm that border the cell walls, and the appearance of the nucleus that is visible in this section. The cytoplasm with Golgi bodies with associated vesicles and a high density of ribosomes and polysomes, sometimes associated with the ER, indicate the initially high rate of metabolic activity of the antipodal cells (Fig. 6a). The antipodal cell shown in figure 6e contains extensive ER at the chalazal side. Some of the vacuoles apparently contain cytoplasmic contents (arrowhead in Fig. 6a). Microtubules can be seen throughout the cytoplasm (arrows in Fig. 6a). Starch containing plastids are initially also present in the cytoplasm (Fig. 6a,b). Different to the egg apparatus cells the antipodal cells are completely surrounded by cell walls. Cell wall ingrowths are present in some areas in the most chalazal part of the embryo sac, but only protruding into the bordering chalazal cells and not into the antipodal cells (not shown). Figure 6d shows part of the cell wall between one of the antipodal cells and the central cell. In both cells a thin layer of cytoplasm is bordering the plasma membrane in this area. In this layer strands of

Fig. 5a-c. Electron micrographs of the *P.* x *hybrida* central cell. See inset for ovule orientation. (a) Part of the central cell cytoplasm bordering the egg apparatus, showing one of the polar nuclei (*n*) and many large starch containing plastids (*p*). (b) Detail of the border between the egg cell, one of the synergid cells and the central cell. Note the close association of the membranes, a vesicle attached to the egg cell plasma membrane (*arrowhead*), and plasma membrane associated microtubules (*arrows*). (c) The two polar nuclei lay very closely together (*n, arrow*). *CC*, central cell; *EC*, egg cell; *er*, endoplasmic reticulum; *g*, Golgi bodies; *m*, mitochondrion; *p*, plastid; *SY*, synergid cell. Bars are (a) 1 μm and (b,c) 200 nm.

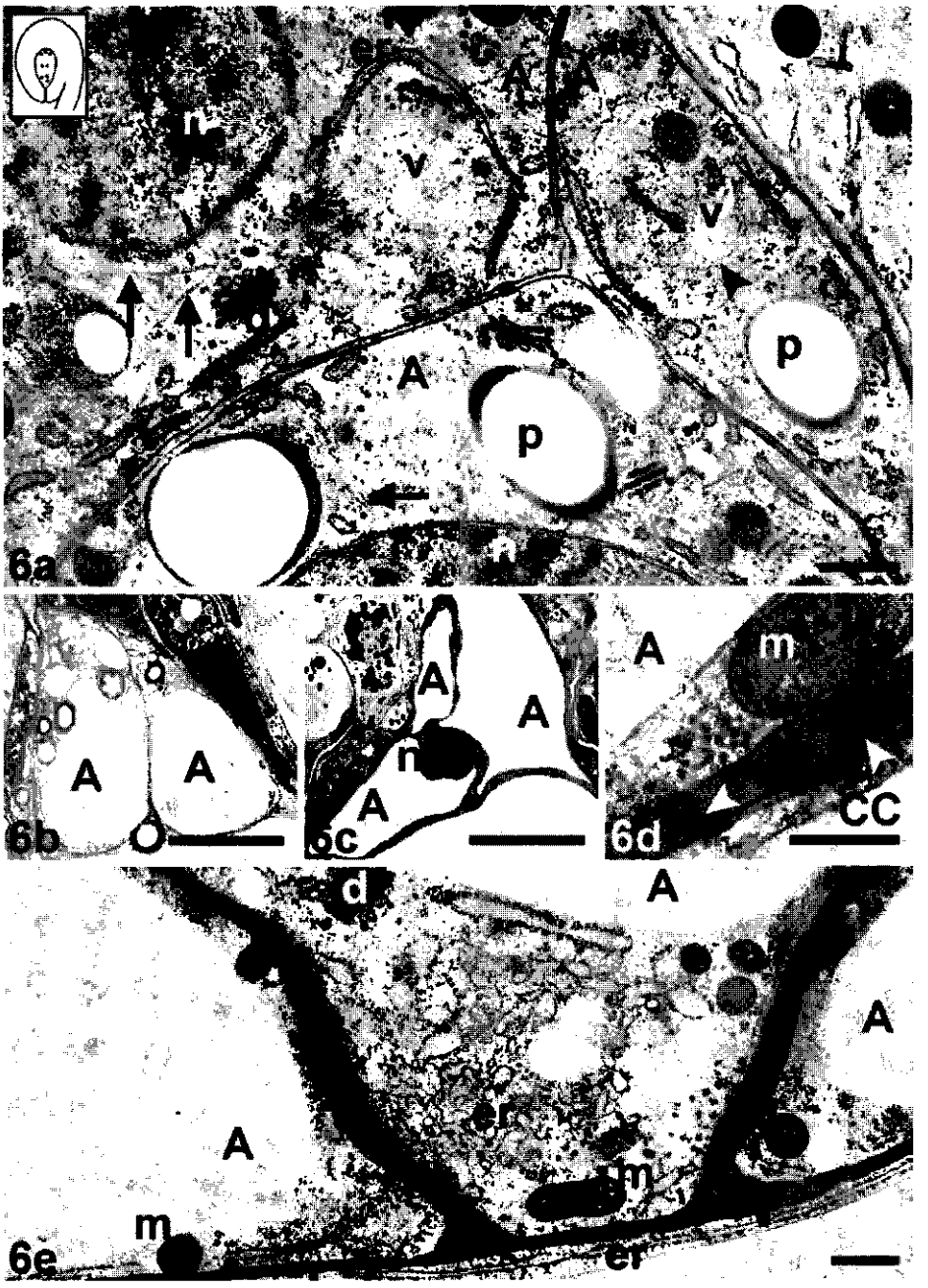
6a
n
v
A
p
6b
A
6c
n
6d
m
CC
6e
d
er
m

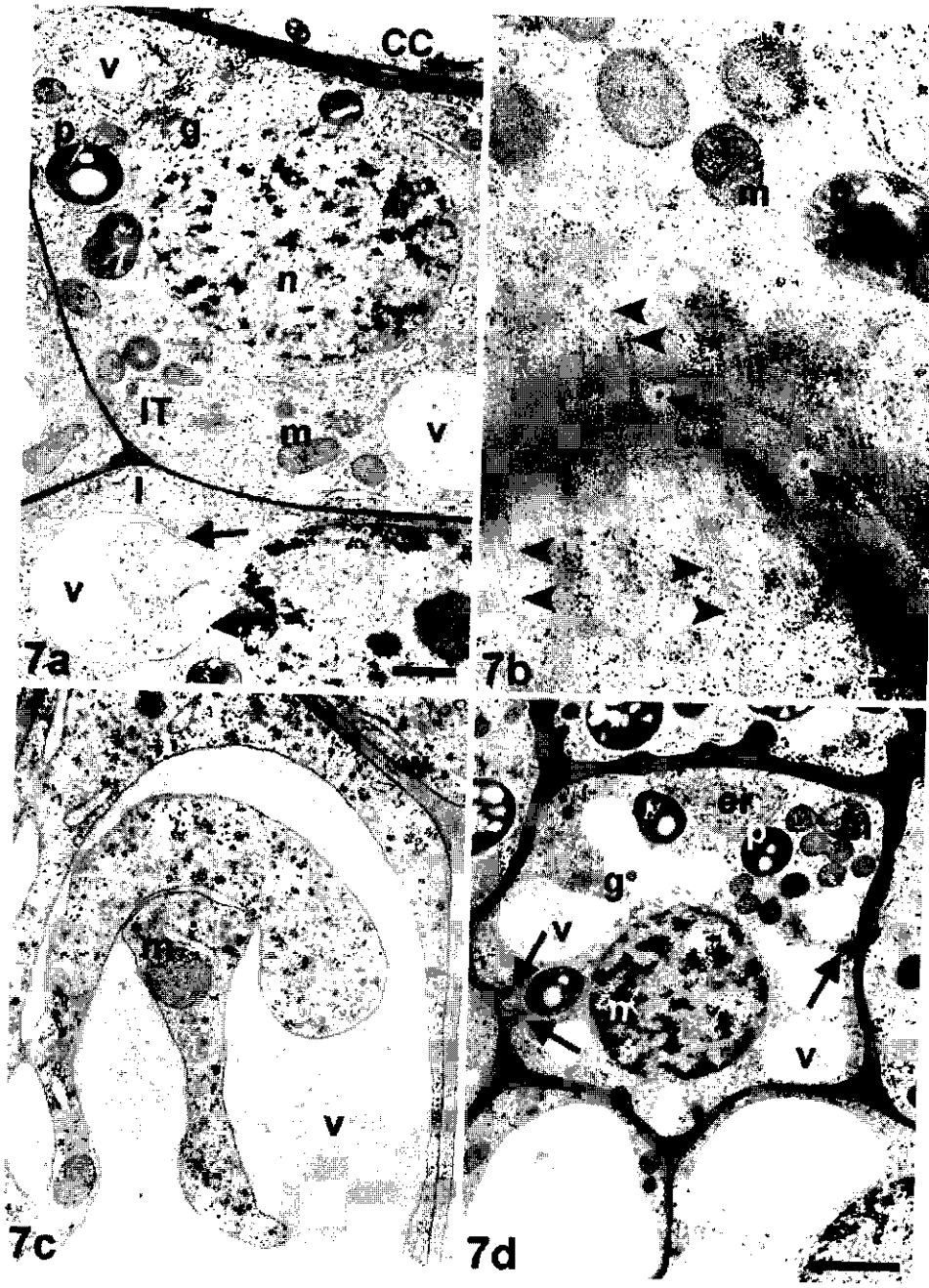
CC
v
p
g
n
IT
m
v
I
v
7a
n
7b
m
v
7c
er
p
g
v
m
v
7d

RER can be detected traversing the wall at several places by plasmodesmata (arrowheads in Fig. 6d). Plasmodesmata are also present between the antipodal cells. Moreover, plasmodesmata are present between antipodal cells and surrounding degenerating nucellus cells at the most chalazal side of the embryo sac; sometimes these seem to be occluded (not shown).

Integuments

Whereas in the coenocytic megagametophyte the cells of the integument tapetum are radially stretched compared to the micropylar-chalazal embryo sac axis, at embryo sac maturity they have become square to elongated (Fig. 7a). The cells contain a centrally located nucleus that occupies a large part of the cell volume. Golgi bodies, RER and starch containing plastids are evenly distributed throughout the cytoplasm. In cross section, often only small vacuoles appear in the cytoplasm, which may however be connected as can be deduced from the irregularly shaped vacuole of the integument cell in figure 7a (arrows). Figure 7c shows the very complex organization of the vacuole of another integument cell, at further distance from the embryo sac. The closer to the outer epidermis of the ovule the more vacuolated the integument cells become (Fig. 1a).

Fig. 6 a-e. Electron micrographs of the antipodal cells of *P.* x *hybrida* embryo sacs of flowers at anthesis. See inset for ovule orientation. (a) Part of the dense cytoplasm of three young antipodal cells. Note the vacuole with cytoplasmic contents (*arrowhead*). (b) Overview of highly vacuolated antipodal cells. (c) Overview of antipodal cells in a degenerating state. Note the degenerating nucleus (*n*). (d) Cell wall between the central cell and an antipodal cell. Note the plasmodesmata (*arrowheads*). (e) Most micropylar side of highly vacuolated antipodal cells. Note the endoplasmic reticulum (*er*). *A*, antipodal cell; *CC*, central cell; *er*, endoplasmic reticulum; *g*, Golgi bodies; *m*, mitochondrion; *n*, nucleus; *p*, plastid; *v*, vacuole; *arrow*, microtubule. Bars are (a,e) 500 nm, (b,c) 5 μm and (d) 200 nm.

Fig. 7 a-d. Electron micrographs of the integument cells of *P.* x *hybrida* ovules of flowers at anthesis. (a) Cell of the integument tapetum (*IT*). Arrows point to irregularly shaped vacuole in an adjacent integument cell (*I*). (b) Detail of the cortical microtubule cytoskeleton of an integument cell. Note the evenly spaced microtubules (*arrowheads*) and the plasmodesmata within the cell wall (*arrows*). (c) Very irregularly shaped vacuole within one of the integument cells. (d) Cell of the hypostase with cell wall ingrowths (*arrows*). *CC*, central cell; *er*, endoplasmic reticulum; *g*, Golgi bodies; *m*, mitochondrion; *n*, nucleus; *p*, plastid; *v*, vacuole; *w*, cell wall. Bars are (a) 1 μm, (b) 200 nm, (c) 500 nm, and (d) 2 μm.

Figure 7b shows parallel oriented microtubules of the cortical microtubule cytoskeleton of an integument cell. Within the cell wall plasmodesmata in cross section are visible (arrows). At the chalazal side the embryo sac is bordered by the cells of the hypostase (Fig. 7d). Typical for these cells are the thick cell walls and cell wall ingrowths (arrows). Often plasmodesmata are visible within these cell wall ingrowths (not visible at this magnification).

Discussion

With high pressure freezing and freeze substitution the ultrastructure of *P.* x *hybrida* ovules and embryo sacs can be very well preserved. Artifacts typical for chemical fixation, and also observed in chemically fixed *P.* x *hybrida* embryo sacs, like collapsed cells, collapsed vacuoles, membranous structures within vacuoles and within nuclei, lobed nuclei, irregular electron translucent spaces within the cytoplasm, and cell shrinkage (Van Went *et al.*, 1970a, 1970b; Thijssen *et al.*, 1997), were not observed in ovules cryofixed by high pressure freezing. High pressure freezing and freeze substitution results in the turgescent appearance of cells. Vacuoles and organelles are bordered by smooth membrane profiles. Many vesicles are present along with and attached to the plasma membranes. The microtubule cytoskeleton is well preserved. Even in degenerating cells many cellular details are still visible.

In the *Polygonum* type of embryo sac, which is also the type present in *P.* x *hybrida*, seven cells of four different types are formed after the third mitotic division: two synergid cells, the egg cell, the central cell containing two nuclei, and three antipodal cells. Within the embryo sac, these cell types have their own location, morphology and cytoarchitecture, related to their specific function in the reproductive processes.

The synergid cells have a role in mediating fertilization by pollen tube attraction and acceptance (Ray *et al.*, 1997; Higashiyama, 2002; Higashiyama *et al.*, 2001), sperm cell release (Rotman *et al.*, 2003), and enabling the migration of the male gametes to the female gametes (Huang & Russell, 1994). The synergid cells of angiosperms in general (Willemse & Van Went, 1984), including those of *P.* x *hybrida*, are highly differentiated, metabolically active cells with a high number of mitochondria, Golgi bodies with associated vesicles and extensive rough endoplasmic reticulum present in their cytoplasm.

Another common feature in angiosperms is the presence of a filiform apparatus at the micropylar side (Huang & Russell, 1992). This specialized thickened cell wall is thought to serve as a diffusion pathway for chemo attractant substances of yet unknown

nature, involved in the attraction of the pollen tube (Higashiyama *et al.*, 2003). In most species the filiform apparatus shows extensive cell wall projections extending into the cytoplasm, believed to function in the amplification of the plasma membrane surface, facilitating transport between the apoplast and the symplast (reviewed by Huang & Russell, 1992). In *P.* x *hybrida* the filiform apparatus is very regular in outline, after cryofixation even more regular that after chemical fixation (Van Went *et al.*, 1970a). Microtubules that are aligned longitudinally compared to the micropylar-chalazal embryo sac axis, and extend into the cytoplasm, like observed by immunocytochemistry in maize synergid cells (Huang & Sheridan, 1994), and immunogold electron microscopy of rapid-frozen tobacco embryo sacs (Huang & Russell, 1994b), are also observed in electron micrographs of *P.* x *hybrida* synergid cells. The presence of many vesicles in the micropylar synergid area, and the presence of substances in the micropyle, is in accordance with the proposed function of the synergid cells in secreting chemo-attractant substances (Higashiyama *et al.*, 2001). The two *P.* x *hybrida* synergid cells show a similar cell organization at embryo sac maturity. In contrast to many other species (Huang & Russell, 1992), synergid cell degeneration does not occur before pollen tube penetration.

Mature egg cells are waiting for the trigger of fertilization, to activate the planned programme of events that leads to the development of the embryo (Antoine *et al.*, 2000). Compared to their neighboring cells, the synergid cells, unfertilized egg cells of angiosperms generally have the cell organization and ultrastructure of quiescent unspecialized cells (Russell, 1993). Generally, only few Golgi bodies are present, with few associated vesicles, and polysomes are rarely observed (Russell, 1993). Variability between angiosperm species in egg cell ultrastructure is reflected in differences in numbers and distribution of plastids, mitochondria and endoplasmic reticulum, and the appearance of the vacuole, visible as one large vacuole or as a large number of small vesicles (Russell, 1993). The *P.* x *hybrida* egg cell is extremely vacuolated, with a large central vacuole and only a thin layer of cytoplasm with few organelles along the plasma membrane and around the chalazally located nucleus.

At the most chalazal side of the *P.* x *hybrida* egg cell and synergid cells, and the micropylar side of the central cell, plasma membranes are aligned very closely. The absence of rigid cell walls in this area, might aid in male - female gamete fusion (Russell, 1993).

During the double fertilization process, typical for angiosperms, the second male gamete fuses with the central cell to form the endosperm, a tissue with a nutritive function for the developing embryo (reviewed by Berger, 2003). The major part of the *P.*

x *hybrida* embryo sac is occupied by this second female gamete. Typical for the *P.* x *hybrida* central cell, as compared to other species, is the high accumulation of starch at maturity (Willemse & Van Went, 1984; Van Went *et al.*, 1970b).

One of the functions of antipodal cells mentioned, is the transport of nutrients from the nucellar tissues to the central cell (Willemse & Van Went, 1984). Initially, the antipodal cells of P. x hybrida show a cytoplasmic constitution of metabolically active cells. However, the cells degenerate upon embryo sac maturity, implying that they can only support embryo sac function for a short time. Cell wall ingrowths are present in a restricted chalazal area of the embryo sac, only extending into the hypostase cells. Though some plasmodesmata are present in the chalazal embryo sac wall, these seem to be occluded. This would imply symplastic isolation of the embryo sac from the surrounding integument tissues.

In the *P.* x *hybrida* egg apparatus cells strands of ER are closely aligning the plasma membranes. Hepler *et al.* (1990) suggest that cortical ER, anchored to the plasma membrane, has a function in attaching actin microfilament bundles, to drive endoplasmic streaming. We did not observe microfilaments in high pressure frozen *P.* x *hybrida* ovules. This may be due to inadequate staining (Murata *et al.*, 2002). Plasmodesmata are present between all embryo sac cells, indicating a close relationship between the embryo sac cells. High symplastic permeability between embryo sac cells before fertilization, and reduced symplastic permeability after fertilization, as was shown in *Torenia fournieri* by Han *et al.* (2000), might be related to the transport of molecules with a role in the functional organization of the cells, related to the coordination of the fertilization process (Han *et al.*, 2000).

Transfer cells are often present between donor and recipient tissues, increasing the surface area available for transport. Whereas in *Vicia* and *Lathyrus* the cells of the integument tapetum showed a typical transfer cell appearance (Johansson & Walles, 1993), in *P.* x *hybrida* the cytoplasm of the integument tapetum cells shows an organization typical for secretary cells, but transfer walls are not present. Cell wall extensions in the central cell have been reported for a number of species (Willemse & Van Went, 1984); these are absent in the central cell of the unfertilized *P.* x *hybrida* embryo sac.

The *P.* x *hybrida* hypostase cells, located at the chalazal side of the embryo sac, seem metabolically active cells. Also cell wall ingrowths are present. Hypostase cells are supposed to be involved in the transport of nutrients from the placenta and ovary vascular tissues to the ovule tissues and the gametophyte cells (Batygina & Shamrov,

1999). They might well have this function in *P.* x *hybrida*.

In the *Polygonum* type of embryo sac, cell plates are formed after the third mitotic division, resulting in the seven-celled embryo sac. The molecular and genetic basis of cell specification and differentiation in the megagametophyte is not known yet. Although of clonal origin, the embryo sac cells differentiate along four alternative developmental pathways, into the functional synergid cells, egg cell, central cell and antipodal cells. Positional information and/or local signaling processes are supposed to play a crucial role in cell fate determination, but the molecular processes that establish the structural features during female gametophyte development still have to be elucidated (Grosniklaus & Schneitz, 1998; Drews *et al.*, 1998; Drews & Yadegari, 2002).

Over the past few years many female gametophyte mutants, mainly in *Arabidopsis*, have been identified (reviewed by Drews & Yadegari, 2002). Studies addressing wild type gametophyte development can provide essential reference data to locate and recognize developmental disturbances in these mutants. The challenge for the coming years is to identify the genes required for female gametophyte function, and to understand their function (Drews & Yadegari, 2002). In the integration of the available information at the molecular level with the level of cellular organization, electron microscopy data obtained with high pressure freezing may play a crucial role.

Acknowledgements

We thank Martin Müller for giving Marja Thijssen the opportunity to visit the Laboratory for Electron Microscopy I, ETH Zurich. We thank Felix Thiel, Johan Hazekamp, Bruno Humbel, Paul Walther and Eyal Shimoni for assistance with the high pressure freezing and useful discussion. Critical reading of the manuscript by André van Lammeren is appreciated.

References

Antoine, A.F., Dumas, C., Faure, J.-E., Feijó, J.A. & Rougier, M. (2001). Egg activation in flowering plants. Sex. Plant Reprod. 14, 21-26.

Batygina, T.B. & Shamrov, I.I. (1999). New approach to interpreting the ovular basic structures. Phytomorphology 49, 111-221.

Berger, F. (2003). Endosperm: The crossroad of seed development. Curr. Opin. Plant Biol. 6, 42-50.

Bethke, P.C. & Jones, R.L. (2000). Vacuoles and prevacuolar compartments. Curr. Opin. Plant Biol. 3, 469-475.

Drews, G.N., Lee, D. & Christensen, C.A. (1998). Genetic analysis of female gametophyte development and function. Plant Cell 10, 5-17.

Drews, G.N. & Yadegari, R. (2002). Development and function of the angiosperm female gametophyte. Annu. Rev. Genet. 36, 99-124.

Grossniklaus, U. & Schneitz, K. (1998). The molecular and genetic basis of ovule and megagametophyte development. Cell Dev. Biol. 9, 227-238.

Han, Y.-Z., Huang, B.-Q., Zee, S.-Y. & Yuan, M. (2000). Symplastic communication between the central cell and the egg apparatus cells in the embryo sac of *Torenia fournieri* Lind. before and during fertilization. Planta 211, 158-162.

Hepler, P.K., Palevitz, B.A., Lancelle, S.A., McCaulay, M.M. & Lichtscheidl, I. (1990). Cortical endoplasmic reticulum in plants. J. Cell Sci. 96, 355-373.

Higashiyama, T. (2002). The synergid cell: Attractor and acceptor of the pollen tube for double fertilization. J. Plant Res. 115, 149-160.

Higashiyama, T., Kuroiwa, H. & Kuroiwa, T. (2003). Pollen-tube guidance: Beacons from the female gametophyte. Curr. Opin. Plant Biol. 6, 36-41.

Higashiyama, T., Yabe, S., Sasaki, N., Nishimura, Y., Miyagishima, S., Kuroiwa, H. & Kuroiwa, T. (2001). Pollen tube attraction by the synergid cell. Science 293, 1480-1483.

Huang, B.-Q. & Russell, S.D. (1992). Female germ unit: Organization, isolation, and function. Int. Rev. Cytol. 140, 233-293.

Huang, B.-Q. & Russell, S.D. (1994). Fertilization in *Nicotiana tabacum*: Cytoskeletal modifications in the embryo sac during synergid degeneration. A hypothesis for short-distance transport of sperm cells prior to gamete fusion. Planta 194, 200-214.

Huang, B.-Q. & Sheridan, W.F. (1994). Female gametophyte development in maize: Microtubular organization and embryo sac polarity. Plant Cell 6, 845-861.

Johansson, M. & Walles, B. (1993). Functional anatomy of the ovule in broad bean (*Vicia faba* L.) I. Histogenesis prior to and after pollination. Int. J. Plant Sci. 154, 80-89.

Kapil, R.N. & Bhatnagar, A.K. (1981). Ultrastructure and biology of female gametophyte in flowering plants. Int. Rev. Cytol. 70, 291-341.

Ketelaar, T. & Emons, A.M.C. (2001). The cytoskeleton in plant cell growth: Lessons from root hairs. New Phytol. 152, 409-418.

Moor, H. (1987). Theory and practice of high pressure freezing. Cryotechniques in biological electron microscopy (ed. by R.A. Steinbrecht & K. Zierold), pp. 175-191. Springer-Verlag, Berlin.

Müller, M. & Moor, H. (1984). Cryofixation of thick specimens by high pressure freezing. Science of biological specimen preparation (ed. by J.P. Revel, T. Barnard & G.H. Haggins), pp. 131-138. SEM, AMF O'Hare, Chicago.

Murata, T., Karahara, I., Kozuka, T., Giddings Jr, T.H., Staehelin, L.A. & Mineyuki, Y. (2002). Improved method for visualizing coated pits, microfilaments, and microtubules in cryofixed and freeze-substituted plant cells. J. Electron. Microsc. 51. 133-136.

Nebenführ, A. & Staehelin, L.A. (2001). Mobile factories: Golgi dynamics in plant cells. Trends Plant Sci. 6, 160-167.

Ray, S., Park, S.-S. & Ray, A. (1997). Pollen tube guidance by the female gametophyte. Development 124, 2489-2498.

Rotman, N., Rozier, F., Boavida, L., Dumas, C., Berger F. & Faure, J.-E. (2003). Female control of gamete delivery during fertilization in *Arabidopsis thaliana*. Curr. Biol. 13, 432-436.

Russell, S.D. (1993). The egg cell: Development and role in fertilization and early embryogenesis. Plant Cell 5, 1349-1359.

Severs, N.J., Newman, T.M. & Shotton, D.M. (1995). A practical introduction to rapid freezing techniques. Rapid freezing, freeze fracture and deep etching (ed. by N.J. Severs and D.M. Shotton), pp. 31-49. Wiley-Liss, New York.

Spurr, A.R. (1969). A low-viscosity epoxy resin embedding medium for electron microscopy. J. Ultrastruct. Res. 26, 31-43.

Studer, D., Michel, M., Wohlwend, M., Hunziker, E.B. & Buschmann, M.D. (1995). Vitrification of articular cartilage by high-pressure freezing. J. Microsc. 179, 321-332.

Staehelin, L.A. (1997). The plant ER: A dynamic organelle composed of a large number of discrete functional domains. Plant J. 11, 1151-1165.

Thijssen, M.H., Mittempergher, F., Van Aelst, A.C. & Van Went, J.L. (1997). Improved ultrastructural preservation of *Petunia* and *Brassica* ovules and embryo sacs by high pressure freezing and freeze substitution. Protoplasma 197, 199-209.

Thijssen, M.H., Van Went, J.L. & Van Aelst, A.C. (1998). Heptane and isooctane as embedding fluids for high-pressure freezing of *Petunia* ovules followed by freeze-substitution. J. Microsc. 192, 228-235.

Van Went, J.L. (1970a). The ultrastructure of the synergids of *Petunia*. Acta Bot. Neerl. 19, 121-127.

Van Went, J.L. (1970b). The ultrastructure of the egg and the central cell of *Petunia*. Acta Bot. Neerl. 19, 313-322.

Willemse, M.T.M. & Van Went, J.L. (1984). The female gametophyte. Embryology of angiosperms (ed. by B.M. Johri), pp. 159-196. Springer-Verlag, Berlin.

Chapter 6

Isolation, culture and microscopic analysis of female gametophytes of *Petunia* x *hybrida* Effects on cell structure and organization

M.H. THIJSSEN & J.L. VAN WENT

Summary

To obtain further insight in the process of female gametophyte development, we isolated *Petunia* x *hybrida* megagametophytes from the surrounding ovular tissues, characterized the isolated cells, and cultured them *in vitro*. Viable mature embryo sacs of *P.* x *hybrida* were isolated from ovules in high amounts by enzymatic maceration, with 3% driselase in the medium. Viable megaspores with surrounding nucellus cells, and one-nucleate, two-nucleate and four-nucleate megagametophytes were successfully isolated with a medium containing 2-3% cellulase Y-C and 0.1-0.5% Macerozyme. Isolated gametophyte cells were intact and viable and after isolation their structure and organization resembled those of *in planta* female gametophytes. Mature embryo sacs that were cryofixed 1-2 hours after isolation, generally showed a cytoplasmic organization and polarity that resembled *in planta* embryo sacs, although some rearrangements of organelles were observed. *In vitro* cultured egg and synergid cells did not show major changes in cell organization. Cells of the egg apparatus degenerated first. Within the central cell clear organizational changes were observed during culture. Shortly after isolation transvacuolar strands with cytoplasmic streaming were visible. After two days in culture the two polar nuclei had fused and the fusion nucleus had moved from a position close to the egg cell to the centre of the cell. Nuclear divisions were never observed. Generally, isolated mature embryo sacs could be kept alive in microscopic micro-culture chambers with low density culture medium for up to five days, whereas young megagametophytes only survived for up to three days. The culture of isolated megagametophytes in Milli-cell inserts or in agarose, both together with *P.* x *hybrida* nurse cultures did not enhance their life span *in vitro*, nor sustain their further development. Improving the viability of isolated megaspores and megagametophytes and establishing an *in vitro* culture system that sustains the development of the isolated cells, will allow fundamental questions on female gametophyte biology to be addressed experimentally.

Key words: embryo sac isolation, female gametophyte, (ultra)structure, *Petunia* x *hybrida*.

Introduction

The female gametophyte of angiosperms, the embryo sac, develops from a single cell, the megaspore, deeply embedded in the sporophytic tissues of the ovule. The mature embryo sac is composed of a number of cells, which differ in structural organization and in function during the fertilization process (reviewed by Kapil & Bhatnagar, 1981; Willemse & Van Went, 1984; Huang & Russell, 1992). The inaccessibility of the female gametophyte makes the study of gametophyte differentiation difficult, and is one of the reasons that this process is still poorly understood.

Within the last 15 years significant progress has been made on the characterization of the female gametophyte, enabled by the availability of methods to isolate female gametophytes and their component cells from the ovular tissues. Megagametophytes can be isolated by enzymatic maceration of the surrounding sporophytic tissues, by micro-dissection of female gametophyte cells, or by a combination of these two techniques (reviewed by Theunis *et al.*, 1991; Huang & Russell, 1992; Dumas & Mogensen, 1993). Isolation of female gametophytes from the ovular tissues, allows direct microscopic three-dimensional observation of these cells, enabling integration of structural information without labor intensive sectioning. Megaspores and megagametophytes isolated from fixed ovular tissues have been used to study the distribution of DNA-containing organelles during megasporogenesis and megagametogenesis (Huang & Russell, 1993; Huang & Sheridan, 1994). The isolation of female gametophyte cells facilitated the study of the actin and microtubular cytoskeleton during megasporogenesis, megagametogenesis and fertilization (Bednara *et al.*, 1990; Webb & Gunning, 1990, 1994; Huang *et al.*, 1993; Huang & Russell, 1994; Huang & Sheridan, 1994), as well as the behavior of nuclei and the organization of the microtubular cytoskeleton in mutants disturbed in megagametophyte development and fertilization (Huang & Sheridan, 1996, 1998).

In a range of angiosperm species it is now possible to isolate living mature embryo sacs or their component cells, including tobacco (Zhou & Yang, 1985; Huang *et al.*, 1992), *Torenia fournieri* (Mòl, 1986), *Plumbago zeylanica* (Huang & Russell, 1989), lily (Wagner *et al.*, 1989a), maize (Wagner *et al.*,1989b; Kranz *et al.*, 1991), ryegrass (Van der Maas *et al.*, 1993), wheat (Kovács *et al.*, 1994), barley (Holm *et al.*, 1994) as well as *Petunia* x *hybrida* (Van Went & Kwee, 1990). The isolation of viable megasporocytes, megaspores, or immature coenocytic megagametophytes has to our knowledge only been reported for lily (Wagner *et al.*, 1989a), tobacco (Wu *et al.*, 1993), barley (Mouritzen & Holm, 1995) and *Torenia fournieri* (Kristóf & Imre, 1996; Imre &

Kristóf, 1999). The access to viable isolated megaspores and immature megagametophytes creates opportunities for experimental studies of megasporogenesis and megagametophyte differentiation at the single cell level and for manipulation of megagametophyte development. This may contribute to a better understanding of the process of gametophyte differentiation and function.

To enhance our insight in the process of female gametophyte development, we isolated female *P.* x *hybrida* gametophytes at different developmental stages, characterized the cells and cultured them *in vitro*. A protocol developed to isolate viable mature embryo sacs (Van Went & Kwee, 1990) was adjusted for the release of megaspores and immature megagametophytes. Because the maintenance of nuclear and cytoplasmic structure and integrity after isolation are essential if the isolated gametophytes are subsequently used for *in vitro* culture experiments, we compared the organization and structure of megagametophytes *in planta* and after isolation. In culture experiments we observed some organizational changes in the isolated gametophytes, but neither immature gametophytes, nor cellular embryo sacs could be induced to divide.

Materials and methods

Plant material

Female gametophytes were isolated from flowers of *Petunia* x *hybrida* (Hook.) Vilm. cv. Bluebedder. Plants were grown in a growth chamber with a day length of 18 hours, a relative humidity of 65%, and a temperature of 20 °C. *P.* x *hybrida* cell suspension cultures that were used to establish the feeder cultures were maintained at 25 °C and at 16 hours light and 8 hours darkness. Cultures were kept on a rotary shaker at 90 rpm and sub-cultured every 10 days. See the media described below under culture of isolated megagametophytes.

Whole ovule preparations

To relate female gametophyte development to flower development, ovaries were dissected from flower buds of different lengths, fixed for 2 days at room temperature in PFA_{50} (paraformaldehyde, propionic acid, and 50% ethanol, 5:5:90) and stored in 70% ethanol at 4 °C. Ovules were cleared with Herr's solution (Herr, 1971) and observed with differential interference contrast (DIC) microscopy.

Isolation of mature embryo sacs

Mature embryo sacs were isolated as previously reported (Van Went & Kwee, 1990), with some modifications. In a number of experiments, for the isolation of aseptic embryo sacs, ovaries were surface sterilized with 70% ethanol and rinsed three times with sterile water. Ovules of 3 to 5 flowers were dissected from the placenta and incubated in 1 ml of enzyme medium in an eppendorf tube for 1.5 hours at 29 °C in a water bath shaking at 140 rpm, and for 1 hour at room temperature without shaking. The maceration medium consisted of 3% driselase (Sigma, USA; or Kyowa Hakko Kogya, Japan; or Fluka, Switzerland) in 5 mM MES-buffer (pH 5.5) with 5 mM $CaCl_2.2H_2O$, adjusted to 600 mOsm/kg H_2O with mannitol. Before use the maceration medium was centrifuged and filtrated through a 0.22 μm Millipore filter (Millipore) to remove the insoluble fraction of the driselase. The solution was heated for 10 minutes at 45 °C to inactivate proteases (Robinson, pers. com.). After the incubation period, the suspension was washed over a 25 μm nylon mesh with a solution of CPW-salts (Frearson *et al.*, 1973) in 5mM MES-buffer (pH 5.8), adjusted to 600 mOsm/kg H_2O with mannitol. Cells were removed from the filter and brought into a 3.5 cm plastic petri-dish with CPW-medium. The liberated embryo sacs were individually collected with a micro-capillary, observed under an inverted microscope.

Isolation of immature megagametophytes

For the isolation of megaspores and immature *P.* x *hybrida* megagametophytes a similar method was used as for the isolation of mature embryo sacs; however, a different enzyme composition of the maceration medium was required. Megaspores and immature megagametophytes could be isolated with a maceration medium containing 2 to 3% cellulase Y-C (Seishin, Japan) and 0.1 to 0.5% Macerozyme (Serva, Germany) in 5 mM MES-buffer (pH 5.5) with 5 mM $CaCl_2.2H_2O$, adjusted to 600 mOsm/kg H_2O with mannitol. This maceration medium could also be used for the isolation of mature cellular embryo sacs.

Light microscopic characterization

For light microscopic characterization isolated megagametophytes were brought into micro-culture chambers consisting of a small droplet of medium, surrounded by paraffin oil on a microscopic cavity slide with a cover slip placed on top of it (Jones *et al.*, 1960); cells were observed with bright field or DIC microscopy. Isolated cells were cultured in the low cell density culture C medium (100 cells per ml), as used by Muller *et al.* (1983)

for low density growth of cells derived from *Petunia* protoplasts. The medium contains macro- and micronutrients, 3 mM MES-buffer (pH 5.8), 0.15 g/l glutamine, 90 mg/l inositol, 0.5 mg/l pyroxidin-HCl, 0.1 mg/l naphthaleneacetic acid (NAA), 0.2 mg/l N_6-benzyladenine (BA) and 2% sucrose, and was adjusted to 600 mOsm/kg H_2O with mannitol. Isolated gametophytes in petri-dishes were observed with inverted phase contrast microscopy. Cell viability was tested with fluorescein diacetate (FDA) (Heslop-Harrison & Heslop-Harrison, 1970). Nuclei of the isolated megagametophytes were stained with 4',6-diamidino-2-phenylindole (DAPI, Sigma). In some cases the DNA-binding fluorescent dye Hoechst 33258 was added to the maceration medium (Zhou, 1987).

Ultrastructural analysis

When aiming a comparative analysis of *in vitro* and *in planta* megagametophyte development, analysis of the ultrastructure can be an important tool to detect degenerative changes after isolation as well as to monitor the developmental process in culture. Because isolated *P.* x *hybrida* embryo sacs appeared to collapse during chemical fixation, they were adhered to nickel wire loops with 2.5% agar films (Tiwari & Polito, 1988) and cryofixed by plunge freezing in liquid propane that was pre-cooled by liquid nitrogen. Embryo sacs were freeze substituted for 48 hours at -80 °C and 8 hours at -40 °C with acetone containing 1% OsO_4 and 0.1% uranyl acetate in the FreasySub freeze substitution unit (Cryotech Benelux, Schagen-NL). Preparations were embedded in Spurr's resin (Spurr, 1969), in a flat embedding mold. Semi-thin sections were stained with toluidine blue. Ultrathin sections were post-stained with uranyl acetate and lead citrate and observed with a JEOL 1200 EXII transmission electron microscope at 60 or 80 kV. Because of ice crystal damage, cryofixed preparations could not be used for detailed characterization of isolated female gametophytes at the ultrastructural level.

Culture of isolated megagametophytes

Besides keeping isolated megagametophytes in micro-culture chambers for light microscopic observation, female gametophyte cells were cultured according to Kranz *et al.* (1991), which means in 12 mm Millicell-CM inserts (Millipore). The inserts were filled with 100 µl of medium, and positioned in 3.5-cm plastic dishes containing 1.5 ml of suspension culture cells of *P.* x *hybrida* as feeder cells. Gametophytes were also cultured in 3.5-cm plastic dishes in medium solidified with 1% of ultra-low gelling temperature agarose, (type IX, Sigma), with on top a *P.* x *hybrida* suspension culture,

comparable to the double layer culture system as described by Mòl *et al.* (1995). Cultures were maintained at 25 °C and at 16 hours light and 8 hours darkness. Two different culture media were used for the *P.* x *hybrida* gametophytes and feeder cells: an MS medium (Murashige & Skoog, 1962), with modifications according to Kranz and Lörz (1993), containing 1 mg/l thiamine-HCl, 1 mg/l nicotic acid, 1 mg/l pyroxidin-HCl, 1.0 mg/l 2,4-dichlorophenoxyacetic acid (2,4-D), 0.02 mg/l kinetin and 2% sucrose, adjusted to 550 mOsm/kg H_2O with mannitol, pH 5.8. The second medium used was the Comanche medium, a modified MS medium containing 9.9 mg/l thiamine-HCl, 4.5 mg/l nicotic acid, 9.5 mg/l pyroxidin-HCl, 2.0 g/l caseinhydrolysate, 1.0 mg/l 2,4-D, 0.02 mg/l kinetin and 2% sucrose, adjusted to 550 mOsm/kg H_2O with mannitol, pH 5.8.

Results

Megagametophyte development in relation to flower development

Ovary development of fixed and cleared flower buds of various lengths were analyzed in order to correlate ovary development and flower bud size. Within ovaries a gradient in developmental stages existed, with the oldest stages located at the apical part of the ovary and the youngest stages at the basal part of the ovary, see the example in table 1. In one flower bud of 2.8 cm of which the ovary was divided into three parts, in the apical quarter part, 70% of megagametophytes appeared to be in the two-nucleate and four-nucleate stage, whereas in the basal quarter part, 88% of megagametophytes were still in the one-nucleate stage. Also between flower buds with the same length differences in developmental stages of the megagametophytes existed, see table 1: whereas in flower bud (1) most gametophytes are in the one-nucleate stage, in flower bud (3) and (4) most gametophytes are in the four-nucleate stage. Grouping flower buds in different classes according to length, the general progression in megagametophyte development during flower growth is as shown in figure 1. 2 cm flower buds will reach anthesis after three days. In 1.5 % of the ovules mitotic divisions of the gametophyte could be observed. At the onset of anthesis 97% of the ovules have reached the mature stage; in 95% of the embryo sacs the two polar nuclei of the central cell have not fused yet.

Table 1. Percental distribution of female gametophyte developmental stages of four flower buds of a length of 2.8 cm of *Petunia* x *hybrida* cv. Bluebedder.

flower number	ovary part	tetrad	1N	2N	4N	8N
1	apical	3	20	33	37	7
1	middle	4	48	41	7	-
1	basal	6	88	6	-	-
2	middle	3	30	39	26	2
3	middle	-	14	38	44	4
4	middle	1	16	32	43	8

Ovary (1) was divided into a top quarter, middle half and bottom quarter part and the developmental stages in each part were scored. Of the other three flowers only the middle half part was scored. Of each ovary at least 100 ovules were scored.

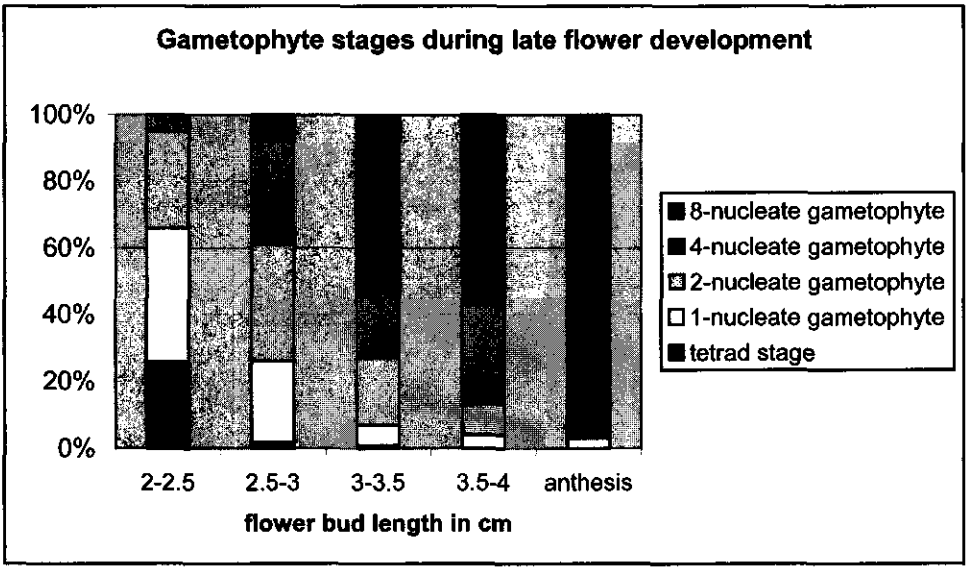

Fig. 1. Percental distribution of female gametophyte stages in different classes of flower bud length. In each class at least 5 flowers were scored and of each flower at least 100 ovules of the middle half part of the ovary were scored for female developmental stage.

Isolation of mature embryo sacs

With a medium containing the enzyme driselase, mature *P.* x *hybrida* embryo sacs can be isolated from the ovular tissues of flowers at anthesis (Van Went & Kwee, 1990). The embryo sac isolation procedure appears to be very sensitive and the yield of isolated embryo sacs depended on factors like the plant variety (high with cv. Bluebedder), the growth stage of the plant (higher with younger plants), and the growth conditions (higher under constant growth chamber conditions compared to high temperature greenhouse conditions in summer). Driselase is a crude fungal enzyme preparation and also the brand and batch of the enzymes used appeared to be important for the yield of isolated embryo sacs. Of the three brands of driselase that we used in our experiments, Sigma (USA), Kyowa Hakko Kogya (Japan), and Fluka (Switzerland), the driselase of Sigma gave the highest yield of isolated mature embryo sacs, which reached up to 20%.

Figures 2a,b show DIC images of a mature embryo sac isolated with driselase. Directly after isolation embryo sacs showed a morphology and organization comparable to the *in planta* situation. All embryo sac cells have retained their position and polarity, with the egg cell nucleus and most of the egg cell cytoplasm located at the chalazal side and the two synergid nuclei and the majority of synergid cell cytoplasm located at the micropylar side of the embryo sac (Fig. 2a,b). Most prominent is the central cell, which possesses a large central vacuole, and a thin layer of peripheral cytoplasm. From PFA_{50}-fixed and Herr-cleared ovaries we know that in flowers at anthesis, in 95% of the megagametophytes, the two polar nuclei of the central cell have not fused yet. In Fig. 2a,b the polar nuclei are invisible because of the large amount of surrounding starch grains. At the chalazal end of the embryo sac, two of the three small antipodal cells can be distinguished (Fig. 2b). Staining with FDA shows viability of the embryo sacs cells (Fig. 2f,h).

Mature embryo sacs could also be isolated with the enzymes cellulase Y-C and Macerozyme (Fig. 2c-e). However, we found that the amount of free embryo sacs in the maceration medium was much lower than when driselase was used, and was never higher than 5%. Whereas the component cells of the embryo sac stayed together when driselase was used in the maceration medium, the cells often appeared as separate protoplasts when cellulase Y-C and Macerozyme were used (Fig. 2c-e).

Though ice crystal damage could not be avoided with the cryofixation procedure employed, the ultrastructure of the cryofixed isolated embryo sacs showed reliable structural details that are not visible with light microscopy (Fig. 3). It appears that two

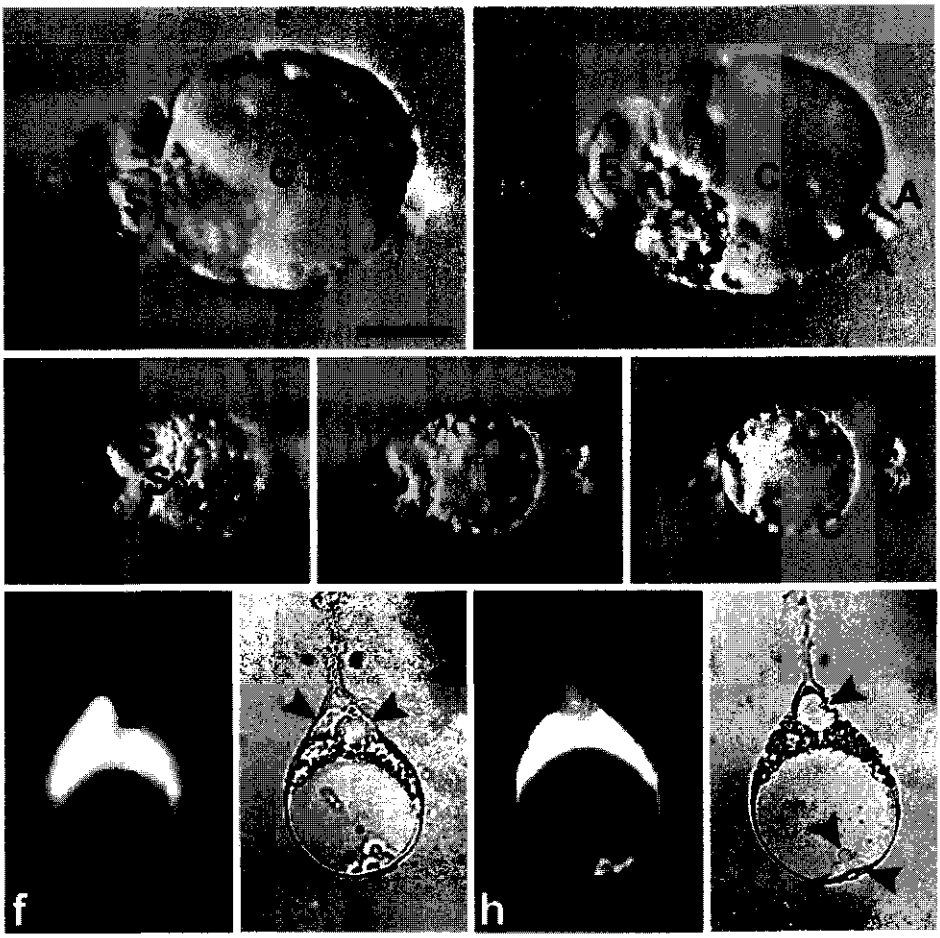

Fig. 2 a-f. Mature embryo sacs two hours after isolation. (a,b) DIC images of an embryo sac isolated with the enzyme driselase, and showing the egg cell (*E*), the two synergid cells (*S*), the central cell (*C*) and two of the three antipodal cells (*A*). (c-e) DIC images of embryo sac cells isolated with the enzymes cellulase Y-C and Macerozyme, showing the separate synergid cells (*S*), the egg cell (*E*), the central cell (*C*) and two of the three antipodal cells (*A*). (f,h) Embryo sac demonstrating fluorescence after treatment with FDA, indicative of viability. (g,i) Bright field images of the same embryo sac as shown in (f,h). Arrowheads point at the different embryo sac cells. Bar (a,b) is 25 μm; Bar (c-i) is 25 μm.

hours after isolation cell walls and the filiform apparatus have completely dissolved (arrows in Fig. 3). In some chalazal areas of the egg cell and synergid cells, plasma membranes are still very closely aligned with the central cell plasma membrane (arrowheads in Fig. 3c,d,f), whereas in other areas they have completely separated. The vacuoles of the highly vacuolated cells are intact. A thin layer of cytoplasm is located at the periphery of the cells and the major cytoplasmic volume is located at either the micropylar pole (synergid cells, Fig. 3b; central cell, Fig. 3e) or chalazal pole (egg cell, Fig. 3c) of the embryo sac cells. Cytoplasmic organization is largely comparable to the *in planta* situation (chapter 5 of this thesis). However, the occurrence of e.g. concentric rings of endoplasmic reticulum at the chalazal side of one synergid cell (Fig. 3d), which was never observed in *P.* x *hybrida* synergid cells *in planta* (chapter 5 of this thesis) indicates that the isolation procedure may cause some changes in cytoplasm organization. Nuclei of the egg cell (Fig. 3c), synergid cells (Fig. 3b) and central cell (Fig. 3e) are largely euchromatic and comparable in organization to the *in planta* situation (chapter 5 of this thesis).

Isolation of immature megagametophytes

By incubating ovules of flower buds in a maceration medium containing the enzymes cellulase Y-C and Macerozyme, megaspores with surrounding nucellar cells and immature megagametophytes could be isolated. However, the yield of isolated gametophyte cells did not reach the yield of isolated mature embryo sacs, and was never higher than 5%. Figure 4 shows DIC images of megagametophytes isolated at the one-nucleate (a), two-nucleate (b), and four-nucleate (c,d) stage.

Megaspores are still surrounded by nucellar cells, and their nuclei can not be observed with light microscopy (not shown). From electron microscopy sections it appeared that all cell walls have dissolved and that megaspores and nucellus cells were kept together by a cuticle-like structure that surrounds them (not shown). Cell walls of the hypostase cells have not dissolved. In one-nucleate gametophytes degenerating cells are still present at the micropylar side of the gametophyte (Fig. 4a). The megagametophyte has already formed a central vacuole and the nucleus is located at its lateral side (arrowheads in Fig. 4a).

Whereas in the maceration medium used for isolating mature embryo sacs, driselase caused the degeneration of the integument cells, in the maceration medium with cellulase Y-C and Macerozyme, many integument protoplasts could be found. Also fusion products of integument cells appeared in the medium, containing up to 12 nuclei

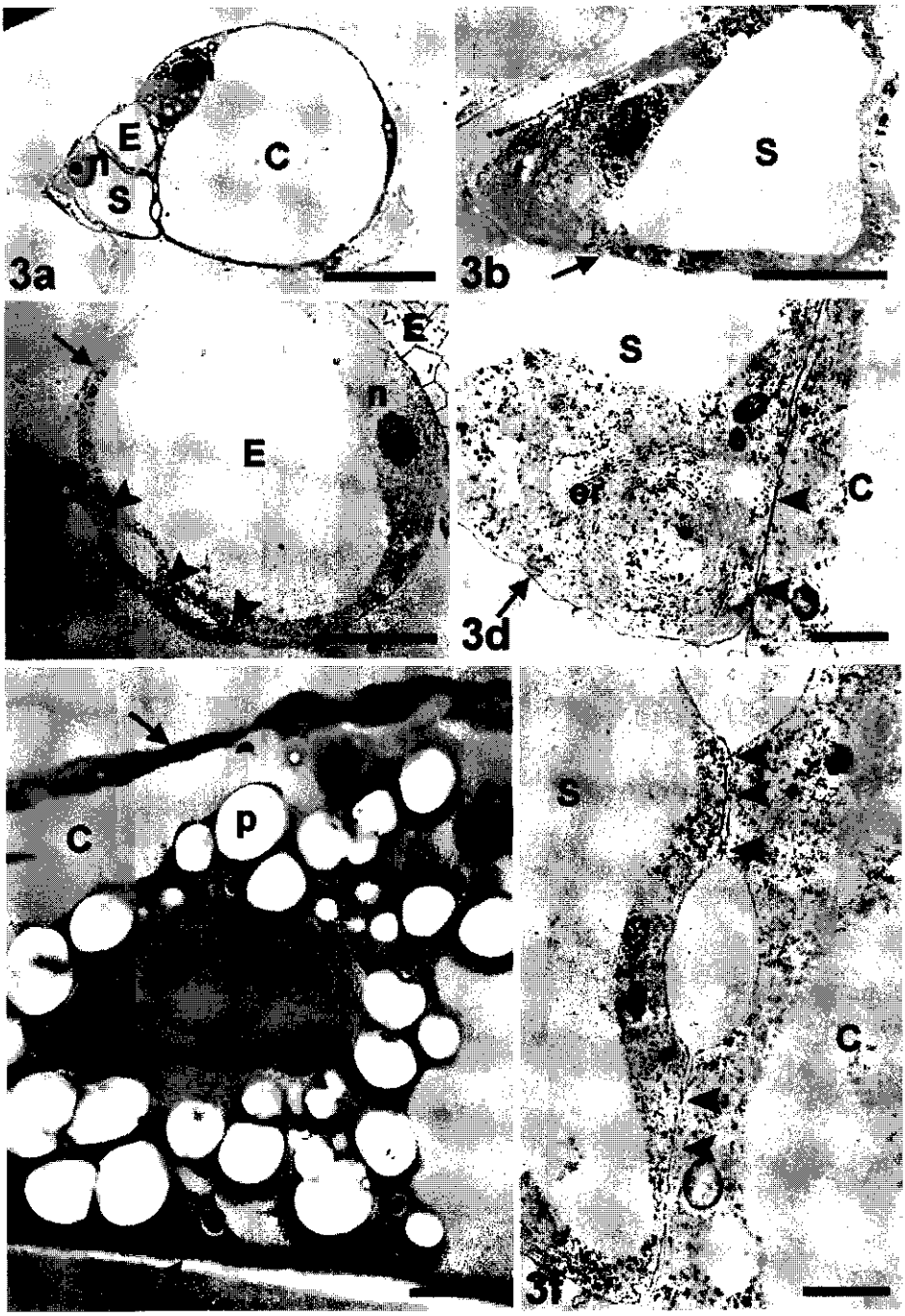
E
C
n
S
3a
S
3b
E
n
E
S
er
C
3d
C
p
S
C
3f

(results not shown). The two-nucleate and four-nucleate gametophytes could be recognized in the mixture of protoplasts by the attached hypostases (Fig. 4b-d). Figure 4b shows a two-nucleate megagametophyte, with one nucleus located at its chalazal pole and one nucleus at its lateral side (arrowheads). The four-nucleate megagametophyte has two nuclei at its chalazal and two nuclei at its micropylar pole (arrowheads in Fig. 4c,d), with a large central vacuole in between, which is comparable to the *in planta* situation.

Coenocytic eight-nucleate embryo sacs were never found. Staining with FDA showed that gametophytes were viable directly after isolation (Fig. 4e).

Culture experiments with isolated megagametophytes

Directly after isolation megagametophyte organization strongly resembles the organization *in planta* (compare Fig. 4 with Fig. 1 in chapter 4 of this thesis). Figure 5 shows young megagametophytes at two hours after isolation (a,d,g), one day after isolation (b,e,h), and two days after isolation (c,f,i). In Fig. 5a-c the same one-nucleate megagametophyte was observed, within a microscopic micro-culture chamber. During culture the megagametophyte became more spherical in shape. Though the megagametophyte still seemed turgescent two days after isolation, four days after isolation it had collapsed. Culture of megagametophytes in Milli-cell inserts (Fig. 5d-f) or embedding megagametophytes in agarose (Fig. 5g-i) did not improve the life span of young isolated megagametophytes *in vitro*, and generally, three days after isolation all gametophytes had died. With the latter two culture methods it appeared difficult to monitor organizational changes within the gametophytes. Nuclear divisions were never observed.

Fig. 3 a-f. Mature cryofixed embryo sacs two hours after isolation. (a) Light microscopic image of a section of an embryo sac stained with toluidine blue, showing the egg cell, one of the synergid cells and the central cell. (b-f) Electron micrographs. In all micrographs the micropylar part of the embryo sac is oriented to the left. (b) Overview of one of the synergid cells. (c) Overview of the egg cell. The egg cell plasma membrane is still very closely aligned with the synergid cell plasma membrane in some areas (*arrowheads*). (d) Detail of chalazally located synergid cell cytoplasm, with concentric rings of endoplasmic reticulum (*er*). (e) Detail of the central cell cytoplasm with one of the polar nuclei (*pn*), and many starch containing plastids (*p*). (f) Whereas plasma membranes of the synergid cell (*S*) and the central cell (*C*) have completely separated in some areas, in other areas they are still very closely aligned (*arrowheads*). *C*, central cell; *E*, egg cell; *n*, nucleus; *no*, nucleolus; *S*, synergid cell; *arrows*, plasma membranes. Bars are (a) 20 μm, (b,c) 5 μm, (d,f) 1 μm and (e) 2 μm.

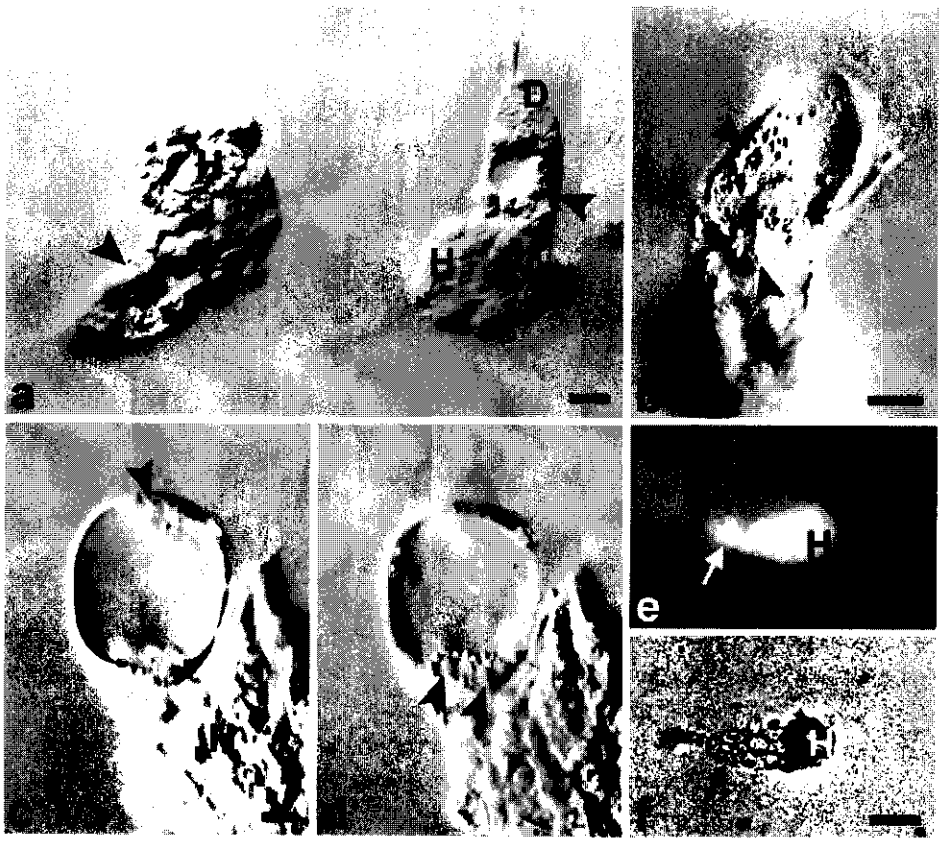

Fig. 4 a-f. Immature megagametophytes 2-4 hours after isolation. DIC images of two one-nucleate megagametophytes (a), a two-nucleate megagametophyte (b), and a four-nucleate megagametophyte (c,d). Arrowheads indicate the positions of the nuclei. (e) Immature megagametophyte (*arrow*) demonstrating fluorescence after treatment with FDA, indicative of viability. (f) Bright field image of the same megagametophyte (*arrow*) as shown in (e). *D*, degenerating cells, *H*, hypostase. Bars are (a-d) 10 μm and (e,f) 25 μm.

Directly after isolation also mature isolated embryo sacs have an organization similar to *in planta* embryo sacs (compare Fig. 6a,b with Fig. 1 in chapter 5 of this thesis). After a few hours in culture, the embryo sac cells became spherical in shape and they partly separated from each other. (Fig. 3c,f). Generally, the embryo sac cells stayed together, but even if cells had completely separated from each other, they could still be recognized because of their size and their amount of cytoplasm (Fig. 2c-e).

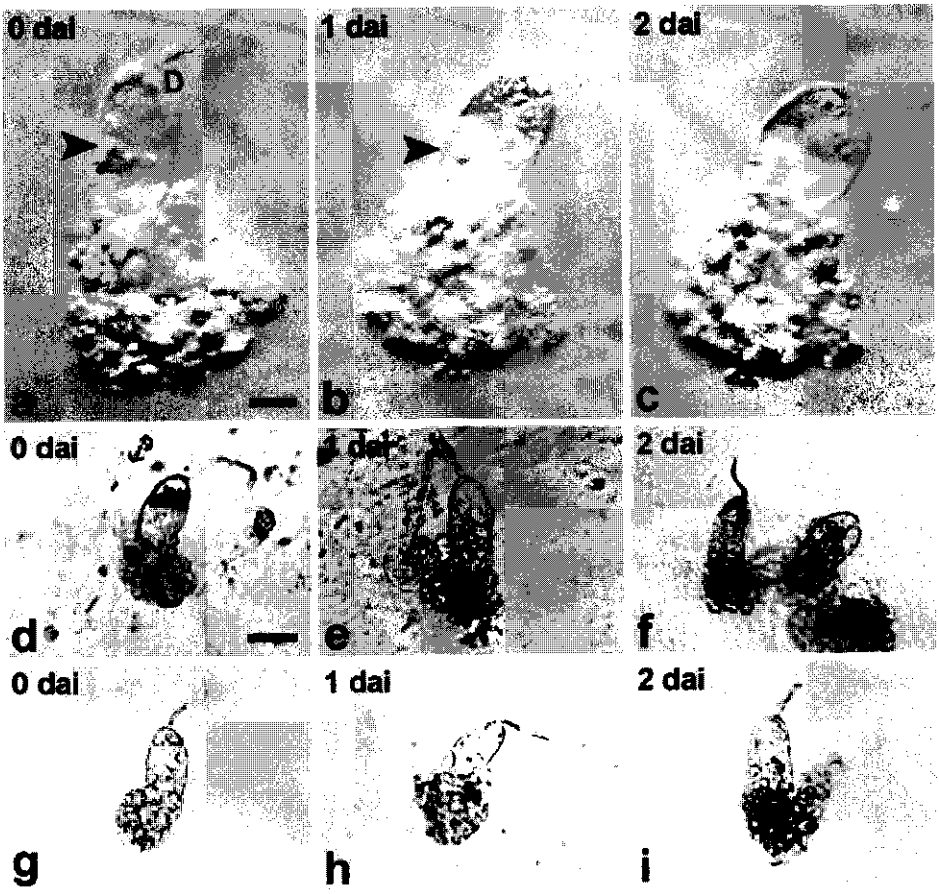

Fig. 5 a-i. Immature megagametophytes at two hours after isolation (0 DAI), one day after isolation (1 DAI) and two days after isolation (2 DAI). (a-c) DIC images of the same isolated one-nucleate megagametophyte in a microscopic micro-culture chamber at 0 DAI (a), 1 DAI (b) and 2 DAI (c). Arrowheads point at the nucleus. (d-f) Bright field images of megagametophytes in Millicell inserts, cultured with a *P.* x *hybrida* feeder suspension at 0 DAI (d), 1 DAI (e) and 2 DAI (f). (g-i) Bright field images of megagametophytes embedded in agarose, cultured with a *P.* x *hybrida* feeder suspension at 0 DAI (g), 1 DAI (h) and 2 DAI (i). Bars are (a-c) 10 μm and (d-i) 25 μm.

In the synergid cells and egg cells hardly any organizational changes were observed during culture. After three days the cells of the egg apparatus generally had degenerated (Fig. 6h).

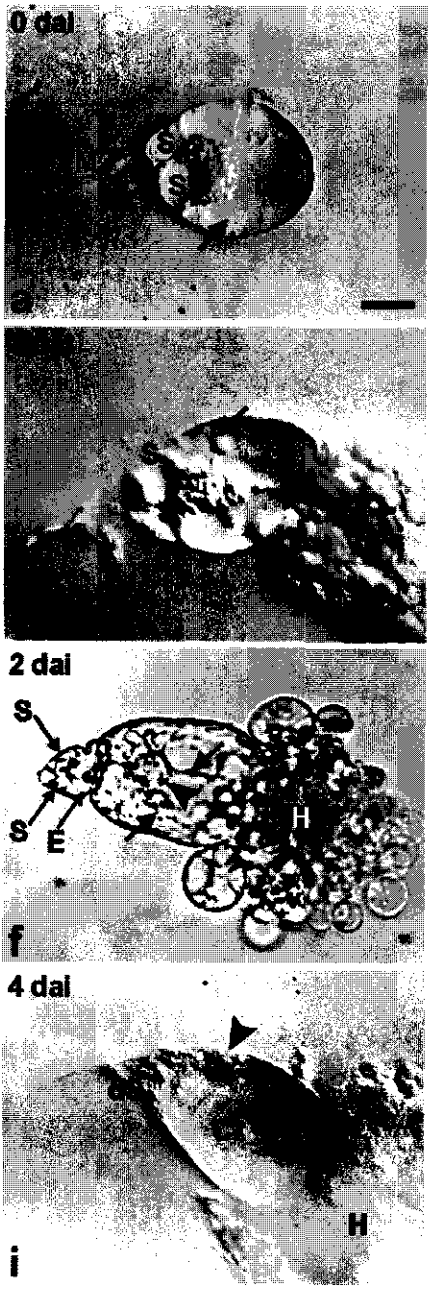

Fig. 6 a-k. Mature isolated embryo sacs at different days after isolation (DAI) and feeder suspension cells. (a,c, f, h, i) Isolated embryo sacs in a microscopic micro-culture chamber at 0 DAI (a), 1 DAI (c), 2 DAI (f), 3 DAI (h), and 4 DAI (i). (b,d,g) Isolated embryo sacs in Milli-cell inserts, cultured with a *P.* x *hybrida* feeder suspension at 0 DAI (b), 1 DAI (d) and 2 DAI (g). (e) Isolated embryo sac, embedded in agarose, cultured with a *P.* x *hybrida* feeder suspension at 1 DAI. (j) *P.* x *hybrida* feeder suspension cells in Comanche medium. (k) *P.* x *hybrida* feeder suspension cells in MS medium. *C*, central cell; *E*, egg cell; *H*, hypostase; *M*, remnants of a cuticle aligning the micropyle; *S*, synergid cell; *dS*, degenerated synergid cells; *arrow*, cytoplasmic strands in the central cell; *arrowhead*, central cell nucleus.
Bar is (a-k) 25 μm.

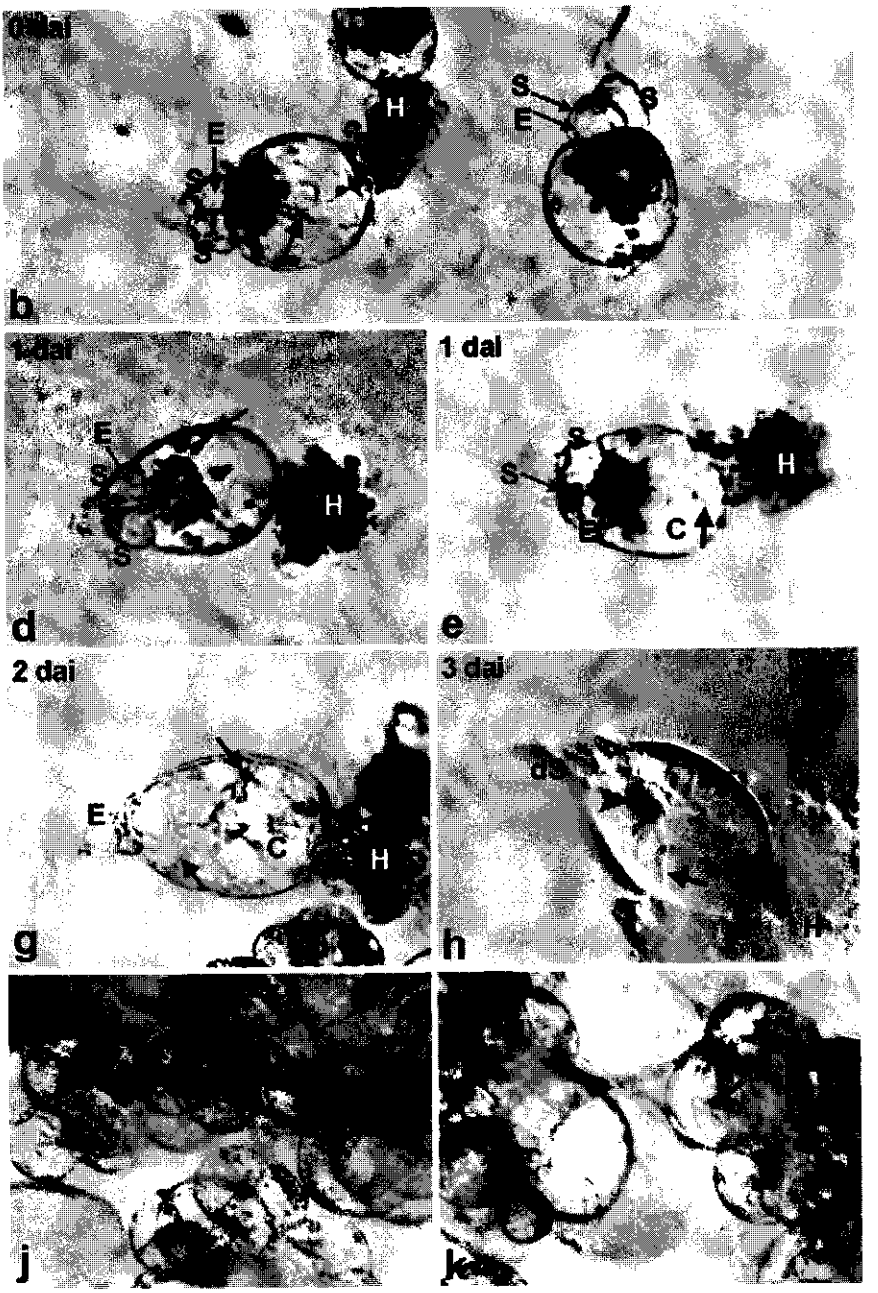
0 dai
H
E
S
S
S
S
S
E
S
b
1 dai
E
S
S
H
d
1 dai
S
S
E
C
H
e
2 dai
E
S
C
H
g
3 dai
H
h
j
k

The central cell changed dramatically during culture. Within a few hours after isolation transvacuolar strands were formed (arrows in Fig. 6). Within these strands a rapid directional movement of organelles was visible, indicating the viability of the cell. The majority of central cell cytoplasm, including the nuclei, moved from a position close to the egg apparatus, to a more central position in the cell (Fig. 6c,d). Surrounded by the large amount of starch grains, the central cell nuclei can not be discerned with light microscopy (Fig. 6a-e). From Herr-cleared ovules we know that at anthesis 92% of the embryo sacs show central cells with two polar nuclei, whereas in 5% of the embryo sacs the polar nuclei have already fused. During culture the starch grains gradually disappeared from the central cell and after two days in culture hardly any starch was present (Fig. 6f,g), which demonstrates the metabolic activity of the central cell *in vitro*. It is visible that the two polar nuclei have fused, with the fusion nucleus located in the centre of the cell (Fig. 6f). After four days of culture, the transvacuolar strands had disappeared and the central cell nucleus had moved to the cell periphery, but the cell still remained turgescent (Fig. 6i). In some cases the plasma membranes and vacuolar membranes remained stable for up to five days after isolation.

Comparing the different culture systems, microscopic micro-culture chambers (Fig. 6a,c,f,h,i) and Milli-cell inserts (Fig. 6b,d,g) or agarose (Fig. 6e) with a *P.* x *hybrida* feeder suspension, no differences in viability of the cells could be observed. More than 100 megagametophytes have been monitored in the three different culture systems each.

Figure 6j shows *P.* x *hybrida* suspension cells cultured in Comanche medium and figure 6k shows suspension cells in MS medium. In both media cell suspensions consisted of highly vacuolated cells. No differences between both media in relation to viability of isolated embryo sacs could be observed.

Discussion

Isolation procedures

At our laboratory an enzymatic maceration method in which the enzyme driselase is used was developed to isolate mature *P.* x *hybrida* embryo sacs of flowers at anthesis from the surrounding integuments (Van Went & Kwee, 1990). To keep damaging effects of the maceration medium on the gametophytic cells as minimal as possible and to enhance their life span *in vitro* we made some modifications to the isolation procedure. However, the embryo sac isolation procedure appeared to be very sensitive.

In general, the successful isolation of protoplasts depends on many factors, including the kind of tissue, plant species and variety, enzyme combination and concentration, and physiological status of the plant (Power & Chapman, 1985). Also for the successful isolation of female gametophytes it has been reported that each species and female gametophyte developmental stage need its own combination and concentration of enzymes, pH of the medium, osmotic pressure, duration of enzyme incubation time, temperature, and force of mechanical agitation (see review by Huang & Russell, 1992). These factors also appeared to be important for *P.* x *hybrida* gametophyte isolation. Additionally, the yield of isolated embryo sacs appeared to depend on the brand of the enzymes used. Driselase is a mixture of endo- and exo-enzymes from the fungus *Irpex lacteus* with amongst others cellulase, galactanase, arabinase, pectinase, mannase and xylanase activity. Of the three brands of driselase that we used, Sigma (USA), Kyowa Hakko Kogya (Japan), and Fluka (Switzerland), driselase of Sigma gave the highest yield of isolated mature embryo sacs, which reached up to 20%.

Several authors used driselase in the maceration mixture for the isolation of viable megagametophytes (Hu *et al.*, 1985; Wu *et al.*, 1993; Li & Hu, 1986; Mouritzen & Holm, 1995; Sidorova, 1985). The incubation of *P.* x *hybrida* ovules of flowers at anthesis with a driselase containing maceration medium, resulted in the degeneration of all ovular cells with the exception of the mature, cellular embryo sacs. If young flower buds were macerated in the same medium, hardly any intact immature megagametophytes could be discerned after the incubation period. Deleterious effects of the enzymes on the megagametophytes can not be ruled out. Leduc and coworkers (1995) reported an adverse effect of enzymatic treatment on the development of isolated maize embryo sacs in culture. In their studies enzymatically isolated egg cells were not able to fuse with sperm cells. Kranz and co-workers (1995) found no differences in the fusing ability of maize egg protoplasts that were isolated after a treatment with cell wall degrading enzymes, or were completely mechanically isolated.

P. x *hybrida* megaspores and one-nucleate, two-nucleate, and four-nucleate megagametophytes were more efficiently isolated with a medium in which the driselase was replaced by cellulase Y-C and Macerozyme. Also mature embryo sacs could be isolated from their surrounding sporophytic tissues with a cellulase Y-C and Macerozyme containing medium, though only in very low amounts. And whereas the yield of mature embryo sacs, isolated with driselase reached up to 20%, the yield of immature megagametophytes, isolated with cellulase Y-C and Macerozyme, was never higher than 5%. The one-nucleate stage was more efficiently isolated than the two- and four-nucleate stages.

Imre and Kristof (1999) reported changes in osmotic pressure during *Torenia fournieri* gametophyte development. Osmotic pressure was lowest at the megaspore stage, increased until the four-nucleate megagametophyte stage and then gradually decreased until the mature embryo sac stage. For the isolation of the different developmental stages of *Torenia* megagametophytes, adjustment of the osmolarity of the enzyme solution for each specific stage appeared crucial. We used the same maceration medium with an osmolarity of 600 mOsm/kg H_2O for the isolation of all developmental megagametophyte stages. Sub-optimal osmolarity of the enzymatic maceration medium for certain *P.* x *hybrida* megagametophyte stages might have influenced the yield of isolated megagametophytes in our experiments.

After incubation of *P.* x *hybrida* ovules with a cellulase Y-C and Macerozyme containing medium many protoplasts were present in the cell suspension; moreover multinucleate cells, fusion products of integument cells caused by Macerozyme were identified. Precise developmental staging of megagametophytes appeared impossible due to a gradient in megagametophyte developmental stages within one ovary. For these reasons recognition of immature megagametophytes in the cell suspension resulting after the enzymatic incubation was very difficult. Female gametophytes could only be recognized as such if the hypostases stayed attached to them.

Structure of isolated megagametophytes

Light microscopic analysis by DIC optics suggests that the morphology and structure of the megagametophytes directly after isolation were not greatly affected by the isolation procedure (see Figs. 2 and 4). FDA staining proved their viability. However, because the maintenance of nuclear and cytoplasmic structure and integrity after isolation are essential when aiming subsequent *in vitro* culture and development, we fixed, embedded and sectioned isolated megagametophytes for a more detailed structural analysis.

In preliminary experiments isolated *P.* x *hybrida* megagametophytes were prepared for microscopy by embedding them in ultra-low gelling temperature agarose, followed by chemical fixation. This methodology enabled a successful ultrastructural characterization of isolated maize egg cells (Faure *et al.*, 1992) and *Plumbago* egg cells (Cao & Russell, 1997). From our experiments it appears that after enzymatic maceration the cell walls of most cells have completely dissolved, including the cell walls of the nucellus cells located around the megaspores. Like already supposed for snapdragon embryo sacs (Zhou & Yang, 1985), *P.* x *hybrida* megaspores and nucellus

protoplasts are kept together by a cuticle-like structure that surrounds them (not shown). Cell walls of the chalazal tissues did not dissolve.

Because isolated *P.* x *hybrida* embryo sacs appeared to be very fragile structures, which were observed to change in structure and collapse during chemical fixation, we cryofixed and freeze substituted a number of isolated mature embryo sacs. These experiments showed that though the individual cells of the embryo sac seemed without cell walls, membranes between the individual cells still stayed very closely aligned to each other in some areas. In some places remnants of a cuticle-like structure were present at the surface of the embryo sac. Cell polarity and nuclear structure appeared comparable to the situation *in planta* (chapter 5 of this thesis).

Faure and co-workers (1992) reported in an ultrastructural study on isolated egg cells of maize, that, though the cells change in shape after isolation, the organelles appeared to be ultrastructurally intact, i.e. comparable to the *in planta* situation. Cao and Russell (1997) reported the same for *Plumbago*, i.e. a comparable ultrastructural organization of isolated egg cells and *in planta* egg cells; however, the accumulation of electron dense particles within the plastids of isolated egg cells might reflect a degenerating state of these organelles. Though at first sight isolated megagametophytes seem ultrastructurally intact, ice crystal damage in the isolated cells rendered *P.* x *hybrida* preparations unsuitable for detailed ultrastructural comparisons with *in planta* megagametophytes. Enclosing isolated megagametophytes in cellulose capillary tubes, and cryofixing them by high pressure freezing, as described for cell suspensions by Hohenberg *et al.* (1994), might be an option to adequately preserve the ultrastructure of isolated *P.* x *hybrida* megagametophytes. This may allow the detection of degenerative changes after isolation, as well as the accurate monitoring of developmental changes during *in vitro* culture.

Culture experiments

Pollen protoplasts cultured under appropriate conditions can sustain gametophyte development as well as be triggered into sporophytic development (reviewed by Yang & Zhou, 1992). Within a number of species, ovules and ovaries cultured *in vitro*, can sustain the normal pattern of megagametophyte development, but *in vitro* culture can also lead to gynogenesis, i.e. the *in vitro* development of embryos and plants from unfertilized embryo sacs (reviewed by Mòl, 1999). The isolation of viable megagametophytes creates opportunities for experimental studies of megagametophyte development at the single cell level, which will enhance insight in the

process of gametophyte differentiation and function. A prerequisite for studies on gametophyte *in vitro* development is the availability of a culture system that sustains the development of the isolated cells. Different from pollen protoplasts, female gametophytes can only be isolated in small quantities, restricting their culture to the use of conditioned media, the culture together with nurse cells, or growing the cells in very low culture volumes (Spangenberg & Koop, 1992).

Jones *et al.* (1960) reported the division and growth of single vacuolated somatic cells of tobacco in micro-culture chambers made of microscope slides; the small volume of medium in this chamber had been previously conditioned by a mass of growing cells. This type of micro-culture chamber together with the low density culture medium for the growth of cells derived from *Petunia* protoplasts, as described by Muller *et al.* (1983), made it possible to characterize the isolated *P.* x *hybrida* megagametophytes and follow them for a number of days with high optical resolution. Though megagametophyte cells stayed viable for a maximum of five days and some changes in cell structure and organization could be observed, cell divisions were never detected.

The cultivation of *in vivo* fertilized isolated zygotes of barley (Holm *et al.*, 1994), maize (Leduc *et al.*, 1996), and wheat (Holm *et al.*, 1994; Kumlehn *et al.*, 1998) resulted in the formation of embryos or embryo-like structures, and subsequent plant regeneration was possible. Also *in vitro* fertilized egg cells of maize are able to develop into embryos in culture (Kranz & Lörz, 1993), whereas *in vitro* fertilized central cells are able to develop into an endosperm tissue (Kranz *et al.*, 1998), thus being able to self-organize without the presence of maternal tissues. In all these studies the quality of the feeder cell culture appeared to be important for sustained development (reviewed by Kranz & Kumlehn, 1999). The *P.* x *hybrida* feeder cell suspension that we used in our experiments may lack the qualities for sustaining the development of isolated female gametophytes.

Only few reports have been published on the culture of isolated mature unfertilized embryo sacs or their component cells (Holm *et al.*, 1994; Kovács *et al.*, 1995; Kranz *et al.*, 1991; Kranz & Lörz, 1993; Mòl, 1986; Tian & Russell, 1997). Under standard culture conditions (2 mg/l 2,4-D in the culture medium), in which *in vitro* fertilized egg cells of maize developed into structures resembling *in vivo* zygotic embryos, unfertilized maize egg cells remained viable for three weeks but never divided (Kranz *et al.*, 1991, 1995, Kranz & Lörz, 1993). It was still possible to fuse isolated egg cells, cultured for six to nine days, with sperm cells, once the cell membrane was free of cell wall material (Kranz *et al.*, 1995). Also *in vitro* cultured isolated central cells of maize (Kranz *et al.*, 1998) and egg cells of wheat (Kovács *et al.*, 1995) and barley (Holm *et al.*,

1994) stayed viable for several days or more, but only divided after fusion with sperm cells. In similarity to the above mentioned cereals, in mature isolated embryo sacs of tobacco (Wu *et al.*, 1993) and *Torenia fournieri* (Mòl, 1986) cell division was never observed within the culture period of one week and two weeks after isolation, respectively. However, Tian and Russell (1997) did report a first nuclear division of isolated unfertilized tobacco egg cells and synergid cells within a feeder cell supported micro-chamber culture, with a medium containing 1 mg/l 2,4D, in which both cell types required a specific osmolarity of the culture medium (460-480 mOsm/kg H_2O and 530 mOsm/kg H_2O respectively). After three days in solid-drop culture some unfertilized egg cells divided to form a small apical cell and a larger basal cell (Tian & Russell, 1997). In isolated unfertilized maize egg cells only short treatments with high amounts of 2,4-D (concentrations of 25 up to 40 mg/l 2,4-D) could induce cell division, but only in four out of 68 isolated egg cells (Kranz *et al.*, 1995).

When mature isolated *P.* x *hybrida* embryo sacs were cultured in Milli-cell inserts surrounded by a *P.* x *hybrida* cell suspension culture, embryo sacs remained alive in culture for up to five days. The egg cell and synergid cells had generally degenerated after three days. *In planta* one of the *P.* x *hybrida* synergids degenerates after it has been penetrated by the pollen tube; the other synergid degenerates at a later stage (Van Went, 1970). The most prominent changes during culture appeared in the central cell and were the formation of transvacuolar strands, the fusion of the two polar nuclei and the movement of the central cell fusion nucleus to the centre of the cell, comparable to the *in planta* situation after fertilization (Van Went, 1970). However, in none of our culture experiments division of embryo sac cells could be detected.

Mòl *et al.* (1995) found that for the culture of zygotes of maize a double layer system, with the isolated embryo sacs in a solidified medium covered with liquid medium, was much more efficient for embryo development compared to liquid medium only. In our experiments with isolated agarose embedded *P.* x *hybrida* female gametophytes, with on top a feeder suspension, we could not detect any differences in cell longevity compared to the feeder cell supported culture in liquid medium.

The isolation of living megasporocytes, megaspores, and/or immature coenocytic megagametophytes has only been reported for few angiosperm species (Wagner *et al.*, 1989a; Wu *et al.*, 1993; Mouritzen & Holm, 1995; Kristóf & Imre, 1996, Imre & Kristóf, 1999). Though sustained development of these cells *in vitro* may be easier compared to mature embryo sac cells, that are completely differentiated cells, and that *in planta* wait for the trigger of fertilization to continue development, this has not been published yet. Mouritzen and Holm (1995) reported on the culture of isolated barley megasporocytes

with the aim of their studies to analyze and eventually manipulate meiosis. The co-cultivation of megasporocytes with barley microspores undergoing embryogenesis prolonged the viability from three days to one week or longer, but division of the cells never occurred (Mouritzen & Holm, 1995). In our *in vitro* studies with isolated megaspores and immature *P.* x *hybrida* megagametophytes nuclear or cellular divisions were never observed either.

In conclusion: If techniques can be developed that prolong the viability and induce division in culture, the isolation of immature megagametophytes and their *in vitro* culture may be a promising tool for the study of the early stages of female gametophyte development. The induction of division of isolated mature megagametophyte cells seems to require a strong trigger, either high concentrations of growth regulators or (*in vitro*) fertilization, or so far undiscovered other triggers. Such triggers need to be discovered in order to induce divisions and open the possibility to use the described technology for production of gynogenic (doubled) haploids. Successful female gametophyte culture will open possibilities for both, fundamental and applied research.

Acknowledgements

We are grateful to Prof. H. Lörz and Dr. E. Kranz for giving M. Thijssen the opportunity to visit the Institut für Allgemeine Botanik, Angewandte Molekularbiologie der Pflanzen II, Universität Hamburg, Germany. The visit was supported by a grant from the EC, project BIOT-0180-NL. Critical reading of the manuscript by Dr. A. Mordhorst and Prof. A.M.C. Emons is appreciated.

References

Bednara, J., Willemse, M.T.M. & Van Lammeren, A.A.M. (1990). Organization of the actin cytoskeleton during megasporogenesis in *Gasteria verrucosa* visualized with fluorescent-labelled phalloidin. Acta Bot. Neerl. 39, 43-48.

Cao, Y. & Russell, S.D. (1997). Mechanical isolation and ultrastructural characterization of viable egg cells in *Plumbago zeylanica*. Sex. Plant Reprod. 10, 368-373.

Dumas, C. & Mogensen, H.L. (1993). Gametes and fertilization: Maize as a model system for experimental embryogenesis in flowering plants. Plant Cell 5, 1337-1348.

Faure, J.-E., Mogensen, H.L., Kranz, E., Digonnet, C. & Dumas, C. (1992). Ultrastructural characterization and three-dimensional reconstruction of isolated maize (*Zea mays* L.) egg cell protoplasts. Protoplasma 171, 97-103.

Frearson, E.M., Power, J.B. & Cocking, E.C. (1973). The isolation, culture and regeneration of *Petunia* leaf protoplasts. Dev. Biol. 33, 130-137.

Herr, J.M. Jr (1971). A new clearing-squash technique for the study of ovule development in angiosperms. Am. J. Bot. 58, 785-790.

Heslop-Harrison, J. & Heslop-Harrison, Y. (1970). Evaluation of pollen viability by enzymatically-induced fluorescence: Intracellular hydrolysis of fluorescein diacetate. Stain. Technol. 45, 1115-120.

Hohenberg, H., Mannweiler, K. & Müller, M. (1994). High-pressure freezing of cell suspensions in cellulose capillary tubes. J. Microsc. 175, 34-43.

Holm, P.B., Knudsen, S., Mouritzen, P., Negri, D., Olsen, F.L. & Roué, C. (1994). Regeneration of fertile barley plants from mechanically isolated protoplasts of the fertilized egg cell. Plant Cell 6, 531-543.

Hu, S.-Y., Li, L.-G. & Zu, C. (1985) Isolation of viable embryo sacs and their protoplasts of *Nicotiana tabacum*. Acta Bot. Sin. 27, 337-344.

Huang, B.-Q., Pierson, E.S., Russell, S.D., Tiezzi, A. & Cresti, M. (1992). Video microscopic observations of living, isolated embryo sacs of *Nicotiana* and their component cells. Sex. Plant Reprod. 5, 156-162.

Huang, B.-Q., Pierson, E.S., Russell, S.D., Tiezzi, A. & Cresti, M. (1993). Cytoskeletal organisation and modification during pollen tube arrival, gamete delivery and fertilisation in *Plumbago zeylanica*. Zygote 1, 143-154.

Huang, B.-Q. & Russell, S.D. (1989). Isolation of fixed and viable eggs, central cells, and embryo sacs from ovules of *Plumbago zeylanica*. Plant Physiol. 90, 9-12.

Huang, B.-Q. & Russell, S.D. (1992). Female germ unit: Organization, isolation, and function. Int. Rev. Cytol. 140, 233-293.

Huang, B.-Q. & Russell, S.D. (1993). Polarity of nuclear and organellar DNA during megasporogenesis and megagametogenesis in *Plumbago zeylanica*. Sex. Plant Reprod. 6, 205-211.

Huang, B.-Q. & Russell, S.D. (1994). Fertilization in *Nicotiana tabacum*: Cytoskeletal modifications in the embryo sac during synergid degeneration. A hypothesis for short-distance transport of sperm cells prior to gamete fusion. Planta 194, 200-214.

Huang, B.-Q. & Sheridan, W.F. (1994). Female gametophyte development in maize: Microtubular organization and embryo sac polarity. Plant Cell 6, 845-861.

Huang, B.-Q. & Sheridan, W.F. (1996). Embryo sac development in the maize *indeterminate gametophyte1* mutant: Abnormal nuclear behavior and defective microtubule organization. Plant Cell 8, 1391-1407.

Huang, B.-Q. & Sheridan, W.F. (1998). Actin coronas in normal and *indeterminate gametophyte1* embryo sacs of maize. Sex. Plant Reprod. 11, 257-264.

Imre, K. & Kristóf, Z. (1999). Isolation and osmotic relations of developing megagametophytes of *Torenia fournieri*. Sex. Plant Reprod. 12, 152-157.

Jones, L.E., Hildebrandt, A.C., Riker, A.J. & Wu, J.H. (1960). Growth of somatic tobacco cells in microculture. Am. J. Bot. 47, 468-475.

Kapil, R.N. & Bhatnagar, A.K. (1981). Ultrastructure and biology of female gametophyte in flowering plants. Int. Rev. Cytol. 70, 291-341.

Kovács, M., Barnabás, B. & Kranz, E. (1994). The isolation of viable egg cells of wheat (*Triticum aestivum* L.). Sex. Plant Reprod. 7, 311-312.

Kovács, M., Barnabás, B. & Kranz, E. (1995). Electro-fused isolated wheat (*Triticum aestivum* L.) gametes develop into multicellular structures. Plant Cell Rep. 15, 178-180.

Kranz, E., Bautor, J. & Lörz, H. (1991). *In vitro* fertilization of single, isolated gametes of maize mediated by electrofusion. Sex. Plant Reprod. 4, 12-16.

Kranz, E. & Kuhmlehn, J. (1999). Angiosperm fertilisation, embryo and endosperm development *in vitro*. Plant Sci. 142, 183-197.

Kranz, E. & Lörz, H. (1993). *In vitro* fertilization with isolated, single gametes results in zygotic embryogenesis and fertile maize plants. Plant Cell 5, 739-746.

Kranz, E., Von Wiegen, P. & Lörz, H. (1995). Early cytological events after induction of cell division in egg cells and zygote development following *in vitro* fertilization with angiosperm gametes. Plant J. 8, 9-23.

Kranz, E., Von Wiegen, P., Quader, H. & Lörz, H. (1998). Endosperm development after fusion of isolated, single maize sperm and central cells *in vitro*. Plant Cell 10, 511-524.

Kristóf, Z. & Imre, K. (1996). Isolation of living megaspores of *Torenia fournieri*. Protoplasma 192, 245-248.

Kumlehn, J., Lörz, H. & Kranz, E. (1998). Differentiation of isolated wheat zygotes into embryos and normal plants. Planta 205, 327-333.

Leduc, N., Matthys-Rochon, E. & Dumas, C. (1995). Deleterious effect of minimal enzymatic treatments on the development of isolated maize embryo sacs in culture. Sex. Plant Reprod. 8, 313-317.

Leduc, N., Matthys-Rochon, E., Rougier, M., Mogensen, L., Holm, P., Magnard, J.-L. & Dumas, C. (1996). Isolated maize zygotes mimic *in vivo* embryonic development and express microinjected genes when cultured *in vitro*. Dev. Biol. 177, 190-203.

Li, L.-G. & Hu, S.-Y. (1986). Enzymatic isolation and observation of protoplasts of embryo sac elements of *Atropa belladonna*. Acta Biol. Exp. Sin. 19, 252-259.

Möl, R. (1986). Isolation of protoplasts from female gametophytes of *Torenia fournieri*. Plant Cell Rep. 3, 202-206.

Mòl, R. (1999). Embryological aspects of *in vitro* gynogenesis in plant organ cultures. Acta Biol. Cracoviensia 41: 67-74.

Mòl, R., Matthys-Rochon, E. & Dumas, C. (1995). Embryogenesis and plant regeneration from maize zygotes by *in vitro* culture of fertilized embryo sacs. Plant Cell Rep. 14, 743-747.

Mouritzen, P. & Holm, P.B. (1995). Isolation and culture of barley megasporocyte protoplasts. Sex. Plant Reprod. 8, 321-325.

Muller, J.F., Missionier, C. & Caboche, M. (1983). Low density growth of cells derived from *Nicotiana* and *Petunia* protoplasts: Influence of the source of protoplasts and comparison of the growth-promoting activity of various auxins. Physiol. Plant. 57, 35-41.

Murashige, T. & Skoog, F. (1962). A revised medium for rapid growth and bio assays with tobacco tissue cultures. Physiol. Plant. 15, 473-497.

Power, J.B. & Chapman, J.V. (1985). Isolation, culture and genetic manipulation of plant protoplasts. Plant cell culture – A practical approach (ed. by R.A. Dixon), pp. 37-66. IRL Press, Oxford Washington DC.

Sidorova, N.V. (1985). Characteristics of the ultrastructure of isolated tobacco embryo sacs. Dokl. Akad. Nauk. Ukr. SSR (Ser. B) Geol. Khim. Biol. Nauki. 12, 63-66.

Spangenberg, G. & Koop, H.-U. (1992). Low density cultures: microdroplets and single cell nurse cultures. Plant tissue culture manual A10 (ed. by K. Lindsey), pp. 1-28. Kluwer Academic Publishers, Dordrecht.

Spurr, A.R. (1969). A low-viscosity epoxy resin embedding medium for electron microscopy. J. Ultrastruct. Res. 26, 31-43.

Theunis, C.H., Pierson, E.S. & Cresti, M. (1991). Isolation of male and female gametes in higher plants. Sex. Plant Reprod. 4, 145-154.

Tian, H.Q. & Russell, S.D. (1997). Micromanipulation of male and female gametes of *Nicotiana tabacum*: II. Preliminary attempts for *in vitro* fertilization and egg cell culture. Plant Cell Rep. 16, 657-661.

Tiwari, S.C. & Polito, V.S. (1988). Organization of the cytoskeleton in pollen tubes of *Pyrus communis*: A study employing conventional and freeze-substitution electron microscopy, immunofluorescence, and rhodamine-phalloidin. Protoplasma 147, 100-112.

Van der Maas, H.M., Zaal, M.A.C.M., De Jong, E.R., Krens, F.A. & Van Went, J.L. (1993). Isolation of viable egg cells of perennial ryegrass (*Lolium perenne* L.). Protoplasma 173, 86-89.

Van Went, J.L. (1970). The ultrastructure of the fertilized embryo sac of *Petunia*. Acta Bot. Neerl. 19, 468-480.

Van Went, J.L. & Kwee H.-S. (1990). Enzymatic isolation of living embryo sacs of *Petunia*. Sex. Plant Reprod. 3, 257-262.

Wagner, V.T., Kardolus, J.P. & Van Went, J.L. (1989a). Isolation of the lily embryo sac. Sex. Plant Reprod. 2, 219-224.

Wagner, V.T., Song, Y.C., Matthys-Rochon, E. & Dumas, C. (1989b). Observations on the isolated embryo sac of *Zea mays* L.. Plant Sci. 59, 127-132.

Webb, M.C. & Gunning, B.E.S. (1990). Embryo sac development in *Arabidopsis thaliana*. I. Megasporogenesis, including the microtubular cytoskeleton. Sex. Plant Reprod. 3, 244-256.

Webb, M.C. & Gunning, B.E.S. (1994). Embryo sac development in *Arabidopsis thaliana*. II. The cytoskeleton during megagametogenesis. Sex. Plant Reprod. 7, 153-163.

Willemse, M.T.M. & Van Went, J.L. (1984). The female gametophyte. Embryology of angiosperms (ed. by B.M. Johri), pp. 159-196. Springer-Verlag, Berlin.

Wu, Y., Zhou, C. & Koop, H.-U. (1993). Enzymatic isolation of viable nucelli at the megaspore mother cell stage and in developing embryo sacs in *Nicotiana tabacum*. Sex. Plant Reprod. 6, 171-175.

Yang, H.-Y. & Zhou, C. (1992). Experimental plant reproductive biology and reproductive cell manipulation in higher plants: Now and in the future. Am. J. Bot. 79, 354-363.

Zhou, C. (1987). A study of fertilization events in living embryo sacs isolated from sunflower ovules. Plant Sci. 52, 147-151.

Zhou, C. & Yang, H.Y. (1985). Observations on enzymatically isolated, living and fixed embryo sacs in several angiosperm species. Planta 165, 225-231.

Chapter 7

Immunodetection and immunolocalization of globulin storage proteins during zygotic and somatic embryo development in *Zea mays*

M.H. THIJSSEN, P. SPOELSTRA & A.M.C. EMONS

(1996) Physiol. Plant. 98, 539-549

Summary

Globulins (GLB) are storage proteins that accumulate to high levels during zygotic embryo development of *Zea mays* L. We visualized the distribution of GLB during zygotic embryo development by immunolabelling of polyethylene glycol sections with a GLB-specific antiserum and a fluorescent secondary antibody. In sections of embryos at 10 days after pollination (DAP), GLB were detected in the scutellar node only. Sections of embryos of 17 DAP showed, besides the presence of GLB in the scutellar node, the presence of a low amount of GLB in the coleoptile and the leaf primordia. In 30-DAP embryos GLB were localized in the root, the coleorhiza, the leaf primordia, the coleoptile and in all cells of the scutellum with the exception of the epidermis and the pro-vascular tissues. The subcellular location of GLB was visualized by immunolabelling of ultrathin sections with anti-GLB and a gold-conjugated secondary antibody. Scutellum cells and root cortex cells of 30-DAP embryos were packed with protein storage vacuoles (PSV), which differed in electron density. GLB were either evenly distributed throughout the PSV or were localized in electron-dense inclusions within the PSV. SDS-PAGE and immunoblot analysis of total protein extracts indicated the presence of a low amount of the GLB1 processing intermediate proGLB1' in globular as well as mature somatic embryos. After maturation on an ABA-containing medium, somatic embryos showed the additional presence of the next GLB1 processing intermediate GLB1'. By immuno-electron microscopy it was possible to localize GLB in globular deposits in PSV in scutellum cells of these somatic embryos.

Key words: Abscisic acid, globulin, immunolocalization, maize, protein storage vacuole, seed storage protein, somatic embryo, *Zea mays*, zygotic embryo.

Introduction

Globulins (GLB) are saline-soluble, water-insoluble proteins that accumulate to high levels in zygotic embryos of *Zea mays* L. The two major GLB components, GLB1 and GLB2, account for 10 to 20% of the total protein of the mature zygotic maize embryo (Kriz 1989). The high accumulation during zygotic embryo development, the degradation within 24 h of seed germination, and the amino acid composition, indicate that GLB are storage proteins (Kriz 1989).

The most abundant GLB, GLB1, is a 63-kDa protein encoded by a single gene designated *Glb1* (Belanger and Kriz 1989). Pulse-chase radiolabelling and *in vitro* translation experiments indicated that the primary translation product, preproGLB1', is extensively processed before the mature protein is formed (Kriz and Schwartz 1986). A 70-kDa protein, proGLB1', is the first processing intermediate detected *in vivo* and this protein is further processed into GLB1', a 67-kDa protein. GLB1' is proteolytically cleaved to form GLB1 (Kriz 1989).

Also the storage protein GLB2, a 45-kDa protein, is encoded by a single gene, the *Glb2* gene (Kriz 1989, Kriz and Wallace 1991). No precursor proteins of GLB2 are known, but the presence of a 26- and a 27-kDa protein is always correlated with the presence of GLB2. These proteins may be processed forms of GLB2, possibly derived from GLB2 by proteolytic cleavage (Kriz and Wallace 1991).

Although the maize *Glb1* and *Glb2* genes as well as their corresponding proteins have been characterized at both the molecular and biochemical level (Kriz and Schwartz 1986, Belanger and Kriz 1989, 1991, Kriz 1989, Kriz and Wallace 1991, Wallace and Kriz 1991), no studies have described the cellular location of GLB.

The development of maize somatic embryos originating from exogenic meristems on embryogenic callus (Emons *et al.* 1993b) shows similarities with zygotic embryo development regarding morphogenesis (Emons and De Does 1993), histodifferentiation (Emons and Kieft 1991), starch accumulation (Emons *et al.* 1993a) and the suppression of lignin formation (Mulder and Emons 1993). During embryo maturation, a stage between proliferation and regeneration, the somatic embryos form a starch-containing scutellum and leaf primordia. In addition, plant regeneration is possible under appropriate conditions (for reviews see Emons 1994, Emons and Kieft 1995).

From several angiosperms and conifers it is known that the somatic embryos synthesize and accumulate seed-specific storage proteins, although these may vary quantitatively and/or qualitatively from the storage proteins of the zygotic embryos

(Crouch 1982, Shoemaker et al. 1987, Stuart et al. 1988, Hakman et al. 1990, Tewes et al. 1991, Krochko et al. 1992, 1994, Maquoi et al. 1993). To our knowledge no comparison of storage proteins has been made between maize zygotic and somatic embryos.

In this paper we show GLB accumulation during zygotic and somatic embryo development of maize by means of SDS-PAGE and immunoblot analysis, the histological pattern of GLB accumulation during zygotic embryo development, and the subcellular location of GLB in PSV on immunogold labelled ultrathin sections of zygotic and somatic embryos. The addition of ABA to the somatic embryo maturation medium appeared to be crucial for proGLB1' processing to GLB1'.

Abbreviations: DAP, days after pollination; DAPI, 4'-6-diamidino-2-phenylindole; GLB, globulin; PSV, protein storage vacuole.

Materials and methods

Zygotic embryos

Plants of *Zea mays* L. genotype 4C1 (Mórocz *et al.* 1986) and inbred line A188 were grown under controlled growth chamber conditions. Plants were hand pollinated and seeds were collected 10 to 30 days after pollination (DAP). The embryos were excised from the seeds and processed for microscopy or frozen in liquid nitrogen and used for protein extraction.

Somatic embryos

The initiation and maintenance of embryogenic callus cultures of maize genotype 4C1 were as described by Emons and Kieft (1991). For callus maintenance a 0.7% agar solidified N6 medium (Chu *et al.* 1975) supplemented with 2 mg ml^{-1} 2,4-D, 20 m*M* L-proline, 200 mg l^{-1} casein hydrolysate, 2% sucrose and 3% mannitol was used. On a hormone-free MS medium (Murashige and Skoog 1962) supplemented with 6% sucrose, with or without 0.2 mg l^{-1} ABA, the globular stage somatic embryos develop a starch-containing scutellum. After 14 days of maturation, regeneration can take place on an MS medium containing 2% sucrose. Embryogenic callus and embryos matured for 14 days on MS medium with or without ABA were processed for microscopy or frozen in liquid nitrogen and used for protein extraction.

Globulin-specific antiserum

A rabbit polyclonal maize GLB-specific antiserum was kindly provided by A.L. Kriz (DeKalb Genetics Corp., Mystic, CT, USA). This antiserum reacts with the *Glb1*-encoded proteins, proGLB1', GLB1' and GLB1, with GLB2, and with two GLB of 26 and 27 kDa, further referred to as 27-kDa GLB (Kriz and Wallace 1991).

Protein extraction, SDS-PAGE and electroblotting

Proteins were extracted from A188 zygotic embryos by macerating them in SDS sample buffer (2% [w/v] SDS, 50 m*M* Tris [pH 6.8], 5% [v/v] 2-mercaptoethanol, 0.01% [w/v] bromophenol blue) at a ratio of 50 mg ml^{-1} fresh weight. Dried mature 4C1 embryos were macerated at a ratio of 10 mg ml^{-1}. Somatic embryos were ground in liquid nitrogen and placed into SDS sample buffer at a ratio of 500 mg ml^{-1}.

Extracts were heated to 100 °C for 2 min, centrifuged at 13 500 *g* for 5 min and 1 µl of each sample was applied to a 7.5 or 12.5% homogeneous polyacrylamide gel and subjected to SDS-PAGE. Gels were stained with Coomassie Brilliant Blue R-250 or electroblotted onto a polyvinylidene difluoride filter membrane (Millipore), using a semidry blotting apparatus. Both gel electrophoresis and electroblotting were performed on the PhastSystem of Pharmacia, according to the manufacturer's specifications (Pharmacia, Uppsala, Sweden).

Molecular mass standards were obtained from Pharmacia and were as follows: phosphorylase *b*, 94 kDa; albumin, 67 kDa; ovalbumin, 43 kDa; carbonic anhydrase, 30 kDa; trypsin inhibitor, 20.1 kDa; and *α*-lactalbumin, 14.4 kDa.

Immunoblot analysis

After the completion of the protein transfer, the blots were blocked for 30 min with 0.1 *M* PBS (pH 7.3) containing 6% (w/v) non-fat dried milk and 0.2% (v/v) Tween 20. Antibodies were diluted in PBS containing 3% (w/v) non-fat dried milk and 0.2% (v/v) Tween 20. The filters were incubated overnight with the primary GLB-specific antibody diluted 1:2500 and for 90 min with goat anti-rabbit IgG alkaline phosphatase (BioRad, Hertfordshire, UK) diluted 1:3000. After washing in PBS the blots were briefly dipped in alkaline phosphatase buffer (0.1 *M* Tris-HCl [pH 8.9], 0.1 *M* NaCl, 0.05 *M* $MgCl_2$) and stained with 0.01% (w/v) nitroblue tetrazolium and 0.005% (w/v) 5-bromo-4-chloro-3-indolyl phosphate in alkaline phosphatase buffer.

Light-microscopic immunocytochemistry

Several developmental stages of zygotic and somatic embryos were fixed for 2 h with 3% paraformaldehyde in 0.1 *M* phosphate buffer (pH 7.2), dehydrated in a graded ethanol series and embedded in polyethylene glycol 1500, or a 2:1 mixture of polyethylene glycol 1500 and 4000 (Merck, Darmstadt, Germany). Sections of 2 or 5 µm were mounted on poly-L-lysine coated slides, rinsed in PBS and treated with 0.1 *M* NH_4Cl in PBS for 5 min. Proteins were blocked with 1% BSA in PBS for 30 min. Primary and secondary antibodies were diluted in PBS containing 0.1% BSA. Sections were incubated with GLB antiserum diluted 1:2000 overnight at 4 °C, and incubated with FITC-conjugated goat anti-rabbit IgG (Sigma, St Louis, MO, USA) diluted 1:50 or Bodipy-conjugated goat anti-rabbit IgG (Molecular Probes, Eugene, OR, USA) diluted 1:100 for 45 min at 37 °C. Sections were finally enclosed in Citifluor glycerol solution (Citifluor Ltd, London, UK) containing 0.1 µg ml^{-1} 4'-6-diamidino-2-phenylindole (DAPI) (Sigma) for counterstaining of the nuclei, and examined using a Nikon Labophot or a Nikon Microphot fluorescence microscope equipped with EX 365/DM 400/BA 420 and EX 470-490/DM 510/BA 515 EF filters. Black and white images were recorded on Kodak TMY 135-film.

Electron-microscopic immunocytochemistry

Scutellar parts of zygotic and somatic embryos of several developmental stages were cut into small cubes and fixed for 2 h with 3% paraformaldehyde and 0.1% glutaraldehyde in 0.1 *M* phosphate buffer (pH 7.2), or alternatively with 1% glutaraldehyde and 0.2% picric acid in 0.1 *M* phosphate buffer. Tissues were dehydrated in a graded ethanol series and embedded in London Resin White (Medium Grade) (London Resin Company Co., Hampshire, UK).

Small root segments from 30-DAP zygotic embryos were cryo-fixed in a Balzers HPM10 high pressure freezer followed by freeze substitution in a Reichert-Jung freeze substitution apparatus for 48 h at -80 □C with anhydrous acetone containing 0.1% glutaraldehyde. After freeze substitution the tissues were slowly brought back to room temperature, rinsed in acetone and embedded in London Resin White.

For ultrastructural analysis some scutellar parts of 30-DAP zygotic embryos were fixed for 4 h with 3% glutaraldehyde in 0.1 *M* phosphate buffer (pH 7.2) and post-fixed for 2 h with 1% OsO_4 in the same buffer. Tissues were dehydrated in a graded ethanol series and embedded in Spurr's resin.

Ultrathin sections were cut with glass knifes on a LKB ultramicrotome and

collected on formvar-coated 150-mesh nickel grids. For immunolabelling, sections were treated with 0.05 *M* NH_4Cl in PBS for 5 min and with 0.05% acetylated BSA in PBS for 30 min. Antibodies were diluted in PBS containing 0.02% acetylated BSA. Sections were incubated with GLB antiserum diluted 1:500 for 1 h at 37 °C, and incubated with 10 nm gold-conjugated goat anti-rabbit IgG (Aurion, Wageningen, The Netherlands) diluted 1:30 for 1 h at 37 °C. Sections were post-fixed with 2% glutaraldehyde in PBS for 10 min and, after washing in millipore water, counterstained with uranyl acetate and/ or lead citrate when necessary. Sections were studied with a JEOL 1200 EXII electron microscope.

Results

SDS-PAGE and immunoblot analysis of globulins in zygotic and somatic embryos

High accumulation of GLB during zygotic embryo development is readily apparent from SDS-PAGE (Fig. 1a) and immunoblot analysis (Fig. 1b) of total protein extracts of embryos at different developmental stages. Figure 1b shows the presence of high levels of the *Glb1*- and *Glb2*-encoded proteins in 30-DAP zygotic embryos. In protein extracts of 10-DAP embryos, the youngest stage examined, we could detect the *Glb1*-encoded proteins. In 13-DAP zygotic embryos the presence of a low amount of GLB2 was visible, whereas the 27-kDa GLB was first visible in 20-DAP embryos.

SDS-PAGE and immunoblot analysis of somatic embryo total protein extracts shows the presence of anti-GLB labelled bands in all protein extracts tested. The bands were observed in extracts of the globular stage somatic embryos, i.e. the embryogenic callus, as well as in extracts of the mature somatic embryos (Fig. 2), which have developed a starch containing scutellum. According to histodifferentiation the mature somatic embryos are comparable with 11- to 12-DAP zygotic embryos. *Glb1*-encoded proteins were present in small quantities and did not account for a high percentage of the total protein present in somatic embryos (Fig. 2a). After maturation on a medium without ABA, the embryos showed the same pattern of protein labelling as the globular stage somatic embryos. However, protein extracts of embryos after maturation on a medium supplemented with ABA showed labelling of an extra GLB band (Fig. 2b).

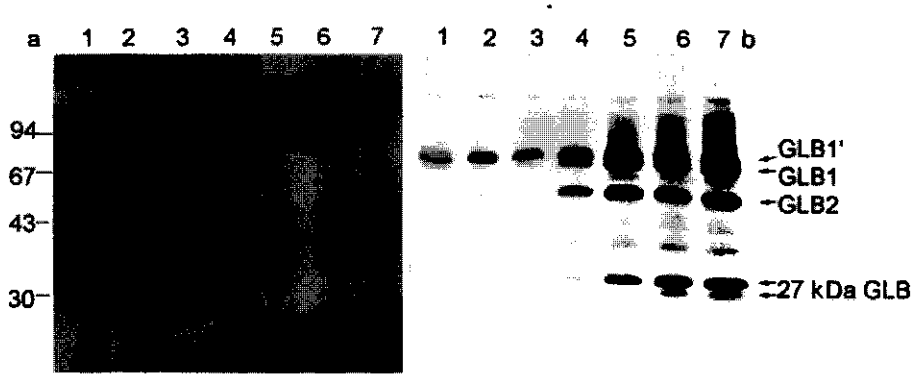

Fig. 1. SDS-PAGE and immunoblot analysis of GLB in zygotic embryo protein extracts showing a high accumulation of GLB during zygotic embryo development. Total protein extracts of A188 zygotic embryos at various times after pollination were subjected to SDS-PAGE and subsequently stained with Coomassie Brilliant Blue (a) or subjected to immunoblot analysis in which a GLB-specific antiserum was used as a probe (b). Lane 1, 10-DAP; lane 2, 13-DAP; lane 3, 17-DAP; lane 4, 20-DAP; lane 5, 24-DAP; lane 6, 27-DAP; lane 7, 30-DAP embryo. Positions of GLB and positions of molecular mass standards in kDa are indicated.

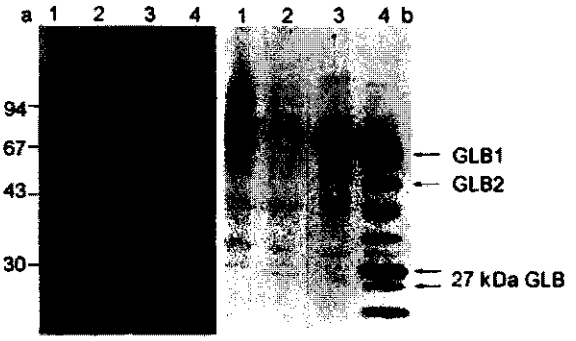

Fig. 2. SDS-PAGE and immunoblot analysis of GLB in somatic embryo protein extracts, showing the presence of *Glb1*-encoded proteins in somatic embryos at different developmental stages. Total protein extracts (500 mg fresh weight ml^{-1} sample buffer) were subjected to SDS-PAGE (12.5% polyacrylamide gels) and subsequently stained with Coomassie Brilliant Blue (a) or subjected to immunoblot analysis in which a GLB-specific antiserum was used as a probe (b). The total protein extract of a mature zygotic embryo (10 mg fresh weight ml^{-1} sample buffer) was used as a control. Lane 1, globular stage somatic embryos; lane 2, somatic embryos after maturation on a medium without ABA; lane 3, somatic embryos after maturation on an ABA-containing medium; lane 4, mature dried zygotic embryo (4C1). Positions of GLB and molecular mass standards in kDa are indicated.

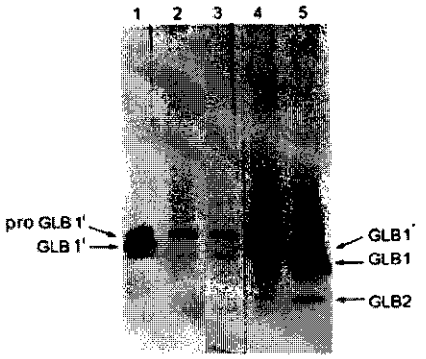

Fig. 3. Immunoblot analysis of GLB in zygotic and somatic embryo protein extracts, showing the presence of proGLB1' in the different developmental stages of the somatic embryos and the additional presence of GLB1' in somatic embryos after maturation on an ABA-containing medium. Total protein extracts were subjected to SDS-PAGE in gels containing 7.5% polyacrylamide. Ratio of sample (fresh weight) to sample buffer: immature zygotic embryo, 50 mg ml^{-1}; somatic embryos 500 mg ml^{-1}; mature zygotic embryo 10 mg ml^{-1}. Gels were subjected to immunoblot analysis in which a GLB-specific antiserum was used as a probe. Lane 1, 17-DAP zygotic embryo (A188); lane 2, globular stage somatic embryos; lane 3, somatic embryos after maturation on a medium without ABA; lane 4, somatic embryos after maturation on an ABA-containing medium; lane 5, mature dried zygotic embryo (4C1). Positions of GLB are indicated.

To determine which *Glb1*-encoded proteins were present in the somatic embryos, (proGLB1' and GLB1' differ by 3 kDa in molecular mass, and are 70 kDa and 67 kDa, respectively), the same somatic embryo protein extracts were separated on a gel with a lower percentage of polyacrylamide and immunoblotting was performed (Fig. 3). Comparison of the somatic embryo protein extracts with zygotic embryo protein extracts of 17-DAP and mature, dried zygotic embryos indicated that in all somatic embryo extracts the labelled band at the highest position in Fig. 3 is proGLB1', whereas in somatic embryos matured on an ABA-containing medium, GLB1' was additionally present. We presume that the lowest faintly labelled bands, at the position where GLB1 is expected, is not correlated to the *Glb1*-encoded proteins, because GLB1' was absent in the other somatic embryo protein extracts.

Distribution of globulins during zygotic embryo development

To examine the spatial pattern of GLB accumulation during zygotic embryo development, tissue sections of embryos collected at different times after pollinationwere used for immunolabelling with a GLB-specific antiserum and a fluorescent secondary antibody. When sections of 10-DAP zygotic embryos, the youngest embryo stage immunolabelled, were examined, an initial deposition of GLB in the area of the scutellum attached to the embryo axis, the scutellar node, became visible (results not shown). Zygotic embryos at 17 DAP showed not only labelling of the scutellar node, but also weak labelling of the coleoptile and the leaf primordia (Fig. 4), whereas the rest of the embryo axis and the scutellum were not labelled. In 30-DAP zygotic embryos GLB had accumulated in all cells of the scutellum, with the exception of the epidermal cells and the pro-vascular regions (Fig. 5a,b). From Fig. 5c,d it is apparent that GLB are present in protein storage vacuoles (PSV) of various sizes, which are randomly distributed in the cells, whereas starch grains are surrounding the cell nucleus (Fig. 5e). Labelling was also observed in the embryo axis in the leaf primordia, the coleoptile and the root. In Fig. 5e,f the presence of GLB in a lane of cells in the root cortex is shown. The control sections, labelled with the secondary antibody without prior incubation in anti-GLB were negative (results not shown).

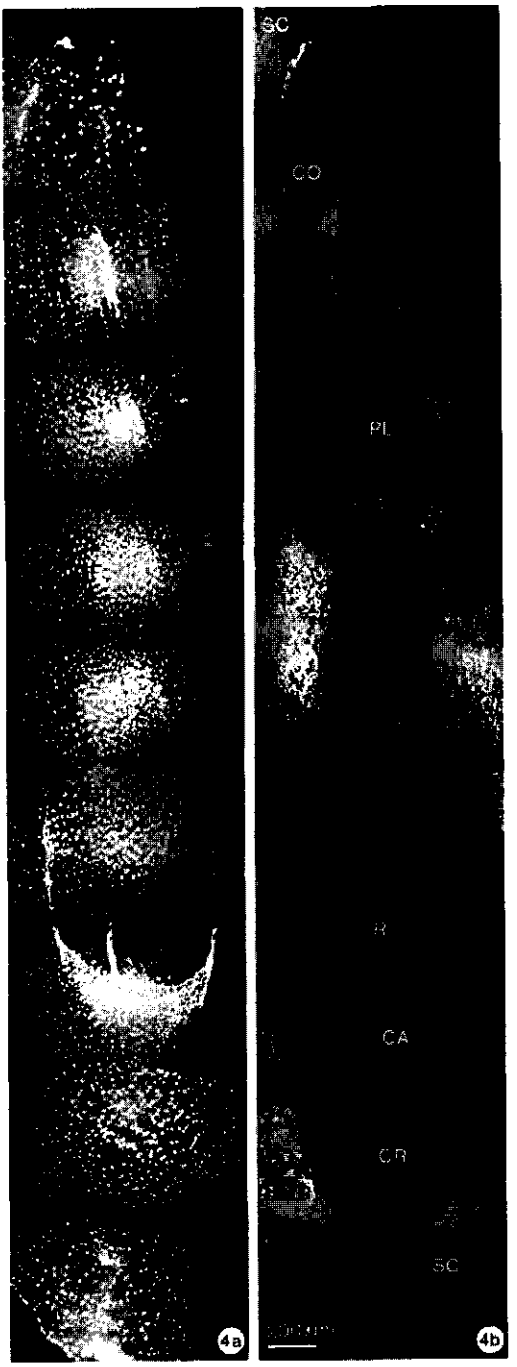

Fig. 4. Semithin polyethylene glycol section through the embryo axis of a 17-DAP zygotic embryo. (a) DAPI staining showing the position of the nuclei, and (b) immunolabelling with GLB-specific antiserum and GAR-IgG-Bodipy, showing GLB deposition in the scutellar node, the coleoptile and the leaf primordia. Calyptra (CA), coleorhiza (CR), coleoptile (CO), plumule (PL), root (R), scutellum (SC), and scutellar node (SN) are indicated.

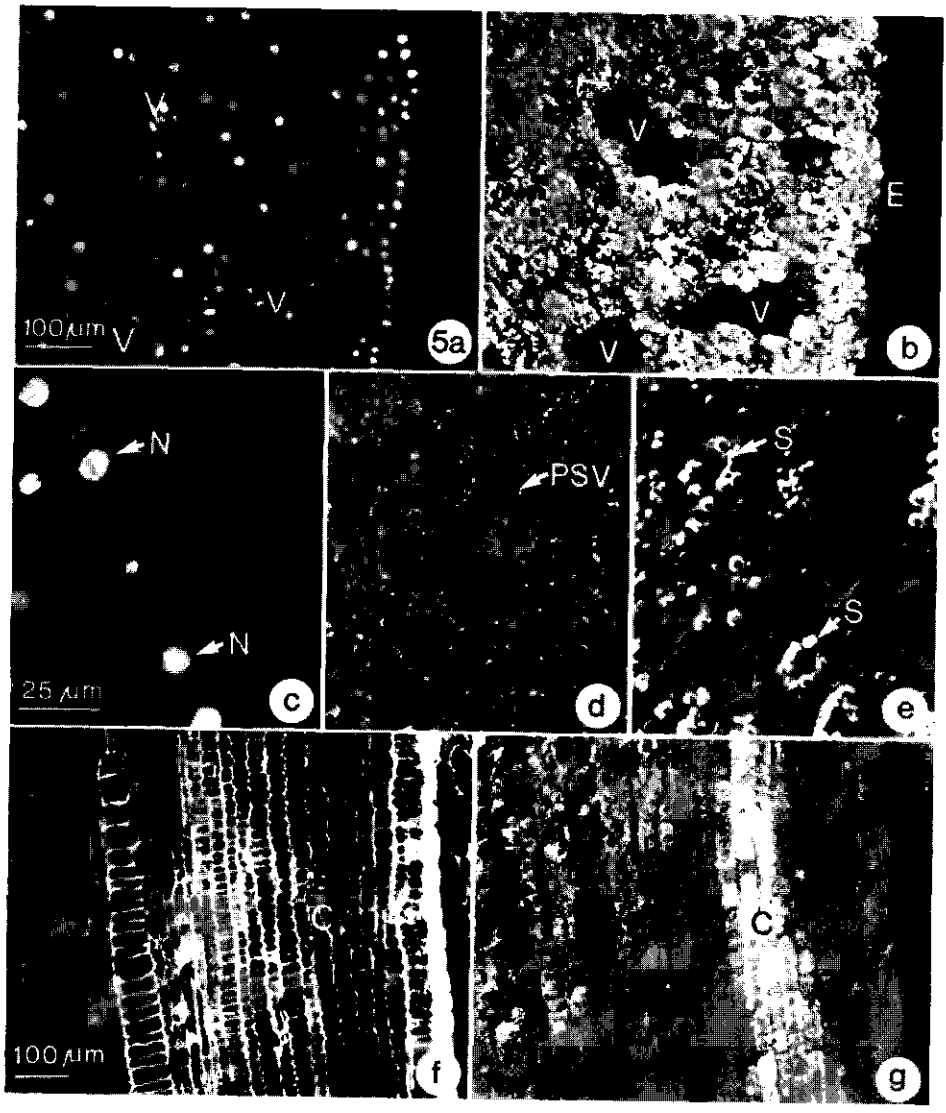
V
V
100 µm
V
5a
V
V
V
E
b
N
N
25 µm
c
PSV
d
S
S
e
C
100 µm
f
C
g

Fig. 5. Semithin polyethylene glycol sections through 30-DAP zygotic embryos. (a-b) Scutellum tissue. (a) DAPI staining showing the position of the nuclei, and (b) immunolabelling with anti-GLB and GAR-IgG-FITC showing the presence of GLB in all cells of the scutellum with the exception of the epidermis and the pro-vascular tissues. (c-e). Detail of scutellum tissue. (c) DAPI staining showing the position of the nuclei, (d) immunolabelling with anti-GLB and GAR-IgG-FITC showing the presence of GLB in protein storage vacuoles of variable sizes, and (e) dark field image showing the starch containing plastids located around the cell nuclei. (f-g). Root tissues. (f) UV fluorescence image showing the root tissues, and (g) immunolabelling with anti-GLB and GAR-IgG-FITC showing the presence of GLB in a part of the root cortex. Epidermis (E), nuclei (N), pro-vascular tissues (V), protein storage vacuoles (PSV), root cortex (C), and starch grains (S) are indicated.

Subcellular location of globulins in zygotic and somatic embryos

In order to study GLB deposition in more detail we immunolabelled ultrathin sections of 30-DAP zygotic and mature somatic embryos with GLB-specific antiserum and gold-conjugated secondary antibody.

In 30-DAP zygotic embryos the scutellum cells were packed with lipids, starch-containing plastids and PSV. In chemically fixed scutellum tissues that were post-fixed with osmium tetroxide, the high accumulation of lipids made it almost impossible to discern other organelles within the cells (Fig. 6). Figure 7a shows the scutellum tissue, chemically fixed for immunocytochemistry and labelled with anti-GLB and goat anti-rabbit-10 nm gold. The cells contain numerous PSV, which differ in staining intensity, and are surrounded by non-staining lipid bodies. In the PSV, proteins were either evenly distributed or aggregated in electron-dense inclusions. At higher magnifications the presence of GLB, as indicated by the gold label, became visible inside the PSV (Fig. 7b). The electron-dense inclusions in the PSV appeared to contain GLB (Fig. 7c).

Figs. 6-8. Ultrathin sections through chemically fixed scutellum tissues. Fig. 6. 30-DAP zygotic embryo fixed with 3% glutaraldehyde and 1% OsO_4. Due to high accumulation of lipids in the scutellum cells, other organelles are hardly discernible. Fig. 7. 30-DAP zygotic embryo fixed with 3% paraformaldehyde and 0.1% glutaraldehyde, and labelled with anti-GLB and GAR-10 nm gold. (a) Overview of cells containing protein storage vacuoles, (b) darkly stained, labelled protein storage vacuole, (c) protein storage vacuole containing a darkly stained, heavily labelled globular inclusion (arrow). Fig. 8. Somatic embryo after maturation on an ABA-containing medium, fixed with 1% glutaraldehyde and 0.2% picric acid, and labelled with anti-GLB and GAR-10 nm gold. (a) Overview of scutellum cells with protein storage vacuoles, (b) gold-labelled globular inclusion in a protein storage vacuole (arrow). Cell wall (CW), protein inclusions (arrows), lipid bodies (L), nuclei (N), protein storage vacuoles (PSV), and starch grains (S) are indicated.

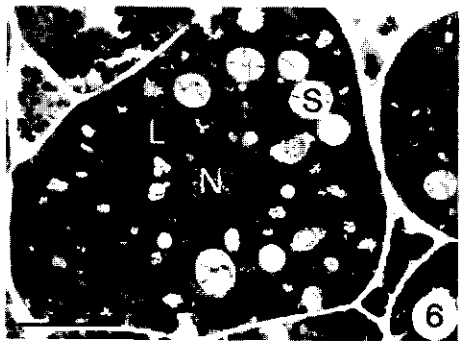

6

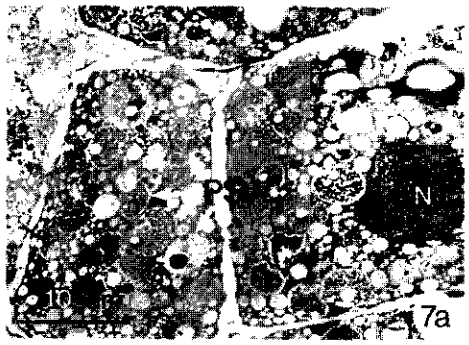

7a

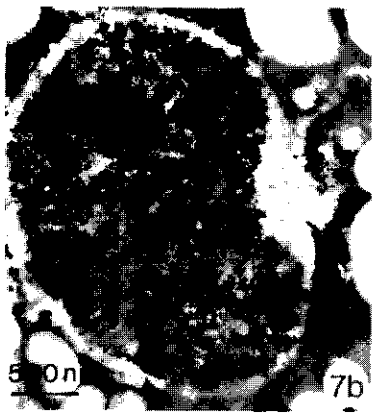

7b

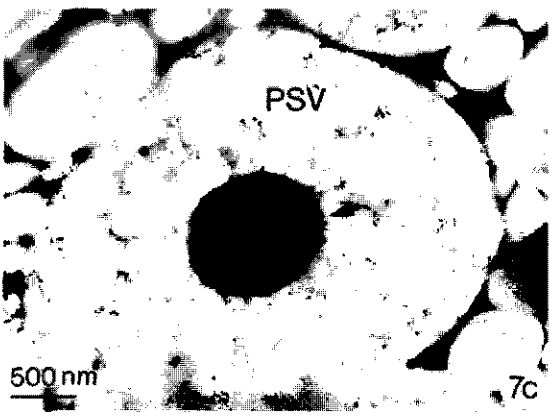

7c

8a

8b

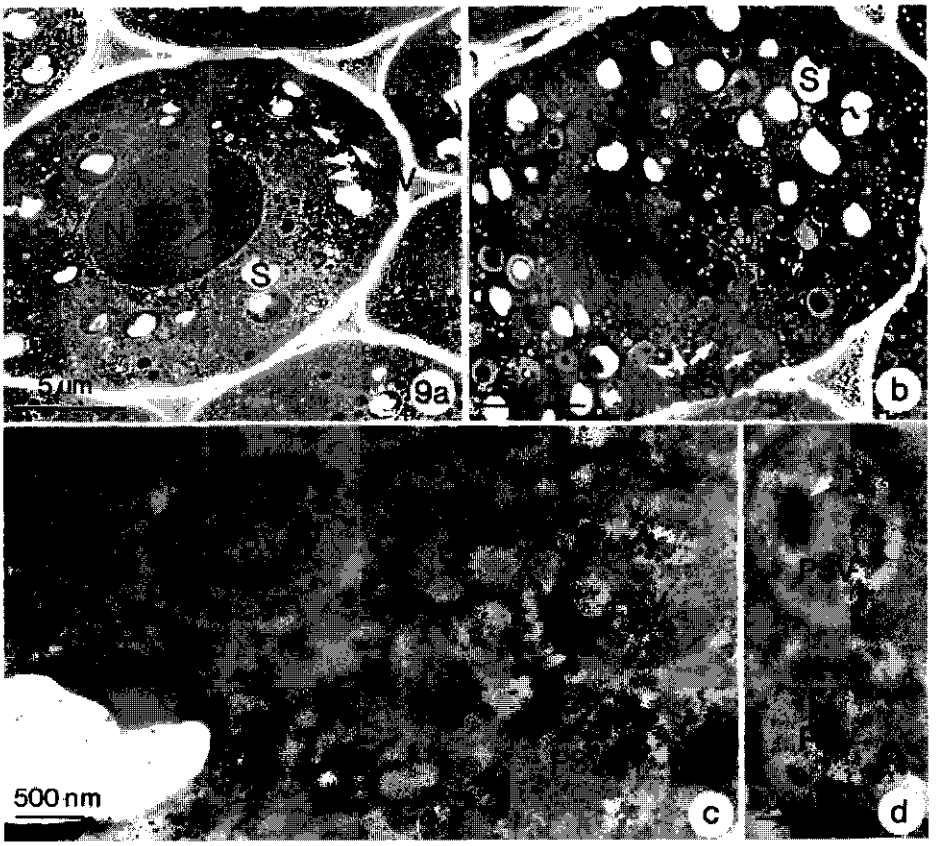

Fig. 9. Ultrathin section through cryo-fixed and freeze-substituted root tissues of a 30-DAP zygotic embryo, labelled with anti-GLB and GAR-10 nm gold. (a) Overview of a root cortex cell close to the epidermis, showing small regularly stained protein storage vacuoles. (b) Overview of a root cortex cell close to the central cylinder, showing protein storage vacuoles with darkly stained inclusions. (c) Detail of tissue in (a), showing gold-labelled protein storage vacuoles. (d) Detail of tissue in (b), showing gold-labelled protein storage vacuoles with a darkly stained inclusion (arrow). Protein inclusion (arrow), nuclei (N), protein storage vacuoles (PSV), and starch grains (S) are indicated.

We also studied GLB deposition in ultrathin sections of scutellar cells of somatic embryos after maturation on an ABA-containing medium. PSV were present in these cells (Fig. 8a) and immunolabelling with GLB-specific antiserum shows the presence of GLB within the PSV (Fig. 8b).

In cryo-fixed roots of 30-DAP zygotic embryos prepared for immunocytochemistry, the root cortex cells contain numerous PSV (Figs. 9a,b). In general, PSV in the root cortex cells were smaller than the PSV in the scutellum tissues. In the PSV in the root cortex cells close to the epidermis GLB are evenly distributed throughout the PSV (Fig. 9c). The PSV in root cortex cells close to the central cylinder contain electron-dense deposits positive for GLB (Fig. 9d). All control sections treated with gold-coupled secondary antibodies, without prior incubation in the GLB-specific antiserum, revealed virtually no gold labelling (results not shown).

Discussion

Kriz (1989) reported that GLB1 was first detectable in zygotic embryos of 21 DAP. Using an optimized detection system, we observed all *Glb1*-encoded proteins in 10-DAP A188 and 4C1 embryos, showing that GLB synthesis is already initiated at this stage in our material. Immunoblotting showed that the different GLB in zygotic embryos are present subsequently during development.

Expression of storage proteins during embryogenesis is known to be under strict developmental control, and is temporally and spatially regulated, mainly at the level of gene transcription (Goldberg *et al.* 1989, Perez-Grau and Goldberg 1989). During embryo development in broad bean the distribution of cell division, followed by cell expansion and endopolyploidisation, follows a developmental gradient, which appeared to be directly related to storage protein deposition (Borisjuk *et al.* 1995). We also found a specific pattern of GLB accumulation in maize zygotic embryos, with an onset of GLB deposition in the scutellar node in 10-DAP embryos, which is also visible in 17-DAP embryos (Fig. 4). In the embryo axis GLB deposition started in the coleoptile and the leaf primordia (Fig. 4). In 30-DAP embryos GLB could be located in the embryo axis within the coleoptile, the leaf primordia, the coleorhiza and the root cortex, and in all cells of the scutellum, with the exception of the epidermis and the pro-vascular tissues (Fig. 5). Based on the negative regulation reported for gene expression of storage proteins in vegetative stem and root tissues of common bean (Burow *et al.* 1992), Borisjuk *et al.* (1995) suggested that transcriptional repression could be involved in preventing storage protein expression in epidermal and pro-vascular tissues.

We were able to locate GLB in protein storage vacuoles in the scutellum tissues as well as in the axis of zygotic embryos. GLB were either evenly distributed throughout the PSV or aggregated in electron-dense deposits within the PSV (Figs. 7 and 9). In the maize endosperm the different zein storage proteins segregate in different areas of the

protein bodies (Lending *et al.* 1988), and in oat endosperm the storage protein GLB and prolamines co-localize within the PSV (Lending *et al.* 1989). Using an antiserum which did not distinguish between the *Glb1*-encoded proteins (proGLB1', GLB1' and GLB1), GLB2, or the two 27-kDa GLB, we could not visualize the deposition of the individual GLB in different PSV, or the segregation in different regions within the same PSV.

Belanger and Kriz (1989) showed that GLB1 exhibits a significant amino acid similarity with the 7S seed globulins of the dicotyledons pea and French bean, and the monocotyledon wheat (Williamson and Quatrano 1988). The 7S and 11S GLB of dicotyledons and related GLB storage proteins in rice and oats are transported from the ER lumen via the Golgi apparatus to the PSV (Shewry *et al.* 1995). In contrast, the major maize endosperm storage protein zein is deposited in protein bodies which are derived directly from the ER (Larkins and Hurkman 1978). These two types of protein processing differ not only between species, but also within the same species for different types of storage proteins (Shewry *et al.* 1995).

In several angiosperms somatic embryos show a pattern of storage protein synthesis, processing and accumulation that parallels the pattern in zygotic embryos. However, storage protein accumulation in somatic embryos often occurs at earlier stages and to a lower extent than in zygotic embryos (Crouch 1982, Shoemaker *et al.* 1987, Tewes *et al.* 1991, Krochko *et al.* 1992). In zygotic embryos of *Brassica napus* the expression of the storage protein napin is under tight developmental control, whereas, in somatic embryos transcripts could be detected during all stages of development as the result of a basal constitutive derepression of the napin gene (Fleming and Hanke 1993). The same could be true in our study in which proGLB1' is already present in embryogenic callus, which is developmentally comparable to globular stage zygotic embryos at 5 to 7 DAP (Fransz and Schel 1991).

From the comparison of the total protein extracts in the gels stained with Coomassie Brilliant Blue with the corresponding immunoblots (Fig. 2) it is, however, clear that in the somatic embryos the GLB only account for a small percentage of the total protein. Even after a maturation period of 14 days (Fig. 2), when histologically the somatic embryos are comparable to zygotic embryos at 11 to 12 DAP (Emons and Kieft 1991), only proGLB1' was present and found in low amounts, while in 10-DAP zygotic embryos we could already detect all of the *Glb1*-encoded proteins (Fig. 1). We can not discriminate between the lack of processing of proGLB1' or the breakdown of the processed proteins as soon as they are formed.

The phytohormone ABA plays a role in many processes during seed

development, like the control of embryo maturation and the suppression of precocious germination (Quatrano 1986). To prevent precocious germination in the developing somatic embryos we included ABA in the maturation medium.

ABA is considered to regulate the expression of specific genes during seed development, by regulating the expression of genes encoding seed storage proteins, osmoprotectants and regulatory proteins (Williamson and Quatrano 1988, Skriver and Mundy 1990). In addition, the *Glb1* and *Glb2* genes in maize zygotic embryos are positively regulated by ABA (Kriz and Schwartz 1986, Kriz *et al.* 1990, Rivin and Grudt 1991, Paiva and Kriz 1994). Kriz and coworkers (1990) showed that the exposure of maize kernels to ABA during germination results in a maintenance of high levels of *Glb1* transcripts in the embryo, whereas these transcripts normally decline to undetectable levels during germination (Kriz and Wallace 1991).

In somatic embryos of several conifers and angiosperms the addition of ABA to the culture medium is a prerequisite for the initiation of storage protein synthesis (Hakman *et al.* 1990, Maquoi *et al.* 1993, Misra 1994). After maturation on an ABA-containing medium the maize somatic embryos showed, besides the presence of proGLB1', the presence of GLB1' (Fig. 3). In ultrathin sections of such somatic embryos a number of cells showed the presence of GLB-containing protein deposits within the PSV (Fig. 8b).

Although the addition of ABA to the culture medium resulted in protein processing, or in the inhibition of protein breakdown, maize somatic embryos were still not able to synthesize all the different GLB present in maize zygotic embryos.

Acknowledgements

We thank Dr. A.L. Kriz for the provision of the globulin-specific antiserum, Prof. A.L. Van Went for critically reading the manuscript, N. de Ruijter and A. Hillen for help with the tissue culture and immunoblotting, and S. Massalt, A. Haasdijk and P. Van Snippenburg for photography and artwork.

References

Belanger, F.C. & Kriz, A.L. (1989). Molecular characterization of the major maize embryo globulin encoded by the *Glb1* gene. Plant Physiol. 91, 636-643.

Belanger, F.C. & Kriz, A.L. (1991). Molecular basis for allelic polymorphism of the maize *globulin-1* gene. Genetics 129, 863-872.

Borisjuk, L., Weber, H., Panitz, R., Manteuffel, R. & Wobus, U. (1995). Embryogenesis of *Vicia faba* L.: Histodifferentiation in relation to starch and storage protein synthesis. J. Plant Physiol. 147, 203-218.

Burow, M.D., Sen, P., Chlan, C.A. & Murai, N. (1992). Developmental control of the ß-phaseolin gene requires positive, negative, and temporal seed-specific transcriptional regulatory elements and a negative element for stem and root expression. Plant J. 2, 537-548.

Chu, C.C., Wang, C.C., Sun, C.S., Hsu, C., Yin, K.C., Chu, C.Y. & By, F.Y. (1975). Establishment of an efficient medium for anther culture of rice through comparative experiments on the nitrogen sources. Sci. Sin. 18, 659-668.

Crouch, M.L. (1982). Non-zygotic embryos of *Brassica napus* L. contain embryo-specific storage proteins. Planta 156, 520-524.

Emons, A.M.C. (1994). Somatic embryogenesis: Cell biological aspects. Acta Bot. Neerl. 43, 1-14.

Emons, A.M.C. & De Does, H. (1993). Origin and development of embryo and bud primordia during maturation of embryogenic calli of *Zea mays*. Can. J. Bot. 71, 1349-1356.

Emons, A.M.C. & Kieft, H. (1991). Histological comparison of single somatic embryos of maize from suspension culture with somatic embryos attached to callus cells. Plant Cell Rep. 10, 485-488.

Emons, A.M.C. & Kieft H. (1995). Somatic embryogenesis in maize (*Zea mays* L.). Biotechnology in agriculture and forestry, Vol. 31, Somatic embryogenesis and synthetic seed II (ed. by Y.P.S. Bajaj), pp. 24-39. Springer-Verlag, Berlin.

Emons, A.M.C., Mulder, M.M. & Kieft, H. (1993a). Pyrolysis mass spectrometry of developmental stages of maize somatic embryos. Acta Bot. Neerl. 42, 319-339.

Emons, A.M.C., Samallo-Droppers, A. & Van der Toorn, C. (1993b). The influence of sucrose, mannitol, L-proline, abscisic acid and gibberellic acid on the maturation of somatic embryos of *Zea mays* L. from suspension cultures. J. Plant Physiol. 142, 597-604.

Fleming, A.J. & Hanke, D.E. (1993). The regulation of napin gene expression in secondary embryos of *Brassica napus*. Physiol. Plant. 87, 396-402.

Fransz, P.F. & Schel, J.H.N. (1991). An ultrastructural study on the early development of *Zea mays* somatic embryos. Can. J. Bot. 69, 858-865.

Goldberg, R.B., Baker, S.J. & Perez-Grau, L. (1989). Regulation of gene expression during plant embryogenesis. Cell 56, 149-160.

Hakman, I., Stabel, P., Engström, P. & Eriksson, T. (1990). Storage protein accumulation during zygotic and somatic embryo development in *Picea abies* (Norway spruce). Physiol. Plant. 80, 441-445.

Kriz, A.L. (1989). Characterization of embryo globulins encoded by the maize *Glb* genes. Biochem. Genet. 27, 239-251.

Kriz, A.L. & Schwartz, D. (1986). Synthesis of globulins in maize embryos. Plant Physiol. 82, 1069-1075.

Kriz, A.L. & Wallace, N.H. (1991). Characterization of the maize *Globulin-2* gene and analysis of two null alleles. Biochem. Genet. 29, 241-254.

Kriz, A.L., Wallace, M.S. & Paiva, R. (1990). Globulin gene expression in embryos of maize *viviparous* mutants. Evidence for regulation of the *Glb1* gene by ABA. Plant Physiol. 92, 538-542.

Krochko, J.E., Bantroch, D.J., Greenwood, J.S. & Bewley, J.D. (1994). Seed storage proteins in developing somatic embryos of alfalfa: Defects in accumulation compared to zygotic embryos. J. Exp. Bot. 45, 699-708.

Krochko, J.E., Pramanik, S.K. & Bewley, J.D. (1992). Contrasting storage protein synthesis and messenger RNA accumulation during development of zygotic and somatic embryos of alfalfa (*Medicago sativa* L.). Plant Physiol. 99, 46-53.

Larkins, B.A. & Hurkman, W.J. (1978). Synthesis and deposition of zein in protein bodies of maize endosperm. Plant Physiol. 62, 256-263.

Lending, C.R., Chesnut, R.S., Shaw, K.L. & Larkins, B.A. (1989). Immunolocalization of avenin and globulin storage proteins in developing endosperm of *Avena sativa* L. Planta 178, 315-324.

Lending, C.R., Kriz, A.L., Larkins, B.A. & Bracker, C.E. (1988). Structure of maize protein bodies and immunocytochemical localization of zeins. Protoplasma 143, 51-62.

Maquoi, E., Hanke, D.E. & Deltour, R. (1993). The effects of abscisic acid on the maturation of *Brassica napus* somatic embryos - An ultrastructural study. Protoplasma 174, 147-157.

Misra, S. (1994). Conifer zygotic embryogenesis, somatic embryogenesis, and seed germination: Biochemical and molecular advances. Seed Sci. Res. 4, 357-384.

Mórocz, S., Dudits, D.G. & Nemeth, J. (1986). Two approaches to rendering *Zea mays* L. applicable to tissue culture manipulations. Proceedings of the 6th International congress of plant tissue and cell culture, Minneapolis, MN. August 3-8, 1986 (ed. by D.A. Somers, B.G. Gegenbach, D.D. Biesboer, W.P. Hackett and C.E. Green), p. 190. (Abstract).

Mulder, M.M. & Emons, A.M.C. (1993). Cell wall development in maize somatic embryos studied by pyrolysis mass spectrometry. J. Anal. Appl. Pyrolysis 25, 255-264.

Murashige, T. & Skoog, F. (1962). A revised medium for rapid growth and bio assays with tobacco tissue cultures. Physiol. Plant. 15, 473-497.

Paiva, R. & Kriz, A.L. (1994). Effect of abscisic acid on embryo-specific gene expression during normal and precocious germination in normal and *viviparous* maize (*Zea mays*) embryos. Planta 192, 332-339.

Perez-Grau, L. & Goldberg, R.B. (1989). Soybean seed protein genes are regulated spatially during embryogenesis. Plant Cell 1, 1095-1109.

Quatrano, R.S. (1986). Regulation of gene expression by abscisic acid during angiosperm embryo development. Oxf. Surv. Plant Mol. Cell Biol. 3, 467-477.

Rivin, C.J. & Grudt, T. (1991). Abscisic acid and the developmental regulation of embryo storage proteins in maize. Plant Physiol. 95, 358-365.

Shewry, P.R., Napier, J.A. & Tatham, A.S. (1995). Seed storage proteins: Structures and biosynthesis. Plant Cell 7, 945-956.

Shoemaker, R.C., Christofferson, S.E. & Galbraith, D.W. (1987). Storage protein accumulation patterns in somatic embryos of cotton (*Gossypium hirsutum* L.). Plant Cell Rep. 6, 12-15.

Skriver, K. & Mundy, J. (1990). Gene expression in response to abscisic acid and osmotic stress. Plant Cell 2, 503-512.

Stuart, D.A., Nelsen, J. & Nichol, J.W. (1988). Expression of 7S and 11S alfalfa seed storage proteins in somatic embryos. J. Plant Physiol. 132, 134-139.

Tewes, A., Manteuffel, R., Adler, K., Weber, E. & Wobus, U. (1991). Long-term cultures of barley synthesize and correctly deposit seed storage proteins. Plant Cell Rep. 10, 467-470.

Wallace, N.H. & Kriz, A.L. (1991). Nucleotide sequence of a cDNA clone corresponding to the maize *Globulin-2* gene. Plant Physiol. 95, 973-975.

Williamson, J.D. & Quatrano, R.S. (1988). ABA-regulation of two classes of embryo-specific sequences in mature wheat embryos. Plant Physiol. 86, 208-215.

Chapter 8

Angiosperm female gametophyte development

M.H. THIJSSEN

Introduction

Male gametophyte cells develop within the stamen's anther, are released from the plant as pollen, and thereby easily accessible for cytological, biochemical and molecular characterization. The female gametophyte of angiosperms, the megagametophyte or embryo sac develops from a single cell, the megaspore, which is located within several layers of ovular cells and within the carpel's ovary. The inaccessibility of the female gametophyte makes the study of gametophyte differentiation difficult, and though the structural organization of the embryo sac has already been studied for decades, the process of gametogenesis is still poorly understood.

Cryofixation is now a generally accepted method to preserve cells closer to their native state than chemical fixation methods (reviewed by Menco, 1986; Galway *et al.*, 1995). High pressure freezing and freeze substitution allow the adequate preservation of tissues as large as 600 µm (Müller & Moor, 1984), including ovules (Thijssen *et al.*, 1997, chapter 2 of this thesis). By employing this cryofixation method, it is now possible to obtain high resolution structural information on female gametophyte organization that may be destroyed by chemical fixation, for a better understanding of the functioning of megagametophyte cells.

Over the last decade, techniques have emerged to isolate megagametophytes from their ovular environment, providing a new approach for gaining insight in female gametophyte development, fertilization, and embryological development, allowing detailed studies to be conducted from a structural, biochemical and molecular perspective (reviewed by Theunis *et al.*, 1991; Huang & Russell, 1992a; Dumas & Mogensen, 1993). Also living gametophytes and gametophytic cells can be isolated (Huang & Russell, 1992a), allowing the study and culture of female reproductive cells, uninfluenced by the tissues that surround them *in planta*.

Hampered by the inaccessibility of the female gametophyte, the genetic and molecular basis controlling female gametophyte development in plants has only begun to be explored. It is only recently that studies are undertaken to identify genes that play a role in the specification and differentiation of female reproductive cells, and genes that are involved in megagametophyte function. A number of interesting mutants that are affected in female gametophyte development, mainly in *Arabidopsis*, have now become available (reviewed by Christensen *et al.*, 1998; Drews *et al.*, 1998; Grossniklaus & Schneitz, 1998; Schneitz, 1999; Drews & Yadegari, 2002). The availability of these mutants makes it possible to characterize the genes required for female gametophyte development.

In this manuscript I have discussed the advantages and limitations of cryofixation by high pressure freezing, the technique I employed in this thesis work for the ultrastructural analysis of female gametophyte development. Moreover I have discussed the impacts that ultrastructural studies, the application of isolation methodologies and molecular and genetic approaches have had so far, on the understanding of female gametophyte development and function. Future directions of research are suggested.

Cryofixation for ultrastructural preservation

Decades of microscopic studies on female gametophyte differentiation and fertilization have yielded an enormous amount of information on the structural aspects of embryo sac organization (reviewed by Kapil & Bhatnagar, 1981; Willemse & Van Went, 1984; Haig, 1990; Reiser & Fischer, 1993). Most of these studies are based on chemically fixed ovules and megagametophytes. To analyze cell architecture and to relate functional roles to the cellular components, which is the aim of ultrastructural studies, cells have to be adequately fixed. Adequate fixation means fixation in a way resembling as much as possible the native state, with spatial and temporal integrity. Due to the nature and duration of a chemical fixation process, a variety of structural artifacts can be induced (Mersey & McCully, 1978; Hayat, 1986). Female gametophytes develop within several layers of ovular tissues and are surrounded by rigid cell walls; female gametophytes consist of relatively large cells and are highly vacuolated, with their osmotic pressure differing from the surrounding ovular tissues, and changing during development (Imre & Kristóf, 1999). These characteristics make them very difficult to preserve adequately for ultrastructural studies with conventional chemical fixatives.

Cryofixation physically arrests cell structure and cellular processes within milliseconds, with the ultrastructure of the cryofixed cells reflecting more closely the living state (reviewed by Menco, 1986; Galway *et al.*, 1995). Whereas with ultra-rapid freezing techniques adequate ultrastructural preservation is generally limited to the outer 8 to 20 μm of the specimen (Sitte *et al.*, 1987), with high pressure freezing (freezing the specimen under a pressure of 2100 bar [Müller & Moor, 1984; Moor, 1987]), the vitrification depth can be increased more than 10-fold (Sartori *et al.*, 1993).

High pressure freezing and freeze substitution have been employed for the ultrastructural analysis of a variety of plant tissues and have changed our views or added significantly to our knowledge on e.g. secretory processes (Meindl *et al.*, 1992), endocytosis (Galway *et al.*, 1993), actin-endoplasmic reticulum complexes (Lichtscheidl

et al., 1990), protein distribution in protein storage vacuoles (Lonsdale *et al.*, 1999), cell plate formation (Samuels *et al.*, 1995), differentiation of Golgi stacks (Staehelin *et al.*, 1990), and chloroplast structure and organization (Bourett *et al.*, 1999).

The combination of high pressure freezing/ freeze substitution and high resolution electron tomography enabled three dimensional analyses of syncytial-type cell plates during endosperm cellularization (Otegui *et al.*, 2001). Water-soluble salts that accumulate during *Arabidopsis* seed development can be preserved with high pressure freezing/ freeze substitution; the distribution of these salts could be visualized with energy-dispersive x-ray spectroscopy (Otegui *et al.*, 2002). Combining high pressure freezing/ freeze substitution with immunocytochemistry enabled the accurate localization of plant proteins at the cellular level, for example in protein storage vacuoles of barley aleurone cells (Lonsdale *et al.*, 1999), and allowed functional compartmentation of the Golgi apparatus in sycamore maple cells (Zhang & Staehelin, 1992).

A number of structural artifacts have been observed in tissues fixed with high pressure freezing. Artifacts are ascribed to exposure of the sample to high pressure before freezing, to the freezing process, or to subsequent steps in specimen handling, like freeze substitution. Artifacts that were attributed to high pressure exposure are: bursting of large vesicles in root cap cells of *Arabidopsis* (Kiss *et al.*, 1990) and in fungal sporangia (Hyde *et al.*, 1991), the appearance of loose wavy microfilament bundles (Ding *et al.*, 1992), tears and folds in plasma membranes (Craig & Staehelin, 1988) and gaps in nuclear envelopes (Kiss & Staehelin, 1995). Craig *et al.* (1987) blame breaks in cell walls and cytoplasmic strands to the vibration of the specimen cups during freezing; according to Studer *et al.* (1989) this might be the result of the conversion of high density ice, which is formed during the freezing under pressure, into ice with a lower density, formed during re-warming to freeze substitution temperatures.

Incomplete freeze substitution may induce the formation of secondary ice crystals, thereby disturbing the ultrastructure. This appeared to be a problem in our studies on *P.* x *hybrida* ovule and female gametophyte development, when we initially used the embedding fluid 1-hexadece to fill the space between the ovules in the specimen sandwich (Thijssen *et al.*, 1997, chapter 2 of this thesis). 1-hexadecene is not soluble at freeze substitution temperatures and hinders substitution when tissues are completely surrounded by this compound (Hohenberg *et al.*, 1994). The application of heptane and isooctane as embedding fluids to fill the specimen sandwich, led to adequate freeze substitution and 90% of crystal-free *P.* x *hybrida* ovules (Thijssen *et al.*, 1998, chapter 3 of this thesis). However, the better the

cryofixation, the more difficult the freeze substitution. In some areas of excellently preserved tissues, the two lipid layers of the plasma membrane separated; this may have been due to water tightly bound to the plasma membrane, which was not removed during freeze substitution (Müller, pers. com.).

Galway *et al.* (1995) mention that the main problem of cryofixation is no longer the freezing process, but the preparation and handling of the specimens before freezing. The way in which ultrastructural preservation reflects the living state greatly depends on physiological control of the sample until freezing is completed; time between dissection of tissues and cryofixation must be kept to a minimum. Heptane and isooctane did have some damaging effects on the outer layers of *P.* x *hybrida* ovules; however, the inner tissues were not affected (Thijssen *et al.*, 1998, chapter 3 of this thesis). In general, in ultrastructural studies compromises on fixation techniques are unavoidable.

Cryofixation technologies provide "snapshots" of subcellular organization. The ability to mark subcellular components in living plant cells with green fluorescent protein (GFP), and follow the marker protein in individual cells in real time, has greatly enhanced our insights in subcellular organization (reviewed by Hawes *et al.*, 1999; Cutler & Ehrhardt, 2000). Marking with GFP showed the remarkable dynamics of the Golgi apparatus (review: Nebenführ & Staehelin, 2001), the endoplasmic reticulum (review: Staehelin, 1997), plastids (Kohler & Hanson, 2000) and the microtubular cytoskeleton (Granger & Cyr, 2000), including dynamic instability (Vos *et al.*, 2003). Randomly marked plant cells may reveal structures and dynamics that have not as yet been described (Cutler & Ehrhardt, 2000). Comparison of high resolution ultrastructural data with data obtained from living cells, and vice versa, will complement and further extend our knowledge on plant cell structure and functional organization.

Female gametophyte development

From functional megaspore to seven-celled embryo sac

In most angiosperm species, including *P.* x *hybrida*, the embryo sac develops according to the *Polygonum* type (Willemse & Van Went, 1984). In this type of female gametophyte development one of the four haploid megaspores undergoes three rounds of mitotic divisions, resulting in an eight-nucleate coenocyte. Formation of cell plates results in the formation of the seven-celled embryo sac which after differentiation consists of one egg cell, two synergid cells, three antipodal cells and one two-nucleate

central cell, with each of these cell types its own location, morphology, cytoarchitecture and function.

In the monosporic gametophyte, after meiosis, three of the megaspores degenerate and one of them, the functional megaspore, will greatly enlarge. The isolation by callose walls is supposed to play a role in the isolation and subsequent degeneration of the non-functional megaspores (reviewed by Huang & Russell, 1992a).

The functional megaspore starts to vacuolize and with the first mitotic division the central vacuole separates the micropylar and chalazal cytoplasm. Whereas in *P.* x *hybrida* the distribution and organization of cytoplasm at the two megagametophyte poles is equal (chapter 4 of this thesis), in some other species it is not (Huang & Russell, 1993). This may have implications for subsequent developmental patterns and ultimate determination of cell fate in the seven-celled embryo sac (Folsom & Cass, 1989; Huang & Russell, 1992a; Huang & Sheridan, 1994).

In *P.* x *hybrida* megagametophyte enlargement goes together with an increase in the number of organelles. The cytoplasmic constitution of the highly vacuolated one-nucleate, two-nucleate and four-nucleate megagametophyte looks similar (chapter 4 of this thesis). The cytoplasm contains extensive rough endoplasmic reticulum, numerous mitochondria and a high number of polysomes. Golgi bodies with associated vesicles and large starch containing plastids are present. This shows that the gametophyte is an active cell. Differences between species have been reported for the moment of increase of the number of organelles, the amount of starch and lipids present at the different developmental stages, and the way of vacuole formation (reviewed by Kapil & Bhatnagar, 1981; Willemse & Van Went, 1984).

Immunofluorescence studies of isolated megaspores and megagametophytes of *Arabidopsis* (Webb & Gunning, 1994) and maize (Huang & Sheridan, 1994) showed microtubules that are distributed throughout the cytoplasm of the functional megaspore and two-nucleate and four-nucleate megagametophyte; these are believed to function in maintaining cytoplasmic organization (Huang & Sheridan, 1994; Webb & Gunning, 1994). In addition, microtubules that seem to radiate from the nuclei are believed to have a role in the positioning of the nuclei within the coenocytic cells (Huang & Sheridan, 1994; Webb & Gunning, 1994). Similar microtubule organizations were also found at the ultrastructural level in *P.* x *hybrida* megagametophytes (chapter 4 of this thesis). The mitotic divisions at the micropylar and chalazal pole are synchronized (Huang & Sheridan, 1994; Webb & Gunning, 1994; chapter 4 of this thesis).

A number of female gametophyte mutants of *Arabidopsis* do not enter the mitotic

phase and are arrested at the functional megaspore stage (*Gf*, Christensen *et al.*, 1997; *fem2*, *fem3*, *gfa4*, *gfa5*, Christensen *et al.*, 1998; *ada*, *tya*, Howden *et al.*, 1998). In another *Arabidopsis* mutant, mitosis is arrested after one or two divisions (*hdd*, Moore *et al.*, 1997). The abnormal distribution of nuclei in the *hdd* megagametophyte suggests that the wild type gene product is required for normal nuclear migration (Moore *et al.*, 1997). The maize *ig* mutant, which shows disturbed nuclear migration as well, has been shown to be defective in the organization of the microtubular cytoskeleton (Huang & Sheridan, 1996).

After the third round of mitotic divisions cell plate formation takes place and seven cells are formed. Different models of embryo sac cell plate formation are proposed in the literature, and there is some disagreement of the total number of cell plates that are involved (reviewed by Russell, 1993). Preprophase bands are absent. Sites of cell plate formation seem to be determined by cytoplasmic domains; cell plates arise at sites where microtubules that radiate from individual nuclei meet (Russell, 1993). Cell plate formation in syncytial endosperm cells is organized in a similar manner (Van Lammeren, 1988; Otegui & Staehelin, 2000).

Mutant *ig* megagametophytes show additional nuclear divisions, or additional divisions of individual micropylar embryo sac cells (Huang & Sheridan, 1994). Mutant *hdd* megagametophytes already form cell plates after the first or second round of mitotic divisions (Moore *et al.*, 1997). These mutants show that the mechanism that regulates the number of mitotic divisions and the mechanism that regulates the timing of cell plate formation are not coupled.

Although of clonal origin in monosporic embryo sacs, the cells in wild type embryo sacs differentiate along four different developmental pathways. Abnormally positioned cells in *ig* embryo sacs (Huang & Sheridan, 1996) and cells in the *hdd* megagametophytes (Moore *et al.*, 1997) do not differentiate into normal gametophytic cells. This suggests that cell specification might depend on correct positioning (Grossniklaus & Schneitz, 1998). In pollen development the first mitosis results in a large vegetative cell and a small generative cell. If division asymmetry is altered, like in the mutant pollen *gem1*, cell fate is altered, with a vegetative cell marker gene activated in both cells (Park *et al.*, 1998).

Egg cell

During fertilization one of the sperm cells fuses with the egg cell, giving rise to the embryo (for reviews, see Russell, 1993; Faure, 2001; Antoine *et al.*, 2001). The specific

physiological and biochemical characteristics of the egg cell that prepare it to readily accept the genome of the male gamete are still poorly understood.

The ultrastructure of egg cells varies between angiosperm species and the number and distribution of plastids, mitochondria, endoplasmic reticulum and lipid bodies differ greatly (Russell, 1993). *P.* x *hybrida* egg cells are extremely vacuolated and contain very few organelles (chapter 5 of this thesis). In general, from its ultrastructural characteristics the unfertilized egg cell appears to be a quiescent unspecialized cell in comparison to the synergid cells (Russell, 1993).

Fertilization triggers "egg activation", a preprogrammed set of events that leads to embryo development (Antoine *et al.*, 2001). High amounts of cDNA encoding eIF-5A, a eukaryotic translation initiation factor, necessary for selective mRNA stabilization and translation, were detected in maize egg cells (Dresselhaus *et al.*, 1999). This may be related to the cell's preparation for selective mRNA translation, which is quickly triggered after fertilization (Dresselhaus *et al.*, 1999).

Generally, at the chalazal side of the egg cell and the synergid cells, the plasma membranes align very closely with the plasma membrane of the central cell, which is presumed to aid in the fusion of female and male gametes (Russell, 1993). We never observed electron-translucent spaces between the plasma membranes like those that have been reported for some species (Willemse & Van Went, 1984), and propose that these spaces are an artifact of chemical fixation (chapter 5 of this thesis).

Synergid cells

The function of the synergid cells is to attract and accept the pollen tube (Ray *et al.*, 1997; Higashiyama, 2002; Higashima *et al.*, 2001). Recently, mutant *sm* embryo sacs showed that the female gametophyte is responsible for male gamete delivery into the embryo sac; pollen tubes do not stop their growth and do not deliver their contents in *sm* embryo sacs (Rotman *et al.*, 2003).

From ultrastructural studies it appears that synergids are highly differentiated, metabolically active cells. Common features between species are the presence of a large number of mitochondria and Golgi bodies, extensive endoplasmic reticulum and abundant ribosomes (Willemse & Van Went, 1984). The same accounts for *P.* x *hybrida* synergid cells (chapter 5 of this thesis). At the most micropylar part of the synergids, a thickened cell wall, called the filiform apparatus is formed. In most species the filiform apparatus shows characteristics of transfer cell walls, with cell wall projections extending deep into the cytoplasm (Willemse & Van Went, 1984). In *P.* x *hybrida* the

filiform apparatus is very regular in outline (chapter 5 of this thesis). An inner and outer core, as observed when ovules are fixed with potassium permanganate (Van Went, 1970), are not present in cryofixed preparations. The filiform apparatus might serve as a diffusion pathway for chemo-attractant substances involved in attraction of the pollen tube (Higashiyama *et al.*, 2003). The high density of vesicles in the micropylar area of *P.* x *hybrida* synergids, and the presence of micropylar exudate at embryo sac maturity, support a secretary function for the synergid cells (chapter 5 of this thesis).

In most species studied, including tobacco, one of the synergid cells begins to degenerate shortly before pollen tube arrival (Huang & Russell, 1992b). Removal of the style before pollen tube arrival in the ovary, prohibited synergid degeneration, suggesting that the degeneration of the synergid cell is triggered only after the pollen tubes have penetrated the ovary (Huang & Russell, 1992b). The degenerate synergid displays high amounts of membrane-bound calcium that may be involved in pollen tube arrest and rupture, releasing the sperm cells into the embryo sac (Huang & Russell, 1992b). High levels of calcium may aid in male gamete – female gamete fusion (Zhang *et al.*, 1997). In other species, including *P.* x *hybrida*, degenerative changes do not occur prior to pollen tube penetration, and at embryo sac maturity, there are no differences in cellular organization between the two synergid cells (chapter 5 of this thesis).

The Arabidopsis *gfa2* mutant is affected in cell death and although pollen tubes penetrate the micropyle, which is normally sufficient to induce synergid cell death, no signs of degeneration could be observed in either of the mutant's synergids (Christensen *et al.*, 2002). GFA2 is targeted to the mitochondria, suggesting a role for mitochondria in cell death in plants (Christensen *et al.*, 2002). Curiously, the mutant also appears affected in polar nuclei fusion (Christensen *et al.*, 2002).

Central cell

During fertilization one of the sperm cells fuses with the central cell to form the endosperm, a tissue with a nutritive function for the developing embryo (for recent review on endosperm development, see Berger, 2003). This cell is the largest cell of the embryo sac and is highly vacuolated, with the major portion of the cytoplasm placed at the micropylar side, close to the egg apparatus cells. The cell contains the two polar nuclei, which eventually fuse. The time of nuclear fusion varies between species (Willemse & Van Went, 1984). Christensen *et al.* (1998) report three *Arabidopsis* mutants, *gfa2*, *gfa3* and *gfa7*, with polar nuclei that fail to fuse; nuclear fusion in

Arabidopsis normally happens before fertilization.

In most species the cytoplasm of the central cell appears metabolically active, with numerous mitochondria, extensive endoplasmic reticulum, a large number of Golgi bodies and numerous ribosomes (Willemse & Van Went, 1984). The central cell of *P.* x *hybrida* has few mitochondria and Golgi bodies and few strands of endoplasmic reticulum (chapter 5 of this thesis). At maturity a lot of large starch containing plastids have accumulated (chapter 5 of this thesis).

In the *Petunia inflata ASRK-13* mutant, which is transformed with an antisense gene encoding the extracellular domain of receptor kinase PRK1, the embryo sacs fail to progress through the maturation stages of cell expansion, polar nuclei fusion, and cell differentiation (Lee *et al.*, 1997). The central cell does not accumulate starch. The role of PRK1 in female gametogenesis remains to be elucidated (Lee *et al.*, 1997).

Antipodal cells

The antipodal cells are the most variable cells in the embryo sac. In some species they degenerate before embryo sac maturity, whereas in others they persist up to the globular pro-embryo stage, and may even proliferate into a multicellular tissue (Willemse & Van Went, 1984). Besides differences in the timing of cell degeneration between species, variability might also exist in the time of antipodal cell degeneration within species, as has been reported for different *Arabidopsis* lines (Murgia *et al.*, 1993). However, this did not influence embryo sac function (Murgia *et al.*, 1993).

Related to their variable organization, different functions have been attributed to the antipodal cells, including (1) the transfer of nutrients from the nucellar tissues to the central cell; (2) the storage of reserves for the developing embryo and endosperm; and (3) a secretory function (Willemse & Van Went, 1984). In *P.* x *hybrida*, transfer like cell wall projections are not present in the antipodal cells. Plasmodesmatal connections with the chalazal tissue are present, but plasmodesmata seem to be occluded (chapter 5 of this thesis). Initially the cells seem highly metabolically active with Golgi bodies that are associated with vesicles and a high density of ribosomes and polysomes, sometimes associated with the endoplasmic reticulum. The *P.* x *hybrida* antipodal cells show signs of degeneration at the stage of embryo sac maturity (chapter 5 of this thesis), and therefore can only support embryo sac function for a short time. Some authors suggest that the antipodal cells are not essential for proper embryo sac function (Murgia *et al.*, 1993).

Cell-cell communication and cell specification

Plant cells communicate by the regulation of plasmodesmatal transport (Heinlein, 2002). Recently, it has been shown that not only small molecules move from cell to cell through plasmodesmata, but also macromolecular proteins, such as transcription factors, plant defense proteins and viral proteins (Heinlein, 2002). Whereas plasmodesmatal connections between the embryo sac and the ovular tissues seem to be restricted to the most chalazal part of the embryo sac, a number of ultrastructural studies have shown the presence of plasmodesmata between the different embryo sac cells (Huang & Russell, 1992a; chapter 5 of this thesis). The microinjection of fluorescent probes into the central cell of *Torenia* embryo sacs showed high symplastic permeability between this cell and the egg apparatus cells before fertilization (Han *et al.*, 2000). Han *et al.* (2000) observed that the symplastic permeability decreased drastically after fertilization and suggest that the symplastic connection might be related to the transport of molecules with a role in the functional organization of the cells, related to the coordination of the double fertilization process. Symplastic isolation is believed to be required in specific cells and tissues to perform distinct functions and for morphogenesis, e.g. the commitment to flowering involves a period of plasmodesmata closure and reduced intercellular communication (Gisel *et al.*, 2001).

Generally, antipodal cells are connected to each other as well as to the central cell through plasmodesmata. Also at the chalazal side of the antipodal cells plasmodesmatal contacts with the bordering chalazal cells are generally present (Willemse & Van Went 1984; chapter 5 of this thesis). In some species, transfer wall like cell projections have been observed (Willemse & Van Went, 1984). These characteristics are thought to be related to one of the functions attributed to the antipodal cells, i.e. the transfer of nutrients from the nucellar tissues to the central cell (Willemse & Van Went, 1984).

Genes that are specifically expressed in the different gametophytic cells suggest a role in the specification or the function of the cells (Grossniklaus & Schneitz, 1998). However, embryo sac cell specification may also depend on signals that are produced locally by the surrounding ovular cells (Grossniklaus & Schneitz, 1998). Sporophytically acting mutants that disrupt megagametophyte development may provide insight into external factors acting on megagametophyte development (Grossniklaus & Schneitz, 1998).

At what developmental point the embryo sac cells become committed to their specific type is not clear. Pollination can accelerate differentiation, as has been shown

for maize egg cells (Mòl *et al.*, 2000). From cytological studies it appeared that pollination accelerated the late steps of egg cell differentiation, with the non-species-specific pollination signal acting immediately after pollen deposition (Mòl *et al.*, 2000).

Additional mitotic divisions in the mutant *ig* maize embryo sac result in more than three cells at the micropylar pole of the embryo sac. The cells have no obvious polarity and all show uniform cytoplasmic features (Huang & Sheridan, 1996). And though these cells lack the ultrastructural characteristics common for synergid cells, still some of them do function as such, and are able to receive a pollen tube. Fertilization gives rise to polyembryony and endosperm with variations in ploidy level (Huang & Sheridan, 1994).

Conclusions and prospects

The study and culture of living gametophytes and gametophytic cells, uninfluenced by the tissues that surround them *in planta* can contribute to the understanding of megagametophyte differentiation and function. *In planta* fertilized isolated zygotes of barley (Holm *et al.*, 1994), maize (Mòl *et al.*, 1995; Leduc *et al.*, 1996), and wheat (Holm *et al.*, 1994; Kumlehn *et al.*, 1998) and *in vitro* fertilized egg cells of maize (Kranz & Lörz, 1993) and wheat (Kovács *et al.*, 1995) are able to develop into embryos or embryo-like structures in culture. Only few data are available on the division of isolated mature unfertilized embryo sac cells in culture. Cell division has been reported for unfertilized tobacco egg cells (Tian & Russell, 1997) and unfertilized rice egg cells and central cells (Zhao *et al.*, 1999). High pulses of 2,4-dichlorophenoxyacetic acid could induce cell division in unfertilized maize egg cells (Kranz *et al.*, 1995). Our attempts to induce *in vitro* development of unfertilized embryo sacs of *P.* x *hybrida* proved to be unsuccessful so far (chapter 6 of this thesis).

Whereas mature embryo sacs *in planta* need the trigger of fertilization for cell division and further development, the induction of cell division of isolated megaspores and immature megagametophytes *in vitro* might be expected to be easier. Though some attempts have been reported (Mouritzen & Holm, 1995; chapter 6 of this thesis), to our knowledge there are as yet no publications, in which the successful culture of megasporocytes, megaspores, or megagametophytes have been described. Improving the viability of isolated megaspores and megagametophytes and establishing an *in vitro* culture system that sustains the development of the isolated cells, will allow fundamental questions on female gametophyte biology to be addressed experimentally. With the induction of parthenogenesis in isolated embryo sac cells, an

in vitro system for gynogenetic-haploid plant production comes within reach.

Decroocq-Ferrant (1994) prepared an embryo sac cDNA library, starting from about 10,000 isolated female gametophytes of *P.* x *hybrida*. With the RT-PCR (reverse transcription-polymerase chain reaction method) Dresselhaus *et al.* (1994) were able to create representative cDNA libraries from as few as 128 unfertilized egg cells and 104 *in vitro* zygotes. From these libraries they were able to isolate several clones that were specifically expressed in these cells. With a sensitive RT-PCR assay gene expression can be studied at the single cell level (Richert *et al.*, 1996). Construction of stage specific cDNA libraries from isolated megaspores and megagametophytes at different developmental stages could allow the isolation of genes that are expressed at specific stages of female gametophyte development, revealing critical transition points during this development.

With an increasing number of identified genes that play a role in female gametophyte development, the challenge will be to understand their function. The integration of information at the molecular level, with the level of cell organization will contribute to further insight into this process. The use of mutants that are disturbed in female gametophyte development and studies on wild type female gametophyte structure and development, provide the essential framework upon which mutagenic approaches are based. Concerning these aspects, electron microscopy data obtained with high pressure freezing may play a crucial role.

Acknowledgements

I thank Prof. Jacques Van Went and Prof. Anne Mie Emons for discussions and Dr. Daphne Wittich-Rainey for English corrections on this chapter.

References

Antoine, A.F., Dumas, C., Faure, J.-E., Feijó, J.A. & Rougier, M. (2001). Egg activation in flowering plants. Sex. Plant Reprod. 14, 21-26.

Berger, F. (2003). Endosperm: The crossroad of seed development. Curr. Opin. Plant Biol. 6, 42-50.

Bourett, T.M., Czymmek, K.J. & Howard, R.J. (1999). Ultrastructure of chloroplast protuberances in rice leaves preserved by high-pressure freezing. Planta 208, 472-479.

Christensen, C.A., Gorisch, S.W., Brown, R.H., Jones, L.G., Brown, J., Shaw, J.M. & Drews, G.N. (2002). Mitochondrial GFA2 is required for synergid cell death in *Arabidopsis*. Plant Cell 14, 2215-2232.

Christensen, C.A., King, E.J., Jordan, J.R. & Drews, G.N. (1997). Megagametogenesis in *Arabidopsis* wild type and the *Gf* mutant. Sex. Plant Reprod. 10, 49-64.

Christensen, C.A., Subramanian, S. & Drews, G.N. (1998). Identification of gametophytic mutations affecting female gametophyte development in *Arabidopsis*. Dev. Biol. 202, 136-151.

Craig, S., Gilkey, J.C. & Staehelin, L.A. (1987). Improved specimen support cups and auxiliary devices for the Balzer's high pressure freezing apparatus. J. Microsc. 148, 103-106.

Craig, S. & Staehelin, L.A. (1988). High pressure freezing of intact plant tissues. Evaluation and characterization of novel features of the endoplasmic reticulum and associated membrane systems. Eur. J. Cell Biol. 46, 80-93.

Cutler, S. & Ehrhardt, D. (2000). Dead cells don't dance: Insights from live-cell imaging in plants. Curr. Opin. Plant Biol. 3, 532-537.

Decroocq-Ferrant, V., Van Went, J. & Kreis, M. (1994). Embryo sac and ovule cDNA libraries of *Petunia hybrida*. Recherche et charactérisation de gènes codant des protéines kinases potentiellement impliquées dans le développement des organes reproducteurs chez *Petunia hybrida* L. PhD thesis V. Decroocq-Ferrant, pp. 23-30. Université Paris-Sud, Centre d'Orsay.

Ding, B., Turgeon, R. & Parthasarathy, M.V. (1992). Effect of high-pressure freezing on plant microfilament bundles. J. Microsc. 165, 367-376.

Dresselhaus, T., Cordts, S. & Lörz, H. (1999). A transcript encoding translation initiation factor eIF-5A is stored in unfertilized egg cells of maize. Plant Mol. Biol. 39, 1063-1071.

Dresselhaus, T., Lörz, H. & Kranz, E. (1994). Representative cDNA libraries from few plant cells. Plant J. 5, 605-610.

Drews, G.N., Lee, D. & Christensen, C.A. (1998). Genetic analysis of female gametophyte development and function. Plant Cell 10, 5-17.

Drews, G.N. & Yadegari, R. (2002). Development and function of the angiosperm female gametophyte. Annu. Rev. Genet. 36, 99-124.

Dumas, C. & Mogensen, H.L. (1993). Gametes and fertilization: Maize as a model system for experimental embryogenesis in flowering plants. Plant Cell 5, 1337-1348.

Faure, J.-E. (2001). Double fertilization in flowering plants: Discovery, study methods and mechanisms. C.R. Acad. Sci. Paris, Life Sciences 324, 551-558.

Folsom, M.W. & Cass, D.D. (1989). Embryo sac development in soybean: Ultrastructure of megasporogenesis and early megagametogenesis. Can. J. Bot. 67, 2841-2849.

Galway, M.E., Heckman, J.W. Jr, Hyde, G.J. & Fowke, L.C. (1995). Advances in high-pressure and plunge-freeze fixation. Methods in cell biology, Vol. 49 (ed. by D.W. Galbraith, H.J. Bohnert and D.P. Bourque), pp. 3-19. Academic Press, Inc., San Diego, CA.

Galway, M.E., Rennie, P.J. & Fowke, L.C. (1993). Ultrastructure of the endocytotic pathway in glutaraldehyde-fixed and high-pressure frozen/ freeze-substituted protoplasts of white spruce (*Picea glauca*). J. Cell Sci. 106, 847-858.

Gisel A., Hempel, F.D., Barella, S. & Zambryski, P. (2001). Leaf-to-shoot apex movement of symplastic tracer is restricted coincident with flowering in *Arabidopsis*. Proc. Natl. Acad. Sci. USA 99, 1713-1717.

Granger, C.L. & Cyr, R.J. (2000). Microtubule reorganisation in tobacco BY-2 cells stably expressing GFP-MBD. Planta 210, 502-509.

Grossniklaus, U. & Schneitz, K. (1998). The molecular and genetic basis of ovule and megagametophyte development. Cell Dev. Biol. 9, 227-238.

Haig, D. (1990). New perspectives on the angiosperm female gametophyte. Bot. Rev. 56, 236-274.

Han, Y.-Z., Huang, B.-Q., Zee, S.-Y. & Yuan, M. (2000). Symplastic communication between the central cell and the egg apparatus cells in the embryo sac of *Torenia fournieri* Lind. before and during fertilization. Planta 211, 158-162.

Hawes, C.R., Brandizzi, F. & Andreeva, A.V. (1999). Endomembranes and vesicle trafficking. Curr. Opin. Plant Biol. 2, 454-461.

Hayat, M.A. (1986). Glutaraldehyde: Role in electron microscopy. Micron Microsc. Acta 17, 115-135.

Heinlein, M. (2002). Plasmodesmata: Dynamic regulation and role in macromolecular cell-to-cell signaling. Curr. Opin. Plant Biol. 5, 543-552.

Higashiyama, T. (2002). The synergid cell: Attractor and acceptor of the pollen tube for double fertilization. J. Plant Res. 115, 149-160.

Higashiyama, T., Kuroiwa, H. & Kuroiwa, T. (2003). Pollen-tube guidance: Beacons from the female gametophyte. Curr. Opin. Plant Biol. 6, 36-41.

Higashiyama, T., Yabe, S., Sasaki, N., Nishimura, Y., Miyagishima, S., Kuroiwa, H. & Kuroiwa, T. (2001). Pollen tube attraction by the synergid cell. Science 293, 1480-1483.

Hohenberg, H., Mannweiler, K. & Müller, M. (1994). High-pressure freezing of cell suspensions in cellulose capillary tubes. J. Microsc. 175, 34-43.

Holm, P.B., Knudsen, S., Mouritzen, P., Negri, D., Olsen, F.L. & Roué, C. (1994). Regeneration of fertile barley plants from mechanically isolated protoplasts of the fertilized egg cell. Plant Cell 6, 531-543.

Howden, R., Park, S.K., Moore, J.M., Orme, J., Grossniklaus, U. & Twell, D. (1998). Selection of T-DNA-tagged male and female gametophytic mutants by segregation distortion in *Arabidopsis*. Genetics 149, 621-631.

Huang, B.-Q. & Russell, S.D. (1992a). Female germ unit: Organization, isolation, and function. Int. Rev. Cytol. 140, 233-293.

Huang, B.-Q. & Russell, S.D. (1992b). Synergid degeneration in *Nicotiana*: A quantitative, fluorochromatic and chlorotetracycline study. Sex. Plant Reprod. 5, 151-155.

Huang, B.-Q. & Russell, S.D. (1993). Polarity of nuclear and organellar DNA during megasporogenesis and megagametogenesis in *Plumbago zeylanica*. Sex. Plant Reprod. 6, 205-211.

Huang, B.-Q. & Sheridan, W.F. (1994). Female gametophyte development in maize: Microtubular organization and embryo sac polarity. Plant Cell 6, 845-861.

Huang, B.-Q. & Sheridan, W.F. (1996). Embryo sac development in the maize *indeterminate gametophyte1* mutant: Abnormal nuclear behaviour and defective microtubule organization. Plant Cell 8, 1391-1407.

Hyde, G.J., Lancelle, S., Hepler, P.K. & Hardham, A.R. (1991). Sporangial structure in *Phytophthora* is disrupted after high pressure freezing. Protoplasma 165, 203-208.

Imre, K. & Kristóf, Z. (1999). Isolation and osmotic relations of developing megagametophytes of *Torenia fournieri*. Sex. Plant Reprod. 12, 152-157.

Kapil, R.N. & Bhatnagar, A.K. (1981). Ultrastructure and biology of female gametophyte in flowering plants. Int. Rev. Cytol. 70, 291-341.

Kiss, J.Z., Giddings, T.H. Jr, Staehelin, L.A. & Sack, F.D. (1990). Comparison of the ultrastructure of conventionally fixed and high pressure frozen/ freeze substituted root tips of *Nicotiana* and *Arabidopsis*. Protoplasma 157, 64-74.

Kiss, J.Z. & Staehelin, L.A. (1995). High pressure freezing. Rapid freezing, freeze fracture and deep etching (ed. by N.J. Severs and D.M. Shotton), pp. 89-104. Wiley-Liss, New York.

Kohler, R.H. & Hanson, M.R. (2000). Plastid tubules of higher plants are tissue-specific and developmentally regulated. J. Cell Sci. 113, 81-89.

Kovács, M., Barnabás, B. & Kranz, E. (1995). Electro-fused isolated wheat (*Triticum aestivum* L.) gametes develop into multicellular structures. Plant Cell Rep. 15, 178-180.

Kranz, E. & Lörz, H. (1993). *In vitro* fertilization with isolated, single gametes results in zygotic embryogenesis and fertile maize plants. Plant Cell 5, 739-746.

Kranz, E., Von Wiegen, P. & Lörz, H. (1995). Early cytological events after induction of cell division in egg cells and zygote development following *in vitro* fertilization with angiosperm gametes. Plant J. 8, 9-23.

Kumlehn, J., Lörz, H. & Kranz, E. (1998). Differentiation of isolated wheat zygotes into embryos and normal plants. Planta 205, 327-333.

Leduc, N., Matthys-Rochon, E., Rougier, M., Mogensen, L., Holm, P., Magnard, J.-L. & Dumas, C. (1996). Isolated maize zygotes mimic *in vivo* embryonic development and express microinjected genes when cultured *in vitro*. Dev. Biol. 177, 190-203.

Lee, H.-S., Chung, Y.-Y., Das, C., Karunanandaa, B., Van Went, J.L., Mariani, C. & Kao, T.-H. (1997). Embryo sac development is affected in *Petunia inflata* plants transformed with an antisense gene encoding the extracellular domain of receptor kinase PRK1. Sex. Plant Reprod. 10, 341-350.

Lichtscheidl, I.K., Lancelle, S.A. & Hepler, P.K. (1990). Actin-endoplasmic reticulum complexes in *Drosera*. Their structural relationship with the plasmalemma, nucleus, and organelles in cells prepared by high pressure freezing. Protoplasma 155, 116-126.

Lonsdale, J.E., McDonald, K.L. & Jones, R.L. (1999). High pressure freezing and freeze substitution reveal new aspects of fine structure and maintain protein antigenicity in barley aleurone cells. Plant J. 17, 221-229.

Meindl, U., Lancelle, S. & Hepler, P.K. (1992). Vesicle production and fusion during lobe formation in *Micrasterias* visualized by high-pressure freeze fixation. Protoplasma 170, 104-114.

Menco, B.P.M. (1986). A survey of ultra-rapid cryofixation methods with particular emphasis on applications to freeze-fracturing, freeze-etching, and freeze-substitution. J. Electron Microsc. Tech. 4, 177-240.

Mersey, B. & McCully, M.E. (1978). Monitoring the course of fixation in plant cells. J. Microsc. 114, 49-76.

Mòl, R., Idzikowska, K., Dumas, C. & Matthys-Rochon, E. (2000). Late steps of egg cell differentaition are accelerated by pollination in *Zea mays* L. Planta 210, 749-757.

Mòl, R., Matthys-Rochon, E. & Dumas, C. (1995). Embryogenesis and plant regeneration from maize zygotes by *in vitro* culture of fertilized embryo sacs. Plant Cell Rep. 14, 743-747.

Moor, H. (1987). Theory and practice of high pressure freezing. Cryotechniques in biological electron microscopy (ed. by R.A. Steinbrecht and K. Zierold), pp. 175-191. Springer-Verlag, Berlin.

Moore, J.M., Vielle-Calzada, J.-P., Gagliano, W. & Grossniklaus, U. (1997). Genetic characterization of *hadad*, a mutant disrupting female gametopgenesis in *Arabidopsis thaliana*. Cold Spring Harbor Symp. Quant. Biol. 62, 35-47.

Mouritzen, P. & Holm, P.B. (1995). Isolation and culture of barley megasporocyte protoplasts. Sex. Plant Reprod. 8, 321-325.

Müller, M. & Moor, H. (1984). Cryofixation of thick specimens by high pressure freezing. Science of biological specimen preparation (ed. by J.P. Revel, T. Barnard and G.H. Haggins), pp. 131-138. SEM, AMF O'Hare, Chicago.

Murgia, M., Huang, B.-Q., Tucker, S.C. & Musgrave, M.E. (1993). Embryo sac lacking antipodal cells in *Arabidopsis thaliana* (Brassicaceae). Am. J. Bot. 80, 824-838.

Nebenführ, A. & Staehelin, L.A. (2001). Mobile factories: Golgi dynamics in plant cells. Trends Plant Sci. 6, 160-167.

Otegui, M.S., Cap, R. & Staehelin, L.A. (2002). Developing seeds of *Arabidopsis* store different minerals in two types of vacuoles and in the endoplasmic reticulum. Plant Cell 14, 1311-1327.

Otegui, M.S., Mastronarde, D.N., Kang, B.-H., Bednarek, S.Y. & Staehelin, L.A. (2001). Three-dimensional analysis of synsytial-type cell plates during endosperm cellularization visualized by high resolution electron tomography. Plant Cell 13, 2033-2051.

Otegui, M. & Staehelin, L.A. (2000). Cytokinesis in flowering plants: More than one way to divide a cell. Curr. Opin. Plant Biol. 3, 493-502.

Park, S.K., Howden, R. & Twell, D. (1998). The *Arabidopsis thaliana* gametophytic mutation *gemini pollen1* disrupts microspore polarity, division asymmetry and pollen cell fate. Development 125, 3789-3799.

Ray, S., Park, S.-S. & Ray, A. (1997). Pollen tube guidance by the female gametophyte. Development 124, 2489-2498.

Reiser, L. & Fischer, R.L. (1993). The ovule and the embryo sac. Plant Cell 5, 1291-1301.

Richert, J., Kranz, E., Lörz, H. & Dresselhaus, T. (1996). A reverse transcriptase-polymerase chain reaction assay for gene expression studies at the single cell level. Plant Sci. 114, 93-99.

Rotman, N., Rozier, F., Boavida, L., Dumas, C., Berger, F. & Faure, J.-E. (2003). Female control of gamete delivery during fertilization in *Arabidopsis thaliana*. Curr. Biol. 13, 432-436.

Russell, S.D. (1993). The egg cell: Development and role in fertilization and early embryogenesis. Plant Cell 5, 1349-1359.

Samuels, A.L., Giddings, T.H. & Staehelin, L.A. (1995). Cytokinesis in tobacco BY-2 and root tip cells: A new model of cell plate formation in higher plants. J. Cell Biol. 130, 1-13.

Sartori, N., Richter, K. & Dubochet, J. (1993). Vitrification depth can be increased more than 10-fold by high-pressure freezing. J. Microsc. 172, 55-61.

Schneitz, K. (1999). The molecular and genetic control of ovule development. Curr. Opin. Plant Biol. 2, 13-17.

Sitte, H., Edelmann, L. & Neumann, K. (1987). Cryofixation without pretreatment at ambient pressure. Cryotechniques in biological electron microscopy (ed. by R.A. Steinbrecht and K. Zierold) pp. 87-113. Springer-Verlag, Berlin.

Staehelin, L.A. (1997). The plant ER: A dynamic organelle composed of a large number of discrete functional domains. Plant J. 11, 1151-1165.

Staehelin, L.A., Giddings, T.H. Jr, Kiss, J.Z. & Sack, F.D. (1990). Macromolecular differentiation of Golgi stacks in root tips of *Arabidopsis* and *Nicotiana* seedlings as visualized in high pressure frozen and freeze-substituted samples. Protoplasma 157, 75-91.

Studer, D., Michel, M. & Müller, M. (1989). High pressure freezing comes of age. Scanning Microsc. Suppl. 3, 253-269.

Theunis, C.H., Pierson, E.S. & Cresti, M. (1991). Isolation of male and female gametes in higher plants. Sex. Plant Reprod. 4, 145-154.

Thijssen, M.H., Mittempergher, F., Van Aelst, A.C. & Van Went, J.L. (1997). Improved ultrastructural preservation of *Petunia* and *Brassica* ovules and embryo sacs by high pressure freezing and freeze substitution. Protoplasma 197, 199-209.

Thijssen, M.H., Van Went, J.L. & Van Aelst, A.C. (1998). Heptane and isooctane as embedding fluids for high-pressure freezing of *Petunia* ovules followed by freeze-substitution. J. Microsc. 192, 228-235.

Tian, H.Q. & Russell, S.D. (1997). Micromanipulation of male and female gametes of *Nicotiana tabacum*: II. Preliminary attempts for *in vitro* fertilization and egg cell culture. Plant Cell Rep. 16, 657-661.

Van Lammeren, A.M.M. (1988). Structure and function of the microtubular cytoskeleton during endosperm development in wheat: An immunofluorescence study. Protoplasma 146, 18-27.

Van Went, J.L. (1970). The ultrastructure of the synergids of *Petunia*. Acta Bot. Neerl. 19, 121-132.

Vos, J.W., Sieberer, B., Timmers, A.C.J. & Emons, A.M.C. (2003). Microtubule dynamics during preprophase band formation and the role of endoplasmic microtubules during root hair elongation. Cell Biol. Int. 27, 295.

Webb, M.C. & Gunning, B.E.S. (1994). Embryo sac development in *Arabidopsis thaliana*. II. The cytoskeleton during megagametogenesis. Sex. Plant Reprod. 7, 153-163.

Willemse, M.T.M. & Van Went, J.L. (1984). The female gametophyte. Embryology of angiosperms (ed. by B.M. Johri), pp. 159-196. Springer-Verlag, Berlin.

Zhang, G., Liu, D. & Cass, D.D. (1997). Calcium-induced sperm fusion in *Zea mays* L. Sex. Plant Reprod. 10, 74-82.

Zhang, G.F. & Staehelin, L.A. (1992). Functional compartmentation of the Golgi apparatus of plant cells. Immunocytochemical analysis of high-pressure frozen- and freeze-substituted sycamore maple suspension culture cells. Plant Physiol. 99, 1070-1083.

Zhao, J., Zhou, C. & Yang, H.Y. (1999). Isolation and *in vitro* culture of zygotes and central cells of *Oryza sativa* L. Plant Cell Rep. 19, 321-326.

Summary

The female gametophyte of angiosperms, also called the megagametophyte or the embryo sac, develops from a single cell, the megaspore. The megaspore is located within several layers of ovular cells and contained within the carpel's ovary. This location makes the study of gametophyte development and differentiation difficult and therefore these processes are still poorly understood. The aim of the thesis work was to obtain further insight into these processes. The work focused on two aspects. One aspect was the analysis of the cytological and ultrastructural changes during megagametophyte development *in planta*, with the aim to identify and characterize factors and mechanisms playing a role in this process. The second aspect was the isolation of viable female megagametophytes from their surrounding ovular tissues and subsequent *in vitro* culture. Successful female gametophyte cell culture could create possibilities for *in vitro* manipulation of megagametophyte development.

In our studies, we mainly used *Petunia* x *hybrida* with its *Polygonum* type of embryo sac as a representative angiosperm. In this type, one of the four haploid megaspores undergoes three rounds of mitotic divisions, resulting in an eight-nucleate coenocyte. Formation of cell plates results in the establishment of the seven-celled embryo sac. Differentiation results in the formation of one egg cell, two synergid cells, three antipodal cells and one two-nucleate central cell, with each of these cell types having its own location, morphology, cytoarchitecture and function.

Most structural studies on female gametophyte development are based on chemically fixed ovules and embryo sacs. Chemical fixation methods are known to induce a variety of structural artifacts. The ultrastructure of cryofixed cells is supposed to reflect more closely the living state of the cells. However, ice crystals formed during freezing may destroy cellular ultrastructure. With high pressure freezing, relatively large samples of tissue can be preserved without subcellular distortion due to ice crystal formation.

In chapter 2 we show that high pressure freezing of *P.* x *hybrida* and *Brassica napus* ovules, followed by freeze substitution resulted in improved ultrastructural preservation of all ovular tissues. Many details that are often destroyed with chemical fixation were well preserved such as plasma membranes and vacuolar membranes, vesicles along with and attached to the plasma membranes, the microtubule cytoskeleton, and details of cell degeneration.

Although the application of high pressure freezing and freeze substitution resulted in an improved ultrastructural preservation, only a low percentage of *P.* x

hybrida ovules were found without structure disturbing ice crystals. These crystals were secondary ice crystals formed during freeze substitution. 1-hexadecene is generally used as an embedding fluid for high pressure freezing to fill the space between samples in the specimen sandwich. However, 1-hexadecene is not soluble in the substitution fluid acetone at freeze substitution temperatures and hinders substitution when tissues are completely surrounded by this compound. Chapter 3 describes the comparisons of different compounds for their suitability as embedding fluid in the high pressure freezing/ freeze substitution procedure. The application of heptane and isooctane as embedding fluids led to adequate freeze substitution and 90% of crystal-free *P.* x *hybrida* ovules.

Results of studies on the ultrastructural aspects of female gametophyte development as well as on the ultrastructural organization of the mature embryo sac with the cryofixation procedure as optimized for *P.* x *hybrida* are described in chapters 4 and 5. In *P.* x *hybrida*'s two-nucleate and four-nucleate megagametophyte, cytoplasmic constitution at the two poles is similar and is comparable to the vacuolated one-nucleate megagametophyte. The cytoplasm is packed with rough endoplasmic reticulum, polysomes, mitochondria, Golgi bodies with associated vesicles and starch containing plastids. Microtubules can be observed throughout the cytoplasm and at the two- and four-nucleate gametophyte stage in addition in close association with the nuclear envelope. Plasmodesmata are only present at the most chalazal part of the cell wall of the gametophyte and seem to be occluded.

The synergid cells are highly polarized with high numbers of mitochondria, Golgi bodies with associated vesicles and extensive rough endoplasmic reticulum in the micropylar cytoplasm. The filiform apparatus is regular in appearance, and along the plasma membrane aligning it, many vesicles are located. Cellular organization of both synergid cells is similar and degeneration before pollen tube penetration does not occur. The *P.* x *hybrida* egg cell is extremely vacuolated with only a thin layer of cytoplasm, containing few organelles along the plasma membrane and around the chalazally located nucleus. The central cell is characterized by the accumulation of high amounts of starch at maturity. At the most chalazal side of the synergid cells and the egg cell, cell walls seem absent. The antipodal cells initially have the appearance of highly metabolically active cells, with Golgi bodies and associated vesicles, rough endoplasmic reticulum, polysomes and starch containing plastids, but degeneration starts upon embryo sac maturity. Plasmodesmata are present between all embryo sac cells, but in the embryo sac surrounding cell wall, only at the most chalazal side. Differences in cytoarchitecture obtained after chemical fixation and after fixation with

high pressure freezing are discussed for *P.* x *hybrida* and compared with other species.

Techniques that allow the isolation of viable megagametophytes from their ovular environment provide a new approach for gaining insight into female gametophyte development. We isolated *P.* x *hybrida* megagametophytes, characterized the isolated cells and cultured them *in vitro*. The results of these studies are presented in chapter 6. After isolation the structure and organization of the female gametophytes resembled those of *in planta* gametophytes. *In vitro* cultured egg and synergid cells did not show major changes in cell organization. Within the central cell clear organizational changes were observed during culture. Nuclear divisions were never observed, neither in young megagametophytes, nor in cells of the mature embryo sac. Generally, isolated mature embryo sacs could be kept alive in culture for up to five days, whereas young megagametophytes only survived for up to three days. Improving the viability of isolated megaspores and megagametophytes and establishing an *in vitro* culture system that sustains the development of the isolated cells, will allow fundamental questions on female gametophyte biology to be addressed experimentally.

The development of maize somatic embryos originating from exogenic meristems on embryogenic callus shows many similarities with zygotic embryo development. Chapter 7 presents a study in which maize *in planta* and *in vitro* embryo development were compared, regarding the accumulation and distribution of globulin storage proteins.

With an increasing number of identified genes that play a role in female gametophyte development, the challenge will be to understand their function. The combination of information at the molecular level with information at the level of cellular organization will contribute to further insight into megagametophyte development. The use of mutants that are disturbed in female gametophyte development and studies on wild type female gametophyte structure and development will provide the essential framework upon which mutagenic approaches are based. Electron microscopic data obtained with high pressure freezing and freeze substitution may play a crucial role in these analyses.

Samenvatting

De vrouwelijke gametofyt van angiosperme planten, ook wel megagametofyt of embryozak genoemd, ontstaat uit een enkele cel, de haploide megaspore. De megaspore bevindt zich binnen in het zaadbeginsel en is omgeven door een aantal lagen sporofytisch weefsel. De studie van de gametofyt vorming en differentiatie wordt hierdoor bemoeilijkt en het ontwikkelingsproces van megaspore tot rijpe embryozak wordt nog steeds niet goed begrepen. De centrale doelstelling van dit project was om meer inzicht te krijgen in dit ontwikkelingsproces. De nadruk lag op twee aspecten. Het eerste aspect was de analyse van de cytologische en ultrastructurele veranderingen tijdens de ontwikkeling van de megagametofyt zoals die plaatsvindt in de plant, met als doel het identificeren en karakteriseren van factoren en mechanismen die een rol spelen in het ontwikkelingsproces. Het tweede aspect was de isolatie van levende gametofyten uit de zaadbeginsels en het kweken van deze cellen *in vitro*. Door middel van *in vitro* cultuur wordt manipulatie van gametofyt ontwikkeling mogelijk gemaakt.

In dit project is als modelplant voornamelijk *Petunia* x *hybrida* gebruikt. Deze plant heeft een *Polygonum* type embryozak. In dit embryozak type, ondergaat één van de vier haploide megasporen eerst drie rondes van mitotische kerndelingen, waarbij steeds alle aanwezige kernen gelijktijdig delen, wat resulteert in een cel met acht kernen. Vervolgens worden er celwanden gevormd en treedt celdifferentiatie op. De gedifferentieerde embryozak bestaat uit een eicel, twee synergiden, drie antipoden en een twee-kernige centrale cel. Elk celtype heeft zijn eigen positie, morfologie, cytologie en functie binnen de embryozak.

In de meeste studies van de structurele aspecten van de vrouwelijke gametofyt ontwikkeling, is gebruik gemaakt van chemische fixatietechnieken. Het is bekend dat chemische fixatiemethoden kunnen leiden tot uiteenlopende artefacten in de structuur van cellen. Er wordt verondersteld dat de ultrastructuur van cellen welke gefixeerd zijn door middel van invriezen, of cryofixatie, de structuur van levende cellen dichter benadert. Een probleem bij cryofixatie van meerdere cellen en weefsels is dat vaak er vaak vorming van ijskristallen plaatsvindt. Deze ijskristallen beschadigen de ultrastructuur van de cellen. Bij cryofixatie onder normale druk kunnen slechts enkele cellen, of kleine delen van weefsels goed gefixeerd worden voor ultrastructurele studies. Door middel van het invriezen onder hoge druk, kunnen relatief grote stukken weefsel kristalvrij worden gefixeerd.

In hoofdstuk 2 laten we zien dat het gebruik van de hoge-druk-invriesmethode in combinatie met vriessubstitutie resulteerde in een verbeterde fixatie van de

ultrastructuur in alle weefsels van *P.* x *hybrida* en *Brassica napus* zaadbeginsels. Vele ultrastructurele details die met chemische fixatiemethoden niet bewaard blijven, kunnen met deze methode wel goed gefixeerd en zichtbaar gemaakt worden, zoals de plasmamembranen, de vacuolemembranen, vesikels langs de plasmamembraan, het cytoskelet van microtubuli als ook cellulaire details van degenererende cellen.

Ondanks de toepassing van de hoge-druk-invriesmethode werd aanvankelijk slechts een klein percentage van de *P.* x *hybrida* zaadbeginsels gefixeerd zonder subcellulaire schade door de vorming van ijskristallen. We veronderstelden dat deze kristallen werden gevormd tijdens de vriessubstitutie. 1-hexadeceen wordt gebruikt als inbedvloeistof in de preparaathouders van de hoge-druk-invriezer. 1-Hexadeceen blijft echter vast bij de temperaturen waarbij de vriessubstitutie plaatsvindt en lost niet op in de substitutievloeistof aceton. Hierdoor kan de vriessubstitutie gehinderd worden wanneer weefsels volledig omringd worden door 1-hexadeceen. De vervanging van 1-hexadeceen door heptaan of iso-octaan resulteerde in 90% goed gefixeerde *P.* x *hybrida* zaadbeginsels. De resultaten van dit werk zijn beschreven in hoofdstuk 3.

De resultaten van de studies naar de ultrastructurele aspecten van de ontwikkeling van de vrouwelijke gametofyt en de organisatie van de rijpe embryozak met een voor *P.* x *hybrida* zaadbeginsels geoptimaliseerde cryofixatie procedure zijn beschreven in hoofdstuk 4 en 5. De organisatie van het cytoplasma aan beide polen van de twee-kerninge en vier-kernige megagametofyt is hetzelfde en is vergelijkbaar met het gevacuoliseerde één-kerninge stadium. Het cytoplasma zit vol met ruw endoplasmatisch reticulum, polysomen, mitochondria, Golgi lichaampjes met vesikels en plastiden met zetmeel. Microtubuli zijn zichtbaar door het gehele cytoplasma en in het twee-kernige en vier-kernige stadium ook geassocieerd met de kernmembraan. Plasmodesmata zijn alleen aanwezig in het meest chalazale deel van de celwand van de gametofyt en lijken gesloten.

De synergiden zijn sterk gepolariseerde cellen met in hun micropilaire cytoplasma een groot aantal mitochondrien, Golgi lichaampjes met vesikels en veel ruw endoplasmatisch reticulum. Het filiform apparaat is uniform van structuur en langs de plasmamembraan liggen veel vesikels. De cellulaire organisatie van beide synergiden is gelijk en deze cellen degenereren niet voordat de pollenbuis de embryozak penetreert. De *P.* x *hybrida* eicel is sterk gevacuoliseerd met slechts een dun laagje cytoplasma met weinig organellen langs de plasmamembraan en rondom de kern. De kern ligt aan de chalazale kant van de cel. Karakteristiek voor de centrale cel in het rijpe stadium is de grote hoeveelheid zetmeel. De chalazale zijden van de synergiden en eicel lijken slechts te worden begrensd door plasmamembranen,

celwanden lijken hier afwezig. De antipoden lijken in een vroeg stadium metabolisch zeer actief met Golgi lichaampjes met vesikels, ruw endoplasmatisch reticulum, polysomen en plastiden met zetmeel, maar cel degeneratie begint in de rijpe embryozak. Plasmodesmata zijn aanwezig in alle afzonderlijke cellen van de embryozak, maar in de celwand om de embryozak heen slechts aan de meest chalazale zijde. Verschillen in organisatie en structuur van het cytoplasma na chemische fixatie en na fixatie met de hoge-druk-invriesmethode worden bediscussieerd voor *P.* x *hybrida* en vergeleken met andere soorten.

Technieken die het mogelijk maken om levende megagametofyten uit zaadbeginsels te isoleren bieden een nieuwe mogelijkheid om inzicht te krijgen in het ontwikkelingsproces van de vrouwelijke gametofyt. Hoofdstuk 6 beschrijft de isolatie van *P.* x *hybrida* megagametofyten en de karakterisering en *in vitro* kweek van de geïsoleerde cellen. Direct na isolatie lijkt de structuur en organisatie van de vrouwelijke gametofyten sterk op de gametofyten zoals deze zich bevinden in de plant. De celorganisatie van eicellen en synergiden *in vitro* veranderde nauwelijks. In de centrale cel werden *in vitro* wel sterke veranderingen in celorganisatie waargenomen. Kerndelingen werden niet waargenomen, noch in de jonge megagametofyten, noch in de cellen van rijpe embryozakken. Geïsoleerde rijpe embryozakken konden in cultuur tot vijf dagen in leven worden gehouden; jonge megagametofyten bleven slechts tot drie dagen in leven. Het verbeteren van de vitaliteit van geïsoleerde megasporen en megagametofyten en het opzetten van een *in vitro* cultuur systeem dat ontwikkeling van de geïsoleerde cellen mogelijk maakt, staat een experimentele benadering toe van fundamentele vragen over de biologie van de vrouwelijke gametofyt.

De ontwikkeling van somatische embryo's van maïs, die zich ontwikkelen uit exogene meristemen aan embryogeen callus, lijkt in vele opzichten op de ontwikkeling van zygotische embryos. Hoofdstuk 7 beschrijft een studie waarin de ontwikkeling van zygotische en somatische maïs embryo's vergeleken wordt, met name wat betreft de opslag en distributie van globuline opslageiwitten.

Met de toename van het aantal geïdentificeerde genen dat een rol speelt in de ontwikkeling van de vrouwelijke gametofyt, is het de uitdaging om de functie van deze genen te begrijpen. Het combineren van moleculaire informatie met informatie over celorganisatie zal bijdragen aan een verder inzicht in gametofyt ontwikkeling. Studies naar normale gametofyt ontwikkeling geven referentie data voor de analyse van mutanten die verstoord zijn in gametofyt ontwikkeling. Data verkregen met behulp van elektronenmicroscopie met de hoge-druk-invriesmethode en vriessubstitutie kunnen een grote rol spelen in deze analyses.

Dankwoord

Na al die jaren toch nog? Ja dus. "Proefschrift" is niet langer meer een woord dat in mijn bijzijn niet genoemd mag worden. Er zijn een aantal mensen zonder wie dit proefschrift er nooit geweest zou zijn, en er zijn er velen die me geholpen en gesteund hebben bij de totstandkoming. Het is onmogelijk al die mensen bij naam te noemen, bij voorbaat excuses. Maar een aantal mensen kan ik niet onvermeld laten.

Allereerst wil ik mijn promotor Jacques van Went bedanken. Jacques, bedankt voor de kans die ik heb gekregen om aan dit proefschrift te beginnen en het ook af te maken. Naast de discussies over petunia's, gametofyten en elektronenmicroscopie heb ik veel geleerd van de discussies over onderwijs, onze andere gedeelde interesse.

Anne Mie, jouw hulp, oneindige energie en vooral ook geduld, hebben erin geresulteerd dat dit boekje hier toch maar ligt. Dank voor je vertrouwen en de nodige push.

Mijn promotietijd op PCM was zeer intensief, moeilijk wanneer het in het lab allemaal weer eens niet meezat, maar door de vele leuke collega's vooral ook gezellig.

Allereerst waren er natuurlijk mijn lab-maatjes Carmen, Francesca en Adriaan. Carmen, het promotiefeestje van Ton, waar het eigenlijk allemaal is begonnen, staat me nog duidelijk bij. Net als ons gezamenlijke congres naar Wenen en de sportieve activiteiten als het bommen, keep-fitten bij Frits en de bergrace by night. Ook al zien we elkaar niet meer dagelijks, onze vriendschap blijft. Ik ben blij dat je mijn paranimf wilt zijn.

Francesca, although rape seed is not petunia, we could share a lot of the work and experience; without you it would not have been so enjoyable. Thanks a lot. Adriaan, waar zou ik geweest zijn zonder jouw enorme EM ervaring? Het was hard werken, maar ook gezellig, op onze gedeelde kamer, op het lab in Zürich en tijdens ons reisje door de Yucatan. Ik vind het een eer dat je mijn paranimf wilt zijn.

Twee zwangere vrouwen op een kamer. Vanwege besmettingsgevaar durfden bepaalde mensen niet meer binnen te komen. Daphne, het was leuk. Dank voor de correcties van mijn Denglish. Jan, ook jij was een plezierige kamergenoot. Sorry, dat ik je plantjes heb laten verdrogen.

En dan zijn er mijn generatie collega-AIO's: Peter, Kees en Folbert, bedankt voor het gedeelde plezier, de gezellige etentjes en feestjes, als ook de gedeelde AIO-stress. Tiny, Hetty, Koos, Wilco, Truus, Regina, Michiel, Jan, Henk, Andre, Norbert, Wim, Alfred, Allex, Sijbout, Paul, Gerrit, Leen, Tijs, John, Bjorn, Franck, Anja, Sun, Patrick, Maarten, Anko en alle andere collega's, gasten en studenten op de leerstoelgroep, dank voor jullie belangstelling in mijn werk en mijn persoon en dank voor de prettige samenwerking.

I want to thank Prof. Lörz and Prof. Kranz for the opportunity to work at their laboratory at the Institut für Allgemeine Botanik, Universität Hamburg. Your work on maize *in vitro* fertilization gave a new dimension to research in sexual plant reproduction. Petra, thanks for your kind and skilled assistance.
I want to thank Prof. Müller for the opportunity to work at the Laboratory for Electron Microscopy I, ETH Zürich, THE place to be for cryofixation work. Paul and Eyal, thanks for the nice discussions and for your assistance with the high pressure freezing.
Fyto-collega's uit Utrecht en Agronomen, DL&V-ers, YIPPIES en andere IAC-collega's, bedankt voor jullie steun en belangstelling. Toch nog een feestje.
Kees, toen jij bijna als laatste de hoop had opgegeven, werd het pas echt wat met dat schrijven. We zijn een goed IAC-team! Ik ben nog steeds blij met mijn interessante baan op het IAC.
Hoewel mijn werk op het IAC, door de reisjes, soms letterlijk "ver van mijn bed" is voor mijn ouders, schoonouders, familie en vrienden, was dat het wat dit promotieonderzoek betreft vaak figuurlijk het geval. Dank aan allen voor jullie interesse, steun en de broodnodige afleiding.
Mirjam, bedankt voor jouw hulp bij het ontwerpen van de omslag.
En last but not least, dank aan mijn grote vriend Bart (mooie foto op de kaft!) en mijn kleine vriendje Emiel. Jullie zijn geweldig.

Marja Thijssen
Wageningen, 21 juli 2003

Curriculum vitae

Marja Thijssen werd op 4 oktober 1967 geboren in Venlo. In 1986 behaalde zij het VWO diploma aan het Elzendaal College te Boxmeer. In datzelfde jaar begon zij met de studie plantenveredeling aan de aan de toenmalige Landbouwuniversiteit Wageningen (WU). Haar afstudeerrichtingen waren Entomologie (leerstoelgroep Entomologie, WU), Plantencelbiologie (leerstoelgroep Plantencytologie en –morfologie, WU) en Plantenveredeling (International Maize and Wheat Breeding Center [CIMMYT], Mexico). Na haar afstuderen in 1992 begon zij met haar promotieonderzoek naar zaadbeginsel en megagametofyt ontwikkeling, bij de toenmalige leerstoelgroep Plantencytologie en –morfologie. Het promotieonderzoek werd uitgevoerd in de periode van 1992 tot 1997. De resultaten van dit onderzoek zijn beschreven in dit proefschrift. In 1997 raakte zij als cursusassistent betrokken bij het internationale trainingsprogramma op het gebied van zaadproductie en zaadtechnologie van het Internationaal Agrarisch Centrum (IAC) te Wageningen. In 1998 en 1999 was zij bij het IAC verantwoordelijk voor de coördinatie van het internationale trainingsprogramma op het gebied van de toegepaste plantenveredeling. In 1997-1998 was zij tevens werkzaam als toegevoegd docent aan de WU, waar zij in samenwerking met de Open Universiteit werkte aan de ontwikkeling van een cursus celbiologie voor afstandsonderwijs. In 1999 en 2000 werkte zij als junior onderzoeker in een samenwerkingsproject van het Laboratorium voor Fytopathologie, Universiteit Utrecht, en het Laboratorium voor Plantencytologie en -morfologie aan geïnduceerde systemische resistentie in *Arabidopsis*. In 2001 keerde zij terug naar het IAC waar zij momenteel een aanstelling heeft en werkzaam is op het gebied van training en advisering in de onderwerpen plantenveredeling, biotechnologie en agrobiodiversiteit.

Huidige adres: International Agricultural Centre, P.O. Box 99, 6700 AB Wageningen, the Netherlands

Publications

Duveiller, E., Van Ginkel, M. & Thijssen, M.H. (1993). Genetic analysis of resistance to bacterial leaf streak caused by *Xanthomonas campestris* p.v. *undulosa* in bread wheat. Euphytica 66, 35-43.

Thijssen, M.H., Spoelstra, P. & Emons, A.M.C. (1996). Immunodetection and immunolocalization of globulin storage proteins during zygotic and somatic embryo development in *Zea mays*. Physiol. Plant. 98, 539-549.

Thijssen, M.H., Mittempergher, F., Van Aelst, A.C. & Van Went, J.L. (1997). Improved ultrastructural preservation of *Petunia* and *Brassica* ovules and embryo sacs by high pressure freezing and freeze substitution. Protoplasma 197, 199-209.

Thijssen, M.H., Van Went, J.L. & Van Aelst, A.C. (1998). Heptane and isooctane as embedding fluids for high-pressure freezing of *Petunia* ovules followed by freeze-substitution. J. Microsc. 192, 228-235.

Van Ginkel, M., Rajaram, S. & Thijssen, M.H. (1991). Waterlogging in wheat: Germplasm evaluation and methodology development. Proc. of the 7th Regional Wheat Congress, Kenia, September 1991.